

Material Characterization and Seasonal Variation in Material Properties

**FINAL REPORT
February 2006**

Submitted by

Dr. Sameh Zaghoul, P.E., P.Eng.*
Managing Senior Principal

Dr. Nenad Gucunski**
Professor

Dr. Hudson Jackson, P.E.,*** Pavement Specialist
Mr. Rambod Hadidi,** Graduate Research Assistant



*Stantec Consulting Ltd.
150 Lawrence Bell Drive, Suite 108
Amherst, NY 14221

**Dept. of Civil & Environmental Engineering
Center for Advanced Infrastructure
& Transportation (CAIT)
Rutgers, the State University

***Stantec Consulting Ltd.
9 Princess Road, Unit D
Lawrenceville, NJ 08648



NJDOT
RESEARCH PROJECT MANAGER
Mr. Anthony Chmiel

In cooperation with

New Jersey
Department of Transportation
Bureau of Research
and
U. S. Department of Transportation
Federal Highway Administration

Disclaimer Statement

“The contents of this report reflect the views of the author(s) who is (are) responsible for the facts and the accuracy of the data presented herein. The contents do not necessarily reflect the official views or policies of the New Jersey Department of Transportation or the Federal Highway Administration. This report does not constitute a standard, specification or regulation.”

The contents of this report reflect the views of the authors, who are responsible for the facts and the accuracy of the information presented herein. This document is disseminated under the sponsorship of the Department of Transportation, University Transportation Centers Program, in the interest of information exchange. The U.S. Government assumes no liability for the contents or use thereof.

1. Report No. FHWA NJ-2005-024	2. Government Accession No.	3. Recipient's Catalog No.	
4. Title and Subtitle FINAL REPORT Material Characterization and Seasonal Variation in Material Properties		5. Report Date February 2006	
		6. Performing Organization Code CAIT/Rutgers	
7. Author(s) Dr. Sameh Zaghoul, Dr. Nenad Gucunski, Dr. Hudson Jackson, Mr. Rambod Hadidi		8. Performing Organization Report No. FHWA-NJ-2005-024	
9. Performing Organization Name and Address Rutgers, the State University Dept. of Civil & Env. Engineering Center for Advanced Infrastructure and Transportation 623 Bevier Road Piscataway, NJ 08854-8014		10. Work Unit No.	
		11. Contract or Grant No.	
12. Sponsoring Agency Name and Address New Jersey Department of Transportation Federal Highway Administration PO Box 600 US Department of Transportation Trenton, NJ 08625 Washington, DC		13. Type of Report & Period Covered 1/1/2001-6/30/2005	
		14. Sponsoring Agency Code	
15. Supplementary Notes e-mail addresses: szaghoul@stantec.com gucunski@rci.rutgers.edu hjackson@stantec.com rambodh@rci.rutgers.edu			
16. Abstract The main objective of this study was to calibrate the AASHTO temperature and seasonal adjustment models, or to develop new models. The models developed are based on New Jersey conditions and will be also used in network and project level FWD analysis. To achieve the objective of study, twenty-four pavement sections were instrumented and nondestructive testing (NDT) program was conducted for a period of two years. The main task of the instrumentation was to monitor environmental parameters: air and pavement temperature, moisture, frost/thaw depth and rainfall. Seismic Pavement Analyzer (SPA) and Falling Weight Deflectometer (FWD) were used to evaluate the pavement structural response and it's properties on a monthly basis, except during the spring thaw period when it is on a bi-monthly basis. The models were developed by performing statistical analyses, such as analysis of variance (ANOVA) and regression analysis. Several important conclusions were developed with respect to the applicability of the Enhanced Climatic Model (EICM) to New Jersey conditions. Results of NDT evaluations provided strong correlations between all environmental parameters, except the ground water level and the overall pavement deflection, difference in pavement deflections and the effective pavement modulus obtained from FWD evaluation. Seismic tests provided a strong correlation between the AC modulus and pavement temperature. It is recommended that for the FWD data corrections using the temperature adjustment model be followed by the seasonal adjustment model. A number of other conclusions and recommendations related to measurement and relationships of environmental variables and material characteristics and effects of drainage conditions are provided.			
17. Key Words Pavement materials, seasonal variations, seasonal models, temperature models, nondestructive testing, material characterization, FWD, SPA, instrumentation		18. Distribution Statement	
19. Security Classif (of this report) Unclassified	20. Security Classif. (of this page) Unclassified	21. No of Pages 284	22. Price

SI* (MODERN METRIC) CONVERSION FACTORS

APPROXIMATE CONVERSIONS TO SI UNITS

APPROXIMATE CONVERSIONS FROM SI UNITS

Symbol	When You Know	Multiply By	To Find	Symbol
LENGTH				
in	inches	25.4	millimeters	mm
ft	feet	0.305	meters	m
yd	yards	0.914	meters	m
mi	miles	1.61	kilometers	km
AREA				
in ²	square inches	645.2	square millimeters	mm ²
ft ²	square feet	0.093	square meters	m ²
yd ²	square yards	0.836	square meters	m ²
ac	acres	0.405	hectares	ha
mi ²	square miles	2.59	square kilometers	km ²
VOLUME				
fl oz	fluid ounces	29.57	milliliters	mL
gal	gallons	3.785	liters	L
ft ³	cubic feet	0.028	cubic meters	m ³
yd ³	cubic yards	0.765	cubic meters	m ³
NOTE: Volumes greater than 1000 L shall be shown in m ³ .				
MASS				
oz	ounces	28.35	grams	g
lb	pounds	0.454	kilograms	kg
T	short tons (2000 lb)	0.907	megagrams (or "metric ton")	Mg (or "t")
TEMPERATURE (exact)				
°F	Fahrenheit temperature	5(F-32)/9 or (F-32)/1.8	Celcius temperature	°C
ILLUMINATION				
fc	foot-candles	10.76	lux	lx
fl	foot-Lamberts	3.426	candela/m ²	cd/m ²
FORCE and PRESSURE or STRESS				
lbf	poundforce	4.45	newtons	N
lbf/in ²	poundforce per square inch	6.89	kilopascals	kPa

Symbol	When You Know	Multiply By	To Find	Symbol
LENGTH				
mm	millimeters	0.039	inches	in
m	meters	3.28	feet	ft
m	meters	1.09	yards	yd
km	kilometers	0.621	miles	mi
AREA				
mm ²	square millimeters	0.0016	square inches	in ²
m ²	square meters	10.764	square feet	ft ²
m ²	square meters	1.195	square yards	yd ²
ha	hectares	2.47	acres	ac
km ²	square kilometers	0.386	square miles	mi ²
VOLUME				
mL	milliliters	0.034	fluid ounces	fl oz
L	liters	0.264	gallons	gal
m ³	cubic meters	35.71	cubic feet	ft ³
m ³	cubic meters	1.307	cubic yards	yd ³
MASS				
g	grams	0.035	ounces	oz
kg	kilograms	2.202	pounds	lb
Mg (or "t")	megagrams (or "metric ton")	1.103	short tons (2000 lb)	T
TEMPERATURE (exact)				
°C	Celcius temperature	1.8C + 32	Fahrenheit temperature	°F
ILLUMINATION				
lx	lux	0.0929	foot-candles	fc
cd/m ²	candela/m ²	0.2919	foot-Lamberts	fl
FORCE and PRESSURE or STRESS				
N	newtons	0.225	poundforce	lbf
kPa	kilopascals	0.145	poundforce per square inch	lbf/in ²

* SI is the symbol for the International Symbol of Units.

TABLE OF CONTENTS

	Page
EXECUTIVE SUMMARY	1
INTRODUCTION	3
MAIN REPORT BODY	3
APPENDICES	4
OBJECTIVES AND SCOPE OF STUDY	5
STUDY OBJECTIVES	5
SCOPE OF STUDY	5
LITERATURE SEARCH & REVIEW	6
ENVIRONMENTAL IMPACT ON PAVEMENTS	6
Impact of Seasonal Parameters	6
Impact of Temperature	8
EXISTING MODELS FOR SEASONAL AND TEMPERATURE CORRECTION	9
1993 American Association of State Highway and Transportation Officials (AASHTO) Guide.....	10
Strategic Highway Research Program (SHRP) - Long Term Pavement Performance (LTPP).....	15
Asphalt Institute.....	17
Research-Based Models	19
European Models	25
SUMMARY OF REVIEW	27
TEST SECTION REQUIREMENTS AND SELECTION	28
TEST SECTION REQUIREMENTS	28
Seasonal Adjustment Study	28
Temperature Correction Study	30
Long Term Pavement Performance (LTPP) – Specific Pavement Studies (SPS) Sites	31
TEST SECTION SELECTION	35
FIELD TESTING PROGRAM	40
PAVEMENT INSTRUMENTATION.....	40
Moisture Content Measurement.....	40
Pavement Temperature Measurement.....	40
Frost/Thaw Depth Measurement.....	40
Ground Water Depth Measurement	41
Climatic Measurements (Air Temperature and Rainfall)	41
EQUIPMENT SETUP & INSTALLATION.....	45
Equipment Check/Calibration.....	48
Installation Procedure.....	49
Site Repair and Cleanup	50
Patch/Repair Area Assessment	50
MATERIALS INVESTIGATION PLAN	51
FALLING WEIGHT DEFLECTOMETER TESTING	51
FWD Testing Protocols	52
File Naming Protocols	53
SEISMIC PAVEMENT ANALYZER (SPA) TESTING	53
SPA Testing Protocols	54
File Naming Protocols	55

TABLE OF CONTENTS (continued)

	Page
DATA PROCESSING AND PRELIMINARY ANALYSIS	56
DATA HANDLING.....	56
DATA TRACKING AND QUALITY CHECKS.....	57
CLIMATIC AND FWD DATA PROCESSING.....	59
PRELIMINARY FWD ANALYSIS.....	60
SPA DATA PROCESSING AND ANALYSIS.....	61
Data Transfer and Data Storage.....	62
Backcalculation Analysis.....	63
LABORATORY DATA PROCESSING AND ANALYSIS.....	65
STATISTICAL ANALYSIS	66
STATISTICAL ANALYSIS OF THE SEASONAL AND TEMPERATURE IMPACTS.....	66
DEVELOPMENT OF REGRESSION MODELS.....	69
SENSITIVITY ANALYSIS.....	76
SUMMARY OF FINDINGS AND IMPLEMENTATION PLAN.....	76
EICM MODEL EVALUATION.....	78
OVERVIEW OF EICM CAPABILITIES.....	78
EVALUATION PROCESS.....	78
Calibration and Validation.....	78
Sensitivity Analysis.....	80
Evaluation Results.....	81
Correlation Analysis.....	89
Summary of Findings.....	91
EMPIRICAL SEASONAL AND TEMPERATURE MODELS.....	93
DEVELOPMENT OF OVERALL LAYER MODULI CORRECTION FACTORS (OLCF) – STREAM 1.....	93
DEVELOPMENT OF OVERALL LAYER DEFLECTION CORRECTION FACTORS (ODCF) – STREAM 2.....	94
DEVELOPMENT OF DEFLECTION TEMPERATURE CORRECTION FACTORS (TCF) AND SEASONAL CORRECTION FACTORS (SCF) – STREAM 3.....	96
Development of Temperature Adjustment Models.....	97
Development of SCF.....	99
DEVELOPMENT OF LAYER MODULI TEMPERATURE CORRECTION FACTORS (TCF) AND SEASONAL CORRECTION FACTORS (SCF) – STREAM 4.....	102
DEVELOPMENT OF DEFLECTION MOISTURE CORRECTION FACTORS (MCF) AND ENHANCED SEASONAL CORRECTION FACTORS (ESCF) – STREAM 5.....	105
Development of MCF.....	105
Development of Enhanced Seasonal Correction Factors for Deflection (ESCF).....	107
DEVELOPMENT OF LAYER MODULI MCF AND ESCF – STREAM 6.....	109
DEVELOPMENT OF LAYER MODULI TEMPERATURE CORRECTION FACTORS FOR SPA BASED ON SASW ANALYSIS RESULTS (SPATCF).....	112
Flexible Pavements.....	112
Rigid Pavements.....	114
DEVELOPMENT OF LAYER MODULI TEMPERATURE CORRECTION FACTORS FOR SPA BASED ON USW ANALYSIS RESULTS (SPATCF).....	116
Flexible Pavements.....	116
Rigid Pavements.....	116

TABLE OF CONTENTS (continued)

	Page
VARIATION OF LAYER MODULI WITH MOISTURE BASED ON SPA RESULTS	119
SUMMARY AND CONCLUSIONS.....	119
VALIDATION OF NEW JERSEY TEMPERATURE AND SEASONAL MODELS ON NEW JERSEY LTPP DATA.....	122
BACKGROUND	122
IMPLEMENTATION OF THE MODELS TO LTPP DATA AND RESULTS	123
SUMMARY OF FINDINGS	131
EVALUATION OF NSOG BASE LAYERS	132
STUDY BACKGROUND	132
TEST SITES	132
Site 5 (S5)	132
Site 6 (S6)	133
Characteristics of Study Sites	134
INSTRUMENTATION AND DATA COLLECTION	135
ANALYSIS OF DATA.....	136
Rainfall And Volumetric Moisture Content Trends	136
Drainage Layer Influence on Pavement Performance	138
SUMMARY AND CONCLUSIONS.....	144
EFFECT OF SUBSURFACE DRAINAGE ON FLEXIBLE PAVEMENT LIFE CYCLE COST .	145
INTRODUCTION	145
IMPACT OF SUBSURFACE DRAINAGE QUALITY ON THE IN-SITU STRUCTURAL CAPACITY	145
IMPACT OF SUBSURFACE DRAINAGE QUALITY ON PAVEMENT PERFORMANCE.....	148
LIFE CYCLE COST ANALYSIS (LCCA).....	150
SUMMARY AND CONCLUSIONS.....	153
FWD VS. SPA CORRELATION ANALYSIS	154
SPA SEISMIC METHODS	154
Spectral Analysis of Surface Waves (SASW)	155
Impulse Response (IR).....	155
Ultrasonic Surface Waves (USW)	155
SPECTRAL ANALYSIS OF SURFACE WAVES (SASW) RESULTS.....	156
FWD and SPA (SASW) Pavement Modulus (Ep)	156
FWD and SPA (SASW) Subgrade Modulus (Mr)	161
SASW Results of FWD and SPA AC Modulus (EAC)	166
IMPULSE RESPONSE (IR) RESULTS.....	169
IR Results of FWD and SPA Pavement Modulus (Ep).....	171
ULTRASONIC SURFACE WAVES (USW) RESULTS	174
USW Results of FWD and SPA PCC Modulus for Rigid Pavements	174
SUMMARY.....	175
ENVIRONMENTAL ANALYSIS	176
RAINFALL AND MOISTURE CONTENT	176
Rainfall and Base Moisture Content.....	176
Rainfall and Subbase Moisture Content.....	177
Rainfall and Subgrade Moisture Content	179
AIR TEMPERATURE AND PAVEMENT TEMPERATURE (SURFACE AND MID DEPTH)	180

TABLE OF CONTENTS (continued)

	Page
Air Temperature and Pavement Temperature Models	181
Mid-Depth and Pavement Temperature Relationships	183
FROST DAMAGE	184
Frost/Thaw Depth Measurement.....	185
FROST Software.....	185
Freezing Index Calculations.....	185
Frost Penetration Depths	186
SUMMARY OF FINDINGS	189
PROJECT CONCLUSIONS AND RECOMMENDATIONS FOR FURTHER STUDIES.....	190
CONCLUSIONS.....	190
RECOMMENDATIONS FOR FURTHER STUDIES	191
REFERENCES	192
APPENDIX A	196
APPENDIX B	242

LIST OF FIGURES

	Page
Figure 1: Environmental Factors Affecting Pavement	6
Figure 2: Effect of Site Location on Seasonal Variation of Deflection ⁽⁸⁾	10
Figure 3: Seasonal Elastic Modulus Calculation for Flexible Pavements ⁽⁸⁾	12
Figure 4: Adjustment Factors for AC Temperature for Granular or Asphalt-Treated Base Pavements ⁽⁸⁾	13
Figure 5: Adjustment Factors for AC Temperature for Cement or Pozzolanic-Treated Base Pavements ⁽⁸⁾	14
Figure 6: Adjustment Factors for Deflections for 3-layered AC Pavements ⁽¹³⁾	18
Figure 7: Predicted Pavement Temperature from Surface and 5-days Mean Air Temperature.....	19
Figure 8: Comparison Between New Jersey Environmental Regions	29
Figure 9: Details of the SPS-5 Test Sections	32
Figure 10: Details of the SPS-9A Test Sections.....	33
Figure 11: Locations of Test Sites within New Jersey	37
Figure 12: Flexible Pavement Test Sections	38
Figure 13: Rigid Pavement Test Sections	39
Figure 14: Composite Pavement Test Section	39
Figure 15: Typical Instrumentation Layout	41
Figure 16: Seasonal Adjustment Instrumentation.....	42
Figure 17: Temperature Correction Instrumentation	42
Figure 18: Instrumentation Plan for SPS-5.....	43
Figure 19: Instrumentation Plan for SPS-9.....	44
Figure 20: Tipping Bucket, Solar Panel, and Air Temperature Probe.....	46
Figure 21: TDR and Temperature Probes	46
Figure 22: Resistivity Probe	47
Figure 23: Data Logger and Housing Cabinet.....	47
Figure 24: Sample TDR Trace During Calibration.....	49
Figure 25: Dynatest HWD	51
Figure 26: Seismic Pavement Analyzer (SPA).....	54
Figure 27: Schematic of SPA	55
Figure 28: Typical Field Instrumentation Functionality Check	56
Figure 29: Field Data Handling Process Flow Chart	57
Figure 30: Sample Climatic Data Track Sheet	57
Figure 31: Sample TDR Data Track Sheet.....	58
Figure 32: Sample FWD Data Track Sheet.....	58
Figure 33: FWD Data Tracking and QC/QA Flow Process.....	60
Figure 34: Typical Backcalculated Pavement Modulus (NJ Site 4)	61
Figure 35: Typical SPA Data Storage Structure	62
Figure 36: Screen Shots of SASW-Ver. 2.0 Program.....	63
Figure 37: Screen Shot of IR Program	65
Figure 38: Initial Design of Experiment	67
Figure 39: Revised DOE Considering Pavement Temperature Only	68
Figure 40: Revised DOE Considering Air Temperature Only	68
Figure 41: Normalized Actual D_1 versus Standard D_1	71

LIST OF FIGURES (continued)

	Page
Figure 42: Predicted Δ Deflection for Low Moisture and Low Pavement Temperature	76
Figure 43: Implementation Plan for Model Development	77
Figure 44: Flowchart for EICM Validation Procedure	79
Figure 45: Hourly Temperature Variation on September 10, 2002 and 2003 at LTPP Sections 5E and 9C.....	80
Figure 46: Sensitivity Analysis Results.....	81
Figure 47a: July 2003 Temperature Comparison for LTPP Section 5E.....	82
Figure 47b: September 2003 Temperature Comparison for LTPP Section 5E	83
Figure 48a: July 2003 Temperature Comparison for LTPP Section 9C	84
Figure 48b: September 2003 Temperature Comparison for LTPP Section 9C	85
Figure 49: Differences in Measured vs. Predicted Temperature in Asphalt Concrete Surface Layer	87
Figure 50: Moisture Content Comparisons for LTPP Section 5E	88
Figure 51: Moisture Content Comparisons for LTPP Section 9C	88
Figure 52: Correlation Analysis Results for Asphalt Concrete Temperature	90
Figure 53: Correlation Analysis Results for Moisture Content (MC).....	91
Figure 54: Different Streams for the Implementation of NJ Specific Models	93
Figure 55a: ODCF for North Region (Sensors 1 to 4)	95
Figure 55b: ODCF for North Region (Sensors 5 to 8)	95
Figure 55c: ODCF for South Region (Sensors 1 to 4).....	96
Figure 55d: ODCF for South Region (Sensors 5 to 8).....	96
Figure 56: Sample Implementation of Temperature Correction Factors.....	99
Figure 57a: Seasonal Correction Factors for Deflection (North Thin Region)	100
Figure 57b: Seasonal Correction Factors for Deflection (North Thick Region).....	100
Figure 58a: Seasonal Correction Factors for M_r - (North Region)	103
Figure 58b: Seasonal Correction Factors for E_p - (North Region)	103
Figure 59a: Seasonal Correction Factors for M_r - (South Region).....	104
Figure 59b: Seasonal Correction Factors for E_p - (South Region).....	104
Figure 60a: Deflection ESCF for North/Thin Region	107
Figure 60b: Deflection ESCF for North/Thick Region	107
Figure 60c: Deflection ESCF for South/Thin Region	108
Figure 60d: Deflection ESCF for South/Thick Region	108
Figure 61a: ESCF for Layer Moduli M_r for North Region	110
Figure 61b: ESCF for Layer Moduli M_r for South Region	110
Figure 61c: ESCF for Layer Moduli E_p for North Region	111
Figure 61d: ESCF for Layer Moduli E^p for South Region	111
Figure 62a: Typical Asphalt Modulus Variation Obtained through SASW Analysis with Date for Test Section No. 3	113
Figure 62b: Typical Asphalt Modulus Variation Obtained through SASW Analysis with Temperature for Test Section No. 3	113
Figure 63: SPATCF Values for Asphalt Modulus and Results of Regression Analysis	114
Figure 64a: Typical Asphalt Modulus Variation Obtained through SASW Analysis with Date - Test Section No. 5	115

LIST OF FIGURES (continued)

	Page
Figure 64b: Typical Asphalt Modulus Variation Obtained through SASW Analysis with Date - Test Section No. 6	115
Figure 65a: Typical Asphalt Modulus Variation Obtained through USW Analysis with Date for Test Section No. 3	117
Figure 65b: Typical Asphalt Modulus Variation Obtained through USW Analysis with Temperature for Test Section No. 3	117
Figure 66: SPATCF-USW Values for Asphalt Modulus and Results of Regression Analysis.....	118
Figure 67a: Typical Asphalt Modulus Variation Obtained through USW Analysis with Date - Test Section No. 5	118
Figure 67b: Typical Asphalt Modulus Variation Obtained through USW Analysis with Date - Test Section No. 6	119
Figure 68a: Typical Variation of Composite Modulus with Moisture Content for Flexible Test Sections.....	120
Figure 68b: Typical Variation of Composite Modulus with Moisture Content for Rigid Test Sections.....	121
Figure 69: Historic Data for SPS-5 in New Jersey (SPS 340504) Based on 1993 AASHTO Analysis	122
Figure 70: Example of the Limitations of the 1993 AASHTO Temperature Correction Factors.....	123
Figure 71: Historic Data for SPS-5 in New Jersey (SPS 340504) – E_p	124
Figure 72: Historic Data for SPS-5 in New Jersey (SPS 340501) – E_p	126
Figure 73: Historic Data for SPS-5 in New Jersey (SPS 340502) – E_p	126
Figure 74: Historic Data for SPS-5 in New Jersey (SPS 340507) – M_r	127
Figure 75: Historic Data for SPS-5 in New Jersey (SPS 340559) – E_p	127
Figure 76: Historic Data for SPS-5 in New Jersey (SPS 340559) – M_r	128
Figure 77: Historic Data for SPS-9A in New Jersey (SPS 340902) – E_p	128
Figure 78: Historic Data for SPS-9A in New Jersey (SPS 340962) – E_p	130
Figure 79: Historic Data for SPS-9A in New Jersey (SPS 340961) – E_p	130
Figure 80: Pavement Profile and Location of Probes at S5.....	133
Figure 81: Pavement Profile and Location of Probes at S6.....	134
Figure 82: Gradations of NSOG (S5) and Crushed Aggregate Bases (S6).....	135
Figure 83: Rainfall Distribution at Case Study Sites.....	136
Figure 84: Moisture Content Distribution at Case Study Sites.....	137
Figure 85: Moisture Content in Base Courses on FWD Testing Days.....	139
Figure 86: Rainfall on FWD Testing Days	140
Figure 87: Average 14-Day Rainfall	140
Figure 88: Variation of Base Layer Moisture Content with Average Rainfall for S5.....	141
Figure 89: Variation of Base Layer Moisture Content with Average Rainfall for S6.....	141
Figure 90: Variation of SAI with Base Layer Moisture Content for S5.....	142
Figure 91: Variation of SAI with Base Layer Moisture Content for S6.....	143
Figure 92: Correlation between Base Course Moisture Content and SAI	148
Figure 93: SAI Performance Prediction Model	149
Figure 94: SAI Performance with Low and High Base Course Moisture Contents	150
Figure 95: Case Studies of Pavement Performance for a 40-year Analysis Period	151

LIST OF FIGURES (continued)

	Page
Figure 96: Seismic Pavement Analyzer (SPA).....	154
Figure 97: Overall Correlation of Pavement Modulus	157
Figure 98: Correlation of Pavement Modulus – Thin Pavements	158
Figure 99: Correlation of Pavement Modulus - Thin Pavements	158
Figure 100: Normal Distributions SPA and FWD Pavement Moduli	159
Figure 101: Normal Distributions SPA and FWD – North Thin	160
Figure 102: Normal Distributions SPA and FWD – North Thick	160
Figure 103: Normal Distributions SPA and FWD – South Thin	161
Figure 104: Normal Distributions SPA and FWD – South Thick.....	161
Figure 105: Overall Correlation of Subgrade Modulus	162
Figure 106: Correlation of Subgrade Modulus – Thin Pavements.....	163
Figure 107: Correlation of Subgrade Modulus – Thick Pavements	163
Figure 108: Normal Distributions SPA and FWD – North Thin	164
Figure 109: Normal Distributions SPA and FWD – North Thick	165
Figure 110: Normal Distributions SPA and FWD – South Thin	165
Figure 111: Normal Distributions SPA and FWD – South Thick.....	166
Figure 112: Overall Correlation of AC Modulus.....	167
Figure 113: Correlation of AC Modulus – Thin Pavements	167
Figure 114: Correlation of AC Modulus – Thick Pavements.....	168
Figure 115: Normal Distributions SPA and FWD Pavement Moduli	169
Figure 116: Correlation of Subgrade Modulus for Rigid Pavements	171
Figure 117: Correlation of Pavement Modulus and Composite Modulus	172
Figure 118: Correlation of Pavement Modulus and Composite Modulus – Thin Pavements.....	173
Figure 119: Correlation of Pavement Modulus and Composite Modulus – Thick Pavements	173
Figure 120: Correlation of PCC Modulus – Thick Pavements	175
Figure 121: Base Moisture Content (M/C) and Rainfall Over an 8-hour Period.....	176
Figure 122: Slope of the Base M/C and Rainfall Trends Over an 8-hour Period	177
Figure 123: Change in Slope with Time Over an 8-hour Period	177
Figure 124: Subbase Moisture Content and Rainfall Over an 8-hour Period.....	178
Figure 125: Slope of the Subbase M/C and Rainfall Trends Over an 8-hour Period	178
Figure 126: Change in Slope with Time Over an 8-hour Period	179
Figure 127: Subgrade Moisture Content and Rainfall Over an 8-hour Period	179
Figure 128: Slope of the Subgrade M/C and Rainfall Trends Over an 8-hour Period.....	180
Figure 129: Change in Slope with Time Over an 8-hour Period	180
Figure 130: Sensor Locations in Pavement Structure	181
Figure 131: Frost Penetration Graph for New Jersey Seasonal Site S5l	185
Figure 132: Cumulative Degree-Day Plot for Section S1 in New Jersey	186
Figure 133: Freezing Index and Frost Penetration Curve (57)	187
Figure 134: Empirical and Measured Frost Depth Correlation	188
Figure 135: Sigmoidal Model and Empirical Frost Penetration Curves	189

LIST OF TABLES

	Page
Table 1: Test Section Requirements for the Seasonal Adjustment Study	29
Table 2: Test Section Requirements for the Seasonal Adjustment and Temperature Correction Studies	30
Table 3: Pavement Structure of the SPS-5 and SPS-9A Test Sections	34
Table 4: Selected Non-LTPP Test Sections	35
Table 5: Pavement Layers of the Selected Test Sections	36
Table 6: Instrumentation Class	42
Table 7: Equipment Installed	45
Table 8: HWD Sensor Spacing	52
Table 9: Target Loads for FWD Testing	52
Table 10: SPA Sensor Distance from Impact Sources	54
Table 11: Sample Preliminary Analysis Results (NJ Site 4)	61
Table 12: Main Effects ANOVA Results for (ΔD_1 , ΔD_7 , $\Delta\{D_1-D_7\}$, ΔM_r and ΔE_p)	70
Table 13: Δ Deflection Regression Coefficients for Different Classes	73
Table 14: CF Regression Coefficients for Different Classes	75
Table 15: Temperature (in °C) Data Comparison for AC layers at LTPP Sites 5E and 9C	86
Table 16: Moisture Content (%) Data Comparison at LTPP Sites 5E and 9C	89
Table 17: Overall Layer Moduli Correction Factors (OLCF)	94
Table 18a: Deflection and Layer Moduli Regression Coefficients for North Region	98
Table 18b: Deflection and Layer Moduli Regression Coefficients for South Region	98
Table 19: Summary of Correction Factors	101
Table 20a: Regression Coefficients for Different Parameters for North Region	106
Table 20b: Regression Coefficients for Different Parameters for South Region	106
Table 21: Results of Implementing the New Jersey Models on SPS-5 and SPS-9A	125
Table 22: Statistical Analysis Results of Rainfall at Sites S-5 and S-6	137
Table 23: Statistical Analysis Results of Rainfall at Sites S-5 and S-6	138
Table 24: Designation of FWD Test Days	139
Table 25: Results of Hypotheses Test on SAI for S5 and S6	143
Table 26: Details of the Instrumented Flexible Pavement Sections	146
Table 27: Max. and Min. Moisture Contents for Instrumented Test Sections at Different Pavement Depths	147
Table 28: Sample LCCA Analysis for Case 1 - High Moisture Content	152
Table 29: Results of LCCA Analysis	152
Table 30: SPA and FWD Comparison Parameters	155
Table 31: Average FWD and SPA Pavement Moduli	157
Table 32: Averages and Standard Deviation of Pavement Modulus (E_p) for SPA and FWD	159
Table 33: Average FWD and SPA Subgrade Moduli	162
Table 34: Averages and Standard Deviation of Subgrade Moduli (M_r) for SPA and FWD	164
Table 35: Average FWD and SPA Subgrade Moduli	166
Table 36: Averages and Standard Deviation of AC Moduli (EAC) for SPA and FWD	168
Table 37: Average Subgrade Moduli in ksi for Rigid Sections	169
Table 38: Monthly Averages for Modulus of Subgrade Reaction	170
Table 39: Average FWD and SPA Pavement Moduli	171

LIST OF TABLES (continued)

	Page
Table 40: Average Subgrade Moduli for Rigid Sections	174
Table 41: Average FWD and SPA PCC Modulus.....	174
Table 42: Frost Penetration Depths Based on Empirical Curve	187
Table 43: Comparison of Empirical and Measured Data for Flexible Sections.....	188

LIST OF ABBREVIATIONS

AASHTO	American Association of State Highway and Transportation Officials
AC	Asphalt Concrete
ADR	Average Daily Rainfall
ANOVA	Analysis of Variance
CAIT	Center for Advanced Infrastructure & Transportation
CF	Correction Factors
DOE	Design of Experiment
E_{AC}	Asphalt Concrete Stiffness
EGB	Granular Base
EICM	Enhanced Integrated Climatic Model
E_p	Pavement Modulus
ESCF	Enhanced Seasonal Correction Factors
E_{SG}	Subgrade Stiffness
FDOT	Florida Department of Transportation
FHWA	Federal Highway Administration
FWD	Falling Weight Deflectometer
GPS	General Pavement Study
GWT	Ground Water Table
HMA	Hot Mix Asphalt
HWD	Heavy Weight Deflectometer
ICM	Integrated Climatic Model
IE	Impact Echo
IR	Impulse Response
LCCA	Life Cycle Cost Analysis
LTPP	Long Term Pavement Performance
MCF	Moisture Correction Factors
M-E	Mechanistic-Empirical
MN/ROAD	Minnesota Research Project
M_R	Subgrade Modulus
NDT	Non-Destructive Testing
NHS	National Highway Network
NJDOT	New Jersey Department of Transportation
NSOG	Non-Stabilized Open Graded
OCF	Overall Correction Factors
ODCF	Development of Overall Layer Deflection Correction Factors
OGDL	Open Graded Drainage Layers
OLCF	Overall Layer Deflection Correction Factors
PCC	Portland Cement Concrete
PWC	Present Worth Cost
QC/QA	Quality Control/Quality Assurance
RAPL	Rutgers' Geotechnical and Asphalt Pavement Laboratories
SAI	Structural Adequacy Indices
SASW	Spectral Analysis of Surface Waves
SCF	Seasonal Correction Factors
SHRP	Strategic Highway Research Program
SMP	Seasonal Monitoring Program
SPA	Seismic Pavement Analyzer
SPS	Specific Pavement Studies
TCF	Temperature Correction Factors
TDR	Time Domain Reflectometry
TXDOT	Texas Department of Transportation
USW	Ultrasonic Surface Waves

EXECUTIVE SUMMARY

Pavement design and performance are highly influenced by environmental factors, such as temperature and moisture. Since temperature and moisture conditions vary with time (daily, seasonal, and longer cycles), adjustment models are required to account for these variations and to bring pavement response parameters measured at different periods to the same standard conditions. A study funded by the New Jersey Department of Transportation (NJDOT) and the Federal Highway Administration (FHWA) was undertaken to develop temperature and seasonal adjustment models to suit New Jersey conditions. These models will be used in network- and project-level pavement evaluation, analysis, and design.

Twenty-four test sections (21 hot-mix asphalt (HMA), 1 composite and 2 Portland Cement Concrete [PCC]) were instrumented to continuously measure environmental and climatic parameters. Deflection and seismic testing was performed on a monthly basis (and bi-monthly during the recovery periods) for two years. In addition, two 24-hour testing cycles, in which tests were repeated every 2 hours for a 24-hour period, were performed on selected sections.

A comprehensive analysis was performed on the collected Falling Weight Deflectometer (FWD) and environmental data from 21 flexible pavement test sites to investigate the impact of the environmental parameters on pavement response. As expected, results of the Analysis Of Variance (ANOVA) performed on the pavement parameters (deflections and backcalculated moduli) and environmental parameters (base course moisture content, average Asphalt Concrete (AC), temperature, ground water table (GWT), rainfall, and air temperature) indicated that all main environmental parameters have a significant impact on the Effective Pavement Modulus (E_p) and Subgrade Modulus (M_r), with the exception of GWT and pavement temperatures, which do not have significant impact on the subgrade modulus. This finding does not agree with the common assumption made in backcalculation analysis that GWT acts as a rigid layer.

Temperature and moisture data from the Seasonal Monitoring Program testing at two locations within Long-Term Pavement Performance (LTPP) test sites were analyzed to evaluate the Enhanced Integrated Climatic Model (EICM) for its applicability to New Jersey conditions. A wide discrepancy was observed between predicted and measured temperature and moisture contents, and no reasonable correlation was found. Because of the inconsistent model output results, it was concluded that EICM in its present form could not be utilized to account for seasonal adjustment on pavement sections within New Jersey. New models were therefore developed specific to New Jersey conditions.

A regression analysis was performed to develop Temperature Correction Factors (TCFs) that account for the impact of temperature changes on measured deflections and backcalculated layer moduli. Overall Correction Factors (OCFs) that account for all seasonal variations were also developed. In addition, Seasonal Correction Factors (SCFs) that account for seasonal variations other than temperature, which should be applied on the temperature-corrected deflections and the resulting backcalculated moduli, were developed.

As part of a validation and verification process, one composite section was used to validate the models developed for the flexible pavement sections. Another of the validation steps was the use of historic FWD data for New Jersey's LTPP- Specific Pavement Study (SPS) sections (17 test sections in total). A comparison was made between the trends obtained when the data was corrected using the current American Association of State Highway and Transportation Officials (AASHTO) temperature correction model and those obtained when NJDOT temperature and

seasonal models were used. The trends obtained for most sections (13 out of 17) had an unrealistic result when the AASHTO temperature correction model was used, i.e. pavements were shown to improve with time. However, for 11 of those 13 sections that had previously showed an improvement with time, the trends were shown to degenerate with time when the NJDOT temperature and seasonal models were used.

Comparative analysis was performed on the data from the two rigid pavement sections to evaluate two types of base course layers used under rigid pavements in terms of their drainage characteristics and corresponding effects on pavement response. One of the base layers was a Non-Stabilized Open Graded (NSOG) material that promotes positive drainage. The second layer was a typical granular soil aggregate material. Assessment was carried out by monitoring rainfall and moisture contents through instrumentation and deflections. Results of the analysis indicated that for similar trends in rainfall, the site having the more permeable NSOG base material drains better in terms of reduced moisture content levels as compared to the typical soil aggregate base material. Statistical analysis was carried out to confirm the conclusion. Analysis and comparison of the Structural Adequacy Indices (SAI) indicate that the permeable base section NSOG does not significantly change the structural condition as compared to the granular soil aggregate base.

Results from testing with the Seismic Pavement Analyzer (SPA) provided a strong correlation between the AC temperature and modulus from both spectral analysis of surface waves (SASW) and ultrasonic surface wave (USW) tests. Small differences are observed in this relationship for pavements of different thicknesses and in different geographical regions. While there was a clear general trend of decrease of the subgrade modulus with moisture content (from the impulse response (IR) test), the data dispersion was high.

One of the study objectives was to compare the results of the FWD and SPA analyses and perform a correlation analysis between the two non-destructive pavement response testing devices. Results provide different levels of linear correlation between pavement parameters backcalculated from both non-destructive devices (from good correlations for AC modulus of thin pavements to poor correlations for subgrade modulus of rigid pavements). The uncorrected FWD pavement moduli showed a greater variability due to seasonal changes compared to those from the SPA.

A comprehensive analysis was also performed on the environmental data to investigate the correlation between different environmental parameters and to develop some statistical models. Statistical models were developed to correlate air and surface temperatures, air and mid-depth temperatures, and surface and mid-depth temperatures.

In summary, this study comprehensively addressed the influence and seasonal fluctuation of environmental factors on long-term pavement performance in New Jersey.

INTRODUCTION

Pavement is one of the essential and key elements of the transportation infrastructure system. Each year billions of dollars are spent on the maintenance and rehabilitation of pavements to keep them functional. This great annual investment has urged many transportation agencies to monitor factors that affect a pavement's performance and to correlate them with a pavement's behavior throughout its service life. The advantage of tracking such factors is that their effect at early stages of design can be accounted for; and pavement life cycle performance can be accordingly improved.

Among the essential factors that influence pavement material properties and performance are environmental effects. In particular, the seasonal variation of pavement material properties has been shown to highly affect pavement performance. The fact that the long-term performance of a pavement structure is strongly dependent on the subgrade soil and the pavement layer properties makes changes in these soil and layer properties a great concern. This is particularly true in areas experiencing seasonal fluctuation in environmental parameters. Therefore, there is a need to correctly address such climatic factors and analytically correlate their effects to pavement stiffness.

The climatic changes from region to region, coupled with the variation of site specific conditions across North America, make it difficult to develop standard models for all regions. Therefore, the development of regional models becomes an essential requirement in the design procedure for most transportation departments. The ability to predict regional environmental effects, and to incorporate seasonal variability of pavement material into current design pavement procedures will greatly enhance pavement performance and reduce maintenance expenditures.

Several environmental parameters are reported to highly affect pavement strength, and accordingly, pavement behavior and performance. The main parameters of great concern are moisture content, ground water table, freeze/thaw, and temperature.

In early 2001, the New Jersey Department of Transportation (NJDOT) in association with the Federal Highway Administration (FHWA) initiated a study to evaluate and calibrate some of the available seasonal and temperature adjustment models, or to develop new models, to suit New Jersey conditions. These models will be used to account for the impact of the temperature and seasonal variations on the deflections measured using FWD.

The document is comprised of the Main Report Body and Appendices A and B; and is structured as follows:

Main Report Body

- Executive Summary
- Introduction
- Objectives and Scope of Study
- Literature Search and Review
- Test Section Requirements and Selection
- Field Testing Program
- Data Processing and Preliminary Analysis
- Statistical Analysis
- EICM Model Evaluation
- Empirical Seasonal and Temperature Models
- Validation of New Jersey Temperature and Seasonal Models on New Jersey LTPP Data

Evaluation of Non-Stabilized Open Graded (NSOG) Base Layers
Effect of Subsurface Drainage on Flexible Pavement Life Cycle Cost
FWD vs. SPA Correlation Analysis
Environmental Analysis
Project Conclusions and Recommendations for Further Studies
References

Appendices

Appendix A: Sample Instrumentation Plan
Appendix B: Results of Sensitivity Analysis for Regression Models

OBJECTIVES AND SCOPE OF STUDY

Study Objectives

The main objective of this study is to provide NJDOT with seasonal and temperature adjustment models, based on New Jersey conditions, that can be used to consider the daily and seasonal variations in the stiffness of pavement materials. These models will be used in the network- and project-level FWD analyses, and will be ultimately incorporated into NJDOT's pavement design procedures.

This objective will be achieved by evaluating some of the available models, such as the EICM, which is incorporated in the new Mechanistic-Empirical Pavement Design Guide. If they are found to be suitable, these models will be calibrated and validated with field-measured data. If the models are not found to be suitable, new models will be developed. In addition to this objective, other objectives include:

- Evaluating the performance of NSOG base layers for rigid pavements under different moisture and temperature conditions.
- Comparing the results of the FWD and the SPA analyses and performing a correlation analysis between them.
- Investigate the impact of the pavement structure; thin vs. thick, and environmental parameters, e.g., temperature, and moisture, on measured deflections.
- Studying the response of pavement structures with different thickness and material properties under different environmental conditions.

Scope of Study

To enable the project objectives to be efficiently achieved, the scope of project was divided into two main components (studies): the Seasonal Adjustment Study and the Temperature Correction Study.

LITERATURE SEARCH & REVIEW

Environmental Impact on Pavements

Several environmental parameters are reported to highly affect pavement strength and therefore pavement behavior and performance. The main parameters of concern are moisture content, GWT, freeze/thaw, and temperature, as illustrated in Figure 1. These parameters can be classified into two main categories: seasonal parameters and temperature.

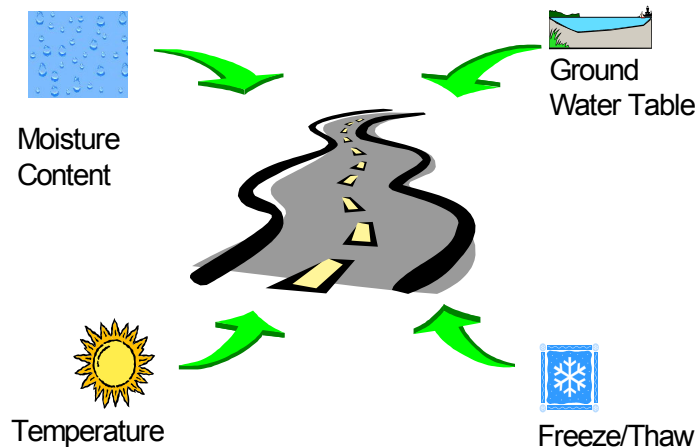


Figure 1: Environmental Factors Affecting Pavement

These parameters receive great consideration in current pavement design procedures and research development. To demonstrate the significance of these parameters, the following sections review their impact on pavements and the ways in which the parameters are addressed in current design procedures and research development.

Impact of Seasonal Parameters

The seasonal variation in weather throughout the year plays an important role in changing the properties of pavement materials, which in turn affects the stiffness and strength of pavements and response of the pavement to traffic loads. Seasonal variation in weather has an impact on pavement through changes in moisture content, GWT, and the freeze/thaw periods during the year. The following sections show in more detail the impact of these parameters on pavement.

Moisture Content

Moisture content has a significant impact on the moduli of subgrades and unbound layers. A dramatic increase in water content will reduce the strength of the unbound materials and roadbed soils, and will also reduce the modulus stiffness values of pavement layers. Such reduction will shorten pavement service life and significantly increase maintenance costs.

Several studies have been conducted to establish a trend between moisture content and pavement strength.^(1,2,3) Ovik et al. carried out a study to investigate the relationship between climatic factors (including moisture content), surface and subsurface condition, and pavement material properties.⁽⁴⁾ The study confirmed that layer moduli vary with the state of moisture in

the pavement. It was shown that fluctuations in the stiffness of base and subgrade layers are related to the seasonal distribution of unfrozen volumetric moisture content in the layers.

Ground Water Table

For pavement sites with a higher ground water table, water content becomes a great concern. The existence of a ground water table close to the depth of the roadway layers plays an important role in increasing the moisture content of the granular material, causing a reduction in pavement strength.

To investigate the effect of GWT, Ksaibati et al. recently performed a study on several Florida State roads to evaluate the decrease in the stiffness of the base and subgrade layers due to the proximity of the water table.⁽³⁾ The main objectives of this study were to correlate the depth of the water table to the backcalculated pavement modulus values and to study the effect of high water table on the increase in moisture contents of the base course and subgrade. These objectives were accomplished by evaluating five test sections in the State of Florida using the Dynaflect and FWD. The testing was performed at different times of the year and the water table fluctuations were recorded throughout the duration of the study. The selected test sections were all in-service primary travel routes that were constructed using approved Florida Department of Transportation (FDOT) materials. All test sections included in this experiment were flexible pavements.

In order to accurately determine the changes in water table levels during the study, 2 inch water pipes with well points were drilled 10 ft deep at each project site. Each time Dynaflect or FWD tests were performed, one of the necessary recordings was the water table level. All measurements were obtained from the pavement surface to the water table. This allowed the correlation between the change in water table, moisture content, and layer modulus values to be established.

The study showed that higher water tables result in high base course and subgrade moisture contents. Both Dynaflect and FWD recordings showed that the water table had a significant impact on the structural strength of the base and subgrade materials. It should be noted that there were differences in the percentage increase in moisture content among different test sites. The study showed a high correlation between ground water table and moisture content.

It was concluded that as the depth from the pavement surface to water table level decreases, there are significant increases in the moisture contents of the base course and the subgrade. FWD testing resulted in magnifying the effect of moisture on backcalculated modulus values of base course and subgrades. The modulus values of one of the test sites experienced up to 96 percent reduction due to moisture increases.

Freeze/Thaw Phenomenon

In seasonal frost areas, pavements experience freeze-thaw cycles that expose the pavement structure to significant moisture and temperature changes. These changes expose the pavement to environmental fatigue in addition to the permanent fatigue caused by traveling vehicles.

In an attempt to investigate this phenomenon, Hanek et al 2000 observed the relationship between moisture content and backcalculated pavement layer moduli, focusing on the Spring thaw period in Montana.⁽¹⁾ It was reported that when thawing began in early March, moisture sensors recorded a large, sharp increase in moisture content to levels well above those

observed immediately prior to freezing. As thawing progressed, an equally rapid sequential decrease in moisture content was observed until a few days following complete thawing. At this point, the slope of the moisture content recovery curve significantly flattened. Concurrently, as thawing began in early March, an apparent decrease in subgrade modulus occurred until it reached its lowest value at a thaw depth of 18 in. It then began to recover as thawing depth increased, until thawing was complete. It should be noted that at other sites, the recovery started at deeper thawing depths. The maximum frost depths below the asphalt were about 43 in and 63 in.

Janoo et al. noticed the same behavior for the base and subbase moisture content during the thawing period.⁽²⁾ The study was also carried out in the State of Montana, and included 10 flexible pavement test sections. The study came to an interesting conclusion – that even though thawing officially started when the temperature reached 32°F on March 30, moisture content records showed that thaw weakening actually started earlier, on March 20. This is an interesting observation that suggests that predicting the start of thaw weakening for both base and subgrade based on base temperature might be misleading.

Impact of Temperature

In flexible pavements, the surface deflection and layer moduli are significantly affected by the temperature of asphalt concrete because the stiffness of the asphalt concrete layers dramatically influences the structural capacity of flexible pavement. As the temperature of asphalt increases, its stiffness decreases, leaving it less able to withstand wheel load. A decrease in asphalt concrete stiffness results in higher stress being transmitted to the base and subgrade. Therefore, it is important to correctly predict pavement temperature and consider it during the design stage, as well as in the evaluation of existing pavements, to ensure more cost-effective flexible pavements. In previous studies, several attempts have been made to develop temperature correction models and reference the temperature to a standard one. The need for such temperature correction models is essential because FWD measurements are always performed at different temperatures.^(5,6,7)

Chen et al. carried out a study to investigate the effects of the test location, structure, level of load, and the influence of cracks on temperature correction factors.⁽⁵⁾ The study highlighted the difference between temperature correction equations developed in the study and those reported in other literature. In this study, FWD tests were repeated at different temperatures and at three different test sites in Texas to develop the temperature correction equations. No traffic load was allowed during the period of repeated FWD testing. Thus, it was reasonable to assume that once FWD deflections were normalized to a specific load, any variation would be due to environmental conditions.

The study reported several response variations in the data collected due to overcast periods during the day. The repeated FWD tests were conducted during times of minimal subsurface moisture variation and no traffic was allowed on any of the test sites. Thus, it can be assumed that these measured response variations were mainly associated with temperature. This would indicate that using the previous 5-day average air temperature to predict pavement temperature may not be accurate when there are rainfalls or overcast conditions.

Though there may be some subsurface moisture variation, Long et al. stated that for flexible pavements, temperature has a much greater effect on FWD deflection than subgrade moisture content.⁽⁶⁾ This study made no attempt to develop or calibrate models that predict mid-depth pavement temperature through air or surface temperatures. Instead, holes were drilled to

collect pavement temperatures during FWD data collection. It was observed that only deflections near the load (sensors 1 and 2) were significantly influenced by pavement temperature while other deflections (sensors 3 to 7) remained almost constant at different temperatures. This same trend was observed at all three sites.

To clearly address the correlation between location and pavement temperature, the effect of pavement structure on temperature correction factors was observed among the 3 different test sites. It was found that temperature did not affect the pavement response on the cracked location as much as on the intact pavement. Temperature correction factors for deflection were observed to differ 1 to 12 percent for intact sites. The average difference was 7 percent. Differences between intact and cracked locations ranged from 2 percent to 30 percent, depending on temperature. The average difference was 15 percent. It was observed that the temperature correction slopes were flatter for the cracked locations, indicating that the cracked locations are less affected by temperature. Since the variation among the intact pavements was less than 10 percent, it was concluded that an equation developed from one structure might perhaps be applied to another structure. However, the equations developed from the intact locations may not be used on cracked locations due to the different temperature-dependent characteristics between intact and cracked locations.

When comparing the deflection correction model initially developed in the present study with the one presented in Kim et al., it was interesting to see that although the two models were developed under different climatic conditions and pavement structures, the temperature correction factors differed, on average, by only 7.9 percent.⁽⁷⁾ The only major difference was observed at temperatures lower than 57°F.

On the other hand, when comparing the modulus temperature correction model developed herein with those from Kim et al. and current Texas Department of Transportation (TXDOT) practice, noticeable variations were found among these three models at temperatures higher than 91°F. Although the equations were developed from two independent studies, there is a close agreement between the current study model and current TXDOT practice model for the temperature range considered. Such comparison showed that there is a close agreement for deflections, but not for moduli.

The study results indicate that the temperature correction factors are not site-structure dependent but are pavement condition (intact or cracked) dependent. It was also concluded that pavements thinner than 3 inches are less affected by temperature changes than the thicker pavements considered in the study.

Existing Models for Seasonal and Temperature Correction

Several models have been developed and are currently available. Some of these models are currently in use in North America and internationally, such as the AASHTO and the Asphalt Institute models, while others were developed through research efforts specifically for certain regions or States. The following sections review some of the existing models and research in this domain.

1993 American Association of State Highway and Transportation Officials (AASHTO) Guide

The 1993 AASHTO Guide is commonly used by most State DOTs.⁽⁸⁾ The AASHTO guide provides standards and guidelines that are mainly used in the design and rehabilitation of flexible, rigid, and composite pavements. The next section highlights how seasonal variation and temperature corrections are addressed in the AASHTO Guide.

AASHTO Seasonal Adjustment Models

The 1993 AASHTO pavement design guide utilizes a non-destructive dynamic deflection testing method, such as FWD testing, as a means of evaluating the *in-situ* structural capacity of existing pavements. As seasonal variation of climate and weather conditions affects the output of deflection testing, seasonal and temperature corrections are needed. Figure 2 shows the deflection of two different sites, each with its own seasonal climate variation. The Rochester, Minnesota, site experienced freeze/thaw conditions that resulted in higher deflection values in March and April. In comparison, the Texas site, which has milder climate, shows a more gradual strength change with peak deflection in late winter.

The AASHTO guide has recognized such seasonal variation effect on pavement design. This variation is addressed in the design as detailed in the following section.

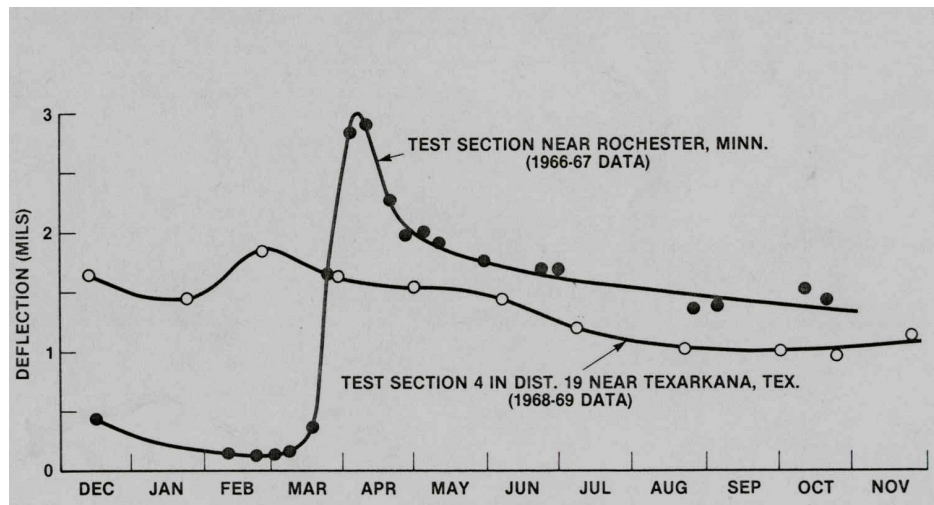


Figure 2: Effect of Site Location on Seasonal Variation of Deflection⁽⁸⁾

Seasonal Variation Models

The seasonal variation in material properties has been addressed in the AASHTO Pavement Design Guide through its effect on the seasonal elastic modulus. The purpose of identifying seasonal modulus is to quantify the relative damage a pavement is subjected to during each season of the year and to treat it as part of the overall design. It is essential at this point to divide the year into equal intervals, representing the seasons the pavement will go through. Two different procedures for determining the seasonal variation of the modulus are suggested as guidelines in the AASHTO guide. One method is to determine a laboratory relationship between resilient modulus and moisture content. Then, with an estimate of the *in-situ* moisture content of the soil beneath the pavement, the resilient modulus for each of the seasons may be estimated. An alternative procedure is to backcalculate the resilient modulus for various seasons using deflection measurements. In both procedures, the mean value is considered to be the seasonal

resilient modulus. For flexible pavements, the seasonal data must be translated into the effective roadbed soil resilient modulus. The first step of this process is to enter the seasonal moduli in their respective time periods as illustrated in Figure 3. Then, the relative damage corresponding to each seasonal modulus is estimated by using the damage function shown in the same figure. The damage values should be added together and then divided by the number of periods used (average damage). The effective roadbed soil resilient modulus, then, is the value corresponding to the average relative damage on the scale. It is obvious that the model introduced in the AASHTO guide for such translation between roadbed resilient modulus and relative change was based on certain site-specific conditions that might not be similar to those of other regions, including the State of New Jersey. In addition, the subgrade modulus at different periods of the year is required. This information is not always available.

The freeze/thaw phenomenon is also addressed in the AASHTO Guide through the damage function shown in Figure 3. Freeze/thaw cycles result in two major effects on pavement: thaw weakening and frost heaving. AASHTO provides guideline procedures for calculating the damage during various seasons of the year as a function of these two factors. The AASHTO guideline shows that the thawing-weakening period can range from a few weeks to a few months, with varying degrees in structural capacity. Even though a well-defined methodology is introduced to calculate the frost penetration depth using the air-freezing index, AASHTO encourages users of the guide to develop their own relationships based on site-specific measurements within their area and compare such experience with both AASHTO and other agencies nationally.

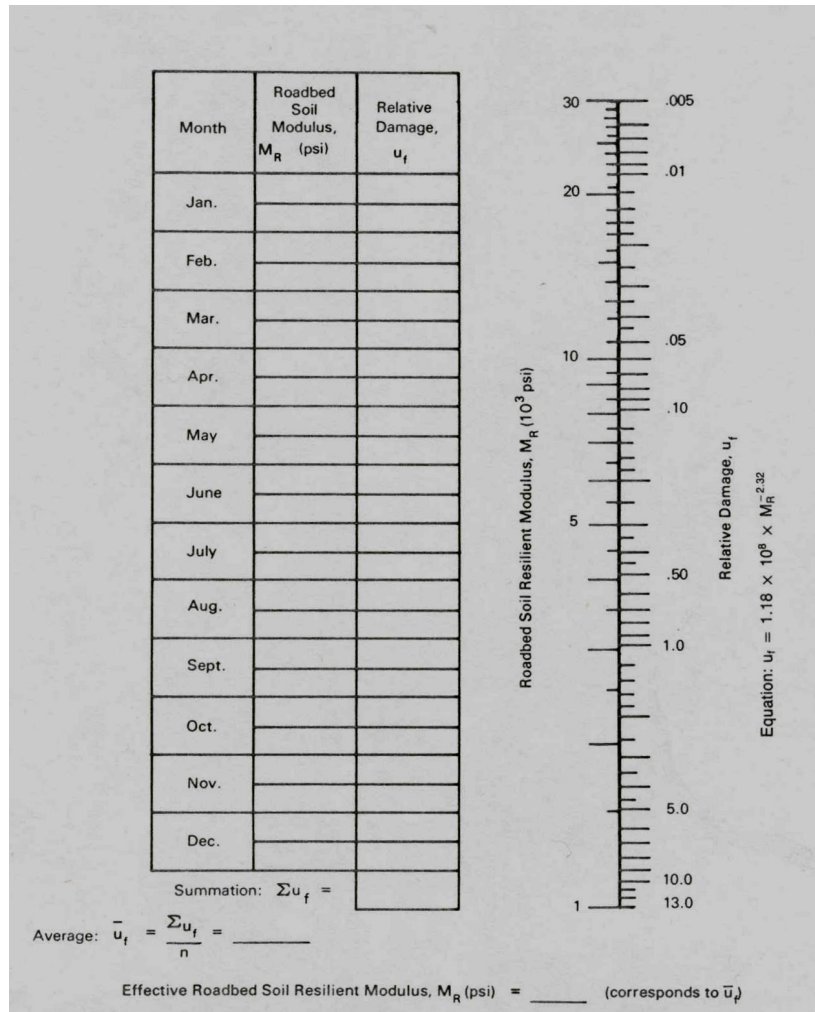


Figure 3: Seasonal Elastic Modulus Calculation for Flexible Pavements⁽⁸⁾

Ground Water Table

For existing pavements, water may enter the pavement due to a higher water table, capillary rise, or adjacent ground water, causing a reduction in the unbound granular materials and roadbed soil strength, as well as pumping and cracking of concrete pavements. The AASHTO guide strongly emphasizes the importance of introducing an effective drainage system to the pavement to provide rapid drainage. However, the effect of existing ground water table was only expressed in terms of the moisture content. Drainage effects were directly considered for flexible pavements in terms of the effect of moisture on roadbed soil and base strength, and for rigid pavements in terms of the effect of moisture on subgrade strength. This might explain why the AASHTO guide strongly recommends undertaking additional site-specific research efforts to accurately document the actual effect of existing water table on pavement life for each region separately.

AASHTO Temperature Correction Model

As detailed in the AASHTO guide, for the purposes of comparison of effective modulus of all pavement layers above the subgrade (E_p) along the length of a project, the deflection measured at the center of the load plate (D_1) should be adjusted to a single reference temperature 20°C to 21°C. Figure 4 shows the adjustment factors for AC pavements with granular or asphalt stabilized base courses, while Figure 5 shows the factors for AC pavements with cement and pozzolanic stabilized base courses. These adjustment factors were calculated based on the average AC mix temperature. The calculation of AC mix average temperature was not an easy task and has been a challenge for numerous projects. AASHTO recommends either directly measuring the AC mix temperature, or estimating it from surface and air temperatures. AASHTO recommends, as a minimum, determining the temperature at top, middle, and bottom of the AC layer and using the average of these temperatures to represent the temperature of the AC layer. These adjustment factors were developed based on data collected from a limited number of sites. The validity of these factors is questionable for pavements located in areas other than those considered. The AASHTO guide recommends that DOTs develop their own temperature factors.

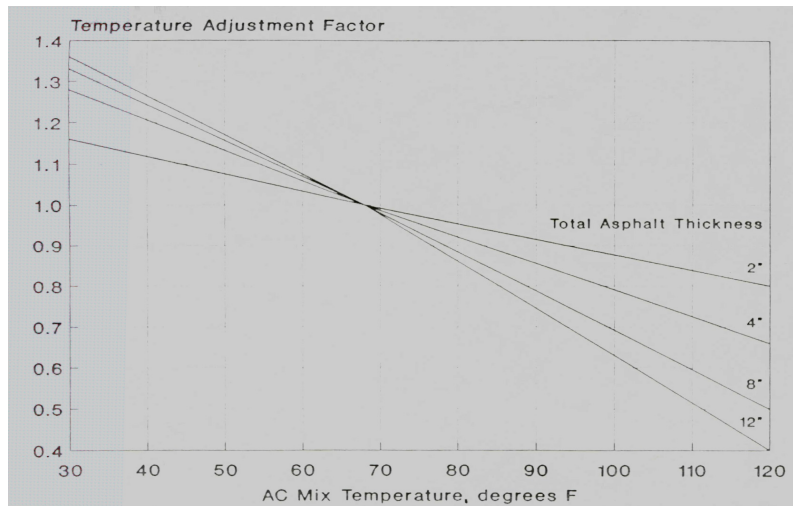


Figure 4: Adjustment Factors for AC Temperature for Granular or Asphalt-Treated Base Pavements⁽⁸⁾

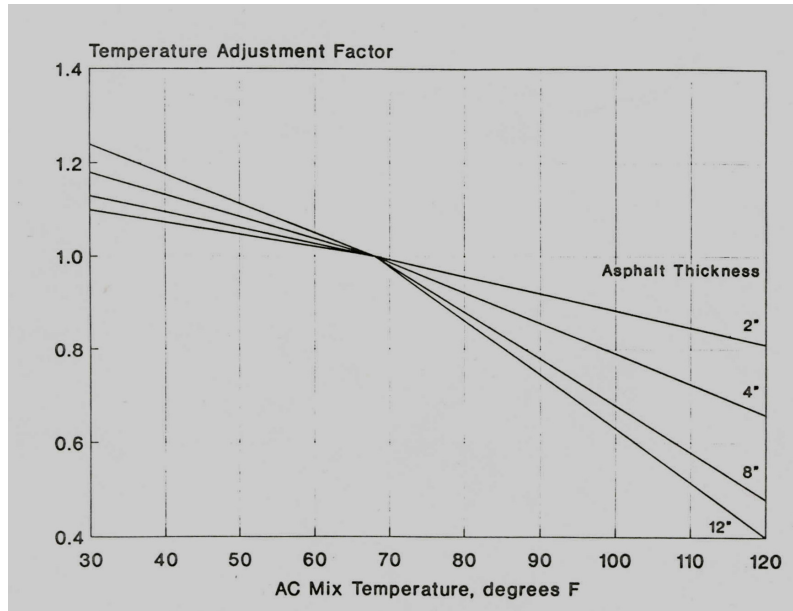


Figure 5: Adjustment Factors for AC Temperature for Cement or Pozzolanic-Treated Base Pavements⁽⁸⁾

Comments on the AASHTO Models

Despite AASHTO's wide recognition among pavement engineers, its capability to produce well-designed and cost-effective pavements has been often questioned in the last decade. The fact that AASHTO specification was implemented based solely on data collected in the State of Illinois makes it obviously difficult to normalize its use for other regions. The conditions under which the AASHTO procedure was developed, including climatic factors, might not be the same for other pavements.

It is obvious from the previous discussion that several gaps in the AASHTO guideline were left open. In many cases, AASHTO indicated that the model introduced for seasonal effect might be used only as a guideline. However, DOTs were encouraged to develop their own models and incorporate their own site-specific conditions.

A recent research effort that addressed the suitability of AASHTO models for New Jersey conditions, was conducted in 1998. In this study, a network-level FWD testing program was performed on a selected subset of the National Highway Network (NHS) highways in New Jersey.⁽⁹⁾ The objective of the study was to analyze deflection data in order to identify the limits of structurally homogeneous sections (sectioning), assess the pavement structural capacity, and predict the future rehabilitation needs. As part of this study, a sensitivity analysis was carried out to investigate the effect of climatic input parameters on the study results. AASHTO guidelines were used to predict the results of the sensitivity analysis process. Therefore, the conclusions from this study would give an indication of whether the AASHTO models might be suitable to New Jersey conditions.

In this study, three main seasonal adjustment factors were considered: effect of the assumed relative subgrade modulus (relative index); effect of locating a section in the wrong climatic zone; and effect of the assumed weather pattern. The weather data was gathered from 26

weather stations scattered over New Jersey. The study suggested that New Jersey had two Climatic Regions, CI (north) and CII (south and coastal).

For the effect of relative index, 8 different scenarios for the above three adjustment factors were tested. The sensitivity results showed that a maximum difference of 0.1 in overlay thickness for the two regions was observed. Then, the effect of climatic region was tested for two cases: assuming that all sections were located in Regions CI, and assuming that all sections were located in Region CII. The sensitivity results showed that the difference in the required overlay thickness ranged from 0.3 in to 0.4 in.

Finally, for the effect of weather pattern, the weather pattern suggested in the 1993 AASHTO guide was assumed for the two New Jersey climatic regions and used in the analysis. This weather pattern consists of 5 periods in which subgrades experience significantly different moisture conditions and stiffness. Another weather pattern was assumed to evaluate the effect of weather pattern on the final results. This weather pattern has four periods only. The comparison between the subgrade moduli adjusted using the main and alternative weather patterns showed that the difference in the required overlay thickness is in the range of 0.6 in to 0.9 in, depending on the traffic level. Due to the limited weather data available from weather stations (temperature and precipitation), the study suggested that the AASHTO main weather pattern could be used to represent New Jersey's weather pattern. However, the weather data does not always accurately represent the subgrade condition. Therefore, the study recommended studying this issue in more detail and calibrating the AASHTO seasonal adjustment models, or developing new models, based on New Jersey conditions.

The above study showed that the combined effect of these three factors could exceed a 1.5 in difference in the required overlay thickness resulting in overestimation in design by 1.5 in. The difference in the estimated rehabilitation cost due to the effect of seasonal adjustment factors (1.5 in AC) is in the range of \$15 million. Another interesting finding of the study is that the seasonal adjustment factors could change the type of rehabilitation activities. For example, based on the AASHTO weather pattern, overlays might be candidate treatments for a section. However, if the actual weather pattern of New Jersey is different than the one used in the analysis, then the actual adjusted subgrade modulus for the same section might be less than the minimum modulus. Therefore, full reconstruction would be required for the section, or vice versa. It was obvious from this study that the environmental factors in New Jersey might highly affect the outcomes of the design and/or reconstruction procedure and it is essential, therefore, to accurately predict their effect.

Strategic Highway Research Program (SHRP) - Long Term Pavement Performance (LTPP)

SHRP is another well-known research program, which is currently in progress across North America. As part of SHRP, the results of analyses performed on data collected under the LTPP program is intended to improve the pavement performance and increase pavement service life.

In 2000, Lukanen et al. carried out a study to investigate the effects of temperature on asphalt pavement deflections using the data collected under the Seasonal Monitoring Program (SMP) of the LTPP program.⁽¹⁰⁾ The objectives of this study were to develop a model that could be used to predict the temperature within an asphalt layer from surface temperature data collected during routine deflection testing and to develop relationships between asphalt temperature, pavement deflections, and backcalculated asphalt modulus.

A series of improvements were introduced in this study to the well-known BELLS equation in an attempt to develop an enhanced temperature prediction model within asphalt pavement.⁽¹¹⁾ The original BELLS model predicts mid-depth asphalt layer temperature using the asphalt layer thickness, 5-day mean air temperature, infrared surface temperature reading, and time of day. It was found that due to faulty infrared surface temperature probes used during data collection, the original BELLS equation is only valid for a temperature range of 59°F–77°F (15°C–25°C). It over-predicts the asphalt temperature at lower temperatures and under-predicts it at higher temperatures.

Therefore, a second model, BELLS2, was developed using corrected infrared surface temperature data and an expanded database. In this model, the average of the previous day's high and low air temperatures was used instead of the 5-day mean air temperature, thus reducing the amount of data required to make use of the model.

When the data used to develop BELLS2 was further investigated, it was found that, as per LTPP data collection protocol, the pavement surface was shaded for an average of six minutes prior to temperature sampling. Thus, the BELLS2 equation was developed based on a biased data. Therefore, a third model, BELLS3, was developed for use during routine FWD testing when the pavement surface is typically shaded for less than a minute.

$$T_d = 0.95 + 0.892T_s + (\log d) - 1.25 \left[1.83 \sin A \left(\frac{2\pi}{18} \right) - 0.448T_s + 0.621T_{avg} \right] + 0.042T_s \sin B \left(\frac{2\pi}{18} \right) \quad (\text{E1})$$

where:

- T_d = Pavement temperature at layer mid-depth, °C
- T_s = Infrared surface temperature, °C
- T_{avg} = Average of high and low air temperature the day before testing, °C
- d = Layer mid-depth, mm

and A and B are computed as follows:

$$A = \begin{cases} t_d + 9.5 & \text{if } 0 \leq t_d < 3 \\ -4.5 & \text{if } 5 \leq t_d < 11 \\ t_d - 15.5 & \text{if } 11 \leq t_d < 24 \end{cases}$$

$$B = \begin{cases} t_d + 9.5 & \text{if } 0 \leq t_d < 3 \\ -4.5 & \text{if } 3 \leq t_d < 9 \\ t_d - 13.5 & \text{if } 9 \leq t_d < 24 \end{cases}$$

A semi-logarithmic format equation relating the asphalt modulus to the mid-depth asphalt temperature was developed to allow for a simple means of adjusting the backcalculated asphalt modulus for the effects of temperature. The approach is to calculate a modulus temperature adjustment factor using the following equation:

$$ATAF = 10^{\text{Slope} * (T_r - T_m)} \quad (\text{E2})$$

Where:

$ATAF$ = Asphalt temperature adjustment factor

slope = Slope of the log modulus versus temperature equation

(-0.0195 for the wheel path and -0.021 for mid-lane are recommended)

T_r = Reference mid-depth hot-mix asphalt (HMA) temperature

T_m = Mid-depth HMA temperature at time of measurement

Even though the BELLS3 has introduced some improvements to the original BELLS model, it has some limitations that might hinder its normalization. The BELLS models are based on daytime surface temperature data collected at above freezing temperatures, so their use during nighttime hours and at below freezing temperatures may be problematic. Also, these equations should only be used for asphalt thickness of 1.75-12 in, which is the range contained in the LTPP database.

Another study was performed in 1993 to correlate temperature to FWD deflection.⁽¹²⁾ In this study, a procedure was developed to implement a temperature correction procedure that would normalize measured maximum deflections to a standard temperature. This procedure was based on a multi-layer analysis so that the properties of each layer within the pavement structure were considered. Typical temperature correction curves were developed in this study for flexible pavement with weak subgrade support (having an elastic modulus of 10 ksi or less), flexible pavements with strong subgrade support, and similarly for composite pavement. However, this procedure has the limitation of ignoring the material properties of the asphalt concrete mix.

Asphalt Institute

Another widely used pavement design procedure is the Asphalt Overlays for Highway and Street Rehabilitation.⁽¹³⁾ For the deflection measurements, the guide considers two environmental adjustment factors: temperature adjustment factor and critical adjustment factor (seasonal adjustment factor).

Within the context of this procedure, the deflection is calculated based on the following equation:

$$RRD = (\bar{x} + 2s)c \tag{E3}$$

Where:

- | | | | |
|-----------|---|--|--------------------------|
| RRD | = | the representative rebound deflection | |
| \bar{x} | = | the arithmetic mean of the individual values that have been adjusted for temperature = | $\frac{\sum X_i f_i}{n}$ |
| s | = | standard deviation | |
| f_i | = | temperature adjustment factor of individual deflections | |
| c | = | critical period adjustment factor | |
| x_i | = | individual deflection values | |
| n | = | number of individual deflection test values | |

For the temperature adjustment factor, the guide provides a model for determining temperature adjustment factors for various thicknesses of dense-graded aggregate base using the mean pavement temperature for 3-layered asphalt concrete pavement similar to the one in AASHTO, as shown in Figure 6. The validation of this model is questionable due to its limitation to certain types of base material and pavement layer structure.

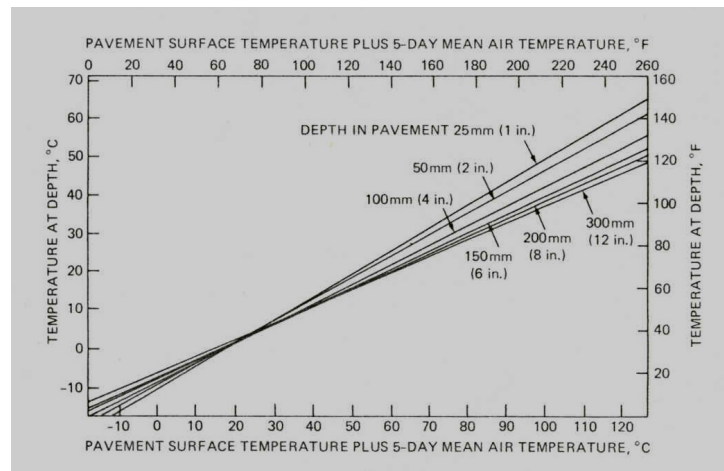


Figure 6: Adjustment Factors for Deflections for 3-layered AC Pavements⁽¹³⁾

The Asphalt Institute Guide also developed a prediction model to accurately estimate the AC temperature at various depths, as shown in Figure 7. This model was based on having the sum of surface temperature and average air temperature for five days prior to testing day as an input to the model. Even though this approach is widely used across the United States, the applicability of these models to all regions is questionable due to the fact that these models were developed at certain locations and under certain environmental conditions which might not necessary be generalized across the nation. The prediction of mean pavement temperature from surface temperature and previous 5-day air temperature needs more investigation.

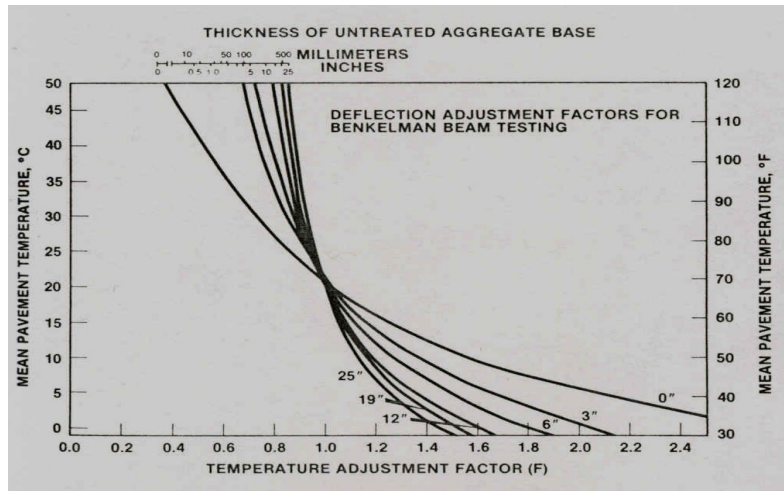


Figure 7: Predicted Pavement Temperature from Surface and 5-days Mean Air Temperature

The guide recommends calculating the seasonal adjustment factor by obtaining a continuous record of measured rebound values over a year for a similar pavement in a similar environment and on a similar subgrade. Deflection should then be determined during the most critical period in which the pavement is most likely to be damaged by heavy loads. At any time when making the rebound measurements, the seasonal adjustment factor is the ratio of the critical period deflection to the deflection for the date of the test. Even though the procedure was clearly stated in the guide, it was left open for DOTs and pavement agencies to develop their own site-specific models for such purpose.

Research-Based Models

Aside from existing models currently in use, DOTs, in conjunction with research institutes, have carried out their own research efforts in order to obtain site-specific models that suit their environment needs. The following sections report such research efforts.

Seasonal Models

Moisture Content

In an attempt to investigate the impact of moisture content and other environmental parameters on pavement strength, an Integrated Climatic Model (ICM) was developed in 1999.⁽¹⁴⁾ ICM was enhanced in 2000 (version 2.6) by Richter et al. to simulate temporal variations in the temperature, moisture, and freeze-thaw conditions internal to the pavement, and their impact on key pavement material properties.⁽¹⁵⁾

The ICM Program is used within the SHRP Superpave and is intended for use in analyzing pavement-soil systems. ICM has the capability to generate patterns of rainfall, solar radiation, cloud cover, wind speed, and air temperature to simulate the upper boundary conditions of a pavement soil system. The program calculates the temperature, suction and pore pressure without loading effects, moisture content, and resilient modulus for each node in the profile for the entire analysis period, as well as frost, infiltration, and drainage behavior.

ICM is composed of four major components, which are:

- A Precipitation Model (Precip Model)
- An Infiltration and Drainage Model (ID Model)
- A Climatic-Materials-Structural Model (CMS Model)
- The CRREL Frost Heave-Thaw Settlement Model (CRREL Model)

The Precip and ID Models were developed at Texas A&M University. The CMS Model was developed at the University of Illinois, while the CRREL Frost Heave and Thaw Settlement Model was developed at the US Army Cold Regions Research and Engineering Laboratory.

The components of the ICM were developed independently of each other for the most part, but were combined into the ICM for the purpose of performing major pavement structure and subgrade analysis. In this study, only predictions from the first three components of the ICM were included.

The inputs to ICM include data such as latitude, geographic region, and number of days in analysis period, as well as background information on the thermal properties associated with the site of interest. The surface temperature is initially established, followed by the calculation of temperatures throughout the pavement layers. Once the surface temperatures are determined, they are used to calculate the temperature throughout the underlying pavement layers. A heat transfer model is used to determine the distribution of temperatures in the pavement layers.

ICM was tested to investigate its capability to accurately predict moisture content, compared with moisture content data actually collected from 10 field sites in U.S. and Canada through the seasonal monitoring program of the LTPP study.⁽¹⁶⁾ The findings of the study showed that in most cases ICM either over-predicts or under-predicts the actual moisture content. The model also showed poor prediction in sites with dry climatic conditions.

Birgisson et al. detailed a comparison between field results and predictions obtained from ICM, entitled "Enhanced Integrated Climatic Model (EICM)".⁽¹⁷⁾ The climatic factors used as inputs into the model included temperature, rainfall, wind speed, and solar radiation. EICM was used to predict seasonal variations in temperature, moisture content, and layer moduli at two representative flexible pavement test sections at the Minnesota Research Project (Mn/ROAD) site. The objective of this study was to evaluate predicted seasonal variations in flexible pavements at Mn/ROAD. EICM was used to predict *in-situ* pavement temperature, moisture content, and layer moduli, allowing for comparisons with actual field-measured values.

The primary source of the field data used in this study was the Mn/ROAD database. Mn/ROAD is located approximately 40 miles west of the Minneapolis-St. Paul metropolitan area. The test facility is comprised of 40 pavement test cells consisting of flexible, rigid, and aggregate sections, each 492 ft long. The test cells were divided between a mainline pavement that carries live interstate traffic and a low-volume test loop subjected to calibrated truck traffic. The total length of pavement at Mn/ROAD is approximately 5.9 miles with over 4,500 sensors monitoring conditions in the atmosphere and in each pavement layer.

For the two base material types considered in the study (dense graded and crushed granite), the predicted moisture content trends follow the measured trends fairly closely, except during spring thaw, when the EICM misses the critical increase in volumetric moisture content. Noticeable differences remain in the winter months, where the EICM assumes that the entire

base is frozen with no unfrozen pore water. The time domain reflectometry (TDR) results indicate some volume of unfrozen water during the winter months. This may be due to the calibration of the TDR probes not adequately reflecting the winter conditions. It should also be noted that the simulations were performed with hydraulic properties measured in the laboratory, and may contain some errors associated with the differences in boundary conditions between the laboratory and the field.

Previous work on the Mn/ROAD site by Ovik et al. established that asphalt concrete stiffness (E_{AC}) is responsive to temperature, and that granular base (E_{GB}) and subgrade (E_{SG}) stiffness are responsive to changes in the state of moisture.⁽⁴⁾ Therefore, the EICM was tested for the changes in stiffness of the pavement materials under the influence of changing temperature and moisture conditions. The next section will highlight the outcome of moisture content effect on granular base and subgrade (the effect of temperature will be discussed later in this report).

It has been reported that one of the EICM drawbacks is the assumption that the stiffness of granular base materials is insensitive to moisture when unfrozen.^(4,18) Therefore, two values, frozen and unfrozen, must be provided in the input data to predict the variations in the base modulus. The program will then select the appropriate value depending on the predicted temperature in the base. Thus, the EICM does not really predict the actual modulus values of the base. Rather, it predicts which of the two user-specified values should be used at each point of time – namely, either the frozen or unfrozen stiffness value. In this context, it is not surprising to see the rather good agreement between the EICM-predicted and backcalculated base modulus values.

EICM considers the subgrade modulus to be in one of three possible states: frozen, unfrozen, or thaw-receiving. The output of the system shows that the initiation of thaw is not captured very well with the EICM. The EICM predicted frozen modulus values until May when in actual fact the thaw began much earlier.⁽⁴⁾

In summary, the results of EICM clearly indicate that it is possible to analytically predict the seasonal variations in moisture content and asphalt layer modulus in flexible pavements using climatic factors. Variations in moisture contents in the various pavement layers were captured reasonably well with EICM, as well as seasonal variations in the asphalt layer modulus. The only exception to this was the inability of EICM to capture the critical increase in volumetric moisture content in the base layer during spring thaw. Also, the transition from frozen to unfrozen moduli for the subgrade was not captured adequately well with EICM. It should be pointed out that the use of EICM currently requires rather extensive material testing. The level of detail in material characterization may be beyond the budget for a typical pavement analysis project.

Another study was carried out by Jin et al. to analyze the seasonal variation of subgrade resilient moduli.⁽¹⁹⁾ A new laboratory testing procedure and system were developed in this study for the design of flexible pavements in Rhode Island and areas that have a similar environment, to replace the AASHTO and ASTM 1990 methods of the resilient-modulus test. The new method included preparing specimens with the split mold and modified rammer. Loading sequences for the sample conditioning and data-collection phase were modified based upon the soil-stress analysis to reproduce the field condition as closely as possible.

Two selected field sites were instrumented with soil moisture-temperature cells. The two sites were selected considering the typical topography and glacial geology of Rhode Island: an upland till plain and an outwash deposit. The soil moisture-temperature cells were used for the following purposes:

- To measure the *in-situ* soil moisture content at different depths, which provided data used to reconstitute samples in the laboratory.
- To measure the *in-situ* soil temperature at different depths, at which the resilient modulus test is conducted in the laboratory.

The results of the resilient-modulus test indicated that the resilient-modulus value increases as the moisture content and temperature decreases, and as the dry density increases.

A multiple regression analysis was performed with the laboratory data to predict the resilient modulus under various environmental conditions. A theoretical model was developed in this study to predict the resilient modulus at different temperatures and moisture conditions. The predicted values obtained by the theoretical model were compared with the laboratory-measured ones for the verification of the developed theoretical model. The comparison indicated that the theoretical model could be used to predict the resilient modulus.

Freeze/Thaw

Ovik et al. conducted a study to quantify the relationships between climate factors, subsurface conditions, and pavement material properties that reflect conditions specific to Minnesota for use in flexible pavement design.⁽⁴⁾ This was achieved by establishing the relationships between climate factors, subgrade parameters, and pavement layer stiffness.

The data used in this study was obtained from Mn/ROAD. An on-site weather station was installed to provide temperature and precipitation data. Four of the flexible pavement test cells of Mn/ROAD, each 492 miles in length, were used in this study. Test cells 14 and 15 from Mn/ROAD are full-depth asphalt concrete cells. Test cells 17 and 21 are asphalt concrete and granular base. The methodology used in this study was to relate specific climate factors to the condition and stiffness of the pavement layers. It was determined that the asphalt concrete stiffness (E_{AC}) is responsive to temperature, and that granular base (E_{GB}) and subgrade (E_{SG}) stiffness is responsive to changes in the state of moisture in the layer.

A tool was developed called the thaw indicator (THAW) in which the moving 3-day average of the freezing degree days and/or forecasted temperatures were used to estimate when thawing events occurred. Precipitation was monitored for effects on the moisture content of the base and subgrade layers. The next step was to relate the seasonal field conditions to the stiffness of the pavement layers. An exponential equation was developed to relate the seasonal variations in the temperature of the asphalt concrete to the stiffness layer.

A typical year was separated into seasons according to variations in pavement layer moduli. The pavement layers were found to be at maximum stiffness in late November, December, January and February. This period was called Season I. The month of March was called Season II since this is typically when the base is thawing and the layer modulus is at minimum stiffness. The months of April and May were called Season III where the subgrade modulus decreases as the layer thaws and the base layer moduli were in the early stages of recovery. The asphalt concrete layer stiffness is at minimum stiffness in June, July and August, Season IV. Season V is September, October, and early November, when all the layer moduli have

reached a value that was used as a baseline for comparison in this study. The moduli were evaluated in terms of percent difference from the baseline moduli of the material or Season V.

It was found that daily precipitation events where the water is drained out of a granular layer within a short period of time (days) were not as influential in the overall moisture content as was the increase in the moisture content during the spring recovery period. It was also found that the moisture content increases with depth for the base materials. This is possibly due to gravitational effects causing the excess moisture to move toward the bottom of the base layer, where it is unable to drain into the embankment or subgrade.

The modulus of the unbound layers was at maximum stiffness when the moisture was frozen and at minimum stiffness when the thawed moisture was still in the layer, before it was able to drain out of the layer. The temperature history data was used to establish the (THAW) indicator and the results showed that frost sensors correspond well with the estimations made by the THAW indicator.

When the moisture is in a solid phase, the modulus of the base is at maximum stiffness (prior to March 14). As the water changes to a liquid phase and cannot drain properly, the modulus decreases to its minimum from March 14 to March 21. As the water is drained from the layer, the modulus rebounds to what is called a baseline value in this study (after May 20).

Then seasonal factors were used to characterize the trends in the layer moduli. These factors were determined by dividing each of the seasonal moduli values by a baseline modulus value. Season V was used as a baseline since these values were between the high and low moduli values. It was observed that the moduli in Season I (when the layers are frozen) were between 1 and 5 times greater than Season V.

On average, the base was less stiff by a factor of 65 percent in Season II, and a factor of 85 percent in Season III when compared to Seasons IV and V. The seasonal modulus values were at a maximum value in Season I, when the pavement is frozen. In general, the average seasonal factor for the subgrade was 75 percent in Season III and 70 percent in Season IV compared to Season V.

The results show that the maximum stiffness for the pavement layers occurs in the winter and the minimum stiffness occurs at different periods in a typical year for the different layers. The asphalt concrete modulus is at a minimum in the summer when temperatures are high. The base layer modulus is at a minimum in the spring thaw period, and the subgrade layer modulus is at a minimum in the late spring and summer months.

Temperature Correction Models

For the temperature correction models, Marshall et al., 2001 used the BELLS3 model, an enhanced mid-depth asphalt layer temperature equation, to predict pavement temperature and compared the results with calibrated temperature measured by thermistors in 4 test sites in Tennessee.⁽²⁰⁾ The BELLS3 predictions matched the measured temperature fairly well below 77°F, but at higher temperatures or below 32°F, it under-predicted the measured one. This study also tried to establish a correlation between flexible pavement layer modulus and calibrated asphalt layer temperature measured *in-situ*. However, the results varied among different sites. A better relation was found when dividing the backcalculated module by the modulus at 68°F for each site. Although the modulus ratio-temperature relationship matched a similar one carried out in North Carolina, it cannot be used for temperature below 32°F.

In the study conducted by Birgisson et al., using the EICM model, it was reported that asphalt concrete stiffness (E_{AC}) is responsive to temperature.⁽¹⁷⁾ Accordingly, when the EICM was tested for the changes in stiffness of the pavement materials under the influence of changing temperature, it was found that trends in the predicted temperatures in the asphalt concrete layer compared very favorably with those observed in the field. The EICM predictions are shown to be reasonably close to the backcalculated moduli, even though the scatter in the backcalculated moduli remains higher. However, the predicted temperatures in the dense graded base material were slightly off – in particular, the peaks of the predicted temperatures were slightly lower than those of the measured temperatures. As reported for the EICM prediction for moisture, it seems that EICM captured the variation in temperature well.

Another study was carried out by Park et al., 2000, to implement an AC mid-depth temperature prediction model based on data collected from test sites in Michigan.⁽²¹⁾ It was validated using seven SMP sites at different locations across the USA from the LTPP database. The model used AC surface pavement temperature, pavement depth, and time when AC surface temperature was measured during the day, to predict the AC temperature at the acquired depth. The model showed good agreement between the measured and predicted data. The study also attempted to establish a model to correct the backcalculated AC modulus at measured mid-depth temperature and reference it to a standard temperature (77°F). The model was validated with data from 5 test sites and showed good agreement between predicted and measured data.

Also, Long et al. conducted a study to investigate the seasonal variation of pavement layer moduli during a one-year period and its correlation to pavement temperature.⁽⁶⁾ The study focused on calculating layer moduli using different modeling methods and evaluating how these methods affected the results. Four 499 ft asphalt pavement sections were selected as test sites in the State of Kansas. Two sites were selected in northeast Kansas, and two sites were selected in southwest Kansas. Deflection data was collected monthly at 10 stations at 49 ft intervals on each test section. Soil moisture measurements were conducted simultaneously with the FWD tests using TDR. Temperature data were also collected for each site.

The pavements were modeled as two types of structural components. First, the pavements were modeled as two-layer systems with an AC layer over a subgrade layer. The subgrade moduli obtained with these models were called 'combined subgrade moduli'. Secondly, the pavements were modeled as three-layer systems with an AC layer, a 18 inches thick compacted subgrade layer, with a natural soil subgrade layer underneath. The natural soil subgrade layers at two sites were considered finite; their thickness values were obtained from the county soil survey data. The natural soil subgrade layers at the other two sites were assumed to be infinite in the vertical direction. The subgrade moduli backcalculated from these models were designated as compacted subgrade moduli and natural soil/rock subgrade moduli.

Comparing the results, it was obvious that the subgrade moduli, irrespective of pavement modeling, varied over seasons. It was anticipated that in the case of pavement models with the subgrade subdivided into compacted and natural subgrades, natural subgrade moduli would not vary much with season. The magnitude of variation of natural subgrade moduli was similar to that of the combined subgrade moduli. Higher variation was observed for compacted subgrade moduli, indicating that modeling subgrades in such a way may well capture the seasonal variation of subgrade moduli.

For northeast sites during months with lower temperatures (November, December, and January), the combined and compacted subgrade moduli increased as expected. In December, when both average pavement and surface temperatures were lower than 32°F, higher subgrade

moduli were computed. Lower subgrade moduli were computed during the summer months. The lowest compacted and combined subgrade moduli were computed for northeastern sites in May, when pavement surface temperature reached 115°F on one day. Lower values of these moduli were obtained again in July, when the pavement surface temperature was normal at 95°F. The moduli of the natural soil subgrade did not appear to vary as much as other subgrade moduli.

It is important to note that subgrade moduli during summer months were lower than during the spring thaw period (February-April). This indicates that temperature played a greater role during tests when evaluating the response of these pavements than thaw weakening played, although freezing and thawing did occur on these sites in northeast Kansas.

For southwest sites, the compacted subgrade moduli obtained from MODULUS were consistently lower than natural soil moduli. The compacted subgrade moduli were lower in winter than in summer. This may imply that it is not appropriate to model the pavement structures as three-layer systems on these sites. It is apparent from this study that some variability in backcalculated subgrade moduli can be avoided by conducting FWD tests in a moderate-temperature regime.

Kim et al. developed a temperature correction model to suit the North Carolina environment, rather than the commonly used AASHTO model.⁽⁷⁾ The data used in developing this model was collected from four pavements in the Piedmont area of North Carolina with various types of layer materials and thickness. Four trips, one in each season, were made to each of these pavements so that deflections in the maximum range of temperatures could be obtained without significant structural deterioration of the pavements. During each trip deflection testing was conducted on an hourly basis for 1 full day per test section. Pavement surface and depth temperatures were measured at the time of deflection testing with FWD. The measured deflection and temperature values were used to validate the temperature correction procedure presented in the 1993 AASHTO Guide for Design of Pavement Structures. It was found that the AASHTO procedure produced significant errors in the corrected deflections. The main reasons for these errors pertained to the fact that AASHTO mean temperature cannot account for the difference in temperature-depth gradients during heating-versus-cooling cycles and that the AASHTO temperature correction factors overcorrect the deflections at higher temperatures.

Accordingly, a new temperature correction procedure for deflections and backcalculated moduli was developed based on the fact that the mid-depth temperature of the AC layer is an effective AC layer temperature. The accuracy of this procedure was validated with deflection and surface temperature data collected from four other pavement sections in North Carolina. The temperature correction procedure based on the temperature at mid-depth of the AC layer was found to greatly improve the accuracy of the temperature-deflection correction.

European Models

In Europe, where the weather is similar to North America, a common practice is to use the Deflectograph (British version of FWD) in measuring the deflection. Similar to FWD, the Deflectograph deflections have to be referenced to a standard temperature in order to normalize the temperature effect on deflections, and hence on the backcalculated properties of all pavement layers. In an attempt to account for such temperature effect, Kennedy and Lister introduced temperature correction charts for the maximum deflection, measured at any temperature between 41°F and 86°F, to be corrected to a standard deflection at a temperature of 68°F.⁽²²⁾ In these charts, broadly linear relations between deflection and pavement

temperature were established for a wide range of pavement types, making the charts more appropriate for generalization. According to the developed models, the study suggested that only the bituminous thickness was affected by the temperature effect.

In another attempt to normalize temperature effect in Northern Ireland, Shaat conducted a tentative study to investigate the seasonal variation of the Deflectograph deflection.⁽²³⁾ This study used the results of the laboratory tests on the bituminous cores recovered from test sections to establish the temperature correction factor to be applied to the backcalculated moduli using the mean pavement temperature at the time of testing. The study also concluded that the temperature effect, in addition to other seasonal parameters, should be considered not only for bituminous layer but for subsequent layers as well.

Bergstedt conducted a comparison of some of the methods used for temperature corrections applied to the measured deflections.⁽²⁴⁾ A test section was used in this study where an FWD test was carried out every 2 hours for a complete 24-hour cycle. The aim of this set-up was to achieve as much temperature variation as possible (54°F to 82°F) without any change in other seasonal factors such as moisture content. The measured FWD maximum deflection was then correlated with the measured mean pavement temperature. The resulting equation was used to provide the adjusted deflection value at four standard temperatures (59°F, 68°F, 70°F, and 80°F). The adjusted deflections were utilized as the basis of comparison with values from selected correction methods. Comparing different methods of deflection correction including AASHTO, Kennedy and Lister, and the method developed during the study itself, and applying them to all the deflection measurements, the study reported a remarkably high accuracy of all the methods stating that their findings were surprising considering that they were developed for different conditions and more importantly, for different types of Non-Destructive Testing (NDT) devices.^(8,22) The study also concluded that only the maximum FWD deflection and deflection ordinates up to 20 inches away from the load centerline are affected by temperature variation and therefore required correction.

Also, Baltzer et al. conducted a study in Denmark for temperature-correction of FWD measurements.⁽²⁵⁾ The asphalt temperature is commonly calculated in Denmark by measuring at a depth of 40mm below the surface. Of the procedures known today, the study suggested that the best way to determine temperature is to drill a hole in the AC layer and measure it with a thermometer. But the optimum depth at which to measure is relative, depending on the thickness of the asphalt layer. Therefore, to find the optimum depth and the relationship between temperature and E-modulus at that depth, field tests have been carried out measuring deflections and temperature gradients simultaneously. Three field tests have been carried out at two different test sections with different AC thicknesses. These tests were conducted over a 24-hour period in order to take both heating and cooling of the asphalt layer into account, leaving out the interference from change in moisture content of the subgrade and subbase.

Using collected data for field temperature, the backcalculated AC modulus was calibrated to a modulus at a reference temperature. The collected data was also used to find the optimum depth at which the AC temperature should be measured in order to represent the temperature of the total AC layer and the corresponding formula for temperature correction of the AC modulus. The backcalculated AC moduli and the measured temperatures have been compared, and showed that there is optimum depth at one third of the thickness of the total AC layer measured from top of the slab.

On the basis of the relationship found between the AC E-modulus and the temperature at one third of the AC thickness, a temperature correction formula was developed, verified, and

showed fine results. Also, the Current Danish Model and an Adjusted Model were tested. The AASHTO temperature prediction was compared to the model developed using the measured test data and AASHTO produced a poor temperature prediction.

In an attempt to investigate other environmental parameters, rather than temperature, Carson et al. in England used the Deflectograph to carry out deflection tests for a period over two years on three test sections with subgrades sensitive to moisture changes (Gault clay and London clay).⁽²⁶⁾ Having installed a number of gypsum cells to measure the moisture content of these subgrades, they developed linear regression equations relating the Deflectograph maximum deflection to the subgrade moisture condition, defining the slope of the linear relationships in deflection 'sensitivity' to subgrade moisture content for a particular section.

For the effect of ground water table in Northern Ireland, Shaat et al. conducted a seasonal study using the Deflectograph to monitor a controlled test section along the shoulder of which three boreholes were cored to a depth of 29.5 ft and the vertical movement of the water table was monitored.⁽²⁷⁾ They correlated the elastic modulus of the subgrade, backcalculated from the Deflectograph deflections, with the depth of the water table measured concurrently. These findings indicated the importance of the moisture content and its seasonal variation effect on the performance of pavement structures in Northern Ireland and similar regions.

Summary of Review

As shown from previous review, moisture content, ground water table, temperature, and freeze/thaw phenomena are highly correlated to pavement material properties. Previous studies have proved that these four environmental factors strongly affect pavement performance. These studies also showed that the impact of seasonal variation on pavement performance varies from one region to another. Models developed based on data collected from one region are valid only for similar environmental regions. The incorporation and handling of these parameters in the AASHTO guideline was investigated herein and it was confirmed that AASHTO specification for handling seasonal parameters might not fit all regions across North America. The current study will attempt to either calibrate EICM models for temperature and seasonal adjustments to suit New Jersey conditions, or develop new models, specifically addressing the New Jersey environment.

TEST SECTION REQUIREMENTS AND SELECTION

As stated earlier, the scope of the project was divided into two main components (studies): the Seasonal Adjustment Study and the Temperature Correction Study.

Since there is some overlap between the two studies, mainly for flexible pavement, the test sections for both studies were selected in a coordinated manner to maximize the benefits and minimize the cost of instrumentation and testing. The NJDOT Pavement Management System was used to identify candidate pavement sections that met the test section requirements. The construction records of the non-highway pavement facilities, such as weigh stations, maintenance yards, etc. were also searched, as were other data sources, such as DataPave for the LTPP sections.

Test Section Requirements

Seasonal Adjustment Study

The influence of seasonal variations on pavement response is very significant on flexible pavements and less significant on rigid and composite pavements. Therefore, the main focus of this study was on flexible pavements. Only two rigid pavement test sections were included in the study in order to allow evaluation of the performance of NSOG layers under different moisture and temperature conditions. The following are the factors that were considered in the Seasonal Adjustment Study:

- Total Pavement Thickness (Total thickness above the subgrade) - two levels:
 1. Thin Pavements (Total thickness < 24 in)
 2. Thick Pavements (Total thickness > 24 in)
- Freezing Index (represented by the geographical location and climatic zone) – two levels:
 1. Northern Region
 2. Southern Region
- Subgrade Type - two levels:
 1. Typical New Jersey silty sand subgrade
 2. Other than the typical silty sand subgrade

In a previous study carried out for NJDOT, climatic data obtained from 26 weather stations covering the whole State was analyzed.⁽⁹⁾ In this analysis, the State was divided into 3 climatic regions: northern, coastal, and southern. Results of the analysis indicated that the difference in the climatic characteristics of the coastal and southern regions is not significant, as shown in Figure 8. Therefore, only the northern region and southern region were considered in the Seasonal Adjustment Study. One additional test section was selected in the coastal region in order to validate the models adopted for the southern region for the coastal region.

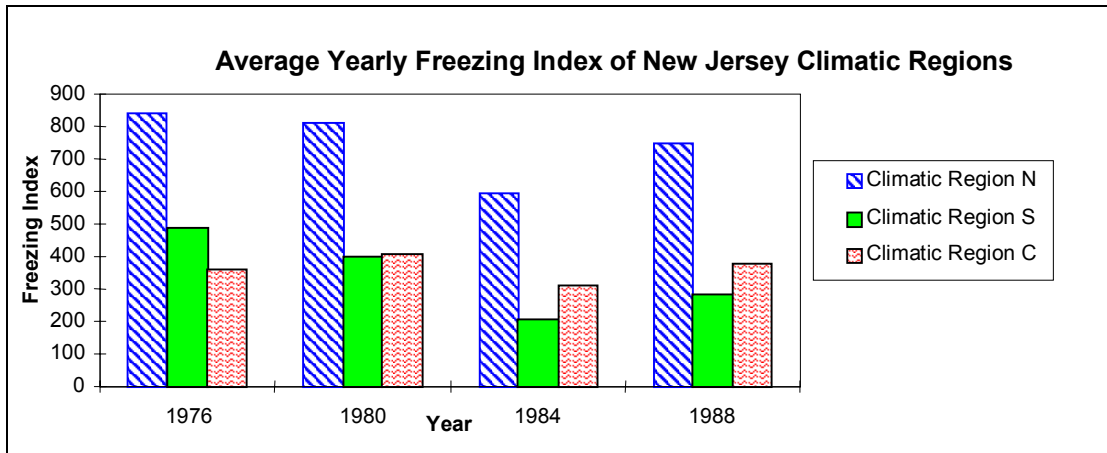


Figure 8: Comparison Between New Jersey Environmental Regions

Table 1 shows the test section requirements for the Seasonal Adjustment Study. Eight test sections are required for this study, as follows:

- Four flexible pavement sections that satisfy the seasonal adjustment study requirements (2 pavement thicknesses and 2 environmental regions).
- One flexible pavement test section that matches one of the above mentioned 4 sections but has different subgrade type.
- One flexible pavement test section located in the Coastal Region.
- Two rigid pavement test sections (with NSOG and without NSOG).

Table 1: Test Section Requirements for the Seasonal Adjustment Study

Section Number	Pavement Type	Climatic Region	Total Thickness	Subgrade Type	Comments
1	Flexible	Northern	>24 in	Type I	
2	Flexible	Northern	<24 in	Type I	
3	Flexible	Southern	>24 in	Type I	
4	Flexible	Southern	<24 in	Type I	
5	Flexible	----	----	Type II	
6	Flexible	Coastal	----	----	
7	Rigid	----	----	----	With NSOG
8	Rigid	----	----	----	Without NSOG

Temperature Correction Study

Since the variation in temperature mainly affects the stiffness of asphalt layers, both flexible and composite pavement sections were considered in this study. The following are the factors that were included in this study:

- Pavement Type - two levels:
 1. Flexible
 2. Composite
- Total Asphalt Thickness
 - Three levels for flexible pavements:
 1. Thin (≤ 4 in)
 2. Medium (> 4 in and ≤ 10 in)
 3. Thick Pavements (> 10 in)
 - Two levels for composite pavements:
 1. Thin (≤ 4 in)
 2. Thick (> 4 in)

In total, 3 flexible pavement test sections and 2 composite test sections are required for the Temperature Correction Study. Two of the 3 flexible pavement test sections will be selected from the sections of the Seasonal Adjustment Study. Therefore, only three additional test sections are required for the Temperature Correction Study, one flexible pavement section and 2 composite pavement sections. Table 2 summarizes the test section requirements of both the Seasonal Adjustment Study and the Temperature Correction Study.

Table 2: Test Section Requirements for the Seasonal Adjustment and Temperature Correction Studies

Section Number	Study	Pavement Type	Climatic Region	Total Thickness	Subgrade Type	Comments
1	Seasonal Adjustment	Flexible	Northern	> 24 in	Type I	
2	Seasonal Adjustment	Flexible	Northern	< 24 in	Type I	
3	Seasonal Adjustment	Flexible	Southern	> 24 in	Type I	
4	Seasonal Adjustment	Flexible	Southern	< 24 in	Type I	
5	Seasonal Adjustment	Flexible	-----	-----	Type II	
6	Seasonal Adjustment	Flexible	Coastal	-----	-----	
7	Seasonal Adjustment	Rigid	-----	-----	-----	With NSOG
8	Seasonal Adjustment	Rigid	-----	-----	-----	Without NSOG
9	Temperature Correction	Flexible	-----	-----	-----	$4 \text{ in} < \text{AC} \leq 10 \text{ in}$
10	Temperature Correction	Composite	-----	-----	-----	$\text{AC} < 4 \text{ in}$
11	Temperature Correction	Composite	-----	-----	-----	$\text{AC} > 4 \text{ in}$

Long Term Pavement Performance (LTPP) – Specific Pavement Studies (SPS) Sites

The LTPP project has been in place since 1987, where a large number of test sections are being steadily monitored to evaluate their performance over the pavement life span. Currently, the project is managed by the Federal Highway Administration and consists of over 2,400 test sections at 932 test sites located across North America. Roughness, distress, and FWD surveys are routinely performed on the LTPP test sections. The LTPP program includes General Pavement Study (GPS) test sites and SPS test sites. The SPS sections are part of a controlled study, in which the test sections were constructed according to a specific protocol with a high level of care and quality control procedures, and are subjected to real-life traffic loading. SPS test sites consist of a number of test sections with different treatments placed along the same highway to help in evaluating the difference in their performance under similar environmental and traffic conditions. For these sites, the environmental, traffic conditions, and construction conditions are nearly identical which allows for easy comparisons. An SPS test site would include a number of core (standard) test sections in addition to a number of supplemental sections. The supplemental sections are constructed by the agency, adjacent to the LTPP study core sections, with special treatments of particular interest to the agency. These sections allow for treatments outside the scope of LTPP program, and generally are not consistent among highway agencies.

New Jersey has two SPS sites, one SPS-5 site (which includes 11 test sections) and one SPS-9A site (which includes 6 test sections). The SPS-5 site in New Jersey was constructed in 1992 as one of 17 projects across North America. It is located in the wet-freeze environment zone. The site includes nine test sections and two other supplemental test sections. The SPS-5 site in New Jersey is located along the westbound lane of I-195. The original pavement was constructed on a silty to clayey sand soil, and consisted of a variable depth soil aggregate mixture subbase, about 10.5 in of an uncrushed gravel base, and about 8.5 in of an AC surface. The details of these 2 sites are shown in Figures 9 and 10, respectively. As can be seen, the SPS-5 site consists of 11 test sections with different pavement structures. Details of the pavement structure of these 11 test sections are presented in Table 3. The SPS-9A site consists of 6 test sections. The pavement structures of these 6 sections are very similar, as shown in Table 3.

The contract for the SPS-9A site in New Jersey was awarded on June 27, 1997, and construction was completed in mid-1998. The objectives of the SPS-9A experiment are to observe the performance of Superpave™ mixes as well as comparable agency mixes, and to verify the asphalt binder selection procedure in SHRPBIND, which is a process for determining the environment in which the pavement is constructed and will function. The New Jersey SPS-9A project is located in the wet-freeze environment zone with a sand to silty sand subgrade/embankment material, 5 inches of granular subbase and 5 inches of granular base of coarse grained soil-aggregate mixture, 6 inches of HMAC binder course, and 3 inches of HMAC surface course. The project is built on the eastbound lanes of I-195. The eastbound lanes involved building three LTPP core sections, 340901 NJ standard mix with AC-20 asphalt cement, 340902 Superpave™ mix with PG 58-28 asphalt cement, and 340903 Superpave™ alternative mix with PG 52-28 asphalt cement in the surface layer. The three supplemental sections were built in the eastbound lanes, 340960 Superpave™ mix with PG 64-22, 340961 Superpave™ mix with PG 78-28 asphalt cement, and 340962 NJ DOT RAP mix with AC-20 asphalt cement in the surface layer. The base layer was paved throughout the project with one inch maximum Superpave™ mix with PG-64-22. However, different asphalt mixtures are used in these test sections, including Superpave Mixes.

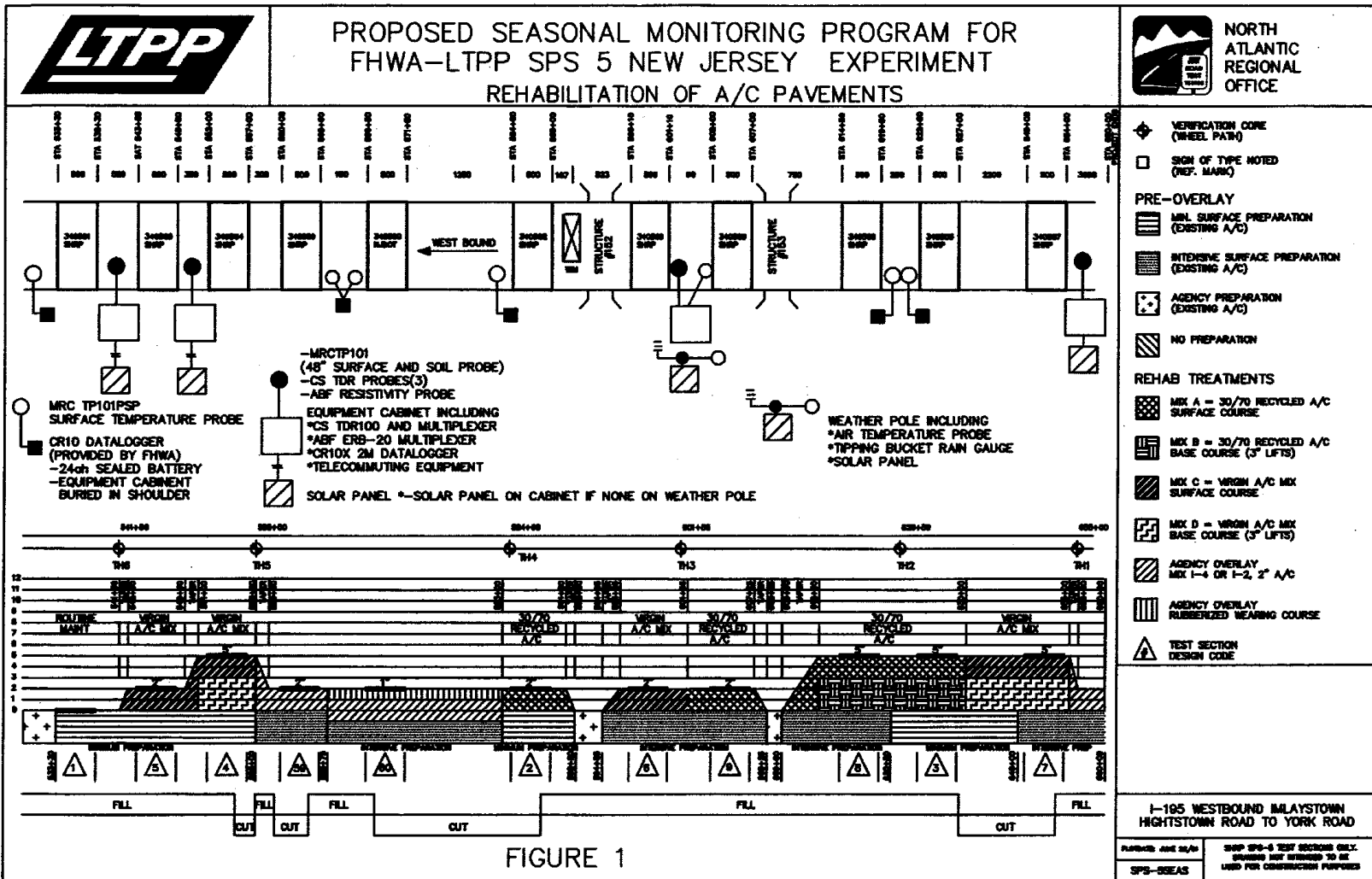


FIGURE 1

Figure 9: Details of the SPS-5 Test Sections

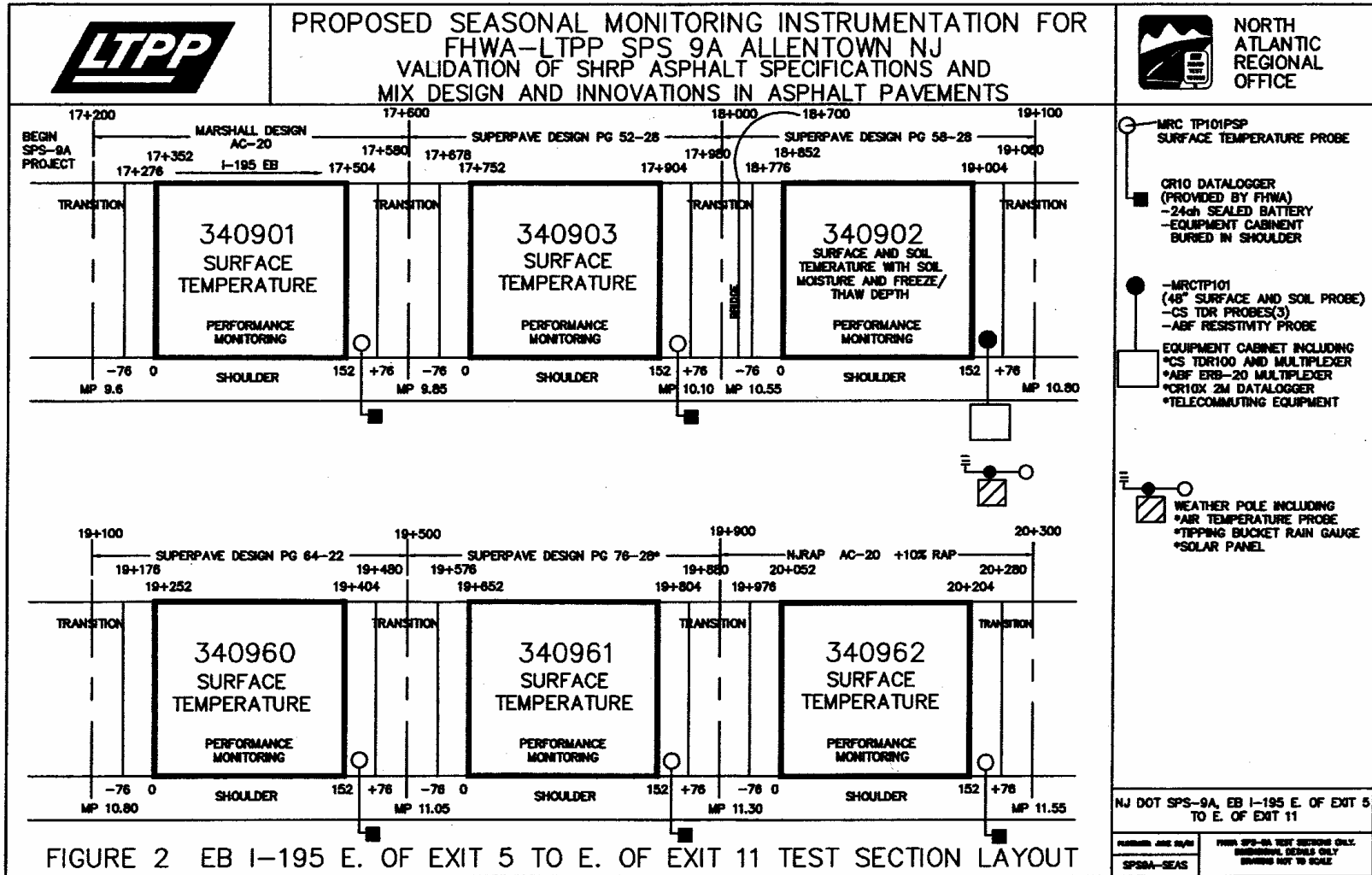


Figure 10: Details of the SPS-9A Test Sections

Table 3: Pavement Structure of the SPS-5 and SPS-9A Test Sections

Region	AC Thickness Class	Total Thickness Class	LTPP	Pavement Type	AC Thickness (in)	Base Thickness (in)	Subbase Thickness (in)	Base Course Type	Subbase Type and Properties	Subgrade Type and Properties
South	Thin	Thick	340501	Flexible	9.5	10	20	Gravel (uncrushed)	Soil Aggregate Mix (predominantly coarse-grained)	Coarse Grained clayey sand
South	Thick	Thick	340502	Flexible	10.8	10.4	19	Gravel (uncrushed)	Soil Aggr. Mix	Coarse grained clayey sand
South	Thick	Thick	340503	Flexible	13.7	11.3	19	Gravel (uncrushed)	Soil Aggr. Mix	Coarse grained clayey sand
South	Thick	Thick	340504	Flexible	13	15	10	Sandy gravel w/stone	Brown silty sand	Clean sand
South	Thick	Thick	340505	Flexible	10.8	22.7	9.5	Brown sandy gravel	Silt sand mix w/some stone	Sand
South	Thick	Thin	340506	Flexible	11.7	3.8	13.5	Coarse stone w/sand mix	Coarse sandy gravel	Silty sand
South	Thick	Thick	340507	Flexible	14.2	10.8	17	Dark brown sand w/stone	Brown sand w/stone	Brown sand over clayey sand
South	Thick	Thick	340508	Flexible	14.9	11.3	22	Gravel (uncrushed)	Soil Aggr. Mix	Coarse grained clayey sand
South	Thick	Thick	340509	Flexible	11.5	11.3	22	Gravel (uncrushed)	Soil Aggr. Mix	Coarse grained clayey sand
South	Thick	Thin	340560	Flexible	10.5	10.5	4	Gravel (uncrushed)	Soil Aggr. Mix	Coarse grained clayey sand
South	Thick	Thick	341559	Flexible	10.2	10.5	22	Gravel (uncrushed)	Soil Aggr. Mix	Coarse grained clayey sand
South	Thick	Thin	340901	Flexible	11	6.5	10	Bituminous Base Course	Soil Aggr. Mix	Coarse grained silty sand
South	Thick	Thick	340902	Flexible	11.5	9.5	26	Sandy gravel w/large granite	Brown silty sand w/small stone	Sandy silt with traces of clay
South	Thick	Thin	340903	Flexible	11	7.4	10	Bituminous Base Course	Soil Aggr. Mix	Coarse grained silty sand
South	Thick	Thin	340960	Flexible	11.5	6.4	10	Bituminous Base Course	Other	Coarse grained silty sand
South	Thick	Thin	340961	Flexible	11.5	5.6	10	Bituminous Base Course	Soil Aggr. Mix	Coarse grained silty sand w/gravel
South	Thick	Thin	340962	Flexible	11	6.6	10	Bituminous Base Course	Soil Aggr. Mix	Coarse grained silty sand w/gravel

Although the LTPP-SPS sites were not a part of the original project work plan, considering them added significant value to the project. Therefore, the project team (NJDOT, Rutgers, and Stantec) jointly with the FHWA made a decision to add the SPS-5 and SPS-9A sites to the study. Based on that, the test section requirements were revised accordingly. Based on initial site testing, coring and preliminary analysis, the site requirements were revised to be as follows for flexible sites:

- AC Thickness
 1. Thin < 10 in
 2. Thick \geq 10 in
- Total Thickness
 1. Thin \leq 30 in
 2. Thick > 30 in

It should be noted that all the test sections of the SPS-5 and SPS-9A sites were instrumented in a way that provided full coverage for the sections.

Test Section Selection

The LTPP SPS-5 and SPS-9A sites provided a total of 17 pavement test sections for meeting the study requirements. An additional seven test sections were selected to complete the study requirements. Several sites were visited and cored to verify the pavement thickness and the sites that matched the study requirements were selected. Table 4 shows the selected non-LTPP test sections, while Table 5 shows the pavement structure of these sections. It should be noted that no composite pavement section with an AC overly thickness greater than 4 in could be identified.

Table 4: Selected Non-LTPP Test Sections

Section	Route	Direction	Mile Post	Location	City in NJ
1	I-80	West Bound	32.5	Truck Rest Area between Exits 34 & 30 across from EB Truck Rest Area	Parsippany
2	66	n/a	n/a	Maintenance Yard Ocean Township at Bowne Rd of Asbury Ave. (Asbury)	Neptune
3	I-287	North Bound	32.5	Rest Area between Exits 30 & 33	Parsippany
4	I-295	North Bound	49.7	Rest Area between Exits 47 & 52	Willingborn
5	I-78	East Bound	4.3	Weigh Station between Exits 3 & 4	Greenwich
6	I-295	North Bound	3.5	Weigh Station between Exits 2 & 4	Deepwater
7	130	North Bound	49.8	Slow Lane	Mt. Holly

Table 5: Pavement Layers of the Selected Test Sections

Region	AC Thickness Class	Total Thickness	Sections	Pavement Type	AC/PCC Thickness (in)	Base Thickness (in)	Subbase Thickness (in)	Base Course Type and Properties	Subbase Type and Properties	Subgrade Type and Properties
North	Thin	Thick	1	Flexible	7.5 (AC)	7	15.75	Crushed stone w/sand	7 in of sand w/crushed agg followed by 8.75 of sand&gravel w/large boulders	Brown sand and gravel w/large boulders
North	Thin	Thin	2	Flexible	4 (AC)	6	14	Recycled aggr. mix	Old AC layer (2 in) followed by sandy gravel	Sand and stone gravel
North	Thick	Thin	3	Flexible	10 (AC)	4	13	Crushed stone w/sand	Med gray-brown sandy gravel w/some cobbles	Dark brown silty sand w/sand stone and decomposed root material
South	Thick	Thin	4	Flexible	10 (AC)	10.5		Crushed aggr. limestone		Sandy clay and silt
North			5	Rigid	9.75 (PCC)	4	8	Aggr. base limestone	Sandy gravel	Sandy loam
South			6	Rigid	10 (PCC)	3	34	Crashed aggr.	Sandy gravel	Clayey silty sand
South	Thin		7	Composite	4 (AC)+9 (PCC)	3	4	Sandy gravel	Old asphalt layer	Sand

The recommended test section length for this study was 250 ft. This length allowed the collecting of enough data points for any statistical analysis, while being short enough to minimize the normal variation in the pavement structure and subgrade condition. The selected test sections were visually inspected to ensure that they were homogeneous, and had defect-free surfaces (i.e. no patches, cracks, etc.). Before the final selection of the 250-ft sections within each site, FWD testing was performed on the entire site length to select a homogeneous 250-ft section. The beginning, ending, and testing points were clearly marked with permanent paint. Stations started at 0.00 at the beginning point of each section and were marked on the shoulder at 25-ft intervals. FWD testing was also performed on the locations of the instrumentation hole and materials sampling hole to ensure consistency with the test section. The final selection of the location of the 250-ft test section, instrumentation hole, and materials sampling hole were selected based on the FWD results, as well as the site geometry and characteristics.

In total, 24 test sections were selected for the study. These 24 test sections are distributed among pavement types as follows:

- 21 flexible pavement sections
- 2 rigid pavement sections
- 1 composite sections

Figure 11 shows the location of the sections within the State of New Jersey. Figures 12 to 14 show the pavement structure distribution of the flexible, rigid, and composite sections, respectively.

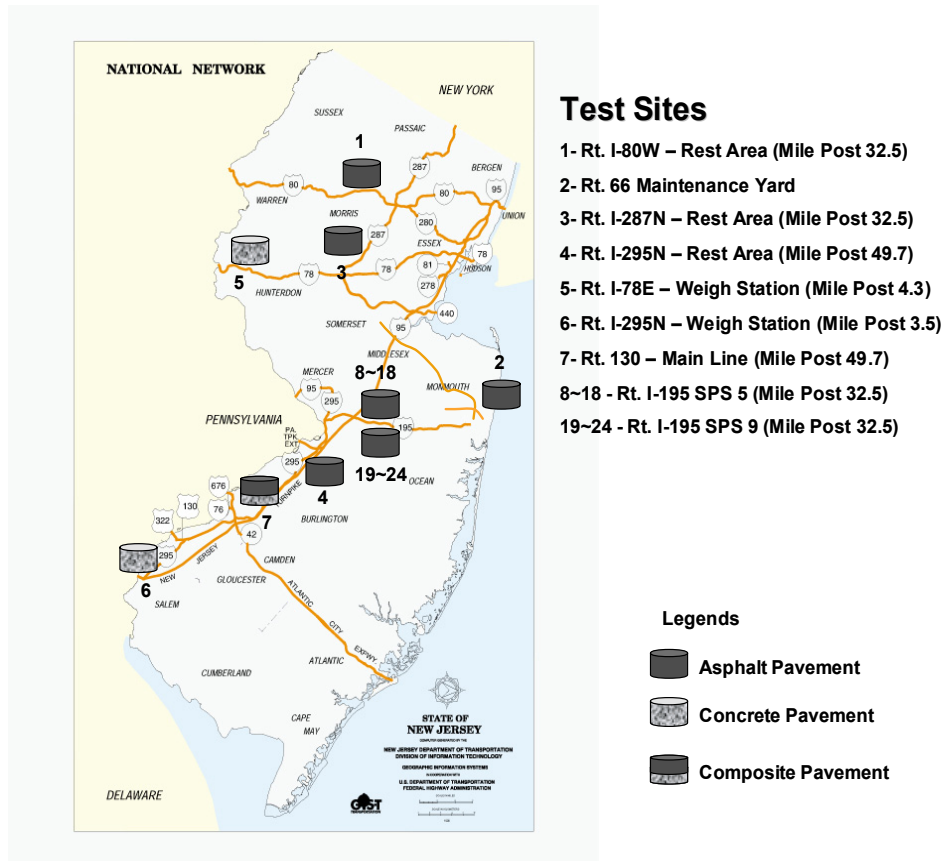


Figure 11: Locations of Test Sites within New Jersey

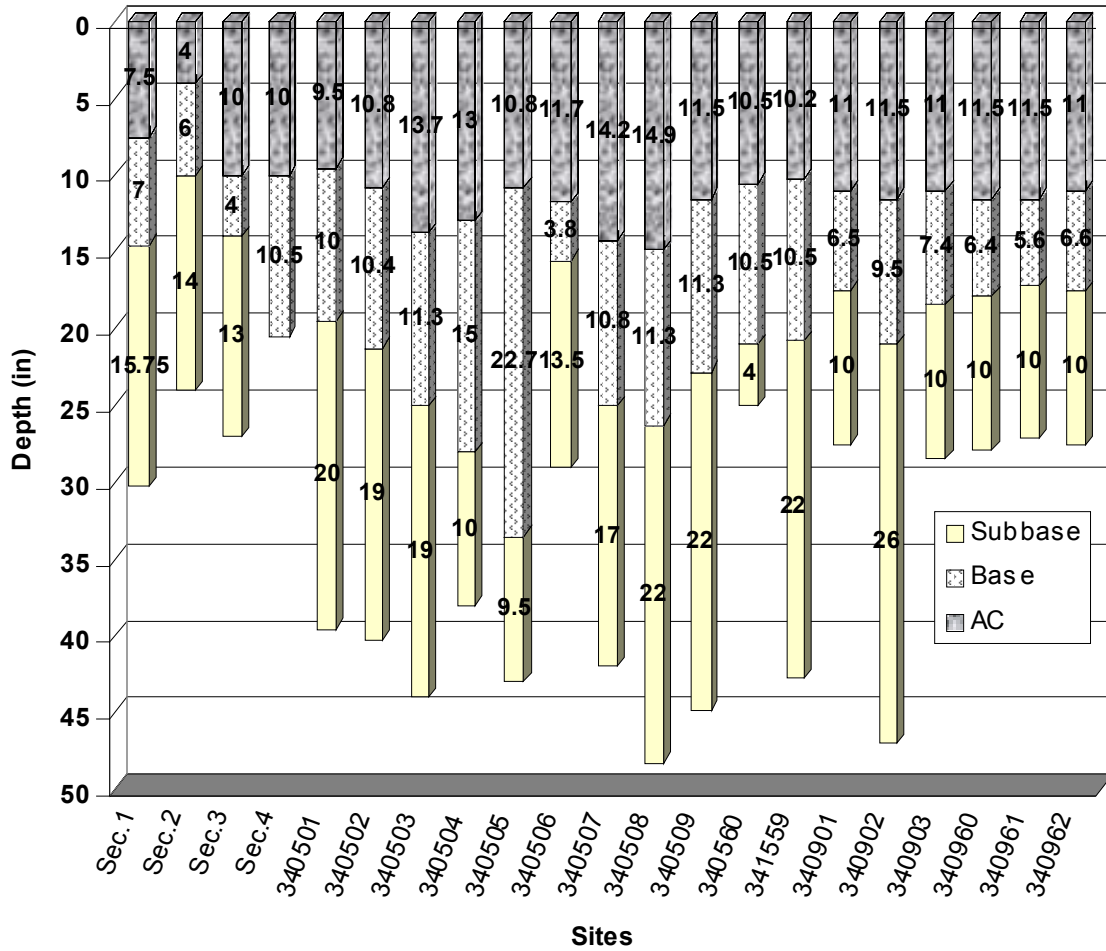


Figure 12: Flexible Pavement Test Sections

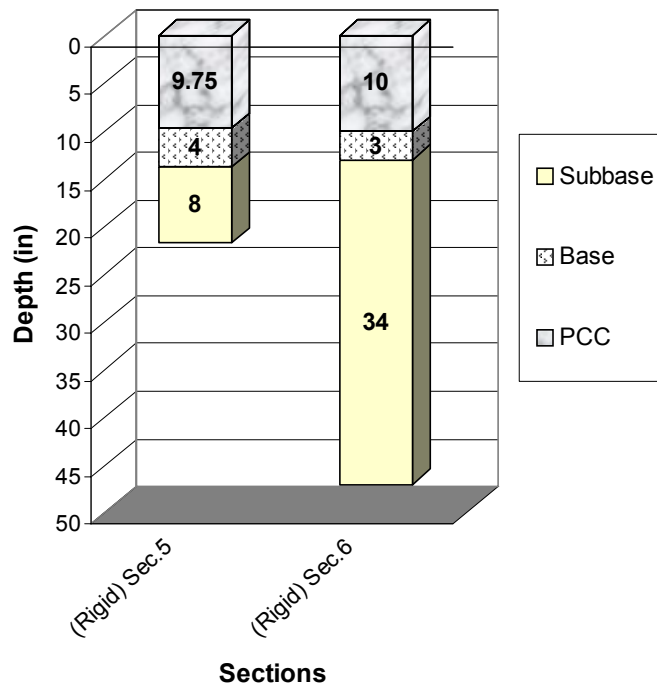


Figure 13: Rigid Pavement Test Sections

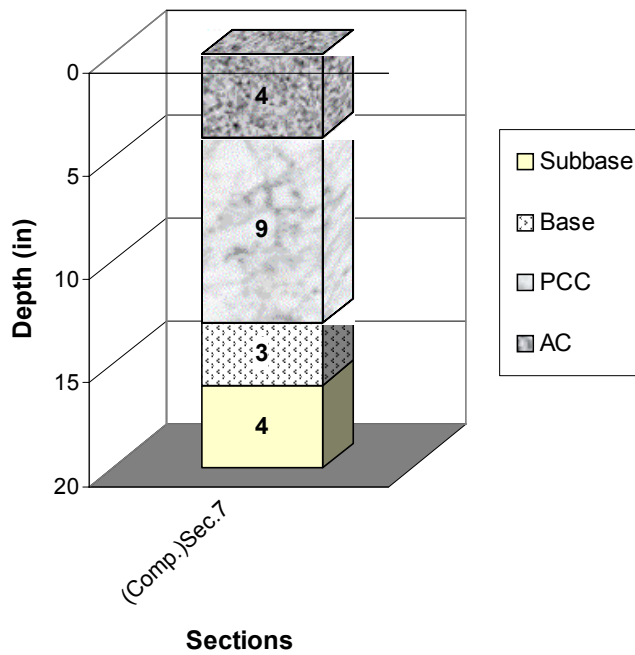


Figure 14: Composite Pavement Test Section

FIELD TESTING PROGRAM

The field testing program included installation of pavement instrumentation at the selected test sites; monitoring and collecting climatic data; performing FWD and SPA testing at the sites on a monthly, biweekly, and seasonal basis; downloading climatic and pavement response data; and performing Quality Control/Quality Assurance (QC/QA) checks on the field data prior to data processing. The sections below describe in detail the field activities carried out as a requirement of this study.

Pavement Instrumentation

To study the seasonal variation in pavement stiffness in the State of New Jersey, several sites across the State were selected for instrumentation. The main purpose of the pavement instrumentation was to monitor the effect that daily and seasonal changes in environmental parameters have on the response of pavements to traffic loads and, hence, on their performance. These parameters include temperature, moisture, and frost/heave penetration depth. Instrumentation selection and the installation procedure was done according to the LTPP-SHRP specifications of the “LTPP Seasonal Monitoring Program”.⁽²⁸⁾ In addition, ground water depth and climatic measurements (air temperature and rainfall) were conducted.

The following are the main components of the pavement instrumentation program. It should be noted that only the AC and air temperatures were monitored for the sections in the Temperature Correction Study.

- Moisture Content Measurement
- Pavement Temperature Measurement
- Frost/Thaw Depth Measurement
- Ground Water Depth Measurement
- Climatic Measurements (air and rainfall)

Details of the instrumentation installation at each of the selected sites have been provided earlier as separate reports. Appendix A shows a sample report from Site 4. Common elements of the installation are described herein.

Moisture Content Measurement

The FHWA’s TDRs were installed and used to monitor the moisture content of the unbound layers (aggregate base, subbase, and subgrade). TDR probes were permanently installed in the slow traffic lane at 2 to 3 ft from the pavement/shoulder joint. Cables were extended to an equipment cabinet located outside the road, where the automatic recording equipment was installed.

Pavement Temperature Measurement

Thermistors were used to monitor the pavement subsurface temperatures. Thermistor probes permanently installed in the pavement continuously measured the surface, base, subbase, and subgrade temperatures. A data logger permanently installed in the equipment cabinet automatically recorded the subsurface temperature profiles.

Frost/Thaw Depth Measurement

Temperature gradients have traditionally been used to determine depth of frost/thaw penetration into a soil. However, since de-icing chemicals can depress the freezing point, the temperature

gradient method can be unreliable. Presently, measuring the electrical resistance and resistivity is the most reliable method of determining depth of frost/thaw penetration. Therefore, electrical resistivity probes permanently installed in the pavement were used to measure the frost/thaw depth.

Ground Water Depth Measurement

The depth of the ground water table was measured through observation piezometers. The piezometers were placed in the shoulder, a few feet outside the pavement.

Climatic Measurements (Air Temperature and Rainfall)

Air temperature and rainfall were measured using an air temperature probe and a tipping-bucket rain gauge on a pole next to the equipment cabinet. The air temperature probe and tipping-bucket gauge were permanently installed and continuous readings were taken through the project duration.

Figure 15 shows a typical instrumentation layout. Table 6 and Figures 16 and 17 show the instrumentation classes.

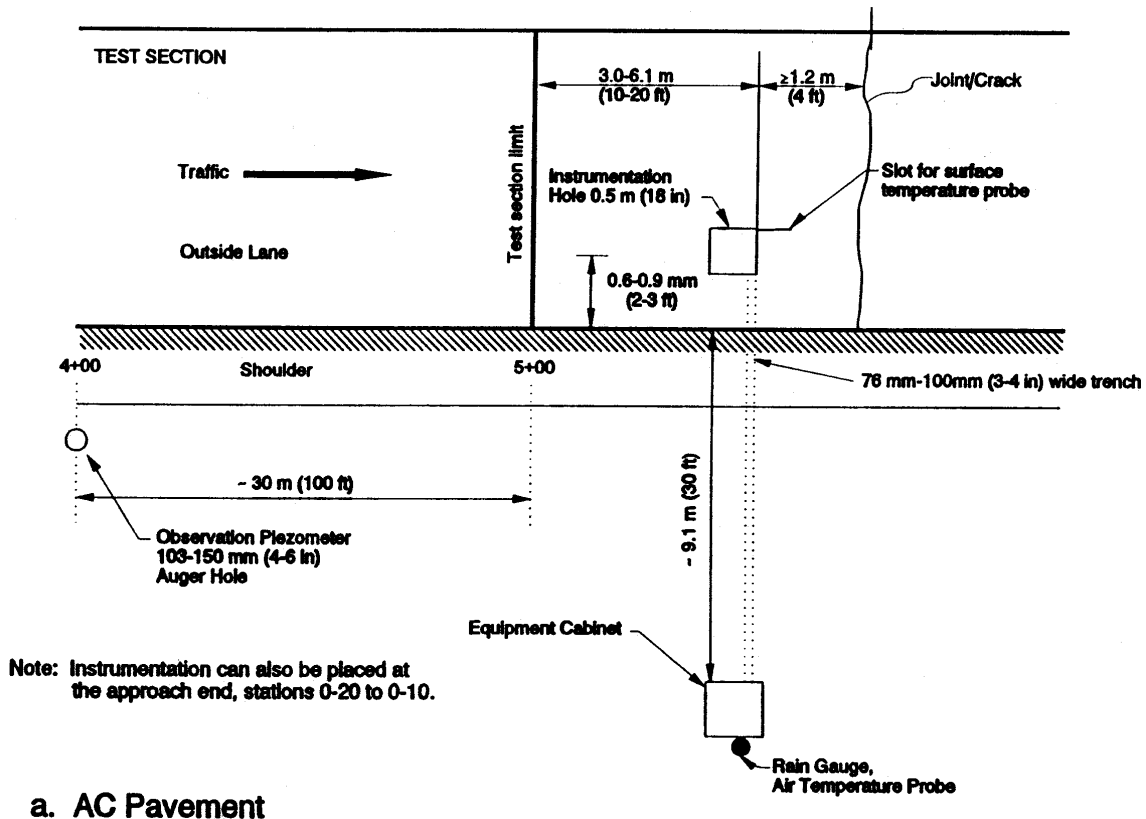


Figure 15: Typical Instrumentation Layout

Table 6: Instrumentation Class

Study	Moisture Content*	Pavement Temperature*	Frost/Thaw Depth	Ground Water Depth	Air Temperature	Rainfall
Seasonal Adjustment	3	11	Yes	Yes	Yes	Yes
Temperature Correction	--	3	--	--	Yes	Yes

* Number of Test Points

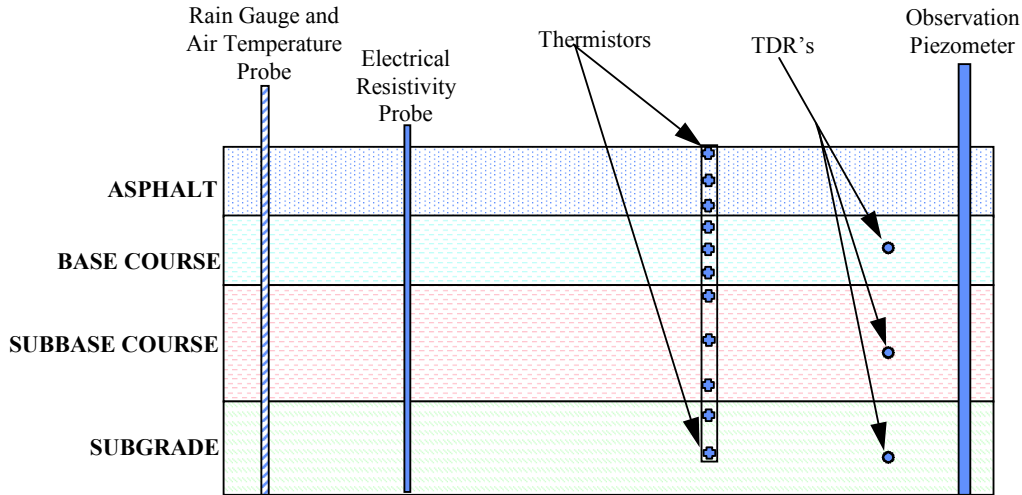


Figure 16: Seasonal Adjustment Instrumentation

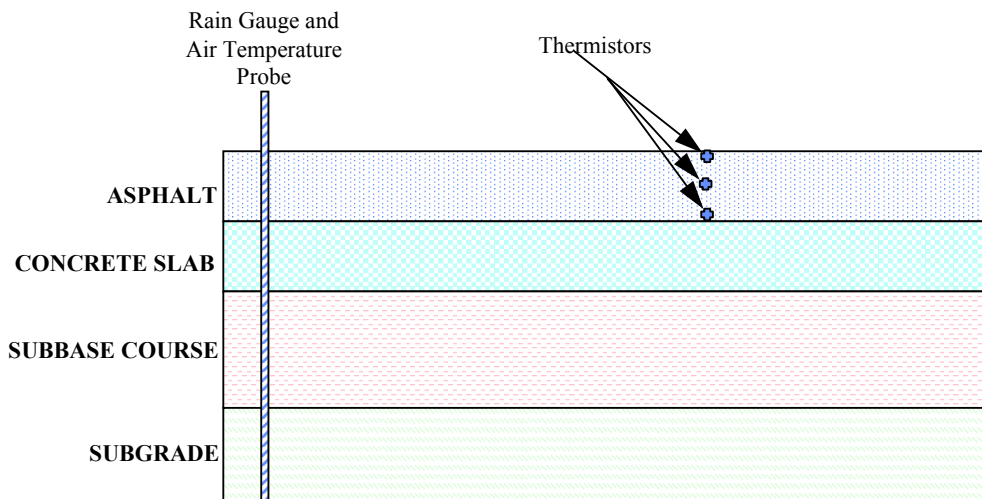


Figure 17: Temperature Correction Instrumentation

A special instrumentation plan was prepared for the LTPP-SPS sites. Figures 18 and 19 show the instrumentation plans for the SPS-5 and SPS-9 sites, respectively.



PROPOSED SEASONAL MONITORING PROGRAM FOR
FHWA-LTPP SPS 5 NEW JERSEY EXPERIMENT
REHABILITATION OF A/C PAVEMENTS

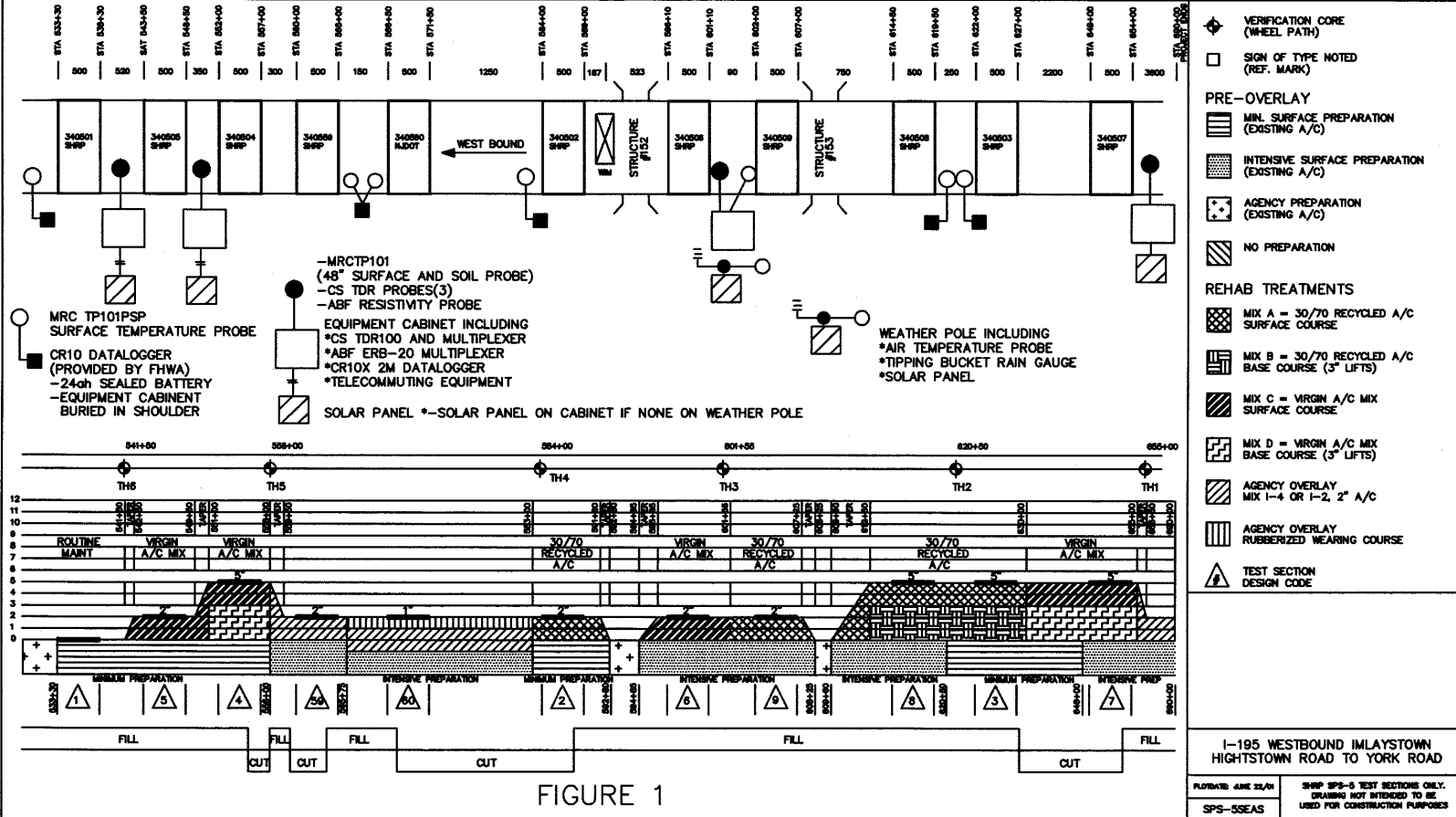


Figure 18: Instrumentation Plan for SPS-5

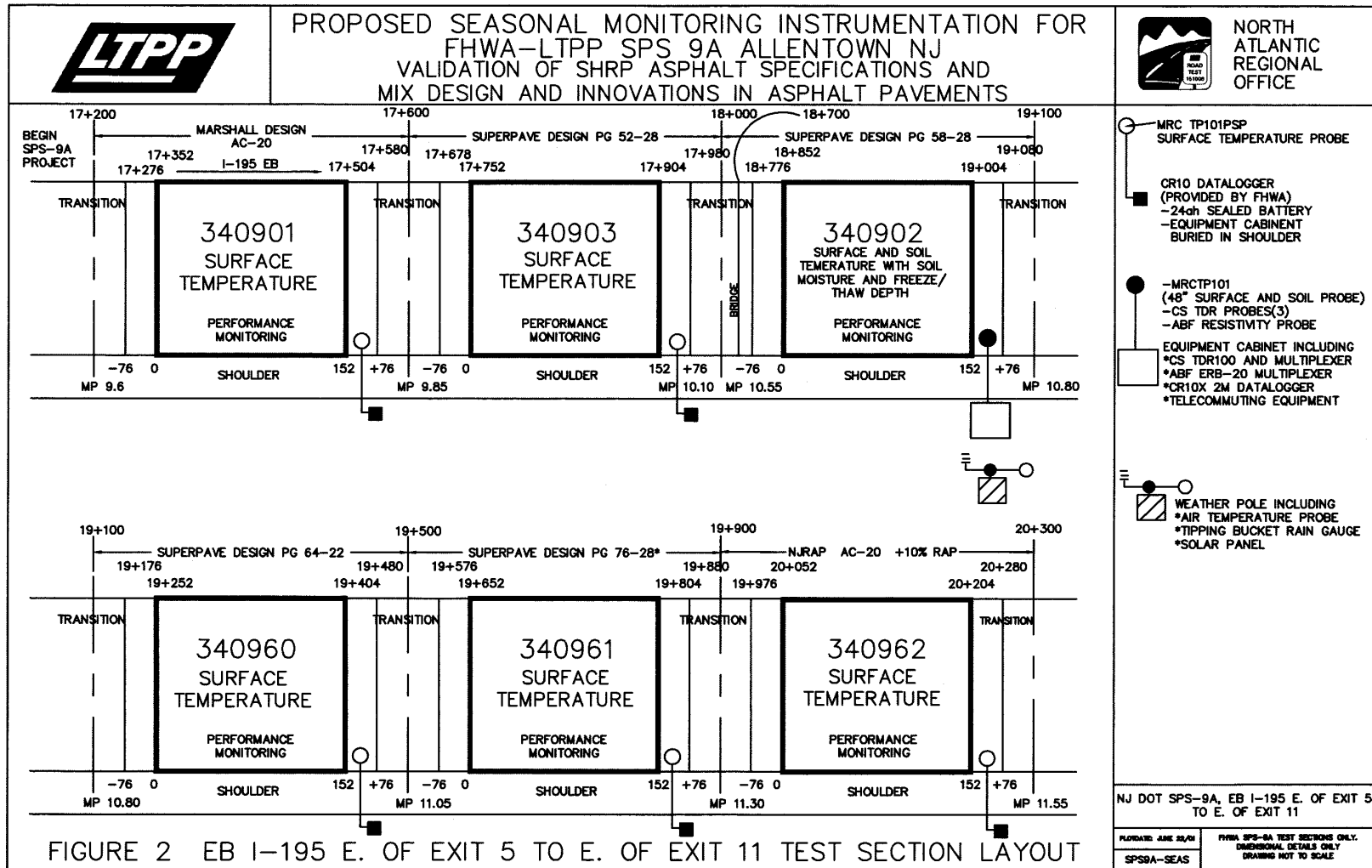


FIGURE 2 EB I-195 E. OF EXIT 5 TO E. OF EXIT 11 TEST SECTION LAYOUT

Figure 19: Instrumentation Plan for SPS-9

Equipment Setup & Installation

The equipment installed at the test site included instrumentation for measuring air, pavement, and subsurface temperature; subsurface moisture content; frost depth; precipitation; and water table. An equipment cabinet was also installed to hold the datalogger, battery pack, and all electrical connections from the instrumentation. A list of the equipment installed is shown in Table 7. Figures 20 to 23 show the various instruments and equipment installed at the test sites.

Table 7: Equipment Installed

Equipment	Quantity	Serial Number
Instrumentation Hole		
TDR Probes (CS610)	3	2-1 to 2-3
MRC Temperature Probe (TP101)	1	101001-NJ-2
ABF Resistivity Probe	1	2
Equipment Cabinet		
Campbell Scientific Datalogger (CR10X)	1	X27903
Campbell Scientific TDR 100 Time Domain Reflectometer	1	1188
Campbell Scientific Multiplexer (SDMX50SP)	1	3138
ABF-ERB 20 Resistivity Multiplexer	1	R001
HD 12V-19AH Battery	1	HD-NJ-2
Crydom Relay	1	CR-NJ-2
AVW1 Vibrating Wire Interface	1	3515
Datalogger Wiring Panel	1	18012
Weather Pole		
TE525 mm Tipping Bucket (rain gauge)	1	29154-801
CS 107 Air Temp. Probe	1	111001-NJ-2
ATP Radiation Shield	1	RS-NJ-2
MSX20R Solar Panel	1	I0101221693406
Other Equipment		
Observation well/benchmark	1	



Figure 20: Tipping Bucket, Solar Panel, and Air Temperature Probe



Figure 21: TDR and Temperature Probes



Figure 22: Resistivity Probe

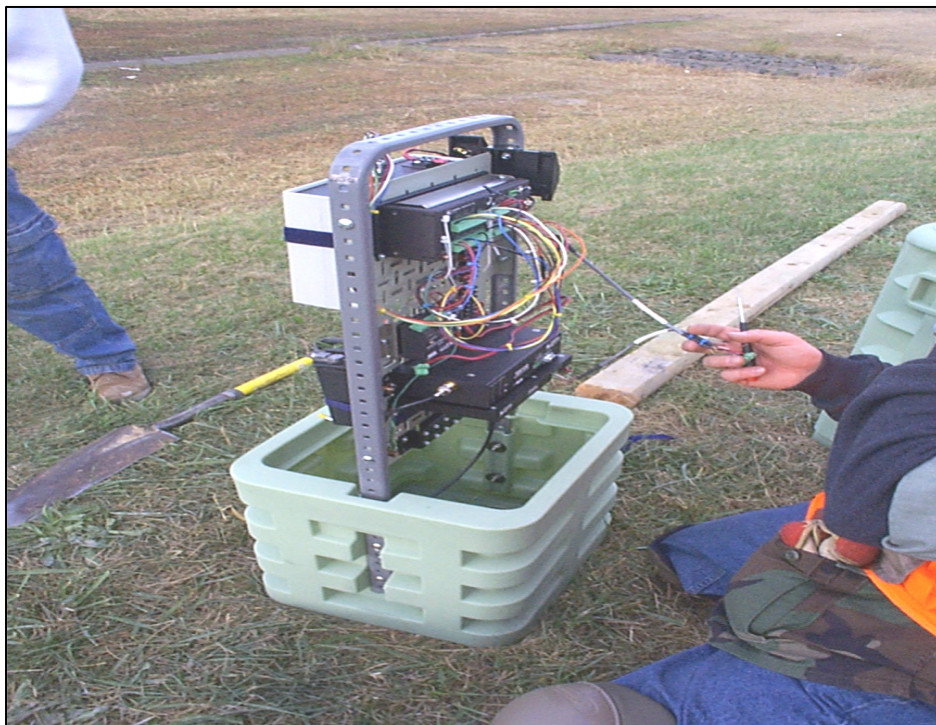


Figure 23: Data Logger and Housing Cabinet

Equipment Check/Calibration

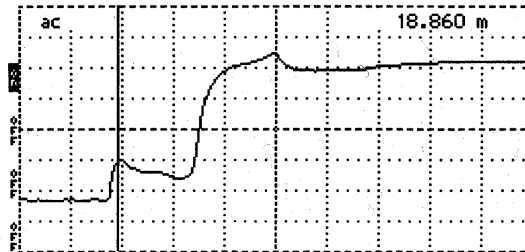
Prior to the installation, each measurement instrument was checked or calibrated. The tipping bucket rain gauge was connected to the CR10X datalogger for calibration. A plastic container with 16 oz. of water was placed in the tipping bucket. The container had a small hole in the bottom, which allowed all the water to be drained out in 45 minutes. For the 16 oz. of water, the tipping bucket should measure 100 tips \pm 3 tips. The results showed 97 tips, which was within specification.

The air temperature and thermistor probes were connected to the CR10X datalogger simultaneously. Functional checks were made by placing the probes in ice and hot water. In order for the probes to pass this check, the temperatures for each probe should correspond to the exact temperature measured with the temperature gauge. The check indicated that the air temperature and thermistor probes were working properly. A second check was made where the air temperature and thermistor probes were connected to the datalogger and run, in air, for 24 hours. The minimum, maximum, and mean temperature for each sensor was checked. All 11 thermistors were similar in their minimum, maximum, and mean readings, therefore the probes were considered to be functioning correctly.

The wiring of the resistivity probe was checked using continuity measurements between each electrode and the corresponding pins on the connector. The distance between each electrode was measured and recorded. The checks on the resistivity probe indicated that all electrodes were functioning properly.

The functioning of the TDR probes was checked by performing measurements in air and water, and with the prongs shorted at the circuit board. The traces were taken and the dielectric constant was calculated for water and air. Figure 24 shows a sample TDR trace obtained during calibration. These values were checked against expected dielectric constants for each medium. The test indicated that all probes were functioning properly.

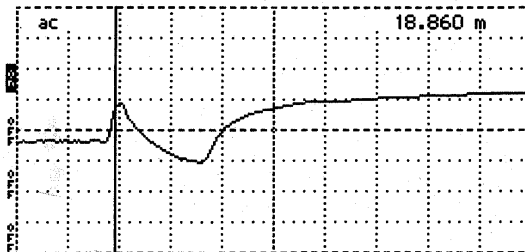
Cursor 18.860 m
 Distance/Div..... 0.5 m/div
 Vertical Scale.... 177 mP/div
 VP 0.99
 Noise Filter..... 1 avs
 Power ac



Tektronix 1502C TDR
 Date DEC 20, 2001
 Cable 3-1 (50SE)
 Notes INSTALLED

Input Trace _____
 Stored Trace _____
 Difference Trace _____

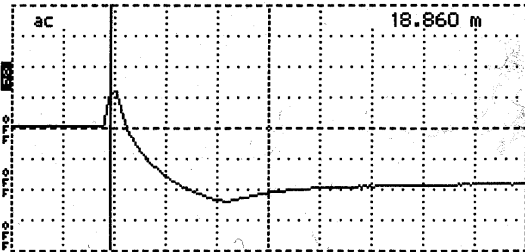
Cursor 18.860 m
 Distance/Div..... 0.5 m/div
 Vertical Scale.... 177 mP/div
 VP 0.99
 Noise Filter..... 1 avs
 Power ac



Tektronix 1502C TDR
 Date DEC 20, 2001
 Cable 3-2
 Notes _____

Input Trace _____
 Stored Trace _____
 Difference Trace _____

Cursor 18.860 m
 Distance/Div..... 0.5 m/div
 Vertical Scale.... 177 mP/div
 VP 0.99
 Noise Filter..... 1 avs
 Power ac



Tektronix 1502C TDR
 Date DEC 20, 2001
 Cable 3-3 (50SE)
 Notes INSTALLED

Input Trace _____
 Stored Trace _____
 Difference Trace _____

Figure 24: Sample TDR Trace During Calibration

Installation Procedure

The pavement surface coring and drilling, augering of the piezometer and instrumentation hole, and the sawing of the trench and cut for the pavement surface temperature probe were performed by agency equipment and drilling crew (Jersey drilling) under the supervision of Stantec staff. Lane closures were provided for the sections located on open highways (the test section on RT-130 and the LTPP-SPS sections on I-195).

Instrumentation bore holes and test pits were dug. A flight auger was used for drilling the hole. A core hole was drilled in the pavement surface using a 12 in thin wall diamond core barrel attached to the truck-mounted drilling unit. A 0.42 ft wide by 0.72 ft deep saw cut was made between the core hole and the edge of the pavement, using a heavy-duty pavement sawing machine. Material was removed in 12 to 16 in lifts. The actual layer thickness of the test sections was measured through the instrumentation holes. Care was taken to ensure that the material was stored in the order of excavation. The material removed was stored in buckets with distinct layers separated. The remainder of the material from the trench was removed with a trencher and shovels.

The measurement equipment, observation piezometer, weather station pole and cabinet were installed by Stantec crew. Assistance was provided by Tony Chmiel of the NJDOT Research Group.

A combination benchmark/piezometer was placed at the instrumented sites at a certain distance (approximately 48 ft) from instrumentation holes and beyond the pavement edge. The cabling from the instrumentation was placed in a 0.42 ft flexible conduit and buried in a trench running from the instrument hole to an equipment cabinet installed on the slope of the roadway embankment. To support the cabinet, existing site materials were spread around the cabinet base. The weather pole was installed outside of the curb. A wet vacuum and sponges were used to remove as much moisture resulting from the coring machine as possible.

Samples of the material placed around each TDR probe were retained for laboratory moisture determination by Center of Advanced Infrastructure and Transportation (CAIT), Rutgers. The equipment cabinet and pole for the rain gauge and air temperature probe were installed as per manual guidelines. The excavation of the extended trench from the edge of the pavement to the cabinet proceeded fairly smoothly as the material was mainly grass.

To check for breakage of the TDR probes during installation, each probe was connected to the cable tester and its waveform monitored during compaction of the material around it. The TDR probes were placed such that the cables coming out of them were evenly spaced around the perimeter of the hole to avoid water migrating along a bundle of cables. The thermistor and resistivity probes were installed at opposite sides of the instrumentation hole, just below the pavement surface. The cables were kept as well-spaced as possible until they converged at the opening of the flexible conduit pipe, placed about 2 in from the edge of the core hole. The cables were then tie-wrapped and passed through the conduit to the equipment cabinet. The ends of the conduit were plugged with a mastic pipe sealant.

Site Repair and Cleanup

The instrumentation hole and material sampling were repaired by reinstalling the 12 in core. Some juggling was required to get the core level with the existing pavement surface. Once the core was leveled it was removed from the hole and the bottom 4 in were heavily covered with a two-part epoxy (PC-7) and reset into the hole, forcing the epoxy against the side and up along the wall of the hole. The holes for the core samples removed for material analysis were then filled with cold mix and compacted.

The trench for the cabling from the instrumentation hole to the edge of pavement was leveled with the native material to the existing bottom of the paved layer and a cold mix was compacted to the level of the existing surface. The remainder of the trench was filled with native material and compacted, followed by a cleanup of loose material from the paved area. The instrument hole was sealed using Corning self-leveling 888 crack sealing compound followed by the removal of the asphalt trench material and other disposable items.

Patch/Repair Area Assessment

The sites were visited one month after the installation and were found, overall, to be in good condition.

Materials Investigation Plan

Field samples, asphalt cores, and Shelby tubes, were recovered from the flexible pavement test sections. Standard characterization of asphalt and aggregate samples was made in Rutgers' geotechnical and asphalt pavement laboratories (RAPL). It should be noted that no laboratory tests were performed on concrete material. The following tests were conducted:

Asphalt Layers

- Rice Test (ASTM D4311)
 - Air Voids
 - Specific Gravity
 - Maximum Theoretical Density
- Asphalt Content

Unbound Layers (Base, Subbase, and Subgrade)

- Standard Soil Characterization Tests
 - Grain Size Analysis (ASTM D422)
 - Atterberg Limits Evaluation (ASTM D4318)

Falling Weight Deflectometer Testing

An LTPP-SHRP calibrated Heavy Weight Deflectometer (HWD), which is a heavier version of the FWD, was used to measure pavement deflections (Figure 25). An initial deflection survey was performed prior to installing the planned instruments. In this survey, FWD testing was performed on the test section, instrumentation hole, and materials sampling hole. Also, a detailed condition survey (visual inspection) was performed prior to the pavement instrumentation.



Figure 25: Dynatest HWD

The deflection testing of the flexible pavement sections was performed on the outer wheel path and mid-lane at 25 ft intervals. For rigid pavement sections, mid-slab tests were performed at the outer wheel path and mid-lane, while joint testing was performed at the outer wheel path only. Composite pavement sections were tested in the same way as rigid pavement sections, if the reflective cracks were visible; otherwise, they were tested in the same way as flexible pavement test sections. No deflection testing was performed directly over the instrumentation. The FWD load plate was placed at least 3 ft away from the instrumentation and materials sampling holes.

FWD testing was performed every month on all sites for two years (February 2002 to March 2004). Two additional tests were performed during the spring thaw and fall periods (spring and fall) at two sites. In total, 28 FWD testing cycles were performed over the 2-year period. FWD tests were performed at three load levels, namely, 7, 9, and 12 kips. Surface and air temperatures were measured before the first testing and every 30 minutes after that. Surface and air temperature were monitored continuously by the FWD during testing. Additionally, manual temperatures were taken before the start of testing and every 30 minutes until completion of FWD testing. The manual temperature measurements were made at three depths of .5 in mid depth and 1 in from the bottom of the AC or slab using an Omega thermometer probe with a digital readout.

Additionally, 24-hour testing (two-hour intervals) was performed on the Non-LTPP Sections S-4 and S-6 in November 2002 and April 2003, respectively.

FWD Testing Protocols

Testing procedures were conducted according to a predefined testing protocol. The following guidelines were used for field staff involved in carrying out FWD/HWD testing for the NJDOT Seasonal Study project.

The Sensor Configuration for HWD was set to have 9 sensors, one before load plate, one at load plate, and 7 after load plate. The spacing is shown in Table 8.

Table 8: HWD Sensor Spacing

Sensor Number	9	1	2	3	4	5	6	7	8
Offset from Load Center (in)	-12	0	8	12	18	24	36	48	60

The Target Loads for flexible and rigid/composite pavements are shown in Table 9.

Table 9: Target Loads for FWD Testing

Drop No.	Target Load for Flexible Pavements (lbs)	Target Loads for Rigid and Composite Pavements (lbs)
1	6500	9000
2	9000	12000
3	12000	14000

The air, surface, and gradient temperature data was collected at various times during the test cycle. For the HWD, automated air (thermistor sensor mounted on HWD trailer) and Infrared pavement surface temperature were collected, as well as manual gradient temperatures.

File Naming Protocols

A file formatting was used for FWD file naming as follows:

File Naming Convention

34S#yyab.f25 for HWD

= site number ; yy = year

a = Month of visit; b=testing category lane spec

To simplify the identification of pavement types, three test setup screens were developed for HWD (Dynatest V. 25). These test setup screens use the same features and drop sequences, but are named differently to allow for easy identification of pavement type tested. The setups are as follows:

- 1-Flex (Metric Units)
- 2-Rigid Basin Edge Test (Metric Units)
- 3-Rigid Load Transfer Test (Metric Units)

The test point naming was set as follows:

For Rigid & Composite Pavement

In Test Category:

Input	J1	for mid-lane mid-slab
	J2	for pavement edge corner
	J3	for pavement edge mid-slab
	J4	for outer wheel path approach slab
	J5	for outer wheel path leave slab

For Flexible Pavement

In Test Category:

Input	F3	for outside wheel path
-------	----	------------------------

Seismic Pavement Analyzer (SPA) Testing

A SPA, developed by University of Texas at El Paso through the SHRP program and manufactured by Geomeia Research and Development, Inc., as shown in Figure 26, was used in elastic modulus profiling of the selected test sections.

Since the speed of pavement evaluation and the size of the test area of the FWD and the SPA are about the same, a testing plan and sequence identical to the FWD testing plan and sequence, as stated previously, were implemented.

Four seismic tests are of primary interest during SPA testing. The first two tests are ultrasonic (or high frequency) tests used in evaluation of elastic moduli and the thickness of the surface layer: ultrasonic surface wave (USW) and impact echo (IE). The USW technique evaluates the surface layer modulus from the velocity of high frequency (short wavelengths) surface waves.

Since the USW technique is an actual direct measurement of elastic moduli, not a backcalculation-based technique, it is considered to be the most reliable seismic method for the AC or PCC modulus evaluation. The second test is the impulse response (IR) test. The primary objective of IR testing is evaluation of the elastic modulus of the subgrade of rigid and composite pavements, and a composite elastic modulus of flexible pavements. The third test, the spectral analysis of SASW, is used in pavement modulus profiling. Since the resolution of the SASW testing decreases with depth, anticipated benefits of the method are higher in the evaluation of moduli of layers closer to the surface.



Figure 26: Seismic Pavement Analyzer (SPA)

SPA testing was performed over a two-year period (February 8, 2002, to February 27, 2004) and involved a total of 19 test cycles at the seasonal sites. Additionally, two 24-hour continuous SPA tests were performed on the Non-LTPP Sections S-4 and S-6 in October 2002 and April 2003, respectively. The testing was not conducted during the coldest winter days, because the pneumatic system of the SPA does not allow data collection at temperatures at or lower than freezing.

SPA Testing Protocols

Testing procedures were conducted according to a pre-defined testing protocol. Since the sensor configuration (5 accelerometers, 3 geophones, and 2 impact sources) cannot be changed, the data was collected using the manufacturer’s pre-defined setup defined in Table 10 and shown in Figure 27.

Table 10: SPA Sensor Distance from Impact Sources

Sensor Number	A1	A2	A3	A4	A5	G1	G2	G3	
Offset from Source Center (in)	3	6	12	24	48	3	30	78	

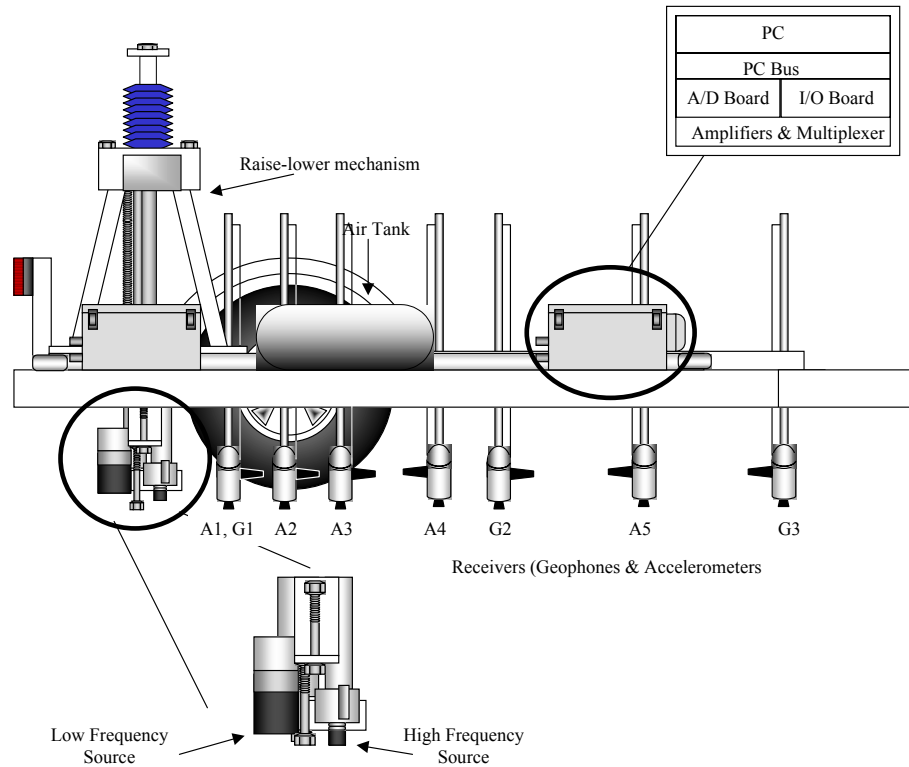


Figure 27: Schematic of SPA

File Naming Protocols

File formatting is predefined by SPA software. However, data for each test section and a particular test date were stored in separate directories. The associated comments file contains information about each particular test file. Six banks of data for a single test point were stored in a single compressed file.⁽²⁹⁾

DATA PROCESSING AND PRELIMINARY ANALYSIS

Data Handling

The climatic and FWD data, sampled materials, and field activity logs were handled and processed at the field office according to the following guidelines to ensure that the highest level of quality data was released for subsequent processing:

- Organize and check field data transmittals;
- Restore to the field-processing computer and check for completeness and readability;
- Store samples for verification of pavement structure information;
- Resolve any missing data or information issues;
- Develop and update track sheets to monitor data flow;
- Copy and archive field data (hard copies, floppies, field logs, field condition survey forms, etc.); and
- Forward data to main office for office quality checks and processing.

Figure 28 shows a typical data check on the instrumentation installed at the study sites, which was carried out during each visit to download the data from the datalogger. The flowchart in Figure 29 presents the entire field data handling process.

<p>Daily Avg/Max/Min Air Temperatures Use ONSFIELD 2.1 (Graph 1) or Visually inspect raw data (<u>Record 1</u> contains Daily values)</p> <p>Rain Data Use ONSFIELD 2.1 (Graphs 1&6) or Visually inspect raw data (<u>Record 1</u> contains Daily values, <u>Record 5</u> contains Hourly values)</p> <p>Hourly Air/MRC Temperatures (5 MRC Temps.) Use ONSFIELD 2.1 (Graph 6) or Visually inspect raw data (<u>Record 5</u> contains Hourly AT values, <u>Record 6</u> contains Hourly MRC values)</p> <p>Daily Avg/Max/Min MRC Temperatures (11 Temps.) Visually inspect raw data (<u>Record 2</u> contains Daily Average values, <u>Record 3</u> contains Daily Maximum values & Times, and <u>Record 4</u> contains Daily Minimum values & Times)</p> <p>Resistivity Use MOBFIELD 3.0 (Graph 2) or Visually inspect raw data (<u>Record 7</u> contains Resistance voltages, <u>Record 27</u> contains Applied voltage & 100 kΩ Resistance voltage)</p> <p>TDRs (Site 1 has 4 Probes, Sites 2-6 have 3 Probes) Visually inspect raw data (<u>Records 10, 11, 12, and 13</u> contain TDR values)</p>
--

Figure 28: Typical Field Instrumentation Functionality Check

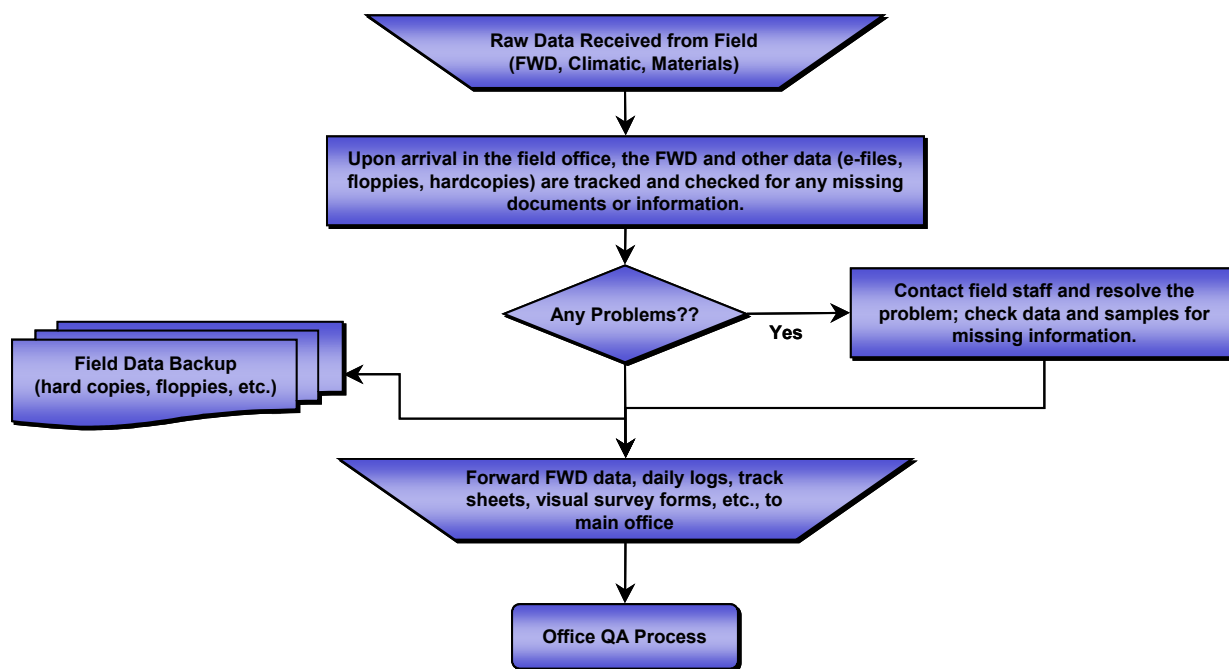


Figure 29: Field Data Handling Process Flow Chart

Data Tracking and Quality Checks

A database was created to store the collected data (climatic, FWD, SPA, etc.). The raw data was checked and reformatted as required for the database. Data quality checks were performed. Questionable data was stored in a separate table for further checking and verification. Data collected from the installed instruments was checked for reasonableness, missing data, or gaps in data due to equipment malfunctioning or other issues. It was also tracked to highlight any problems and to help in rectifying those problems.

Sample spreadsheets for overall tracking and for tracking individual instruments and equipment are shown in Figures 30 through 32.

Section	Automated Data Up To	Air Temperature	Rain-Fall	Freeze/Thaw	Water Depth -Month Collected
1	February 19, 2004	OK	OK	OK	NA**
2	February 18, 2004	OK	Tipping bucket plugged - Data from Sep 6-Oct 10 is suspect	OK	'02-Apr, May (dry), Jun (dry), Jul (dry), Aug (dry), Sep, Dec '03-Feb, Mar, May (2 sets, 1 dry), Jul, Aug, Sep, Oct, Nov, Dec '04-Jan, Feb
3	February 19, 2004	OK	OK	Some bad data sets in 2002	'02-Apr (dry), May (dry), Jun (dry), Jul (dry), Sep (dry), Oct (dry) '03-Feb, Mar, Apr, May (Dry), Jul, Aug, Sep, Oct, Nov, Dec '04-Jan
4	February 17, 2004	OK	Tipping bucket plugged - Data from Sep 1-6 is suspect	Suspect data in sensors 12-15	'02-Jan, Apr, May, Jun, Jul, Aug, Sep, Oct (7 sets), Nov, Dec (2 sets) '03-Feb, Mar, Apr (8 sets), May, Jul, Aug, Sep, Oct, Nov, Dec '04-Jan, Feb
5	March 9, 2004	Not working Apr 27-29, 2003 Jul 26-Nov 29: many spikes in data Nov 29, 2003-Jan 7, 2004: Few spikes in data	Not working Apr 27-29, 2003	OK	'02-Apr (dry), Jun (dry), Jul (dry), Aug (dry), Sep, Oct, Dec (dry) '03-Feb, Mar, Apr, May, Jul, Aug, Sep, Oct, Nov, Dec '04-Mar
6	February 24, 2004	OK	OK	OK	'02-Apr, May, Jun, Jul, Aug, Sep, Nov (6 sets), Dec (2 sets) '03-Feb (2 sets), Mar, Apr (7 sets), May (2 sets), Jul, Aug, Sep, Oct, Nov, Dec '04-Feb
7	February 14, 2004	OK	No rain in Jan & Feb, 2004	NA**	NA**

Figure 30: Sample Climatic Data Track Sheet

Figure 31: Sample TDR Data Track Sheet

SPS 5											
	A	B	C	D	E	F	G	H	I	J	K
Feb-02	Instrumentation Data										
Mar-02	Weather Problem (Rain)										
Apr-02	✓	✓	✓	✓	✓	✓	✓	✓	✓	✓	✓
May-02	Weather Problem (Rain)										
Jun-02	✓	✓	✓	✓	✓	Equipment Breakdown					
Jul-02	✓	Time Constraints			✓	Time Constraints			✓	✓	
Aug-02	Equipment Breakdown										
Sep-02	✓	✓	✓	✓	✓	✓	✓	✓	✓	✓	✓
Oct-02	Weather Problem (Rain)										
Nov-02	✓	✓	✓	✓	✓	✓	✓	✓	✓	✓	✓
Dec-02	✓	✓	✓	✓	✓	No MRC	✓	✓	✓	✓	✓
Jan-03	✓	✓	✓	✓	✓	✓	✓	✓	✓	✓	✓
Feb-03	✓	✓	✓	✓	✓	✓	✓	✓	✓	✓	✓
Mar-03	✓	✓	✓	✓	✓	✓	✓	✓	✓	✓	✓
Apr-03	✓	✓	✓	✓	✓	✓	✓	✓	✓	✓	✓
May-03	✓	✓	✓	✓	✓	✓	✓	✓	✓	✓	✓
Jun-03	✓	✓	✓	✓	Not Scheduled						
Jul-03	✓	✓	✓	✓	✓	✓	✓	✓	✓	✓	✓
Aug-03	✓	✓	✓	✓	✓	✓	✓	✓	✓	✓	✓
Sep-03	✓	✓	✓	✓	✓	✓	✓	✓	✓	✓	✓
Oct-03	✓	✓	✓	✓	✓	✓	✓	✓	✓	✓	✓
Nov-03	✓	✓	✓	✓	✓	✓	✓	✓	✓	✓	✓
Dec-03	✓	✓	✓	✓	✓	✓	✓	✓	✓	✓	✓
Jan-04	✓	✓	✓	✓	✓	✓	✓	✓	✓	✓	✓
Feb-04	Not Scheduled										

Figure 32: Sample FWD Data Track Sheet

Climatic and FWD Data Processing

The field data was handled and processed in the office according to the following guidelines to ensure the highest level of confidence in the collected data:

- Organize and check field data transmittals;
- Update the track sheets used to monitor data flow;
- Set processing and scheduling priorities;
- Restore to the office-processing computer and check for completeness and readability;
- Run QA check on output and resolve errors, if any;
- Carry out preliminary analysis on checked data;
- Check on log files created from the preliminary phase of analysis;
- Process data and resolve data issues;
- Provide processed data to key individuals responsible for carrying out the analyses related to various tasks within the project scope of work.

The climatic data was checked to ensure that the values recorded for rainfall, air and pavement temperatures, moisture content, etc., were within expected limits. TDR traces were checked to ensure reasonableness of the data collected. If major deviations from the expected range of values were found, reasons for the deviations were noted and if related to equipment malfunctioning, the field office was informed to rectify the problems.

The FWD data was processed in a timely fashion to prevent backlogs. Qualified data processors/engineers processed the FWD data at Stantec. Experience with FWD data collection and processing procedures is a requirement for anyone processing this data.

A secondary review of the processed data was carried out for completeness in terms of testing pattern, procedures, file naming, and other key data elements, prior to passing the data for analysis. The data was formatted in Microsoft Excel or equivalent for software setup, and included any additional information or comments.

Any anomalies in the processed data were resolved at this stage, up to and including manual upgrade of FWD data, if required. Figure 33 shows the flow process for the FWD QC/QA process.

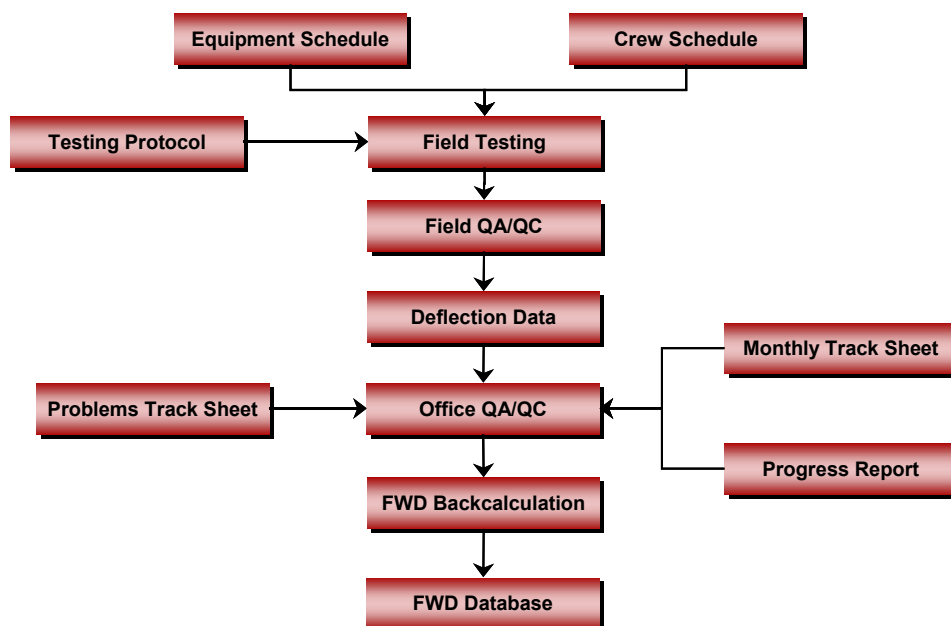


Figure 33: FWD Data Tracking and QC/QA Flow Process

As shown in the above figure, the field testing was carried out according to the previously mentioned protocol and a field QA/QC was performed immediately after testing to check the quality of data and retest the site if necessary. The deflection data, monthly tracking sheets, progress report, and problem tracking sheets were sent later to the main office for further QA/QC and analysis. In this process, the data collected was checked for any erroneous types of data, site information, checks against progress report, file naming convention, and follow ups were filed with technicians if necessary. A software package was implemented to automate the QA/QC, process large data, speed up processing time, and eliminate any human error in the process.

Preliminary FWD Analysis

A preliminary analysis was carried out on the deflection data obtained through the monthly and bi-monthly testing on the asphalt and concrete pavement sections at the project sites. The collected FWD data was first normalized to 9000 lb load level. The normalized deflection basins were corrected for the variation between the testing and the standard temperatures 21°C. This correction was made according to the 1993 AASHTO procedure. An analysis was performed on each deflection basin to backcalculate the effective pavement modulus, as well as the asphalt, aggregate, and subgrade moduli for the flexible pavement sections. A mechanistic analysis based on Boussinesq's Theory and O'dmark's Transformation approach was used for this purpose. For the rigid pavement sections, the deflection data was used to backcalculate the effective modulus of elasticity of the PCC slabs and the modulus of subgrade reaction (k) of the foundation.

A sample of the flexible pavement analysis results is shown in Table 11. Figure 34 shows a graphical representation of the tabulated result for Effective Pavement Modulus ' E_p '.

Table 11: Sample Preliminary Analysis Results (NJ Site 4)

Station (ft)	Deflection 'D ₁ '* (mils)	Resilient Modulus 'M _r ' (psi)	Pavement Modulus 'E _p ' (psi)
20	11.81	7112.24	116291.3
30	12.59	6969.5	113237.7
50	13.27	6044.81	118425.6
75	16.45	7233.42	73868.01
100	15.52	7473	79121.89
125	14.15	7549.75	90420.15
150	13.21	9145.64	91456.41
175	14.94	9185.86	77896.52
200	16.28	8764.31	70324.13
225	15.41	8110.63	77084.84
250	15.64	8579.24	72170.52

*D₁ is deflection at center of load plate.

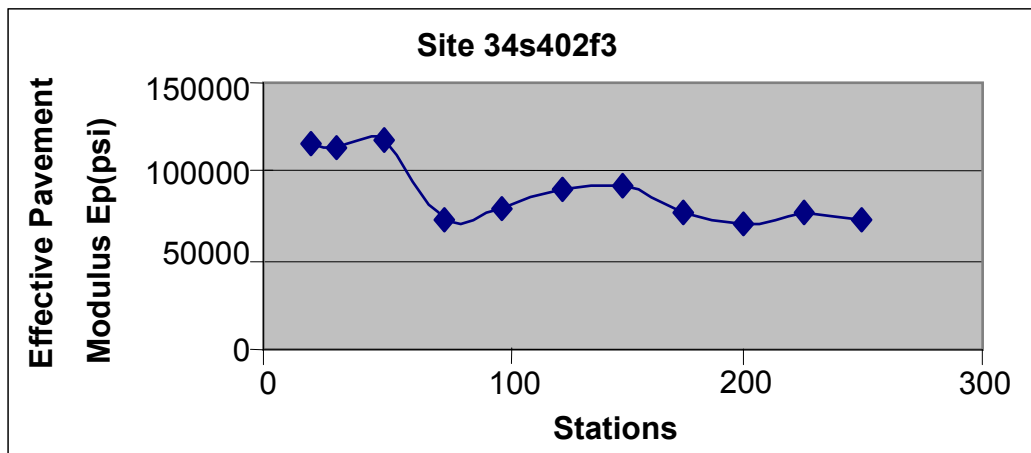


Figure 34: Typical Backcalculated Pavement Modulus (NJ Site 4)

SPA Data Processing and Analysis

The primary objective of the SPA analysis is to establish relationships between the evaluated elastic moduli and seasonal variations in moisture and temperature. While the ultrasonic methods provide direct measurement of elastic properties of the surface layer, moduli of the deeper layers evaluated by the SASW and IR methods require a backcalculation analysis. The backcalculation was conducted using a suite of programs developed by the University of Texas in El Paso. The following sections discuss data transfer, storage structure, and backcalculation of SPA collected field data.

Data Transfer and Data Storage

The collected SPA data is stored in a zip file archive. Each archive file contains four files:

1. Collected waveforms in binary format
2. Comments entered during data collection
3. Calibration factors
4. Structure of data banks

Upon completion of each monthly data collection cycle, collected data archives were transferred to a project dedicated computer and were backed up on a CD-ROM and an external hard drive. For each test section, an electronic log in Excel format was also generated based on the comments recorded during data collection including test location, archive number, date, time of tests, and operator comments. Prints of electronic logs were filed along with the field log.

In preparation for the backcalculation analysis, data archives were organized in a directory structure based on type of analysis, test section, and date. A typical data storage structure is depicted in Figure 35.

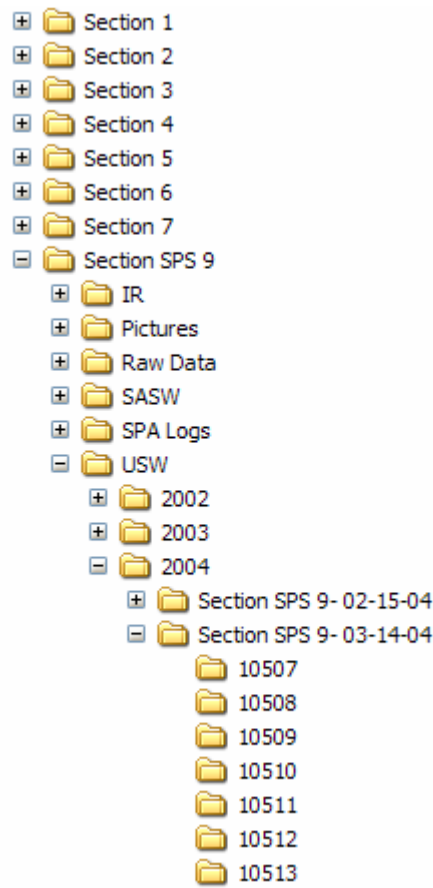


Figure 35: Typical SPA Data Storage Structure

Backcalculation results and any additional analysis, if necessary, were also stored under the same directory structure depicted in Figure 35.

Backcalculation Analysis

Collected field data was analyzed using three seismic techniques: SASW, IR, and USW; and were used to evaluate different mechanical properties of the pavement section. A brief description of each technique, steps involved in each analysis, and a description of corresponding software are presented below. A more detailed description of these techniques and software can be found in other studies.^(30,31)

Spectral Analysis of Surface Waves Analysis (SASW)

The SASW test is a non-destructive seismic technique for the *in-situ* evaluation of elastic moduli and layer thicknesses of layered systems like soils and pavements. The method is based on the phenomenon of Rayleigh wave dispersion in layered systems, i.e. that the velocity of propagation is frequency dependent. The objective of the test is to determine the velocity-frequency relationship described by the dispersion curve, and then, through the process of inversion or backcalculation, to obtain the shear wave velocity profile. The elastic modulus profile can then be easily obtained using simple relationships between the velocity of propagation and measured or approximated values for mass density and Poisson's ratio. The backcalculation of the SPA data was performed using "SASW – Ver. 2.0" program developed at University of Texas in El Paso. Screen shots of the program are presented in Figure 36.

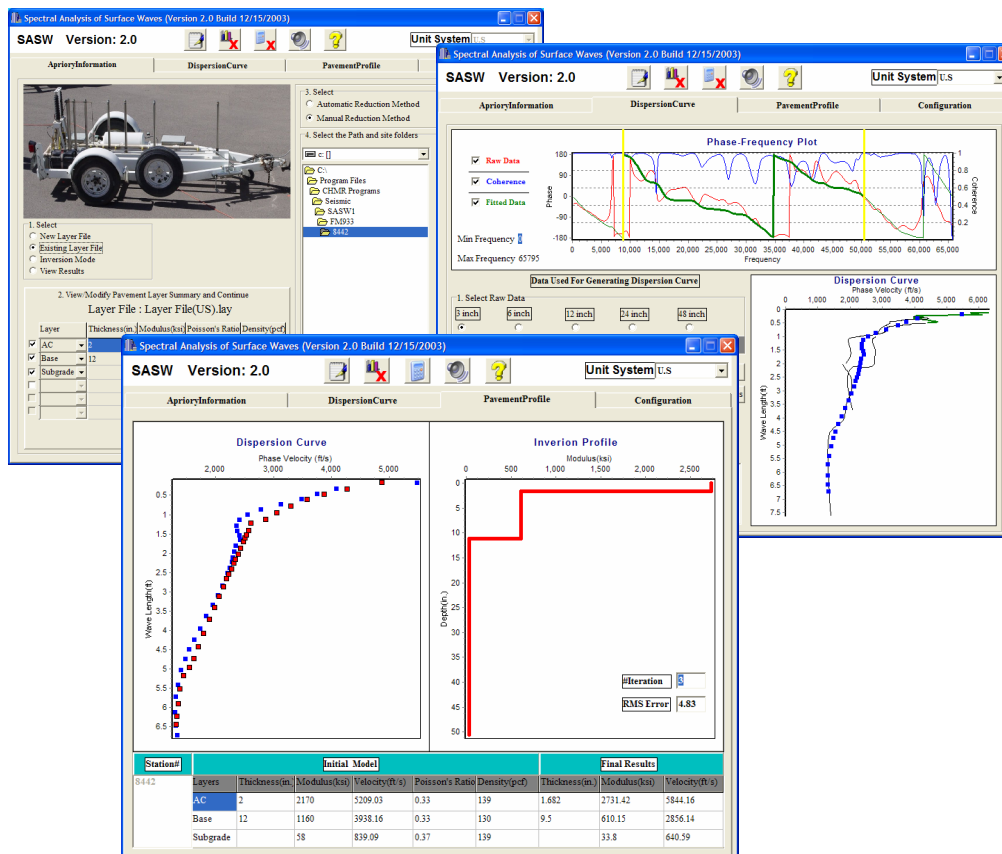


Figure 36: Screen Shots of SASW-Ver. 2.0 Program

Screen shots depict typical steps involved in the backcalculation of the test-developed dispersion curve. The process is briefly explained below:

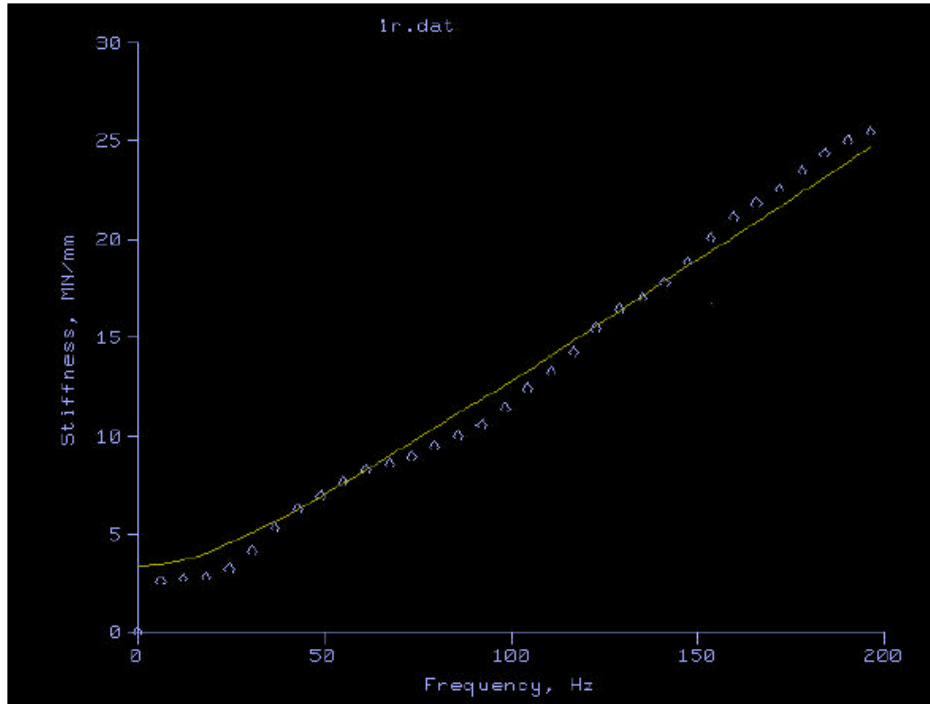
1. **Initial Settings:** The top left window in Figure 36 depicts the window where initial settings of the backcalculation analysis are entered into the program. These settings include file location and the analysis settings for each layer, such as initial or seed moduli values, initial thickness, Poisson's ratio, and density.
2. **Evaluation of Field Dispersion Curve:** Recorded signals from each receiver are transformed from the time to the frequency domain by the means of Fast Fourier Transform. Spectral functions are then applied to obtain information about the velocity as a function of frequency, which is called the phase velocity. Phase velocities for a range of frequencies form a dispersion curve. Dispersion curves are evaluated for a series of receiver spacings and averaged to obtain the average field dispersion. Discrete points on the average dispersion curve are then selected for a comparison with the theoretical dispersion curve. The top right window in Figure 36 depicts typical steps in the evaluation of the field dispersion curve.
3. **Backcalculation:** The last step in the SASW analysis is backcalculation or inversion of the dispersion curve to obtain the modulus profile. The backcalculation process generally involves forward modeling of an assumed pavement profile to obtain the theoretical dispersion curve and comparison of the obtained dispersion curve with the field evaluated dispersion curve. Once a satisfactory match between these two curves is obtained, thickness and moduli (shear wave velocities) of all the layers are evaluated. This is a complex, nonlinear problem that has been solved in a number of different ways. A typical dispersion curve for a pavement, and the backcalculated shear wave velocity profile are shown in the bottom window of Figure 36.

Impulse Response Analysis (IR)

The impulse response technique is used to determine the modulus of subgrade reaction (or the shear modulus of the subgrade) for rigid pavements, or the modulus of the overall system for flexible pavements. Signals from the impact hammer, the forcing function, and the response at the nearby geophone (velocity transducer) are transformed into the frequency domain to obtain the corresponding spectra. The ratio of the displacement and impact spectra represent a flexibility spectrum, while the inverse ratio is termed a mechanical impedance (dynamic stiffness spectrum). The mechanical impedance is matched by a mechanical impedance for an assumed single-degree-of-freedom (SDOF) system. Once the two spectra are matched, the modal properties of the SDOF system provide information about the shear modulus of the subgrade, or the modulus of subgrade reaction, and damping of the system. A screen shot of the IR program used in backcalculation of the test results is depicted in Figure 37. Theoretical and experimentally evaluated pavement impedances are shown in the figure.

Ultrasonic Surface Wave Analysis (USW)

The ultrasonic technique utilizes high frequency/ultrasonic surface waves to measure the shear modulus of a near surface region in layered structures like pavements. To evaluate the shear modulus, the shear wave (S-wave) velocity is measured from the average phase velocity of the surface wave in high frequency and ultrasonic frequency ranges, similar to the process in the SASW test. One of the strengths of the USW technique is that it is capable of measuring variations of the modulus within the top paving layer.



(triangle represents experimental data, solid line represents matched theoretical curve)

Figure 37: Screen Shot of IR Program

Laboratory Data Processing and Analysis

Laboratory testing was conducted on collected samples from a number of pavement sections in New Jersey. All bituminous samples delivered to the laboratory in the form of extracted cores were subjected to the following tests:

- Bulk Specific Gravity (AASHTO T166)
- Maximum Specific Gravity of the Loose Hot Mix Asphalt (AASHTO T209)

After receiving the cores, the cores were separated at the different lifts. The bulk specific gravity and maximum specific gravity of the loose HMA was determined for each lift to provide an air void and density profile of the asphalt pavement layer.

The geotechnical laboratory testing was conducted on the base, subbase, and subgrade materials collected during typical drilling/coring procedures. Unfortunately, only small quantities of materials could be collected and brought back to the laboratory. Therefore, the soil investigation was limited to:

- Grain Size Analysis (ASTM D422)
- Atterberg Limits (ASTM D4318)

All soil samples were air dried with a fan for 96 hours prior to testing. Once dry, the sample was split to provide a grain size distribution and Atterberg Limit determination.

Standard sieve analysis tests were conducted on representative samples that have been retained while washing the material through a No. 200 sieve. Air dried soil passing the No. 40 sieve was used to conduct the Atterberg Limit test.

STATISTICAL ANALYSIS

The major environmental factors that influence and affect pavement design and performance are temperature and moisture. This is particularly true in areas experiencing seasonal fluctuation in climate. Therefore, there is a need to correctly address such environmental factors, and analytically correlate their effects to pavement stiffness.

Statistical Analysis of the Seasonal and Temperature Impacts

Since environmental conditions vary with time (daily, seasonal, and longer cycles), their effect on the stiffness of pavement materials has to be investigated. The first step is to identify the environmental parameters that have significant impact on pavement performance (main effects). In addition, the interactions among these parameters that can significantly influence pavement performance should be considered. ANOVA is one of the tools available to identify the significant main effects, as well as the significant interactions between those effects. For this study, a statistical analysis was carried out using the ANOVA technique to identify the environmental parameters affecting pavement response, either individually or in association with other parameters. The following are parameters that were included in the ANOVA:

- Pavement Performance Parameters:
 1. FWD deflection at the center of the load plate (D_1) to represent the overall pavement structural capacity, including the subgrade.
 2. FWD deflection at 48 in from the center of the load plate (D_7) to represent the subgrade capacity.
 3. Difference between D_1 and D_7 (D_1-D_7) indicating the structural capacity of the pavement only, excluding the subgrade.
 4. The backcalculated effective pavement modulus (E_p).
 5. The backcalculated effective subgrade modulus (M_r).
- Environmental Parameters:
 1. Base course moisture content (M/C).
 2. Mid-depth AC temperature (Pav. Temp.) – the average of all the temperature sensors on the AC layer.
 3. Depth to ground water table (GWT).
 4. Rainfall.
 5. Air temperature (Air Temp.).

A Design of Experiment (DOE) was prepared for each performance parameter as the first step in performing ANOVA. In this DOE, as shown in Figure 38, the environmental parameters were classified into two levels – low (L) and high (H). The limits of each level were determined based on the available data.

A M/C	B PavTemp	C GWT	D Air Temp				E
			L		H		
			Rainfall		Rainfall		
			L	H	L	H	
L	L	H	23	17	6		
		L	5	2			
	H	H	1	5	8	6	
		L	2	1	14	10	
H	L	H	13	7	1		
		L	21	1	3		
	H	H	2		5	7	
		L			12	14	

 No records satisfy this condition

Initial Cutoff Values for Climatic Parameters (Based on Histogram)

	H	L
M/C (%)	>31	<=31
Pavement Temperature (°F)	>59	<=59
GWT (ft)	<=6.5	>6.5
Air Temperature (°F)	>57	<=57
Rainfall (in)	>0	0

Figure 38: Initial Design of Experiment

Statistical analysis was performed on the collected data to identify the limits of each parameter/level that provides balanced DOE, or as balanced as possible. The analysis results indicated that there are some parameter combinations were not available in the data, mainly because of the strong correlation between air and pavement temperatures. Some combinations, such as high air temperature and low pavement temperature, did not exist in the data. Therefore, a decision was made to split the DOE into two parts. In the first part the air temperature was dropped from the DOE, and the pavement temperature was considered (Figure 39); in the second part, the pavement temperature was dropped from the DOE and the air temperature was considered (Figure 40).

D1			E	
A	B	C	Rainfall	
M/C	PavTemp	GWT	L	H
L	L	H	41	28
		L	28	3
	H	H	11	12
		L	19	23
H	L	H	6	1
	H	L	9	1
		H	1	1
		L	1	1

Adjusted Cutoff Values for Climatic Parameters

	H	L
M/C (%)	>45	<=45
Pavement Temperature (°F)	>68	<=68
GWT (m)	<=2	>2
Air Temperature (°F)	>68	<=68
Rainfall (in)	>0	0

Figure 39: Revised DOE Considering Pavement Temperature Only

A	C	D				E
		Air Temp		Rainfall		
		L	H	L	H	
M/C	GWT	L	H	L	H	
L	H	44	32	7	11	
	L	41	4	6	18	
H	H	14	1	1	2	
	L	17	1	1	9	

Adjusted Cutoff Values for Climatic Parameters

	H	L
M/C (%)	>43	<=43
Pavement Temperature (°F)	>68	<=68
GWT (m)	<=2	>2
Air Temperature (°F)	>68	<=68
Rainfall (in)	>0	0

Figure 40: Revised DOE Considering Air Temperature Only

The data available in the project database was then grouped as per the 4 parameters of each DOE. ANOVA was performed to identify the significant main effects. Table 12 shows the results of the ANOVA analysis performed on the pavement temperature and air temperature DOEs, respectively.

As can be seen from Table 12, all main effects (air temperature, pavement temperature, MC%, GWT, and rainfall) have significant impact on overall pavement deflection (D_1), differential pavement deflection (D_1-D_7) and the Effective Pavement Modulus (E_p), which is expected. However, GWT and pavement temperature were found to have no significant impact on the subgrade deflection (D_7). This finding does not agree with the common assumption made in backcalculation analyses that GWT acts as a rigid layer. However, in a previous study performed for the Indiana Department of Transportation (INDOT), the same conclusion was reached.⁽³¹⁾

The next step in the analysis was to consider the main effects and 2-way interactions on each of the performance parameters. Results of the analysis indicated that all main effects and 2-way interactions have significant impact on overall pavement deflection (D_1), differential pavement deflection (D_1-D_7) and the Effective Pavement Modulus (E_p). On the other hand, pavement temperature was found to have no significant impact on the subgrade deflection (D_7) and subgrade resilient modulus (M_r).

Development of Regression Models

The ANOVA results indicated that the environmental parameters have a significant impact on flexible pavement response to FWD testing. The next step in the analysis was to develop regression models to account for the impact of the environmental parameters on pavement response, and, hence, pavement performance. These models are required to estimate the impact of seasonal variation on pavement response parameters and not the pavement response parameters themselves. In other words, regression models developed based on the ANOVA presented herein will estimate the deflection D_1 under different environmental conditions. The estimated D_1 in such cases will not be a function of the pavement cross-section parameters, as this is not the purpose of developing such models. Therefore, similar analysis is required to evaluate the significance of the environmental parameters on the difference between the measured deflection and the deflection expected at some standard conditions, such as a standard deflection basin. The differences considered in this analysis include:

- ΔD_1 : the difference between the measured deflections and forward calculation deflections for the 1st sensor.
- ΔD_7 : the difference between the measured deflections and forward calculation deflections for the 7th sensor.
- $\Delta(D_1-D_7)$: the difference between the measured difference in the deflections of the 1st and 7th sensors and the forward calculation difference in the deflections of the 1st and 7th sensors.
- ΔM_r : the difference between the backcalculated subgrade moduli that were used in the forward calculation.
- ΔE_p : the backcalculated effective pavement moduli that were used in the forward calculation.

Table 12: Main Effects ANOVA Results for (ΔD_1 , ΔD_7 , $\Delta\{D_1-D_7\}$, ΔM_r and ΔE_p)

Environmental Parameter	Temperature Used	F Ratio	Signific.	F Ratio	Signific.	F Ratio	Signific.	F Ratio	Signific.	F Ratio	Signific.
Overall Pavement Structure Source		D₁		D₇		D₁-D₇		M_r		E_p	
MC	Pavement	1121.8	S*	101.7	S	1221.7	S	228.9	S	94.0	S
Pavement Temperature	Pavement	1995.6	S	0.4	NS	2315.7	S	1.6	NS	2985.6	S
GWT	Pavement	745.6	S	295.3	S	758.4	S	500.8	S	79.9	S
Rainfall	Pavement	18.8	S	101.5	S	12.9	S	120.4	S	258.3	S
MC	Air	962.8	S	603.2	S	940.4	S	762.6	S	48.7	S
Air Temperature	Air	953.0	S	1224.6	S	873.2	S	1378.6	S	53.0	S
GWT	Air	1331.8	S	3.6	NS*	1517.1	S	11.2	S	2379.9	S
Rainfall	Air	10.4	S	11.2	S	9.8	S	44.0	S	214.6	S
Overall Pavement Structure Source		ΔD_1		ΔD_7		$\Delta(D_1-D_7)$		ΔM_r		ΔE_p	
MC	Pavement	1.9	NS	533.6	S	134.6	S	22.9	S	137.9	S
Pavement Temperature	Pavement	3787.0	S	121.1	S	6180.8	S	189.7	S	6432.7	S
GWT	Pavement	572.8	S	92.2	S	1130.5	S	216.2	S	21.3	S
Rainfall	Pavement	999.0	S	495.1	S	594.9	S	13.8	S	2.7	NS
MC	Air	82.0	S	459.0	S	1.6	NS	257.2	S	158.5	S
Air Temperature	Air	124.1	S	346.8	S	505.6	S	277.3	S	496.2	S
GWT	Air	3795.8	S	4.0	NS	4943.6	S	15.5	S	5287.8	S
Rainfall	Air	1153.7	S	670.2	S	586.9	S	101.2	S	17.5	S

*S represents significant effect; NS represents Non-Significant effect

A multi-layer analysis approach was used to establish the standard deflection basin for each test section. In this analysis, the average layer modulus values backcalculated from all FWD tests at a particular section (24 test cycles on average) were used in the forward calculation to determine the standard deflection basin for this section. The differences between the deflection basins measured under different environmental conditions (monthly test cycles) and the standard deflection basins were calculated and categorized as per the same DOEs presented earlier. Everstress (version 5) Software was used in the forward calculations. A sample of the results is shown in Figure 41.⁽³²⁾

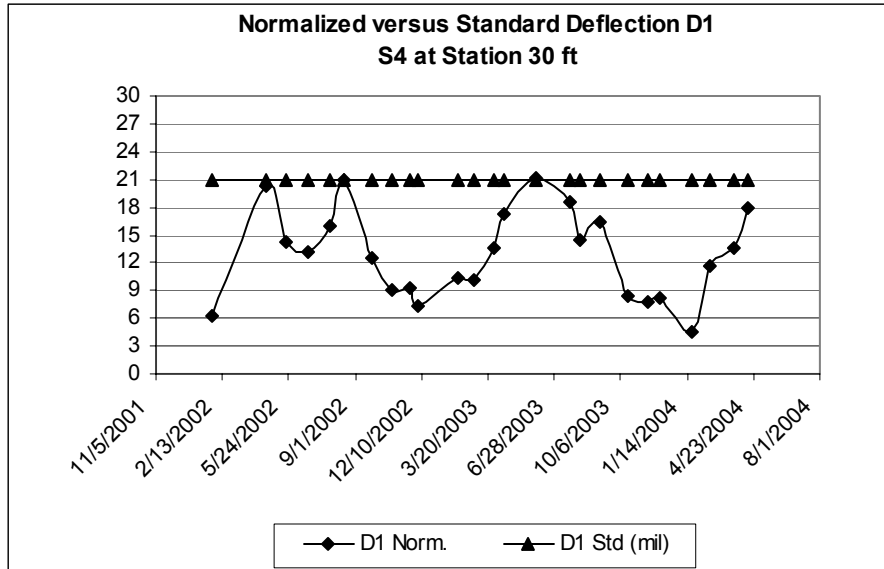


Figure 41: Normalized Actual D_1 versus Standard D_1

The ANOVA analysis was then repeated to identify the significant main effects and 2-way interactions on each of the performance parameters (ΔD_1 , ΔD_7 , $\Delta\{D_1-D_7\}$, ΔM_r and ΔE_p). Results of the main effects ANOVA are also summarized in Table 12. As can be seen from the table, although base course moisture content has significant impact on D_1 and (D_1-D_7) , it has no significant impact on ΔD_1 or $\Delta(D_1-D_7)$. Similarly, rainfall has a significant impact on E_p ; however, it has no significant impact on ΔE_p . The GWT is found to have no significant impact on D_7 or ΔD_7 .

Regression equations were then developed to estimate the differences between the standard deflection and those measured at different months (Δ Deflection), as well as the standard layer moduli and those backcalculated from the measured deflections (ΔM_r and ΔE_p).

The generic equation considering Δ Deflection is of the following form:

$$\Delta\text{Deflection} = a * MC + b * \text{Pavement Temperature} + CE4 \quad (E4)$$

Where:

Δ Deflection (mils)

MC = Base Moisture Content (%)

PavTemp = Mid depth asphalt temperature ($^{\circ}$ C)

a,b,c = regression coefficients

Table 13 shows the values of the regression coefficients a, b, and c for different combinations of deflection sensors.

An example of using the developed models is as follows:

A pavement section with the following parameters:

- Base Course MC at 10% = L class
- Measured Pavement Temperature at 25°C (77 °F) = H class
- GWT at 5 m (16.4 ft)= L class
- Rainfall at 10 mm (0.4 in) = H class

The selection of the Low and High categories are done as per Figure 40. Based on these parameters, the regression parameters a, b, and c are selected from Table 13 for ΔD_1 and are found to be:

- a = 0.22
- b = 0.12
- c = -11.41

These parameters are highlighted in Table 13. This model has an $R^2 = 0.95$

Table 13: Δ Deflection Regression Coefficients for Different Classes

Base M/C	L	L	L	L	L	L	L	L	H	H	H	H	H	H	H	H
PavTemp	L	L	L	L	H	H	H	H	L	L	L	L	H	H	H	H
GWT	L	L	H	H	L	L	H	H	L	L	H	H	L	L	H	H
Rainfall	L	H	L	H	L	H	L	H	L	H	L	H	L	H	L	H
	ΔD_1															
R^2	0.59	0.51	0.13	0.32	0.05	0.95	0.35	0.47	0.61			0.04	0.06		0.05	0.58
a	0.02	0.14	-0.03	-0.05	0.04	0.22	0.00	0.08	0.00			0.03	0.16		0.28	0.02
b	0.16	-0.03	0.05	0.09	0.06	0.12	-0.21	0.30	0.07			0.05	-0.14			1.90
c	-5.54	-7.20	-3.17	-2.79	-4.71	-11.41	2.73	-12.96	-2.23			-5.95	-14.45		-9.34	-49.05
	ΔD_2															
R^2	0.44	0.39	0.04	0.16	0.04	0.90	0.36	0.43	0.73			0.13	0.02		0.02	0.35
a	0.00	0.11	0.00	-0.04	0.03	0.13	0.02	0.06	0.01			0.01	-0.27		0.07	-0.08
b	0.11	-0.01	0.03	0.04	0.05	0.15	0.04	0.20	0.06			0.07	0.06			1.32
c	-2.83	-4.33	-1.92	-0.77	-2.67	-8.33	-2.18	-8.08	-1.95			-2.43	19.73		-2.43	-24.47
	ΔD_3															
R^2	0.33	0.30	0.02	0.13	0.03	0.87	0.31	0.33	0.74			0.09	0.07		0.02	0.39
a	0.00	0.09	0.01	-0.04	0.03	0.10	0.02	0.03	0.01			0.01	0.26		0.05	-0.10
b	0.09	-0.02	0.02	0.03	0.04	0.16	0.02	0.15	0.06			0.05	0.06			0.81
c	-2.25	-3.55	-1.69	-0.37	-2.18	-7.64	-1.44	-5.82	-1.88			-1.90	-21.54		-1.89	-10.55
	ΔD_4															
R^2	0.27	0.19	0.02	0.10	0.02	0.79	0.17	0.03	0.75			0.12			0.05	0.51
a	0.00	0.08	0.01	-0.04	0.03	0.08	0.01	-0.01	0.01			0.02			0.08	-0.12
b	0.08	-0.03	0.02	0.01	0.02	0.15	-0.08	0.06	0.04			0.03				0.30
c	-2.10	-2.98	-1.80	-0.42	-2.03	-6.79	0.73	-2.61	-1.80			-2.40			-2.99	2.45
	ΔD_5															
R^2	0.20	0.62	0.01	0.07	0.03	0.95	0.72	0.01	0.68			0.24			0.04	0.75
a	0.01	0.07	0.01	-0.04	0.02	0.09	0.00	-0.02	0.00			0.02			0.12	-0.15
b	0.06	-0.02	0.01	0.00	0.00	0.13	-0.16	0.04	0.02			0.00				0.35
c	-2.35	-3.31	-1.84	-0.21	-1.68	-6.96	2.55	-2.07	-1.77			-2.67			-4.18	2.24
	ΔD_6															
R^2	0.13	0.25	0.01	0.08	0.15	0.95	0.89	0.19	0.48			0.31			0.03	0.87
a	0.01	0.03	0.01	-0.04	0.02	0.07	-0.01	-0.05	0.00			0.03			0.15	-0.14
b	0.04	-0.02	0.00	-0.01	-0.02	0.09	-0.23	-0.04	0.02			-0.04				0.22
c	-2.46	-2.69	-2.04	-0.84	-1.87	-5.88	3.96	0.22	-1.79			-3.22			-5.48	3.04
	ΔD_7															
R^2	0.13	0.24	0.01	0.05	0.28	0.94	0.90	0.22	0.28			0.30			0.03	0.83
a	0.01	0.03	0.01	-0.02	0.03	0.06	-0.02	-0.04	0.00			0.03			0.17	-0.08
b	0.03	-0.02	0.00	-0.01	-0.02	0.05	-0.25	-0.04	0.01			-0.04				0.19
c	-2.59	-2.67	-2.18	-1.38	-1.98	-4.86	4.32	-0.24	-1.76			-3.58			-6.29	-1.07
	ΔD_8															
R^2	0.14	0.18	0.02	0.04	0.35	0.96	0.91	0.20	0.09			0.27			0.03	0.63
a	0.01	0.02	0.01	-0.02	0.02	0.05	-0.02	-0.03	-0.01			0.02			0.16	-0.04
b	0.03	-0.02	0.00	-0.01	-0.02	0.03	-0.26	-0.03	-0.05			-0.05				0.13
c	-2.60	-2.49	-2.22	-1.53	-2.04	-4.16	4.31	-0.94	2.77			-3.53			-6.23	-3.35

A review of Table 13 indicates the data has been grouped into different sets based on the cutoff values for each climatic parameter. For example, the first column in the table represents the regression model between variation in deflection at sensor 1 (ΔD_1), base moisture content, and pavement temperature, when base moisture content, pavement temperature, GWT, and rainfall (RF) are all at low levels. As can be seen, the regression models could not be implemented for a few combinations due to limited data. These combinations are not expected to exist – such as high moisture content with low temperature. Also, a few models did not produce high correlation due to the fact that limited data existed in these sets.

A second regression model was therefore developed to consider CF rather than the variation in deflection. The regression equation is of the following form:

$$\text{Correction factor (CF)} = a * \text{MC} + b * \text{Pavement Temperature} + C \quad (\text{E5})$$

Table 14 lists the regression coefficients for CF related to Equation E5.

Table 14: CF Regression Coefficients for Different Classes

Base M/C	L	L	L	L	L	L	L	L	H	H	H	H	H	H	H	H
PavTemp	L	L	L	L	H	H	H	H	L	L	L	L	H	H	H	H
GWT	L	L	H	H	L	L	H	H	L	L	H	H	L	L	H	H
Rainfall	L	H	L	H	L	H	L	H	L	H	L	H	L	H	L	H
	CF₁															
<i>R</i> ²	0.32	0.47	0.18	0.44	0.15	0.85	0.34	0.53	0.80		0.29	0.52		0.02	0.51	
<i>a</i>	0.00	-0.03	0.01	0.01	0.00	-0.03	-0.01	-0.01	-0.01		0.00	0.35		-0.03	0.00	
<i>b</i>	-0.03	0.01	-0.02	-0.05	-0.02	-0.03	-0.01	-0.06	-0.04		-0.02	-0.06			-0.17	
<i>c</i>	1.96	2.34	1.74	1.73	1.79	2.99	1.77	3.28	2.18		1.68	-24.88		2.26	5.56	
	CF₂															
<i>R</i> ²	0.29	0.41	0.08	0.31	0.06	0.82	0.53	0.47	0.80		0.24	0.45		0.01	0.28	
<i>a</i>	0.00	-0.02	0.00	0.01	0.00	-0.02	-0.01	-0.01	-0.01		0.00	0.18		-0.02	0.01	
<i>b</i>	-0.02	0.00	-0.01	-0.02	-0.01	-0.04	-0.01	-0.04	-0.04		-0.02	-0.04			-0.11	
<i>c</i>	1.55	1.84	1.48	1.30	1.48	2.74	1.58	2.47	2.05		1.39	-12.66		1.63	3.14	
	CF₃															
<i>R</i> ²	0.22	0.35	0.04	0.27	0.05	0.78	0.51	0.41	0.80		0.17	0.37		0.00	0.28	
<i>a</i>	0.00	-0.02	0.00	0.01	0.00	-0.01	-0.01	-0.01	-0.01		0.00	0.10		-0.01	0.01	
<i>b</i>	-0.02	0.00	-0.01	-0.02	-0.01	-0.05	0.00	-0.03	-0.04		-0.01	-0.03			-0.08	
<i>c</i>	1.47	1.74	1.44	1.18	1.45	2.80	1.47	2.22	2.09		1.36	-6.02		1.42	2.08	
	CF₄															
<i>R</i> ²	0.18	0.26	0.03	0.20	0.05	0.68	0.43	0.15	0.80		0.16	0.37		0.01	0.34	
<i>a</i>	0.00	-0.02	0.00	0.01	0.00	-0.01	-0.01	0.00	0.00		0.00	0.04		-0.01	0.01	
<i>b</i>	-0.02	0.01	-0.01	-0.01	-0.01	-0.06	0.00	-0.02	-0.03		-0.02	-0.03			-0.04	
<i>c</i>	1.50	1.70	1.52	1.21	1.51	2.89	1.47	1.87	2.11		1.59	-1.32		1.54	1.03	
	CF₅															
<i>R</i> ²	0.09	0.62	0.02	0.17	0.05	0.83	0.28	0.13	0.77		0.09	0.58		0.00	0.56	
<i>a</i>	0.00	-0.02	0.00	0.01	0.00	-0.01	-0.01	0.00	0.00		0.00	-0.10		-0.01	0.02	
<i>b</i>	-0.01	0.01	0.00	-0.01	-0.01	-0.07	0.00	-0.02	-0.03		-0.01	-0.03			-0.06	
<i>c</i>	1.59	1.88	1.57	1.14	1.54	3.31	1.44	1.93	2.27		1.68	9.58		1.61	0.96	
	CF₆															
<i>R</i> ²	0.00	0.23	0.03	0.15	0.11	0.68	0.11	0.09	0.67		0.09	0.67		0.00	0.79	
<i>a</i>	0.00	-0.02	0.00	0.01	0.00	0.00	0.00	0.01	0.00		0.00	-0.29		0.00	0.04	
<i>b</i>	0.00	0.01	0.00	0.00	-0.01	-0.08	0.00	0.00	-0.02		0.00	0.00			-0.08	
<i>c</i>	1.77	1.92	1.79	1.46	1.75	3.75	1.82	1.36	2.57		1.94	24.46		1.85	0.46	
	CF₇															
<i>R</i> ²	0.02	0.23	0.05	0.03	0.14	0.46	0.12	0.12	0.50		0.11	0.53		0.02	0.71	
<i>a</i>	0.00	-0.02	0.01	0.01	0.01	0.01	0.00	0.03	0.00		0.00	-0.28		-0.02	0.04	
<i>b</i>	0.01	0.02	0.00	0.00	-0.01	-0.09	-0.01	-0.01	-0.01		0.00	-0.01			-0.13	
<i>c</i>	2.11	2.22	2.14	2.06	1.98	4.00	2.61	1.63	2.81		2.31	23.70		2.70	1.76	
	CF₈															
<i>R</i> ²	0.13	0.17	0.02	0.01	0.23	0.65	0.38	0.05	0.15		0.07	0.17		0.00	0.52	
<i>a</i>	0.00	-0.02	0.00	0.00	0.02	0.03	-0.01	0.02	0.00		0.00	0.18		-0.01	0.03	
<i>b</i>	0.02	0.03	0.00	0.00	-0.01	-0.10	0.00	-0.02	0.01		0.01	0.00			-0.16	
<i>c</i>	2.53	2.45	2.62	2.52	2.17	4.39	3.05	2.41	0.97		2.37	-11.06		2.98	3.52	
	CFM_r															
<i>R</i> ²	0.39	0.21	0.14	0.10	0.49	0.88	0.52	0.27	0.47		0.01	0.78		0.01	0.18	
<i>a</i>	-0.01	0.02	-0.01	0.01	-0.02	-0.03	0.00	-0.02	0.00			-0.25		-0.01	0.00	
<i>b</i>	-0.02	-0.02	0.00	0.01	0.02	0.04	0.02	0.12	0.03		0.00	0.02			0.08	
<i>c</i>	1.58	1.44	1.27	0.96	1.33	1.20	0.59	-0.82	0.49		1.20	20.17		1.17	-0.45	
	CFE_p															
<i>R</i> ²	0.37	0.45	0.11	0.31	0.46	0.79	0.14	0.24	0.75		0.35	0.36		0.04	0.77	
<i>a</i>	0.00	0.00	-0.01	-0.01	0.00	0.03	0.01	0.01	0.002		0.00	-0.42		0.05	0.02	
<i>b</i>	0.02	0.02	0.01	0.02	0.04	0.03	0.00	0.05	0.029		0.02	0.03			0.23	
<i>c</i>	0.77	0.77	0.96	1.10	0.31	-0.24	1.23	-0.48	0.493		0.81	33.58		-0.08	-5.62	

A review of both Tables 13 and 14 indicates an improved correlation with the CF model as compared to the correlations obtained from the Δ Deflection model.

Sensitivity Analysis

A sensitivity analysis was conducted to study the effect of changing base moisture content and pavement temperature on delta deflections, i.e. ΔD_1 , ΔD_7 , $\Delta(D_1-D_7)$. Figure 42 shows a sample of the sensitivity analysis results. In this figure, the predicted ΔD_1 is presented on the y-scale, while the percent MC is presented on the x-scale. The case presented in Figure 42 is for a pavement section with pavement temperature, GWT and rainfall in the low class categories, as they are defined in Figure 40. In Figure 42, the predicted ΔD_1 ranges about 7 mils as a result of the changed pavement temperature from -20°C to $+20^\circ\text{C}$ (-4°C to $+68^\circ\text{F}$). For example, at 15 percent base course MC, the predicted ΔD_1 ranges from -9 mils to -2 mils.

In this sensitivity analysis, the GWT and Rainfall were held constant for a specific run, i.e. Low/Low, Low/High, High/Low and High/High. The pavement temperature and base MC were changed and the delta deflections were predicted for different combinations of pavement temperature, Base MC and GWT/Rainfall categories.

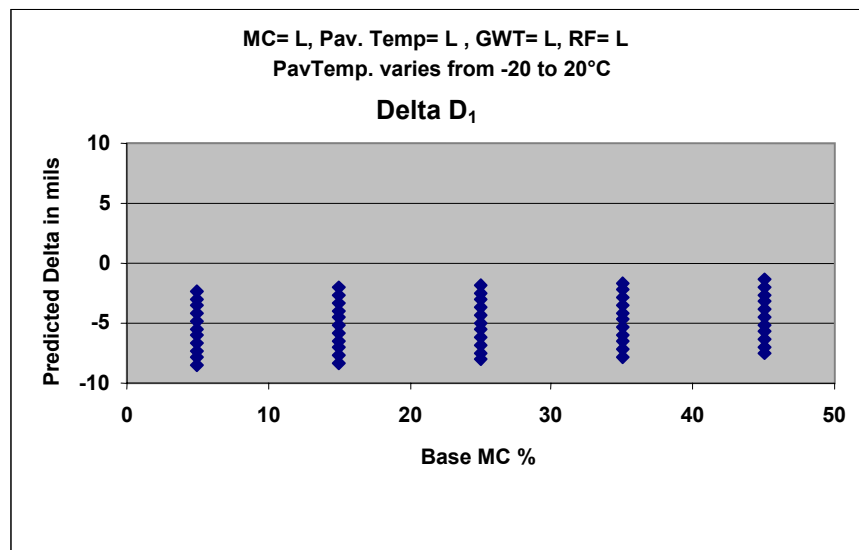


Figure 42: Predicted Δ Deflection for Low Moisture and Low Pavement Temperature

Appendix B provides the full results of the sensitivity analysis for the various combinations. A review of the sensitivity analysis results indicates delta deflection to be sensitive to changes in base moisture and pavement temperature.

Summary of Findings and Implementation Plan

Comprehensive analysis was performed on the collected FWD and environmental data from 21 flexible pavement test sites to investigate the impact of the environmental parameters on pavement response obtained through FWD. Results of the Analysis Of Variance (ANOVA)

performed on the pavement parameters (deflections and backcalculated moduli) and environmental parameters (base course moisture content, average AC temperature, ground water table, rainfall, and air temperature) indicated that all main effects have a significant impact on the overall pavement deflection (D_1), difference in pavement deflection (D_1-D_7), and the Effective Pavement Modulus (E_p), which is expected. However, GWT and pavement temperature were found to have no significant impact on the subgrade deflection (D_7). This finding does not agree with the common assumption made in backcalculation analyses that the GWT acts as a rigid layer.

To achieve the stated object of the study, a plan as shown in Figure 43 was formulated for implementing these models. In this plan, one of the existing seasonal and temperature correction models, namely, the EICM was to be used first to calibrate the model for New Jersey conditions using the data available in the project database. The required input parameters for EICM were to be obtained from field-measured data and from the weather stations. EICM would then generate the inputs required for the developed models. If the results of calibrating EICM for New Jersey conditions were found to be unsatisfactory, then an alternate plan for this study was to develop models that do not require difficult-to-obtain input parameters, such as moisture content.

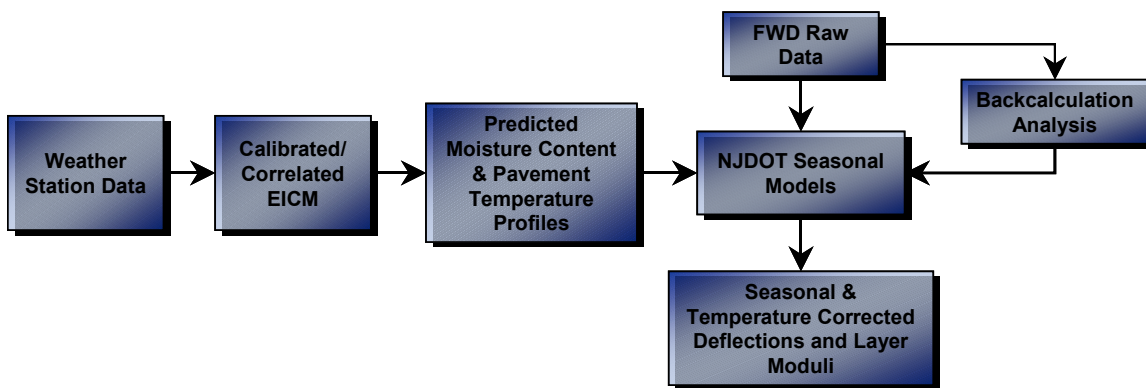


Figure 43: Implementation Plan for Model Development

EICM MODEL EVALUATION

Overview of EICM Capabilities

The EICM is expected to be an integral part of the Mechanistic-Empirical (M-E) Design of New and Rehabilitated Pavement Structures. The EICM program can estimate the pavement environmental parameters if pavement properties and climatic data are known. EICM has undergone major revisions since its initial development and has been designed to simulate the behavior of pavement materials and subgrade conditions or characteristics.⁽¹⁶⁾ EICM incorporates the following three primary sub-models:

1. Infiltration and drainage
2. Climate-materials-structure
3. Frost heave and thaw settlement

The EICM program user has a choice of using either the Hourly Climatic Database supplied with the EICM, or actual field-specific data (if available). As a model input, EICM requires the analysis parameters (exact date and duration of the analysis period at the location), specific climatic data (minimum and maximum daily air temperature, rainfall, wind speed, percent sunshine, and water table depth for the each day in the analysis period), pavement material properties (thermal properties, infiltration, and drainage properties), pavement structure (layer material and thickness), and subgrade properties.

Evaluation Process

The evaluation study was carried out, by comparing the EICM model predictions with measured field data from test sections of the Seasonal Variation and Material Characterization Study. The following subsections describe the procedure and results of the evaluation.

Calibration and Validation

The criteria used to evaluate the applicability of EICM for New Jersey conditions was to compare program-predicted outputs with field-measured data for each of the study test sections, and to establish correlation between predicted and measured parameters. For this evaluation, the latest version of the EICM (Version 3.0) was used. Figure 44 shows the procedure used for the evaluation process.

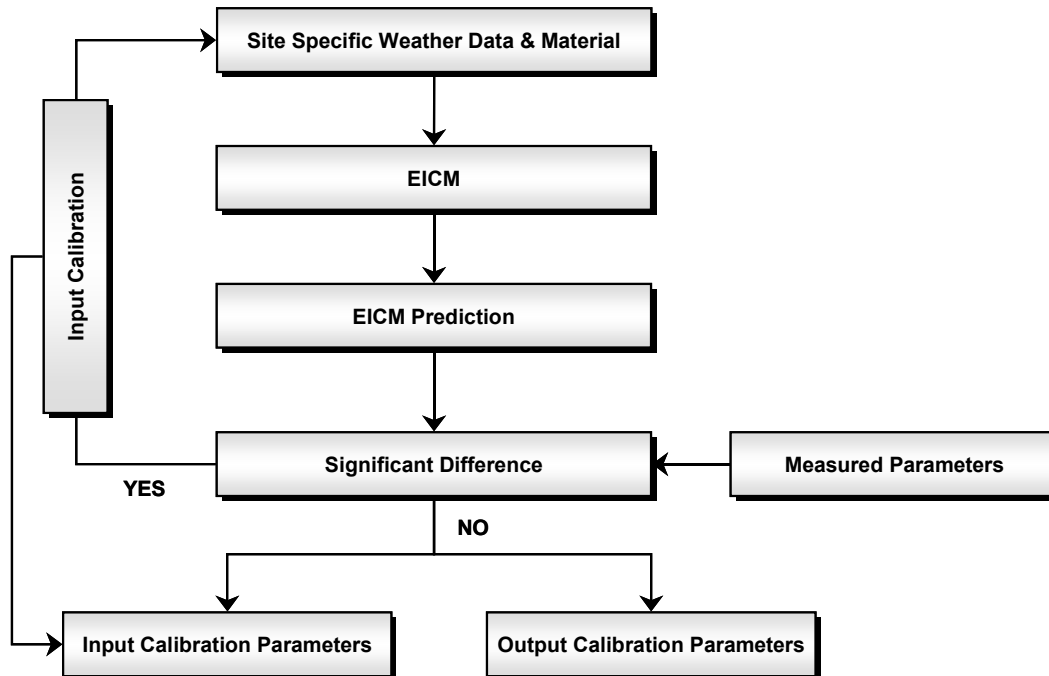


Figure 44: Flowchart for EICM Validation Procedure

The program user has a choice of using either default climatic data supplied with the EICM or actual field-specific data (if available). As a model input, EICM requires the analysis parameters (exact time and duration of the analysis period at the location), specific climatic data (minimum and maximum daily air temperature, rainfall, wind speed, percent sunshine, and water table depth for the each day in the analysis period), pavement structural geometry and material properties (thermal properties, infiltration, and drainage properties), pavement profile (layers and corresponding thickness), and pavement and subgrade material properties. The surface temperature is initially established, followed by the calculation of temperatures throughout the pavement layers. Once the surface temperatures are determined, they are used to calculate the temperature throughout the underlying pavement layers. A heat transfer model is used to determine the distribution of temperatures in the pavement layers.

The influence of seasonal variation on pavement response is very significant in case of flexible pavements and less significant in case of rigid and composite pavements. Therefore, the main focus of this evaluation was chosen to be flexible pavements. The evaluation process was carried out using data from the two LTPP test sites, namely, SPS 5 (11 test sections) and SPS 9 (6 test sections), and four other instrumented test sites from New Jersey having flexible pavement cross sections. Field specific data for a few climatic parameters such as wind speed and percent sunshine were not available. Therefore, initially, a constant wind speed of 6.2 miles/h (10 km/h) and 80 percent sunshine per day were used in all calculations. Pavement structure, layers, was defined based on actual field values from the test sites.

Figure 45 shows the temperature variation recorded at various time intervals during a specific day for two typical sites (LTPP Sections 5E and 9C respectively). The figures indicate the variation of temperature within the surface layer to be more pronounced as compared to the subgrade. There is also a shift in the recorded temperature at the two sites for the two years (2002 and 2003) of data collected. This indicates a warmer season in the year 2002 than in 2003. Similar trends were observed at other instrumented sites.

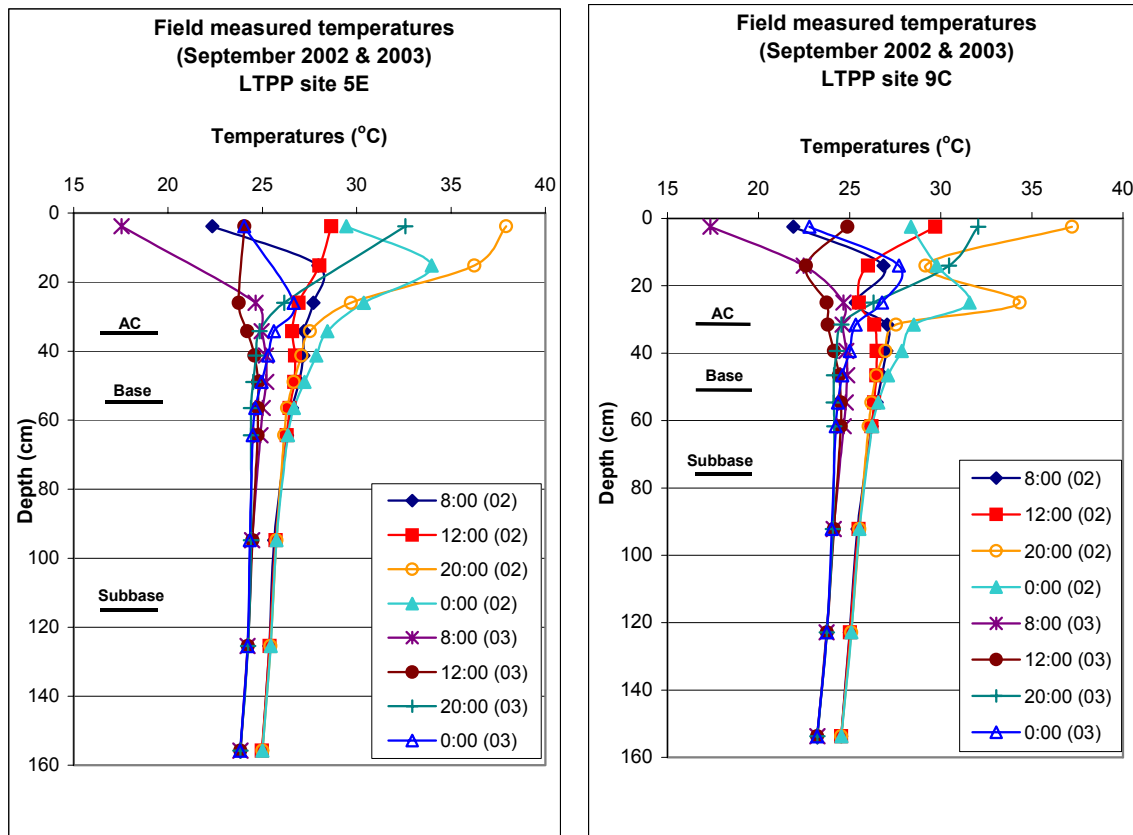


Figure 45: Hourly Temperature Variation on September 10, 2002 and 2003 at LTPP Sections 5E and 9C

Sensitivity Analysis

The EICM model requires a number of input variables, some of which may not be available for particular sites under investigation. In such cases, necessary assumptions need to be made, possibly resulting in differences between predicted and measured values. To minimize possible error, sensitivity analysis was performed to determine the EICM's sensitivity to several climatic parameters.

For this analysis, the EICM model was run a number of times for the same pavement site, while certain climatic or temperature parameters were varied one-by-one. Field-specific data for a few climatic parameters, such as wind speed (ws) and percent sunshine (ss) were not available from the weather stations for the evaluated test sections. Based on the National Oceanic and Atmospheric Administration (NOAA) and Northeast Regional Climate Center (NRCC), the average percent of possible sunshine for the closest weather station (Atlantic City) for past 36 years is 56 percent. The average wind speed, based on the same sources, is approximately 10

miles/h (16 km/h), for the past 40 years, for the same weather station. Therefore, these values were used as default input values for the EICM. The sensitivity of all the program's default parameters was checked. Figure 46 illustrates the impact of variations in wind speed and percent sunshine on program-predicted values for LTPP site 9C. It can be concluded that change in wind speed has a more significant influence on predicted pavement temperature than change in percent sunshine.

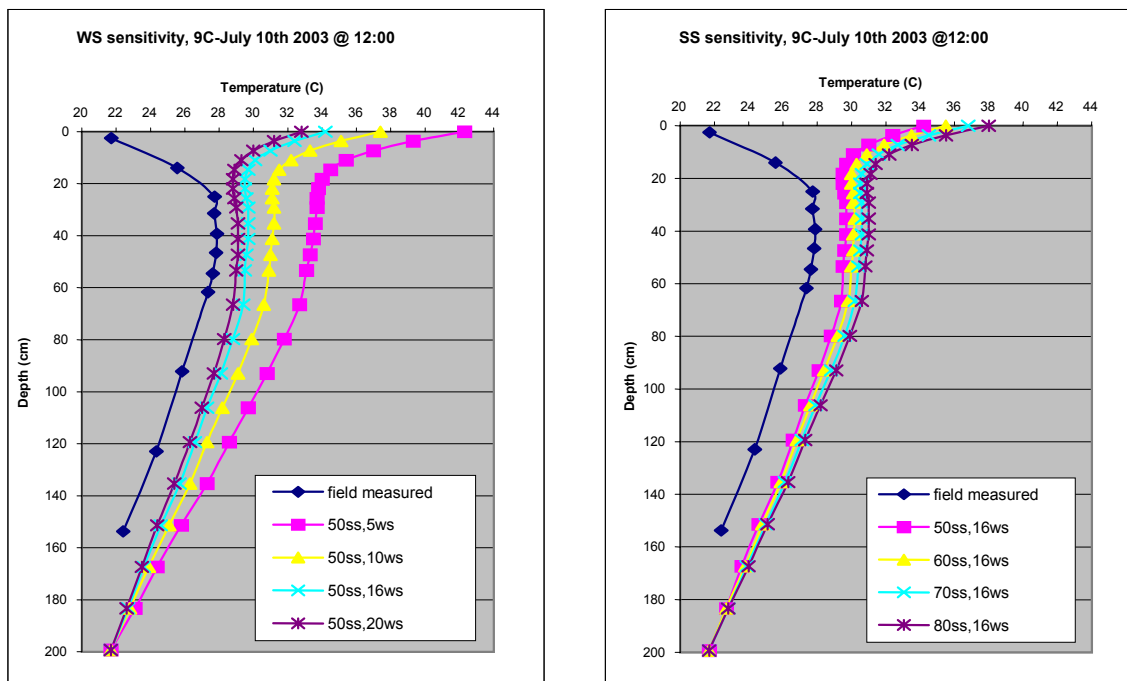


Figure 46: Sensitivity Analysis Results

Other parameters such as internal boundary condition (flux/suction), type of fines added to the base course (silt, clay, inert filler), and linear length of cracks/joints did not appear to influence the predicted data (mostly expected on moisture content). Pavement structure was defined based on actual field values. A similar sensitivity study was carried out in Vermont, by repeatedly modeling the behavior of the same pavement, while varying several climatic parameters and pavement thermal properties, one at a time.⁽³³⁾ The study showed that the maximum seasonal frost penetration predicted by EICM was relatively insensitive to variations in water table depth, percent sunshine, wind speed, and pavement surface absorptivity. Considering the geographical and climatic differences between the two States, the results from both the New Jersey and Vermont studies support the findings that potential inaccuracies in the assumed and/or estimated values for these parameters do not significantly impact the outcome of the sensitivity study analysis.

Evaluation Results

Temperature Data Comparison

The temperature variations measured at different periods of the day across pavement sections for the two LTPP sites 5-E and 9-C are shown in Figures 47 and 48 for the months of July 2003 and September 2003, respectively. Similar temperature variations have been measured at other sites and for April and December, which together with July and September represent the typical months for the four seasons in New Jersey. As can be seen, EICM program-predicted temperatures do not compare well with the actual measured temperatures.

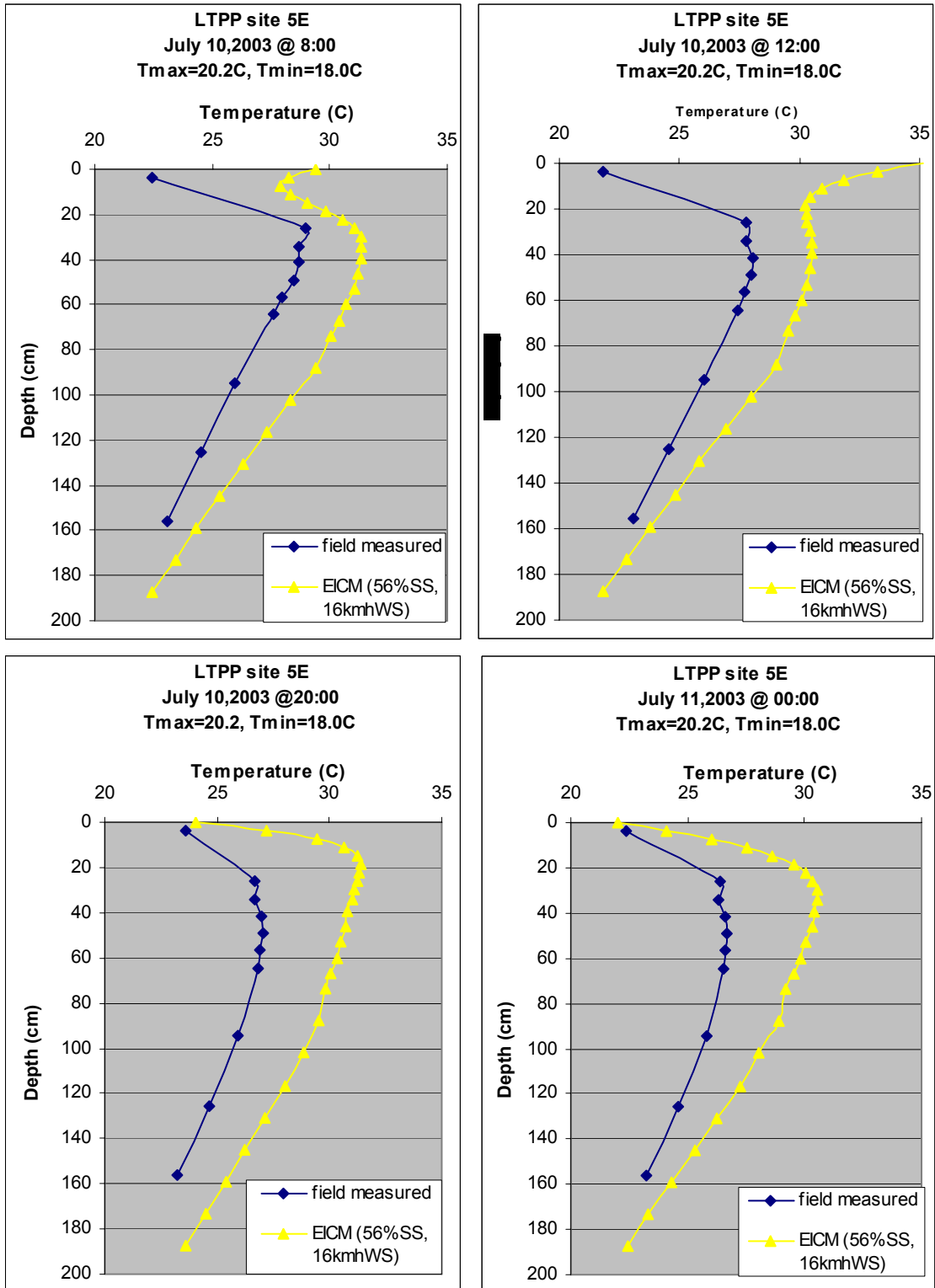


Figure 47a: July 2003 Temperature Comparison for LTPP Section 5E

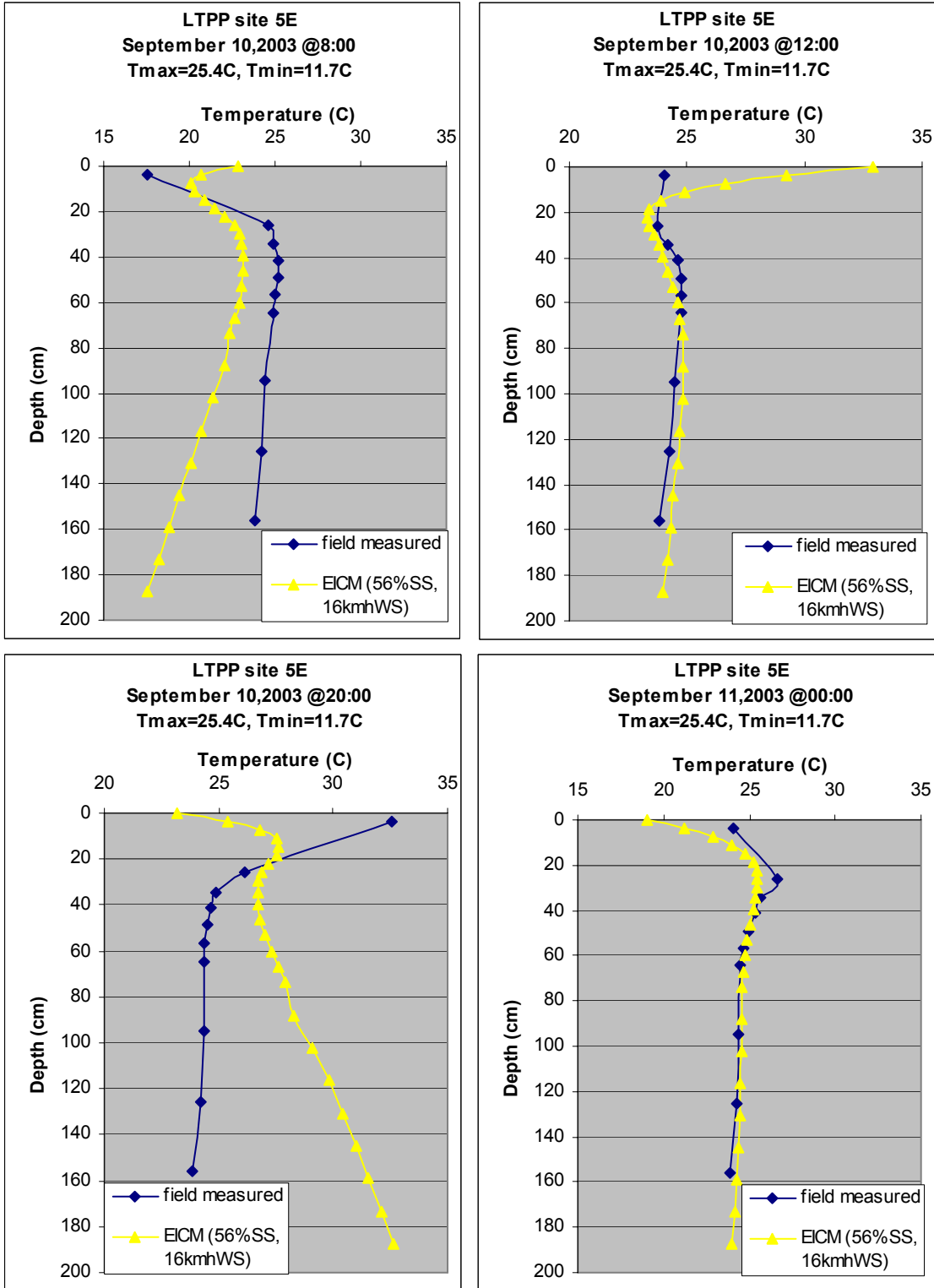


Figure 47b: September 2003 Temperature Comparison for LTPP Section 5E

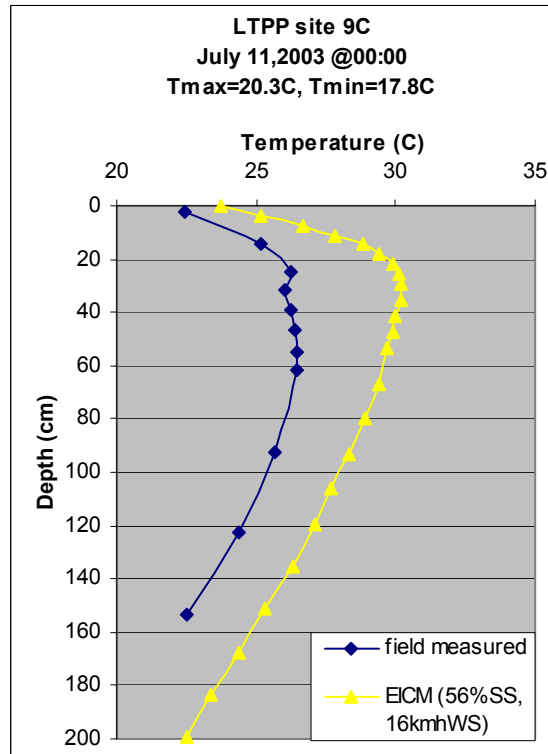
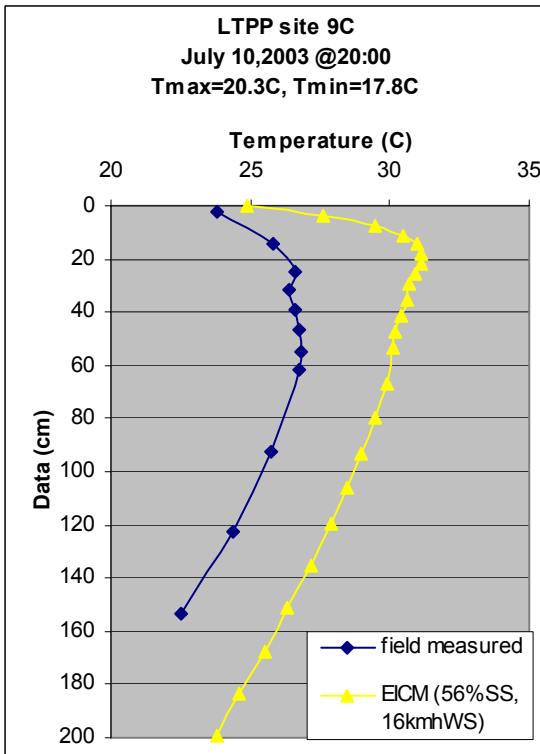
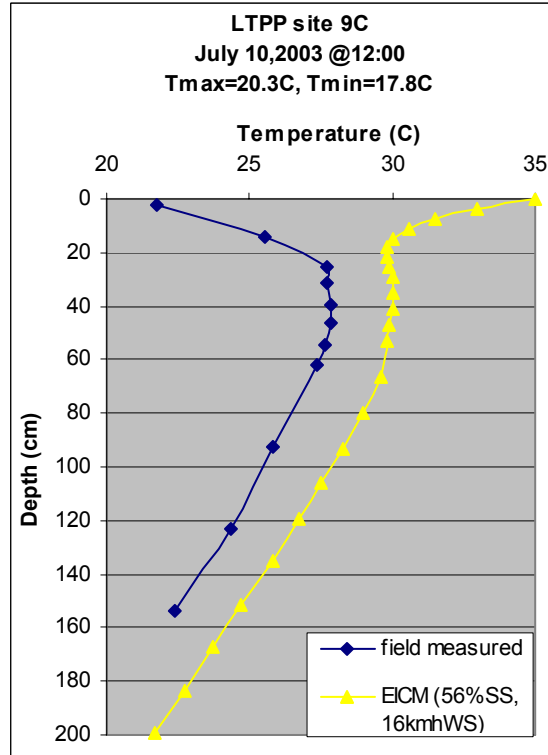
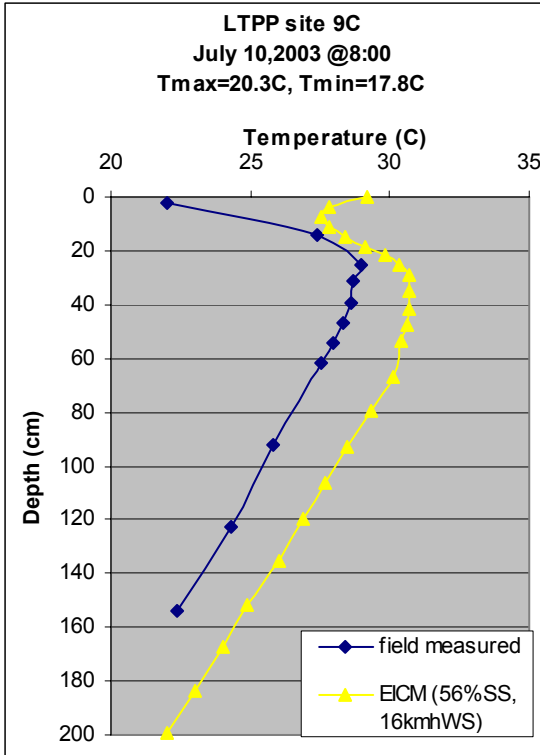


Figure 48a: July 2003 Temperature Comparison for LTPP Section 9C

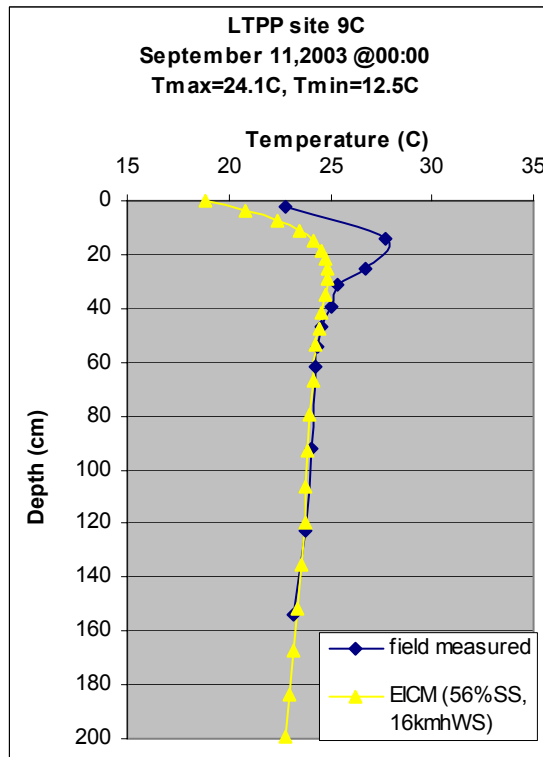
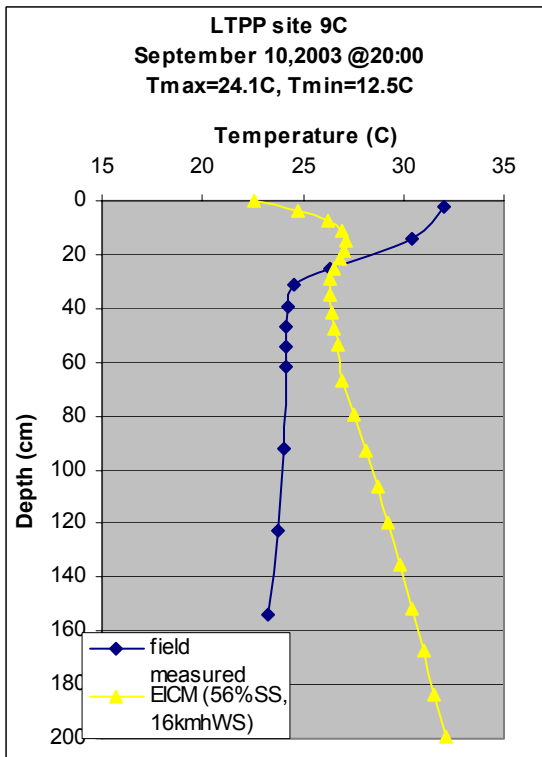
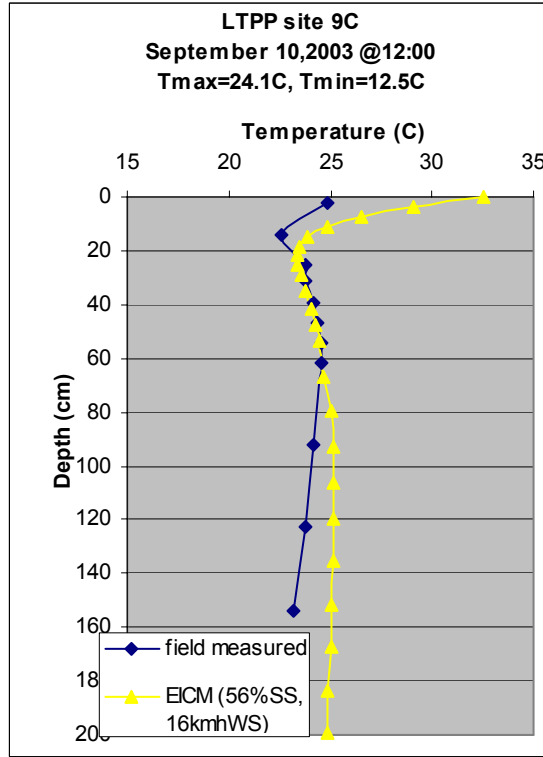
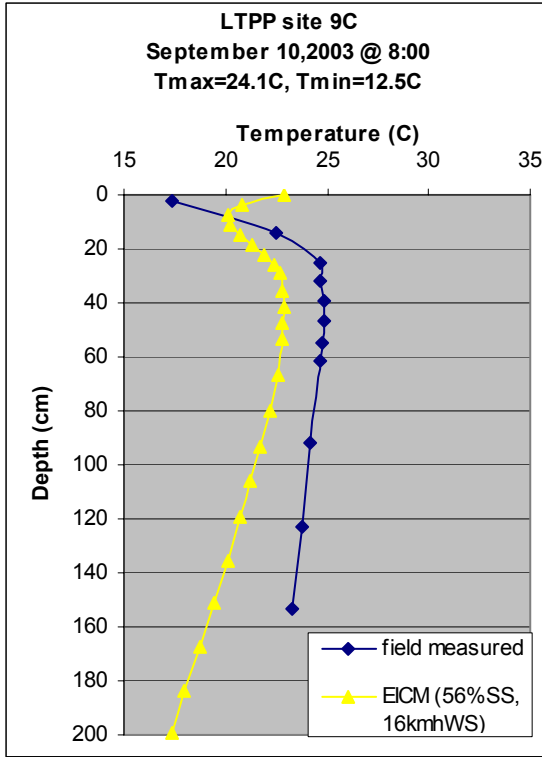


Figure 48b: September 2003 Temperature Comparison for LTPP Section 9C

The variation in temperature within the pavement layer, and specifically the surface layers, is of greater interest in adjusting deflection data to account for environmental effects. For flexible pavements, this is essentially the asphalt concrete layers comprising the pavement cross section. Table 15 shows the difference between predicted and measured temperatures for the asphalt concrete surface layers for a two-year period at the two LTPP sites. Program-predicted surface temperature is more than 15°C (27°F) greater than the measured one in all cases, as shown in Figure 49, even though the actual surface temperature (measured at the site) is an input in the initial temperature profile of the EICM. It should be noted that in this figure, the measured and predicted temperatures were for the same depth, i.e., surface and were 14 cm (5.5 in) from the surface, where the sensors are located.

Table 15: Temperature (in °C) Data Comparison for AC layers at LTPP Sites 5E and 9C

		LTPP Site 5E				LTPP Site 9C			
		2002				2002			
		April	July	Sept.	Dec.	April	July	Sept.	Dec.
AC	Field data	17.5	30.2	27.9	0.9	17.8	29.3	27.1	-2.0
	EICM (56ss/16ws)	20.8	33.5	30.1	-1.3	20.9	33.9	30.0	1.1
Base	Field data	14.6	28.8	26.6	3.3	14.6	28.7	26.4	3.3
	EICM (56ss/16ws)	18.4	32.0	27.4	-1.0	18.4	31.8	27.1	-1.1
Subbase	Field data	14.1	28.8	26.5	5.0	13.3	28.1	26.0	5.8
	EICM (56ss/16ws)	18.5	32.4	27.7	-1.0	18.6	32.1	27.8	-1.0
Subgrade	Field data	12.2	26.4	25.4	8.8	11.6	25.4	24.8	9.5
	EICM (56ss/16ws)	19.4	31.7	28.2	-1.0	20.5	31.8	29.0	-2.1
		LTPP Site 5E				LTPP Site 9C			
		2003				2003			
		April	July	Sept.	Dec.	April	July	Sept.	Dec.
AC	Field data	8.9	24.8	23.9	5.5	18.9	25.0	23.7	1.3
	EICM (56ss/16ws)	11.6	31.4	25.7	4.8	24.4	31.2	25.9	0.7
Base	Field data	6.9	27.8	24.2	5.4	15.6	27.8	24.1	4.3
	EICM (56ss/16ws)	8.9	30.5	23.9	1.9	22.2	30.0	24.0	0.0
Subbase	Field data	7.6	27.8	24.7	6.3	14.5	26.9	24.4	6.9
	EICM (56ss/16ws)	9.6	30.0	24.5	2.4	23.4	28.8	24.9	0.4
Subgrade	Field data	9.2	24.6	24.2	9.7	12.5	23.4	23.5	10.8
	EICM (56ss/16ws)	10.5	25.4	24.5	4.4	24.3	24.2	25.0	-0.2

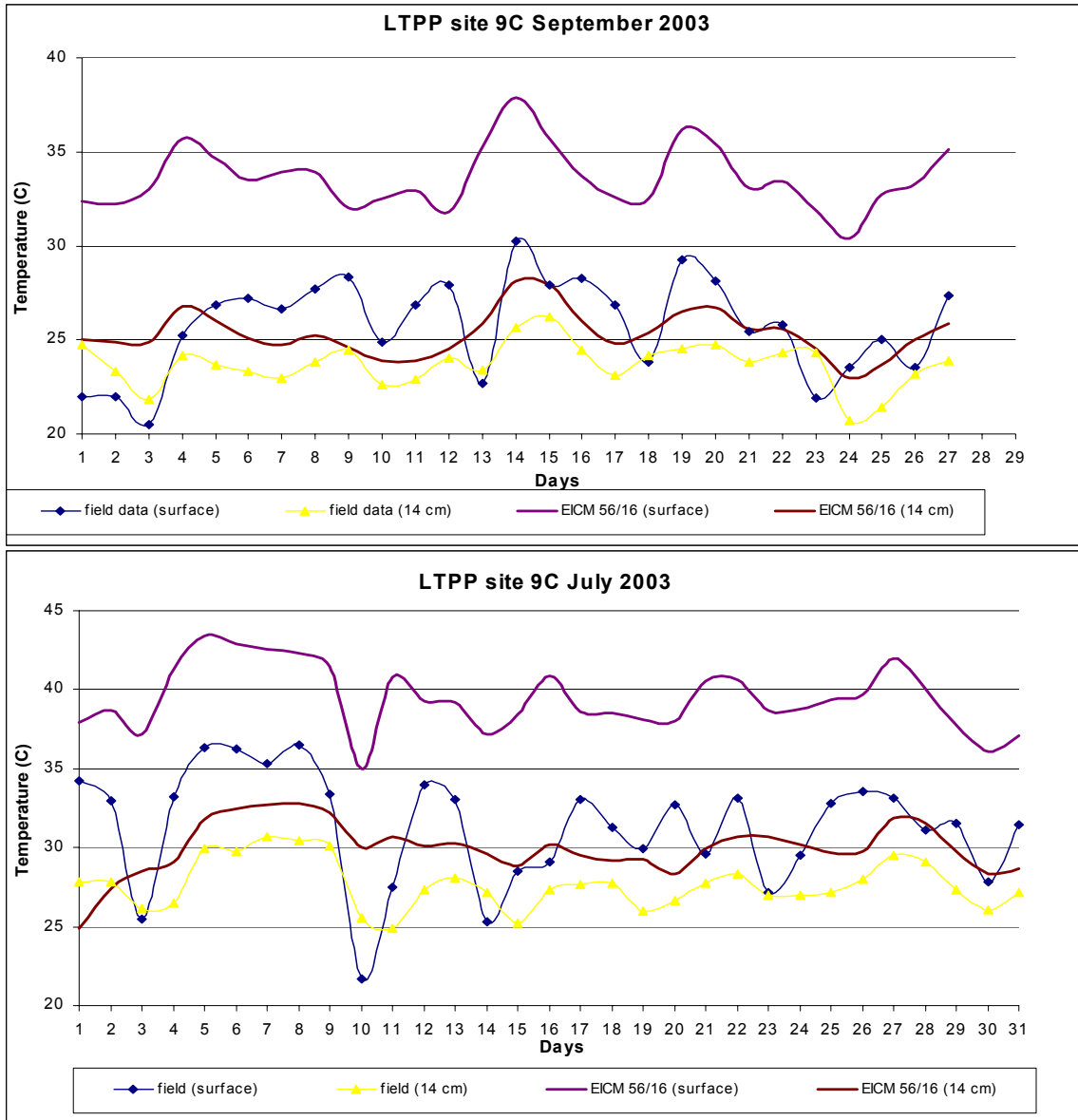


Figure 49: Differences in Measured vs. Predicted Temperature in Asphalt Concrete Surface Layer

Moisture Data Comparison

Comparison of the field-measured and program-predicted moisture content is presented in Figures 50 and 51 for the two LTPP sites (9C and 5E), respectively.

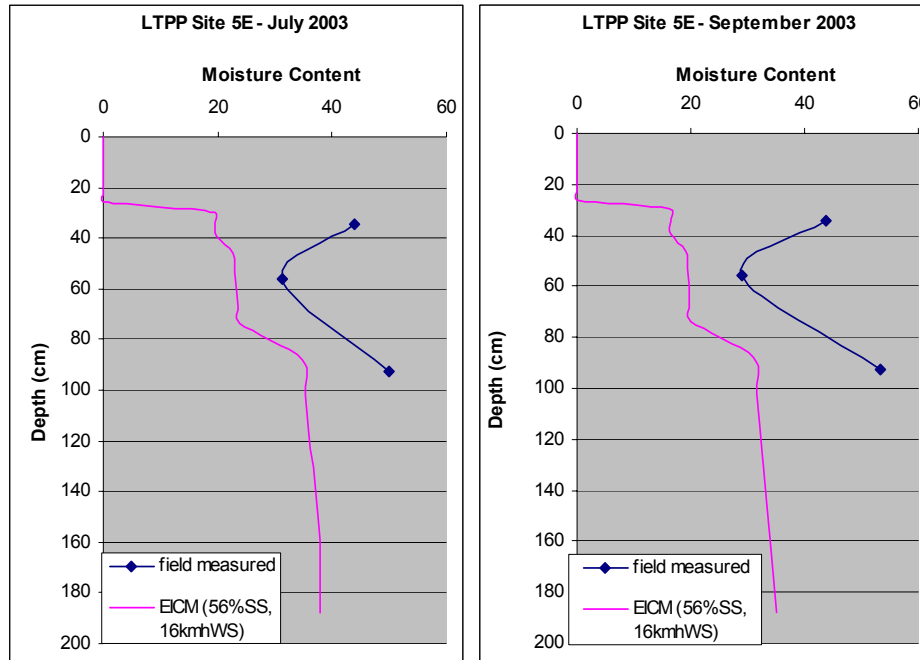


Figure 50: Moisture Content Comparisons for LTPP Section 5E

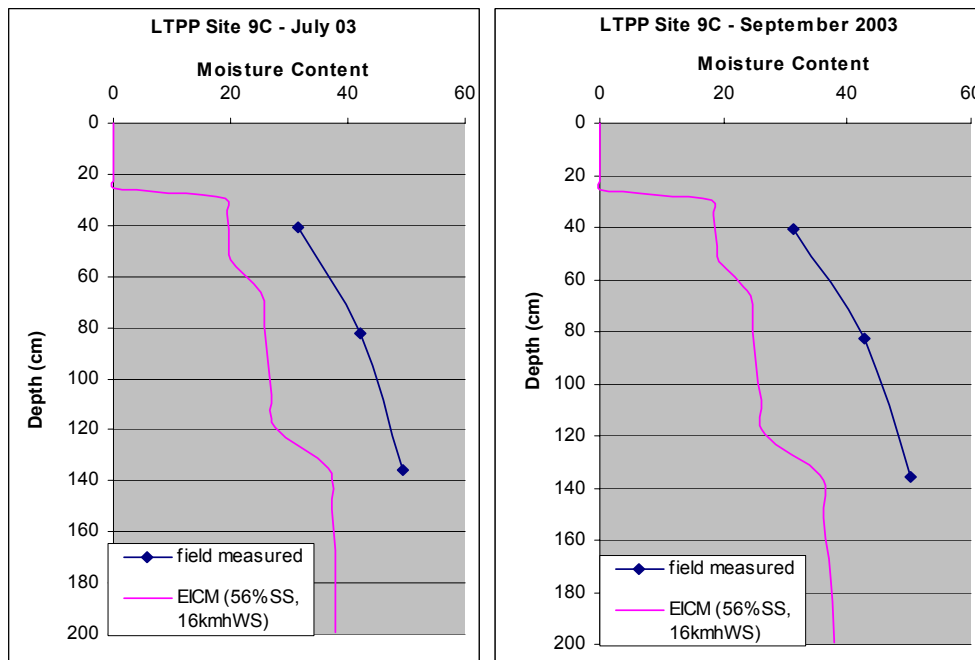


Figure 51: Moisture Content Comparisons for LTPP Section 9C

Table 16 summarizes the difference between EICM-predicted and measured moisture contents for the same locations within the granular layers and subgrades for a two-year period, at the two LTPP sections. As can be observed from the figures and the summary provided in Table 16, there was an inconsistency in the EICM-predicted moisture content as compared to measured moisture content.

Table 16: Moisture Content (%) Data Comparison at LTPP Sites 5E and 9C

		LTPP Site 5E				LTPP Site 9C			
		2002				2002			
		April	July	Sept.	Dec.	April	July	Sept.	Dec.
Base	Field data	41.0	41.0	34.8	-	18.0	22.9	18.0	34.8
	EICM (56ss/16ws)	18.3	15.9	16.2	3.1	18.7	16.0	18.1	9.6
Subbase	Field data	24.2	33.7	20.4	29.4	38.0	34.8	35.9	34.8
	EICM (56ss/16ws)	21.5	18.8	19.1	26.1	24.9	21.6	24.1	12.6
Subgrade	Field data	40.0	39.1	38.0	38.3	48.0	48.7	49.5	48.7
	EICM (56ss/16ws)	33.3	30.2	30.8	12.5	35.6	31.9	34.8	18.3
		LTPP Site 5E				LTPP Site 9C			
		2003				2003			
		April	July	Sept.	Dec.	April	July	Sept.	Dec.
Base	Field data	45.5	43.8	43.8	45.5	29.0	31.4	31.4	22.9
	EICM (56ss/16ws)	19.5	19.6	16.4	19.2	18.5	19.6	18.7	18.9
Subbase	Field data	29.0	31.4	29.0	43.8	46.4	42.1	42.9	38.0
	EICM (56ss/16ws)	22.8	22.9	19.4	22.5	24.7	25.9	24.8	25.1
Subgrade	Field data	54.8	50.0	53.3	29.0	48.7	49.5	50.3	48.0
	EICM (56ss/16ws)	34.7	34.8	31.0	34.3	35.4	36.6	35.6	35.9

Correlation Analysis

As shown earlier in Figure 45, the EICM-predicted temperatures for the two locations within the asphalt surface layer were generally higher than field-measured temperatures. However, the trend in temperature variation within the two months (July and September, 2003), at Site 9C, were almost identical for the EICM-predicted and measured temperatures. To determine whether this trend was repeated for other sites and months, a correlation analysis was carried out between the EICM-predicted and field-measured parameters. The reproducibility of the EICM was evaluated based on two main parameters: temperature and moisture content. Figure 52 provides samples of the correlation analysis results for temperature at the two sections (5E and 9C), whereas Figure 53 provides similar analysis results for the moisture content.

As can be seen from both figures, the EICM-predicted and field-measured temperatures and moisture contents varied significantly. The correlation analysis indicated that even for each particular site, the trend changed with the seasons (issue of repeatability). In addition, the results were not consistent between sites (issue of reproducibility). It should be noted that the data presented in figures 52 and 53 are measured and predicted at the same locations in the pavement structure. The pavement temperatures presented in Figure 52 were measured and predicted at depths of 0 (0); 14 (5.5); 25 (10); 31.5 (12.5); 39.3 (15.5); 46.6 (18.3); 54.6 (21.5); 61.7 (24.3); 92.2 (36.3); 122.9 (48.4) and 153.7 (60.5) cm (in) for the site 9C and 3.8 (1.5); 15.2 (6); 26 (10.2); 34.2 (13.5); 41.3 (16.25); 48.9 (19.25); 56.5 (22.25); 64.4 (25.4); 94.8 (37.3); 125.4 (49.4) and 155.8 (61.3) cm (in) for the site 5E, while the MC presented in Figure 53 was measured and predicted at depths of 40.6 (16); 82.6 (32.5) and 135.9 (53.5) cm (in) for the site 9C and at 34.5 (13.5); 55.9 (22) and 92.7 (36.5) cm (in) for the site 5E.

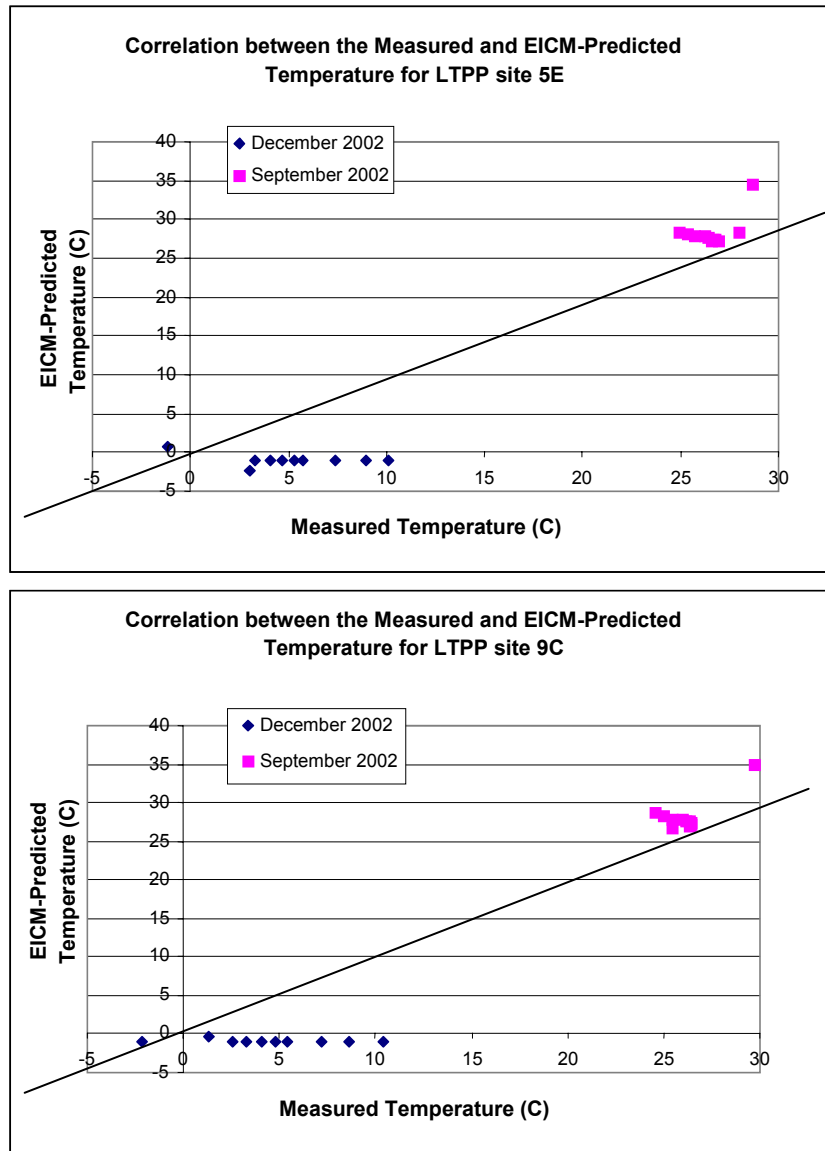


Figure 52: Correlation Analysis Results for Asphalt Concrete Temperature

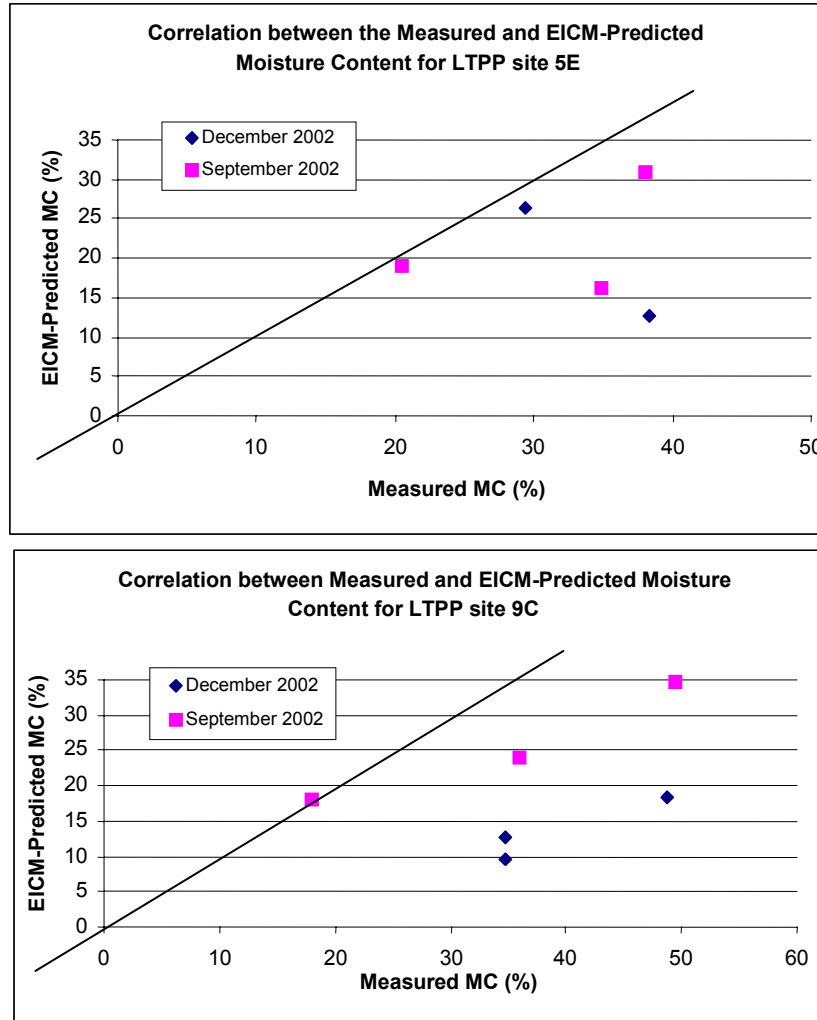


Figure 53: Correlation Analysis Results for Moisture Content (MC)

Summary of Findings

Temperature and moisture data from the SMS testing at two LTPP test sites within New Jersey were analyzed to evaluate the EICM model for its applicability to New Jersey conditions. It was shown that a strong, consistent correlation did not exist between EICM-predicted and field-measured temperature, especially for the surface layers. For some sites/hours an acceptable correlation was found for the subgrade. However, the correlation varied significantly by site and time. Temperature prediction is improved below the 30 cm (11.8 in) depth (granular and subgrade layers). In addition to temperature, the capability of the EICM to predict pavement moisture variation was also evaluated. A wide discrepancy was observed between predicted and measured moisture contents, and no reasonable correlation was found. A sensitivity analysis was carried out using different wind speed and percent sunshine to determine whether these parameters have any significant effect on the gap between the predicted and measured temperatures. It was observed that change in wind speed has a greater influence on predicted data than the change in percent sunshine. However, although a wide range of values for percent sunshine and wind speed was considered in the analysis, the gap between the measured and predicted temperatures was still significant. In addition, a correlation analysis was carried out between EICM-predicted and field-measured temperatures and moisture

contents. The results indicated a significant variation between the two forms of measurements (predicted and measured).

Due to the inconsistent model output results, EICM cannot be utilized in its present form to account for seasonal adjustment on pavement sections within New Jersey. As such, adjustments to the EICM model are required or a new model needs to be developed to suit site-specific New Jersey conditions.

EMPIRICAL SEASONAL AND TEMPERATURE MODELS

The development of the empirical seasonal and temperature models incorporated six alternatives to correct pavement response for different climatic parameters, including temperature and moisture content. As seen in Figure 54, different streams were implemented that can be used for this purpose. The following sub-sections describe the development of these models in more detail.

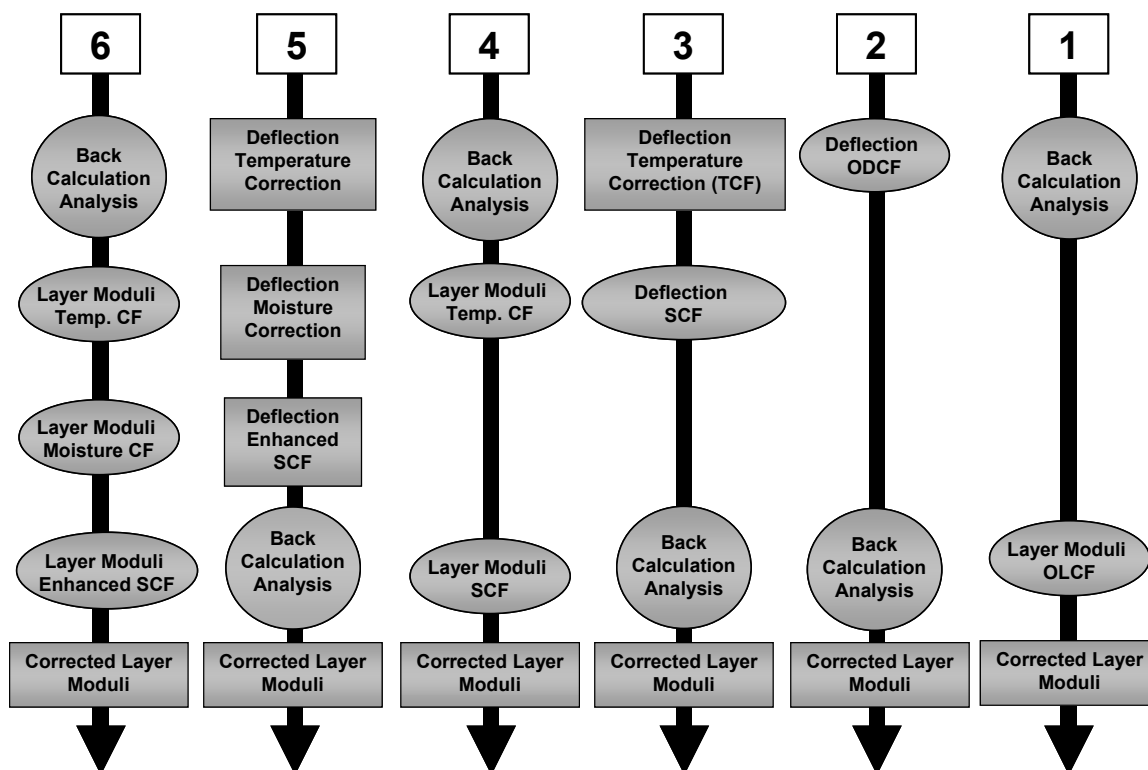


Figure 54: Different Streams for the Implementation of NJ Specific Models

Development of Overall Layer Moduli Correction Factors (OLCF) – Stream 1

An empirical approach was used in modeling the impact of all seasonal variation in pavement performance (i.e. seasonal, moisture, and temperature variation). Overall Correction Factors (OCFs) were developed to reference the pavement response data measured at different conditions to standard conditions. The first Overall Correction Factor accounts for temperature and seasonal variations in layer moduli, termed as OLCF, and should be applied to the backcalculated results from temperature and moisture uncorrected deflections. The following formula was used to calculate the overall correction factors:

$$\text{Standard Parameter}_{(\text{May})} = \text{Measured Parameter} * \text{OLCF} \quad (\text{E6})$$

Where:

- Standard Parameter is the layer moduli used in the forward calculations, as explained earlier.
- Measured Parameter is the layer moduli backcalculated from the FWD data.

The month of May was selected to be the base month for the layer moduli and for the development of overall correction factors, i.e. correction factors to convert measurements made during other months to equivalent May numbers. Table 17 shows the implemented overall correction factors for different thicknesses and regions.

Table 17: Overall Layer Moduli Correction Factors (OLCF)

Region	Month	Thickness Class	OLCF M_r	OLCF E_p	Region	Month	Thickness Class	OLCF M_r	OLCF E_p
North	1	Thin	0.66	0.42	South	1	Thin	0.91	0.38
North	2	Thin	0.67	0.73	South	2	Thin	0.89	0.83
North	3	Thin	1.08	1.01	South	3	Thin	1.04	0.77
North	4	Thin	1.02	0.90	South	4	Thin	0.96	1.01
North	5	Thin	1.00	1.00	South	5	Thin	1.00	1.00
North	6	Thin	0.93	1.42	South	6	Thin	0.83	1.22
North	7	Thin	1.08	1.08	South	7	Thin	0.81	1.36
North	8	Thin	0.86	1.19	South	8	Thin	0.79	1.31
North	9	Thin	0.91	0.88	South	9	Thin	0.82	1.07
North	10	Thin	0.87	0.65	South	10	Thin	1.10	1.54
North	11	Thin	0.76	0.67	South	11	Thin	0.89	0.71
North	12	Thin	0.98	0.61	South	12	Thin	1.00	0.62
North	1	Thick	0.93	0.27	South	1	Thick	0.95	0.60
North	2	Thick	0.92	0.87	South	2	Thick	0.90	1.10
North	3	Thick	0.99	1.02	South	3	Thick	1.07	0.95
North	4	Thick	0.97	0.97	South	4	Thick	0.95	1.26
North	5	Thick	1.00	1.00	South	5	Thick	1.00	1.00
North	6	Thick	0.96	1.08	South	6	Thick	0.87	1.34
North	7	Thick	1.11	0.95	South	7	Thick	0.85	1.41
North	8	Thick	0.86	1.02	South	8	Thick	0.83	1.37
North	9	Thick	0.91	0.83	South	9	Thick	0.86	1.29
North	10	Thick	0.98	0.82	South	10	Thick	0.90	1.16
North	11	Thick	0.79	0.85	South	11	Thick	0.96	0.96
North	12	Thick	1.03	0.83	South	12	Thick	0.99	0.77

Development of Overall layer Deflection Correction Factors (ODCF) – Stream 2

A second approach (Stream 2) was implemented to develop OCFs for deflections. The ODCF was calculated using the same formula as mentioned in the previous subsection (Equation E6), but with standard and measured deflections instead. These correction factors account for all seasonal variations in pavement performance (i.e. seasonal, moisture, and temperature variation). The ODCFs are applied to the uncorrected moisture and temperature deflections. The calculated deflections are then used to backcalculate the layer moduli resulting in corrected E_p and M_r . The resulting correction factors are shown in Figures 55a and 55b for the North Region, and Figures 55c and 55d for the South Region.

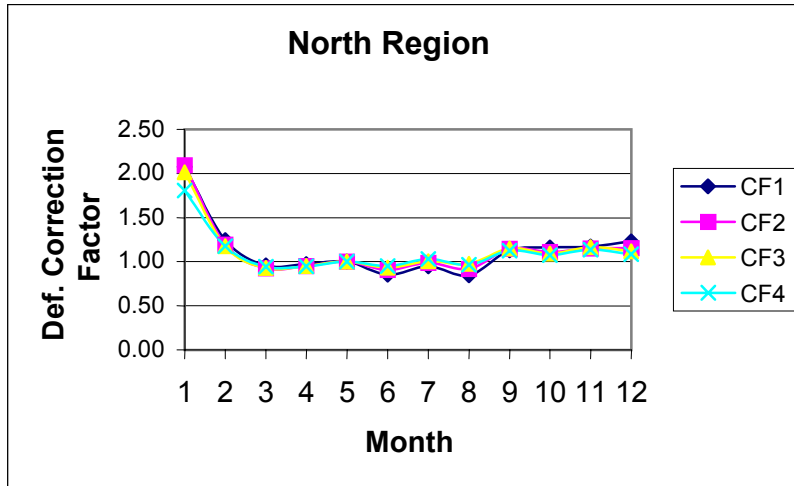


Figure 55a: ODCF for North Region (Sensors 1 to 4)

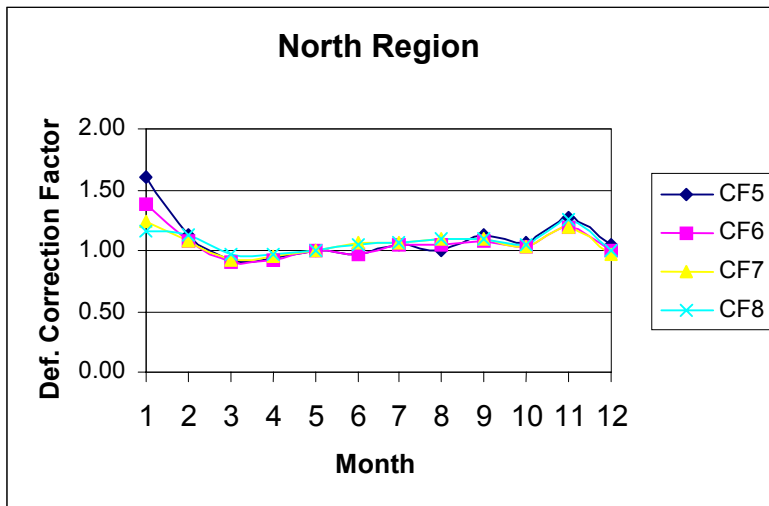


Figure 55b: ODCF for North Region (Sensors 5 to 8)

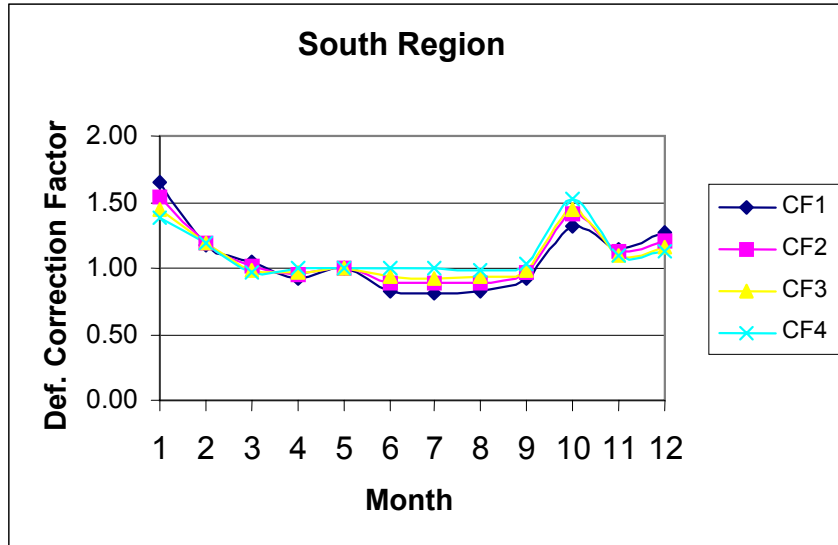


Figure 55c: ODCF for South Region (Sensors 1 to 4)

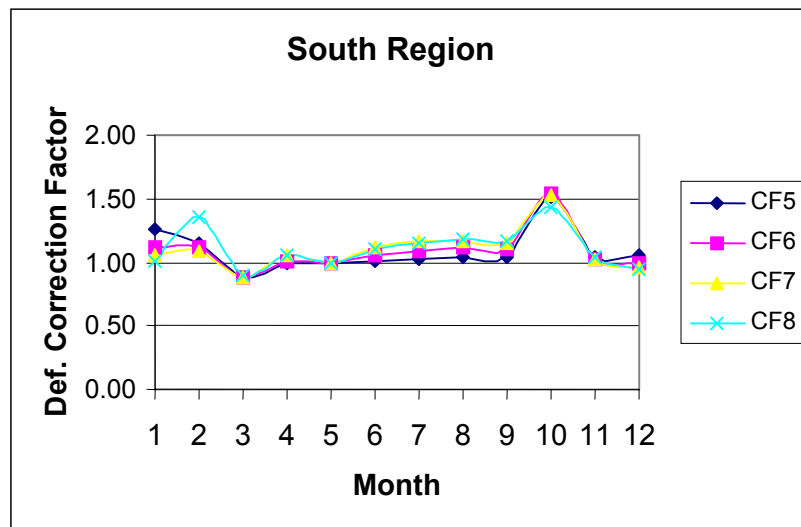


Figure 55d: ODCF for South Region (Sensors 5 to 8)

Development of Deflection Temperature Correction Factors (TCF) and Seasonal Correction Factors (SCF) – Stream 3

The third approach was implemented to take into consideration other climatic parameters such as the variation in temperature. Initially, the deflection temperature correction models were developed and applied to the deflection. Seasonal correction models were then implemented and were subsequently used to correct for any variations other than temperature. Therefore, these seasonal correction models should be applied to the temperature-corrected deflections. The following subsection shows the development of deflection temperature and seasonal correction factors in more details.

Development of Temperature Adjustment Models

Regression analysis was performed to develop TCFs that can be used to account for the impact of temperature changes on the measured deflections. These TCFs are used in the following formula:

$$\text{Standard Parameter} = \text{Measured Parameter} * \text{TCF} \quad (\text{E7})$$

Where:

The Standard Parameter is the temperature corrected D_1 to D_8 .

The Measured Parameter is the temperature uncorrected D_1 to D_8 .

The measured asphalt temperatures (surface, mid-point, and bottom) and the corresponding deflections measured at different offset distances (D_1 to D_8) were grouped by Region (North/South) and by asphalt thickness (Thin/Thick). TCFs were calculated for all the available FWD data, as the ratio between the standard deflection and the temperature uncorrected deflection. Regression analysis was then performed on the TCFs and the corresponding AC thickness and mid-depth asphalt temperature (calculated as the average of the surface, mid-point, and bottom temperatures). The following model form was used in the regression analysis:

$$TCF_i = a*T + b*t_{AC} + c \quad (\text{E8})$$

Where:

TCF_i = Temperature Correction factor for the deflection of sensor i ; $i = 1$ to 8

T = Mid-depth AC Temperature, °C

t_{AC} = Thickness of AC layer, inch

a , b , and c = Regression Coefficients

Table 18a and 18b show the regression coefficients (a , b , and c) for different parameters. The following equation is used to adjust deflection measurements, as well as the backcalculated layer moduli, to a certain standard temperature, e.g. 20°C (68 °F) :

$$FTCF_i = \frac{TCF_i}{TCF_{std}} \quad (\text{E9})$$

Where:

$FTCF_i$ = final temperature correction factor for parameter “ i ” (D_1 to D_8).

TCF_t = temperature correction factor for the mid-depth temperature during the FWD test (t).

TCF_{std} = temperature correction factor for the selected standard temperature, e.g. 20°C (68 °F).

Table 18a: Deflection and Layer Moduli Regression Coefficients for North Region

Independent Variable	Thickness Class	a	b	c
D ₁	Thin	-0.0132	-0.2490	2.9311
D ₂	Thin	-0.0092	-0.2102	2.4900
D ₃	Thin	0.0028	-0.2369	2.5118
D ₄	Thin	0.0031	-0.2516	2.7755
D ₅	Thin	0.0053	-0.2563	3.0021
D ₆	Thin	0.0096	-0.2164	3.3498
D ₇	Thin	0.0103	-0.1357	3.5993
D ₈	Thin	-0.0104	-0.1148	4.5976
M _r	Thin	0.0015	0.0159	0.9059
E _p	Thin	0.0042	0.0128	0.9649
D ₁	Thick	-0.0280	0.0000	2.2361
D ₂	Thick	-0.0183	0.0000	1.7770
D ₃	Thick	-0.0160	0.0000	1.7062
D ₄	Thick	-0.0149	0.0000	1.7650
D ₅	Thick	-0.0186	0.0000	2.0277
D ₆	Thick	-0.0169	0.0000	2.5521
D ₇	Thick	-0.0056	0.0000	2.8447
D ₈	Thick	0.0002	0.0000	3.3269
M _r	Thick	0.0023	0.0000	1.2926
E _p	Thick	0.0351	0.0000	0.5250

Table 18b: Deflection and Layer Moduli Regression Coefficients for South Region

Independent Variable	Thickness Class	a	b	c
D ₁	Thin	-0.0113	0.0000	1.6289
D ₂	Thin	-0.0049	0.0000	1.2024
D ₃	Thin	-0.0027	0.0000	1.1650
D ₄	Thin	0.0027	0.0000	1.1862
D ₅	Thin	0.0073	0.0000	1.3482
D ₆	Thin	0.0212	0.0000	1.7371
D ₇	Thin	0.0352	0.0000	2.2210
D ₈	Thin	0.0343	0.0000	2.8677
M _r	Thin	-0.0106	0.0000	1.1736
E _p	Thin	0.0129	0.0000	0.9678
D ₁	Thick	-0.0265	-0.0221	2.2838
D ₂	Thick	-0.0157	-0.0299	1.9746
D ₃	Thick	-0.0110	-0.0403	2.0220
D ₄	Thick	-0.0051	-0.0605	2.2681
D ₅	Thick	0.0024	-0.0853	2.6055
D ₆	Thick	0.0153	-0.1457	3.5775
D ₇	Thick	0.0267	-0.1845	4.3694
D ₈	Thick	0.0313	-0.1825	4.7931
M _r	Thick	-0.0084	-0.0056	1.2401
E _p	Thick	0.0336	0.0055	0.5608

Sample Implementation of the Temperature Correction Model

A sample implementation of the temperature correction models is presented in Figure 56. In this figure, a temperature-uncorrected deflection basin from one of the SPS-5 test sections in New Jersey is shown along with those that have been temperature corrected using the AASHTO Temperature Correction Model and the developed model herein.⁽⁸⁾ As can be seen, the AASHTO correction model provided unrealistic results, namely, D_1 is less than D_2 , while the developed model provided more realistic results. The results of the backcalculation analysis performed on the three deflection basins can be summarized as follows:

- M_r and E_p (no temperature correction) are 14,231 and 115,803 psi, respectively
- M_r and E_p (AASHTO temperature correction) are 14,231 and 161,053 psi, respectively
- M_r and E_p (developed TCF) are 12,865 and 149,248 psi, respectively

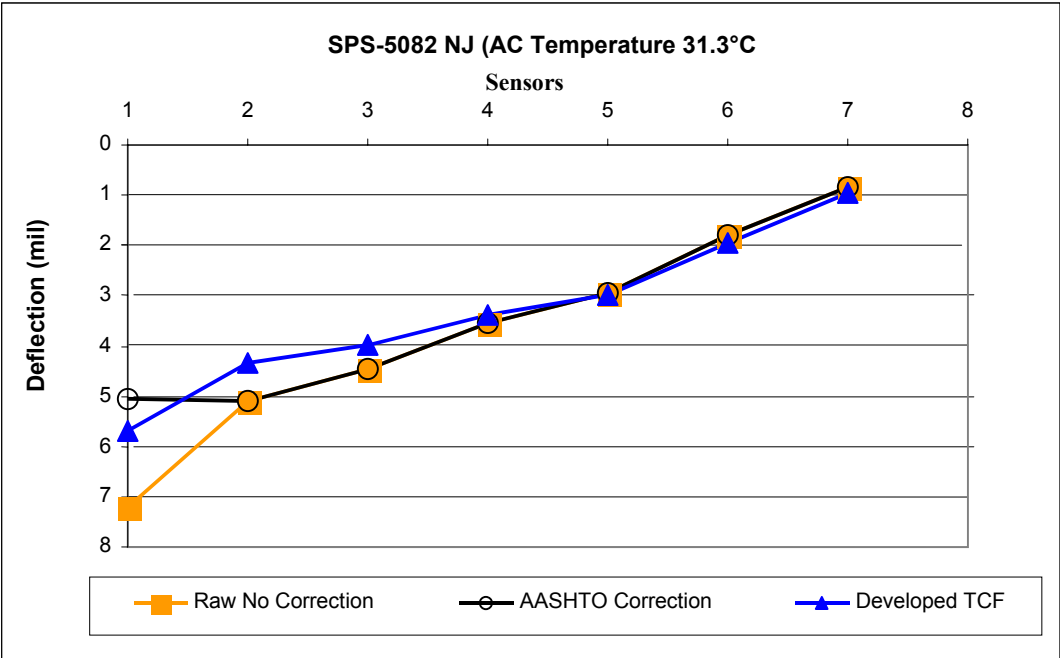


Figure 56: Sample Implementation of Temperature Correction Factors

Development of SCF

An empirical approach was used in modeling the impact of seasonal variation on pavement performance. SCFs were developed to reference the pavement response data measured at different conditions to standard conditions. In this analysis, the measured deflections were corrected first for temperature using the TCF-developed models. The corrected deflections were then grouped by region (North/South) and total thickness class (thin/thick). The SCFs implemented herein account for seasonal variations other than temperature, and they should therefore be applied on the temperature-corrected deflections. Figures 57a and 57b show a sample of the developed SCF for deflections (D) related to thick and thin pavements for the North climatic region.

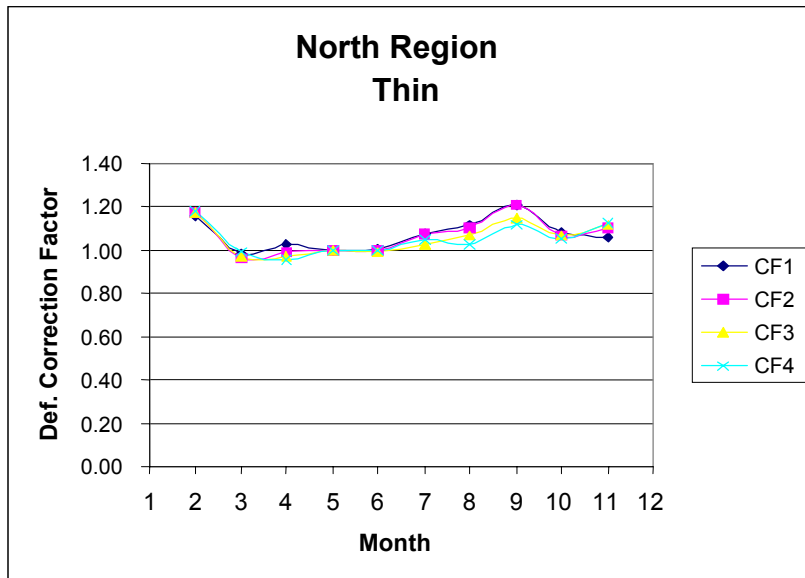


Figure 57a: Seasonal Correction Factors for Deflection (North Thin Region)

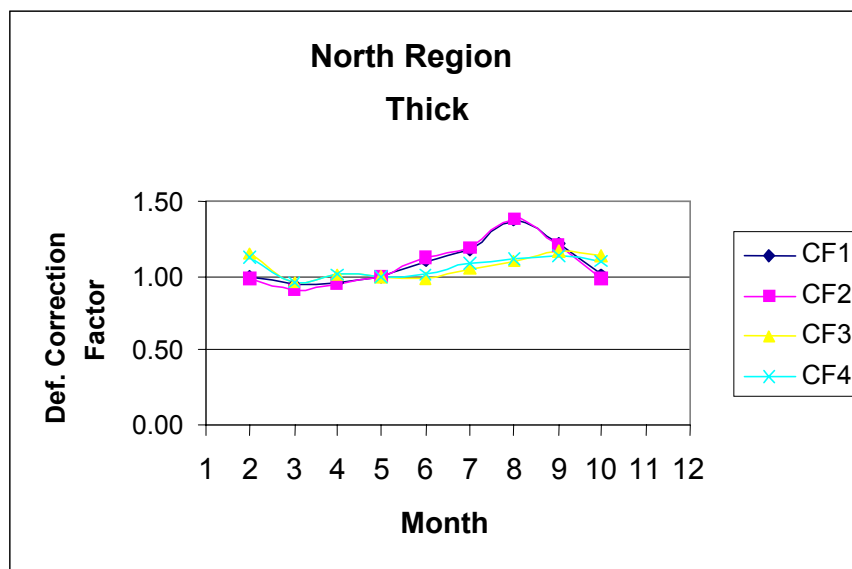


Figure 57b: Seasonal Correction Factors for Deflection (North Thick Region)

Table 19 shows the complete set of results. It should be noted that some cells could not be filled, especially in the winter season. This is due to the fact that limited data was available during this period and also due to the fact that temperature correction models can only be applied for temperatures above 6°C (43°F). Therefore, any deflection measured below 6°C(43°F) was not used in the development of seasonal correction factors.

Table 19: Summary of Correction Factors

Region	Month	Total Thick. Class	CF ₁	CF ₂	CF ₃	CF ₄	CF ₅	CF ₆	CF ₇	CF ₈	CF M _r	CF E _p
N	1	Thin										
N	2	Thin	1.16	1.17	1.18	1.18	1.15	1.07	1.02	0.92	0.77	1.06
N	3	Thin	0.99	0.96	0.97	0.99	0.99	0.96	0.95	0.94	1.19	1.10
N	4	Thin	1.03	0.99	0.97	0.96	0.94	0.92	0.92	0.94	0.98	0.87
N	5	Thin	1.00	1.00	1.00	1.00	1.00	1.00	1.00	1.00	1.00	1.00
N	6	Thin	1.01	1.00	0.99	1.00	1.02	1.02	1.06	1.08	0.91	1.11
N	7	Thin	1.08	1.07	1.03	1.05	1.05	1.05	1.05	1.09	1.06	0.91
N	8	Thin	1.12	1.10	1.07	1.02	1.05	1.06	1.05	1.09	0.79	0.90
N	9	Thin	1.21	1.21	1.15	1.12	1.11	1.08	1.08	1.11	0.90	0.82
N	10	Thin	1.08	1.07	1.07	1.06	1.04	1.04	1.06	1.05	0.85	0.85
N	11	Thin	1.06	1.10	1.12	1.13	1.28	1.21	1.23	1.27	0.76	1.17
N	12	Thin										
N	1	Thick										
N	2	Thick	1.00	0.98	1.15	1.12	1.14	1.02	1.00	1.10	0.93	0.87
N	3	Thick	0.95	0.90	0.95	0.96	0.95	0.89	0.96	1.04	1.00	1.03
N	4	Thick	0.96	0.95	1.01	1.01	1.01	0.94	1.01	1.05	0.98	0.99
N	5	Thick	1.00	1.00	1.00	1.00	1.00	1.00	1.00	1.00	1.00	1.00
N	6	Thick	1.10	1.12	0.98	1.00	0.98	0.94	1.02	1.05	0.94	1.05
N	7	Thick	1.18	1.19	1.05	1.09	1.06	1.02	1.04	1.07	1.09	0.92
N	8	Thick	1.37	1.38	1.10	1.12	1.06	1.06	1.10	1.20	0.84	0.97
N	9	Thick	1.21	1.20	1.17	1.14	1.12	1.03	1.07	1.12	0.91	0.83
N	10	Thick	1.01	0.99	1.13	1.10	1.11	1.00	1.03	1.02	1.00	0.85
N	11	Thick										
N	12	Thick										
S	1	Thin										
S	2	Thin	1.20	1.22	1.25	1.30	1.33	1.41	1.47	1.41	1.02	1.92
S	3	Thin	0.99	0.99	0.99	0.98	0.92	0.93	0.96	0.96	1.00	0.96
S	4	Thin	1.02	1.02	1.01	1.04	1.01	1.00	1.04	1.03	0.98	0.97
S	5	Thin	1.00	1.00	1.00	1.00	1.00	1.00	1.00	1.00	1.00	1.00
S	6	Thin	1.10	1.07	1.05	1.08	1.02	1.00	1.03	1.01	0.92	0.92
S	7	Thin	1.10	1.08	1.06	1.10	1.06	1.04	1.07	1.06	0.91	1.00
S	8	Thin	1.04	1.03	1.04	1.05	1.05	1.07	1.09	1.10	0.86	1.03
S	9	Thin	1.12	1.12	1.11	1.12	1.08	1.08	1.11	1.12	0.87	0.91
S	10	Thin	1.28	1.33	1.32	1.39	1.37	1.40	1.40	1.36	1.06	1.70
S	11	Thin	1.19	1.19	1.17	1.17	1.13	1.08	1.10	1.12	0.86	0.79
S	12	Thin	1.14	1.15	1.13	1.12	1.07	1.03	1.03	1.03	0.89	0.80
S	1	Thick										
S	2	Thick										
S	3	Thick	0.93	0.94	0.94	0.95	0.91	0.96	0.97	0.96	1.05	1.12
S	4	Thick	0.95	0.95	0.94	0.97	0.92	0.93	0.98	0.99	1.00	1.08
S	5	Thick	1.00	1.00	1.00	1.00	1.00	1.00	1.00	1.00	1.00	1.00
S	6	Thick	0.87	0.90	0.91	0.94	0.89	0.89	0.93	0.95	0.95	1.07
S	7	Thick	0.96	0.98	0.97	1.01	0.97	0.99	1.02	1.03	0.96	1.07
S	8	Thick	0.94	0.95	0.96	0.97	0.97	1.02	1.03	1.06	0.91	1.08
S	9	Thick	1.00	1.01	1.00	1.02	0.99	1.03	1.06	1.07	0.93	1.04
S	10	Thick	0.97	0.99	0.99	1.01	1.00	1.02	1.05	1.08	0.97	1.40
S	11	Thick	1.02	1.02	1.02	1.04	1.02	1.05	1.06	1.05	0.95	1.03
S	12	Thick	1.04	1.08	1.08	1.09	1.08	1.10	1.08	1.04	0.94	0.96

Development of Layer Moduli Temperature Correction Factors (TCF) and Seasonal Correction Factors (SCF) – Stream 4

The same process used in Stream 3 for deflection was applied once again for layer moduli (M_r and E_p) to develop temperature correction and seasonal correction for layer moduli (stream 4). The same typical equation for temperature correction (Equation E8) was used as follows:

$$TCF_i = a*T + b*t_{AC} + c \quad (E10)$$

Where:

TCF_i = Correction factor for M_r and E_p

T = Mid-depth AC Temperature, °C

t_{AC} = Thickness of AC layer, inch

a , b , and c = Regression Coefficients

Similarly, seasonal correction factors for layer moduli were developed that account for any seasonal variations other than temperature. The implemented coefficients (a , b , and c) for temperature correction factors for layer moduli are shown in Table 18. Figures 58 and 59 show the developed SCF for Material Properties (M_r and E_p) for the North and South climatic regions, respectively. The complete set is also shown in Table 19. The temperature and seasonal correction factors for layer moduli developed herein should be applied to backcalculation results from temperature uncorrected deflections.

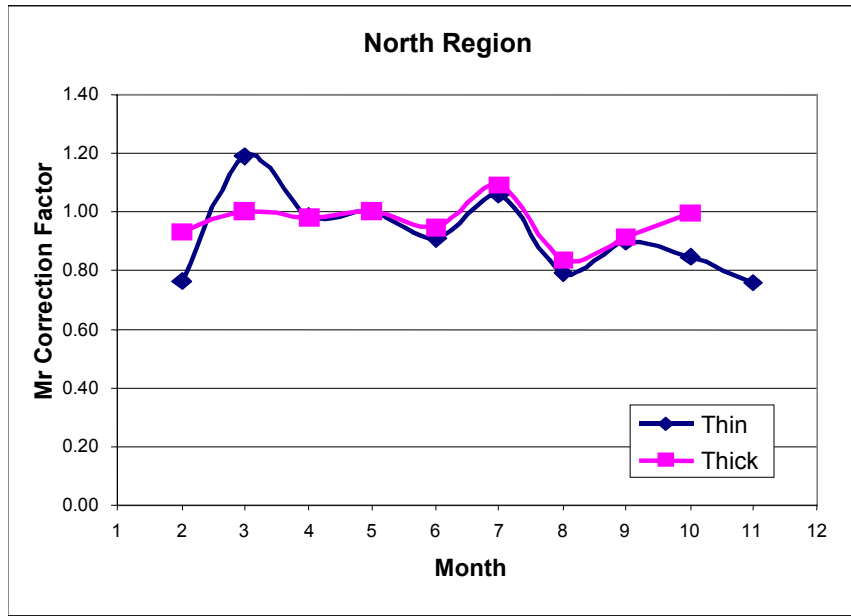


Figure 58a: Seasonal Correction Factors for M_r - (North Region)

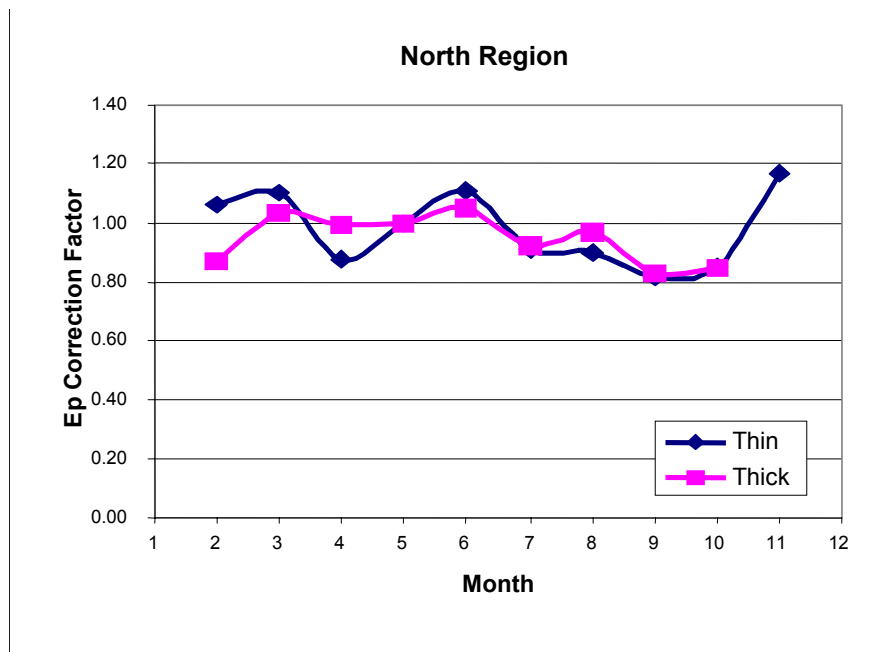


Figure 58b: Seasonal Correction Factors for E_p - (North Region)

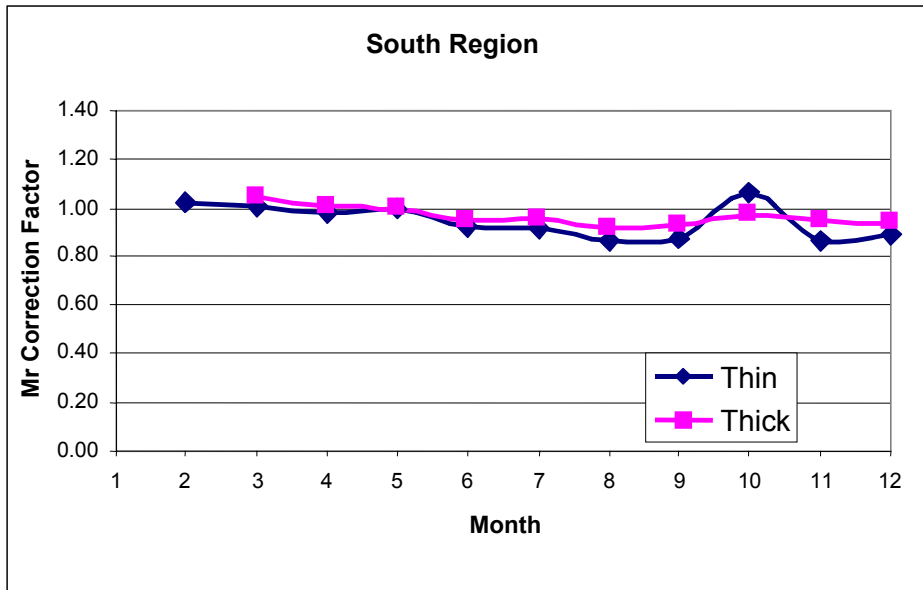


Figure 59a: Seasonal Correction Factors for M_r - (South Region)

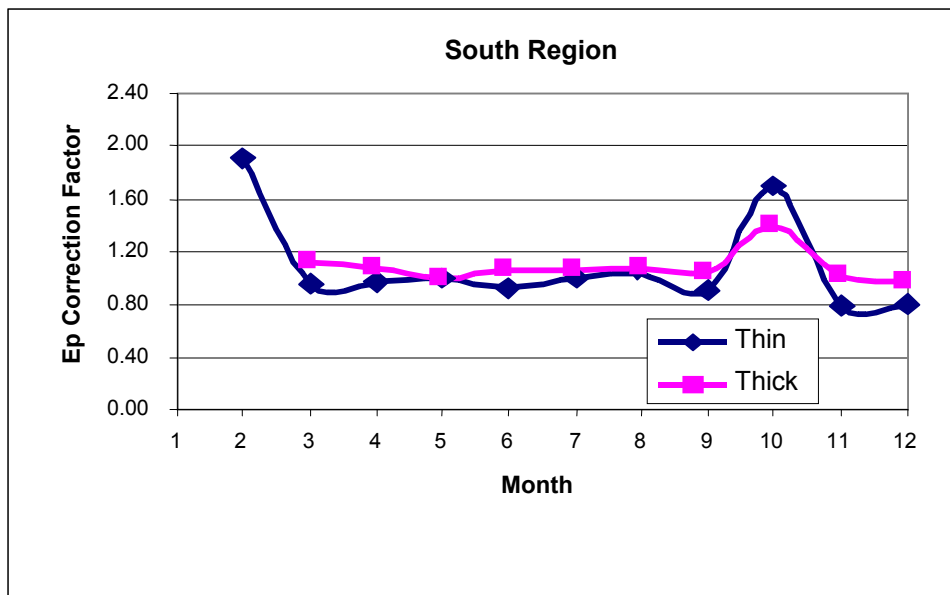


Figure 59b: Seasonal Correction Factors for E_p - (South Region)

Development of Deflection Moisture Correction Factors (MCF) and Enhanced Seasonal Correction Factors (ESCF) – Stream 5

The ANOVA analysis illustrated earlier showed that moisture content has a great influence on the measured deflection. Therefore, the incorporation of the moisture content in the developed models would obviously reduce the expected tolerance in the measurement of deflection. Accordingly, moisture content correction models were developed for correcting both the deflection and layer moduli. These models can be used based on the availability of measuring this parameter in the field. The following section illustrates in detail the implementation of both moisture and enhanced seasonal correction factors.

Development of MCF

The moisture data for base, subbase, and subgrade collected from the field were used to correlate the measured deflection with its corresponding moisture content. Initially, the deflections were corrected for temperature using TCFs developed earlier to eliminate the effect of temperature on the measured deflection. Therefore, the remaining effects are due to the effect of other climatic parameters, including moisture content. Moisture content correction factors (MCCFs) were calculated using the following formula:

$$\text{Standard Parameter} = \text{Measured Parameter} * \text{MCCF} \quad (\text{E11})$$

Where:

Standard Parameter is the moisture-corrected D_1 to D_8 .

Measured Parameter is the moisture-uncorrected D_1 to D_8 .

Next, regression analysis was performed on the MCCFs, the corresponding total thickness, and moisture content. The following model form was used in the regression analysis:

$$\text{MCCF}_i = a * \text{MC} + b * t + c \quad (\text{E12})$$

Where:

MCCF_i = Moisture Content Correction factor for the deflection of sensor i ; $i = 1$ to 8

MC = Volumetric Moisture Content, %

t = Total Thickness of the pavement, inch

a , b , and c = Regression Coefficients

Table 20 shows the regression coefficients (a , b , and c) for different parameters. It should be noted that the moisture content used varies with the deflection sensor under investigation. For instance, it was found that deflection D_1 is highly affected by the base moisture content, while sensors away from the load drop (D_5 to D_8) are more affected by the subgrade moisture content.

Table 20a: Regression Coefficients for Different Parameters for North Region

Independent Variable	Total Thickness Class	Moisture Content	a	b	c
D ₁	Thin	Base	-0.00771	-0.0673	3.6916
D ₂	Thin	Avg(SB+SG)	-0.00301	-0.0651	3.2947
D ₃	Thin	Avg(SB+SG)	-0.00217	-0.0944	4.0285
D ₄	Thin	Avg(SB+SG)	-0.1403	0.0271	5.3942
D ₅	Thin	SG	-0.00633	-0.1274	5.4394
D ₆	Thin	SG	-0.01011	-0.1193	5.9696
D ₇	Thin	SG	-0.00439	-0.0390	2.1356
D ₈	Thin	SG	-0.00572	-0.0135	1.7006
M _r	Thin	SG	0.00426	-0.0207	1.3455
E _p	Thin	Base	0.01075	0.0550	-0.459
D ₁	Thick	Base	-0.0560	0	1.3719
D ₂	Thick	Base	-0.0598	0	1.3356
D ₃	Thick	Avg(SB+SG)	-0.00827	0	1.0873
D ₄	Thick	Avg(SB+SG)	-0.00778	0	1.2191
D ₅	Thick	SG	-0.01511	0	1.7466
D ₆	Thick	SG	-0.02352	0	2.7760
D ₇	Thick	SG	-0.00930	0	1.2295
D ₈	Thick	SG	-0.01256	0	1.5951
M _r	Thick	SG	0.01104	0	0.5849
E _p	Thick	Base	0.00563	0	1.2269

Table 20b: Regression Coefficients for Different Parameters for South Region

Independent Variable	Total Thickness Class	Moisture Content	a	b	c
D ₁	Thin	Base	-0.00565	-0.0250	2.389
D ₂	Thin	Base	-0.00588	-0.0286	2.376
D ₃	Thin	Avg(SB+SG)	-0.01564	-0.0641	3.8984
D ₄	Thin	Avg(SB+SG)	-0.01346	-0.0668	4.0388
D ₅	Thin	SG	-0.01277	-0.0285	3.2321
D ₆	Thin	SG	-0.00805	-0.0420	3.9695
D ₇	Thin	SG	-0.00226	-0.0083	1.2491
D ₈	Thin	SG	-0.00288	0.00184	1.6609
M _r	Thin	SG	0.004077	-0.0163	1.2708
E _p	Thin	Base	0.00604	-0.0017	1.1830
D ₁	Thick	Base	0.000055	-0.0022	1.5596
D ₂	Thick	Base	-0.00098	-0.0075	1.5719
D ₃	Thick	Avg(SB+SG)	-0.00548	-0.0126	1.9709
D ₄	Thick	Avg(SB+SG)	-0.00508	-0.0177	2.2600
D ₅	Thick	SG	-0.00084	-0.0247	2.549
D ₆	Thick	SG	-0.00026	-0.0390	3.5952
D ₇	Thick	SG	-0.00007	-0.0182	1.7061
D ₈	Thick	SG	0.000463	-0.0172	1.8455
M _r	Thick	SG	0.000409	-0.0008	1.0110
E _p	Thick	Base	0.000059	-0.0012	1.2974

Development of Enhanced Seasonal Correction Factors for Deflection (ESCF)

Applying the correction models for each parameter can eliminate tolerance in the measured deflection due to temperature and moisture. Therefore, an ESCF was implemented that accounts for seasonal effects other than temperature and moisture. The corrected deflections for temperature and moisture were grouped by region (North/South) and total thickness class (thin/thick). Correction models for each month were developed and the month of May was selected as a reference month with correction factor = 1. It should be noted that the ESCF should be applied to deflections that are corrected for both temperature and moisture. Figure 60 (a to d) shows the developed ESCFs.

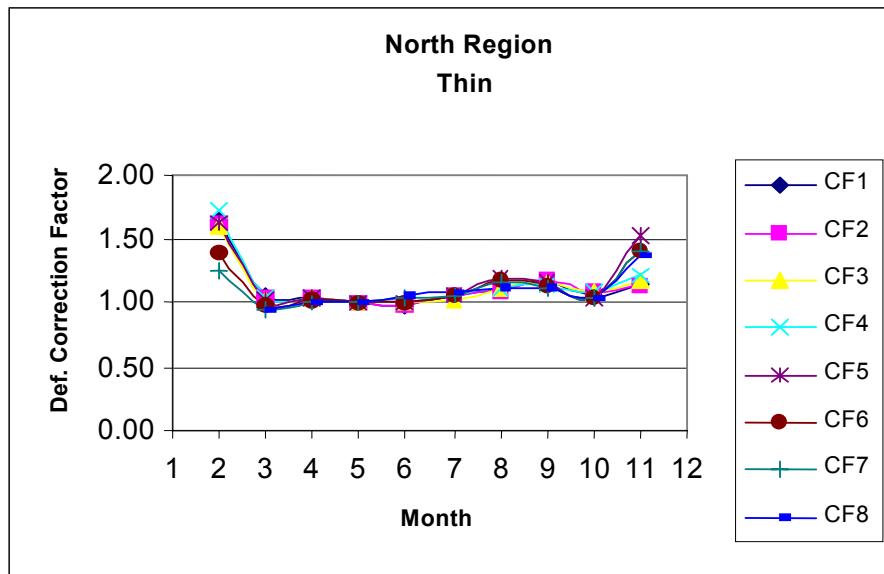


Figure 60a: Deflection ESCF for North/Thin Region

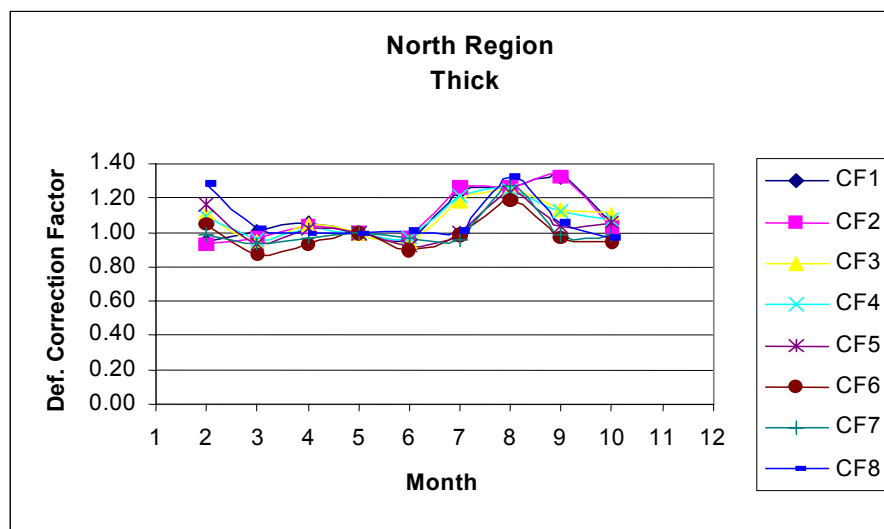


Figure 60b: Deflection ESCF for North/Thick Region

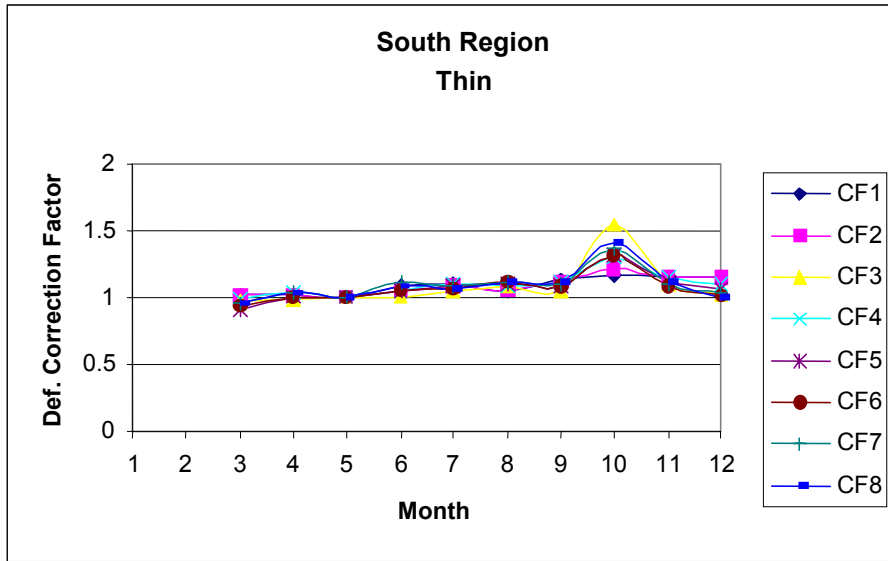


Figure 60c: Deflection ESCF for South/Thin Region

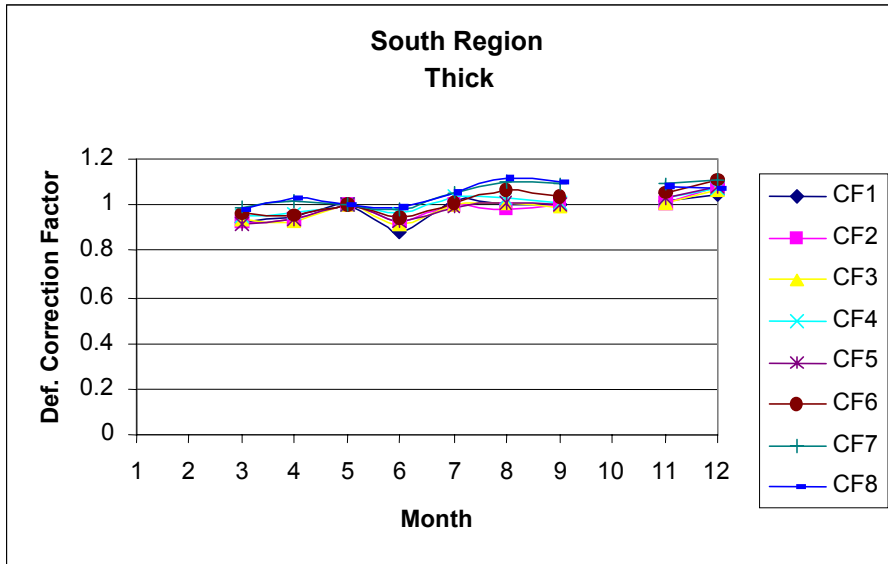


Figure 60d: Deflection ESCF for South/Thick Region

It should be noted that models could not be implemented for certain months (specifically winter months) due to the fact that both moisture and pavement temperature are needed in order to develop the enhanced seasonal correction factors.

Development of Layer Moduli MCF and ESCF – Stream 6

Similar to the deflection models, the layer MCF for moisture were developed using the following form:

$$\text{Standard Parameter} = \text{Measured Parameter} * \text{MCCF} \quad (\text{E13})$$

Where:

Standard Parameter is the moisture-corrected layer moduli (M_r or E_p).

Measured Parameter is the moisture-uncorrected layer moduli (M_r or E_p).

Next, regression analysis was conducted to correlate moisture content and total pavement thickness with the moisture correction factors using the following form:

$$\text{MCCF}_i = a * \text{MC} + b * t + c \quad (\text{E14})$$

Where:

MCCF_i = Moisture Content Correction factor for M_r and E_p

MC = Volumetric Moisture Content, %

t = Total Thickness of the pavement, inch

a, b and c = Regression Coefficients

The layer moduli coefficients have been listed earlier in Table 20a and Table 20b.

Enhanced seasonal correction models were then developed for layer moduli to account for parameters other than temperature and moisture. The monthly data was grouped and classified by total thickness classes (thin/thick) and the month of May was used as a reference with a seasonal correction factor of 1. Figure 61 (a to d) shows the implemented seasonal correction factors for layer moduli. It should be noted that layer moduli correction factors for moisture can only be applied to layer moduli results from backcalculation analysis that have previously been corrected for temperature (Stream 4). Additionally, the deflection that is used in the backcalculation analysis must not be corrected for either temperature or moisture (Stream 6).

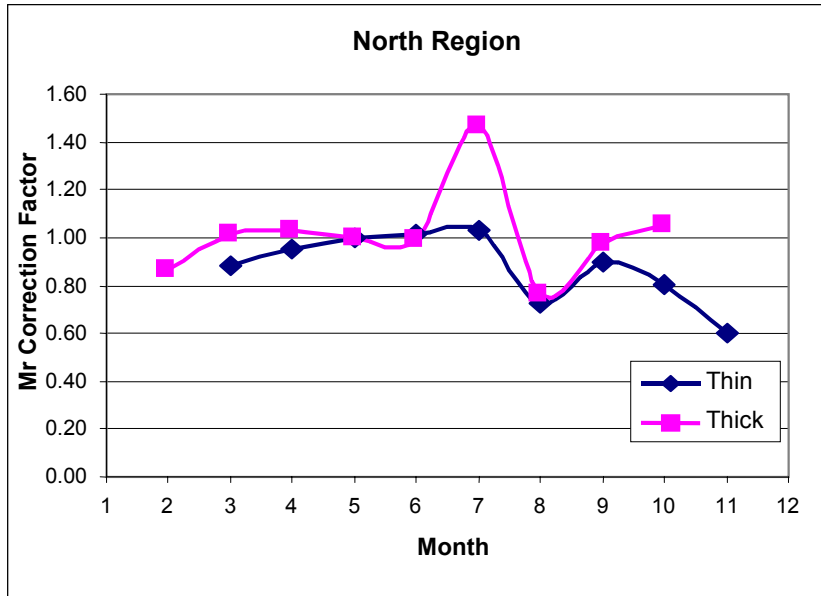


Figure 61a: ESCF for Layer Moduli M_r for North Region

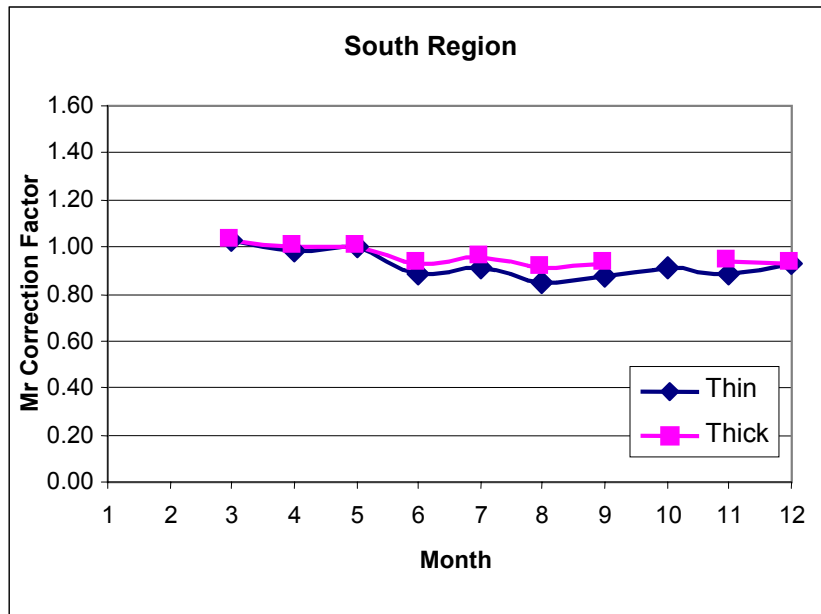


Figure 61b: ESCF for Layer Moduli M_r for South Region

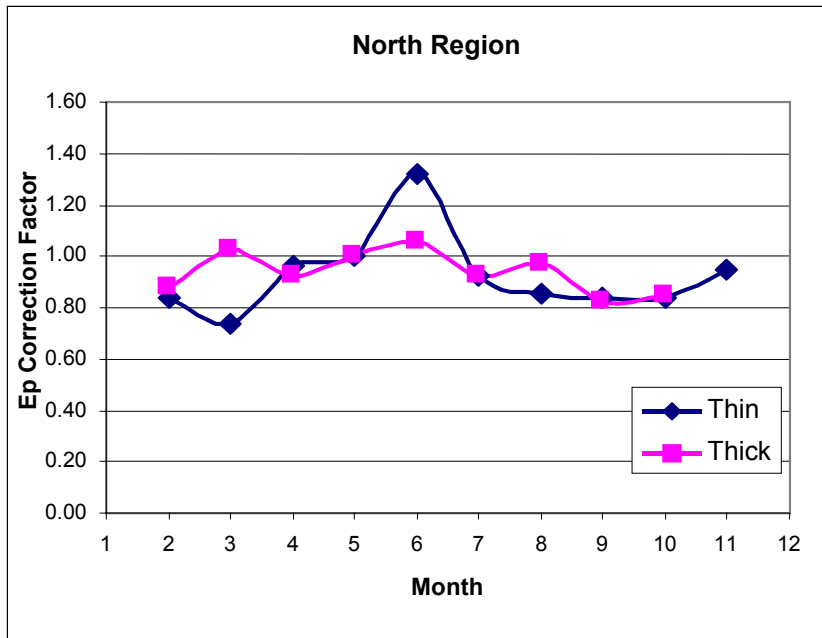


Figure 61c: ESCF for Layer Moduli E_p for North Region

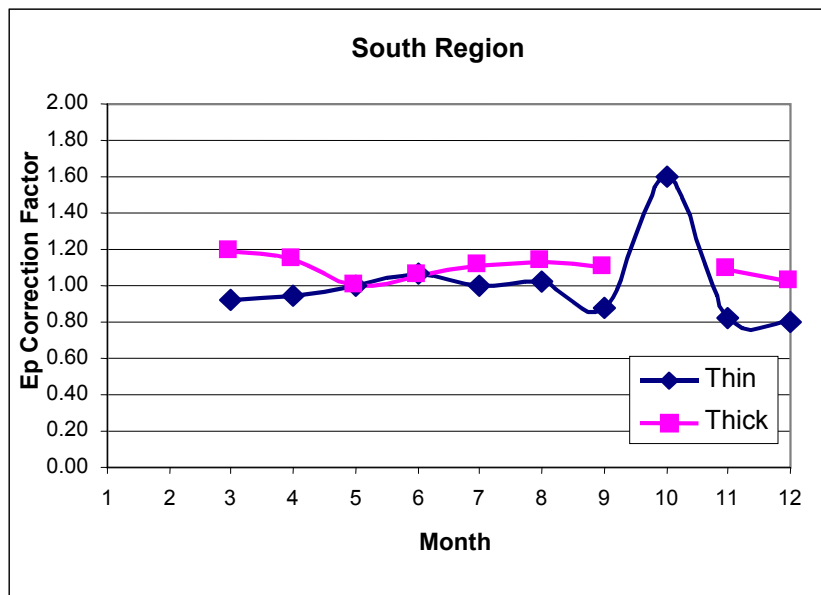


Figure 61d: ESCF for Layer Moduli E_p for South Region

Development of Layer Moduli Temperature Correction Factors for SPA based on SASW Analysis Results (SPATCF)

Flexible Pavements

Backcalculated SPA modulus values using Spectral Analysis of Surface Waves (SASW) analysis suggest a strong influence of temperature on backcalculated asphalt layer modulus. Regression analysis was performed to develop SASW analysis Temperature Correction Factors for SPA (SPATCF) that can be used to account for the impact of temperature changes on the backcalculated paving layer moduli obtained through SASW analysis from field measurements. The developed SPATCF is used in the following formula:

$$\text{Standard Modulus} = \frac{\text{Measured Modulus}}{\text{SPATCF}} \quad (\text{E15})$$

Where:

Standard Modulus is the temperature-corrected modulus (i.e. estimated modulus at 20°C/68 °F).

Measured Modulus is the temperature-uncorrected modulus.

To develop SPATCF, the measured average asphalt temperatures (average of surface, mid-point, and bottom temperatures) and the corresponding backcalculated modulus from SASW analysis were grouped for each test section and regression analysis was performed to obtain a temperature-modulus relationship for each section. Based on this analysis, the backcalculated modulus values of each test section were normalized with respect to modulus at 20°C (68 °F). Typical backcalculated asphalt modulus variation with date and temperature, along with results of regression analysis, are depicted in Figure 62.

Combining results for all sections, a single SPATCF was calculated through a statistical analysis of all available normalized moduli, as the ratio between the measured modulus and the standard temperature-corrected modulus. Results of this analysis are presented in Figure 63. SPATCF variation with temperature and bounds of the SPATCF values (SPATCF plus/minus one standard deviation of error) are depicted in this figure. As presented, the obtained results do not suggest any significant relationship between SPATCF and pavement thickness and/or pavement region (i.e. north or south). This fact can be explained based on the underlying method of analysis of asphalt modulus and development of SPATCF. Since the SASW analysis measures the wave propagation velocity through the whole thickness of the asphalt layer, the backcalculated modulus is calculated with the same assumption. Furthermore, these results are correlated to an average measured temperature in the pavement. Since the temperature temporal distribution is mainly affected by the test section's geographic location, and the spatial (thickness) distribution is mainly affected by the pavement thickness, those two parameters are implicitly considered when developing SPATCF values. Still, the results do not suggest any significant relationship between SPATCF and pavement thickness and/or pavement region.

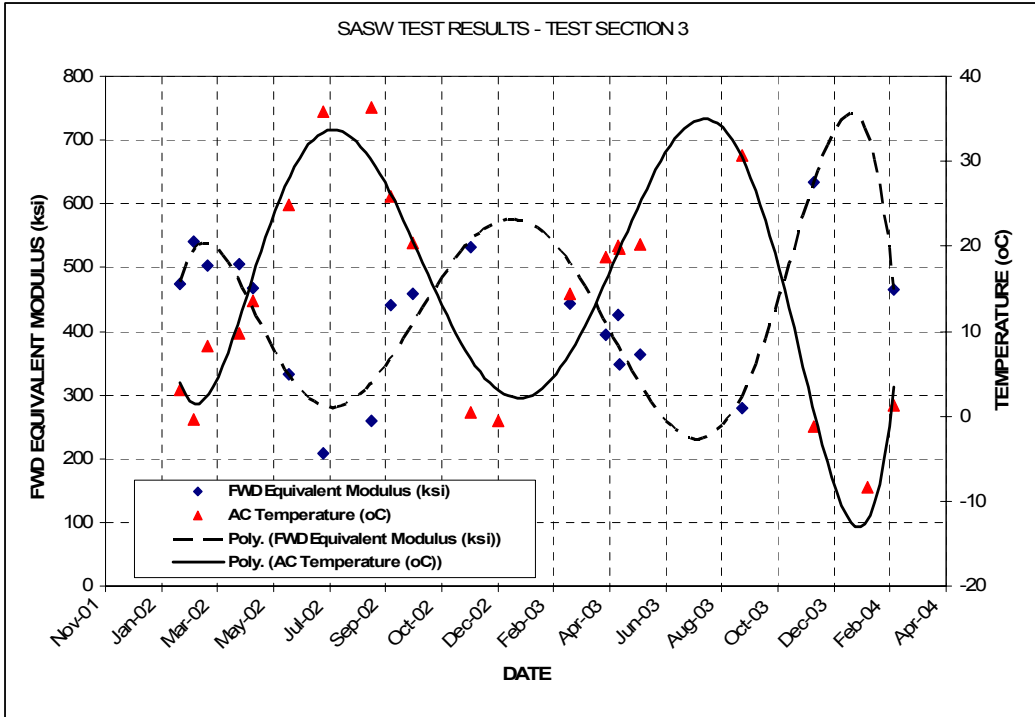


Figure 62a: Typical Asphalt Modulus Variation Obtained through SASW Analysis with Date for Test Section No. 3

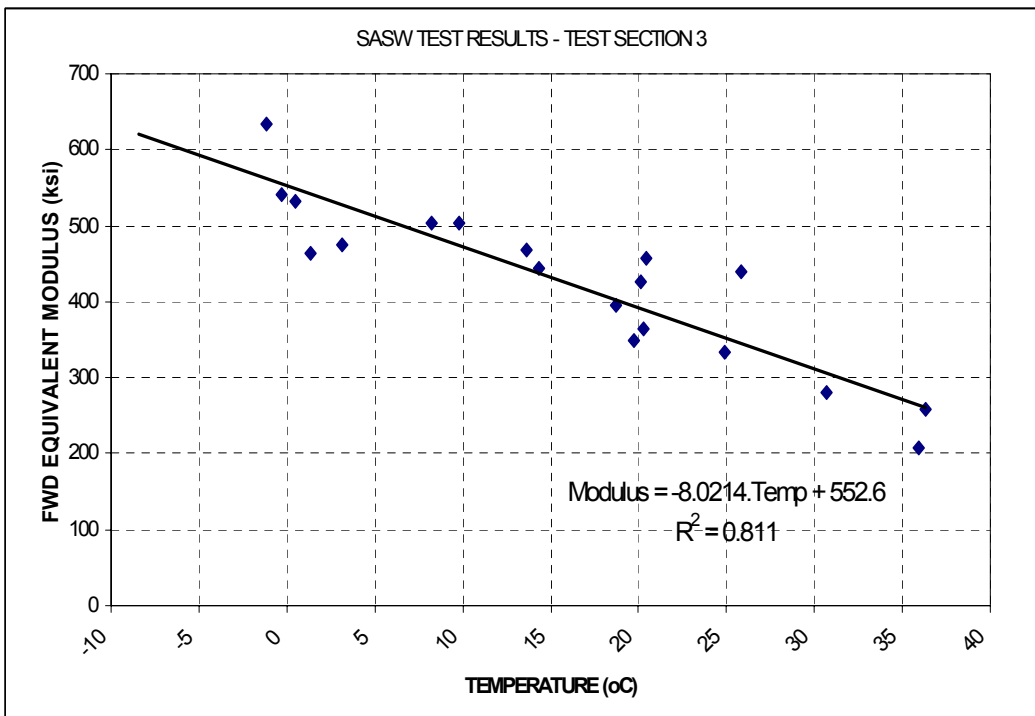
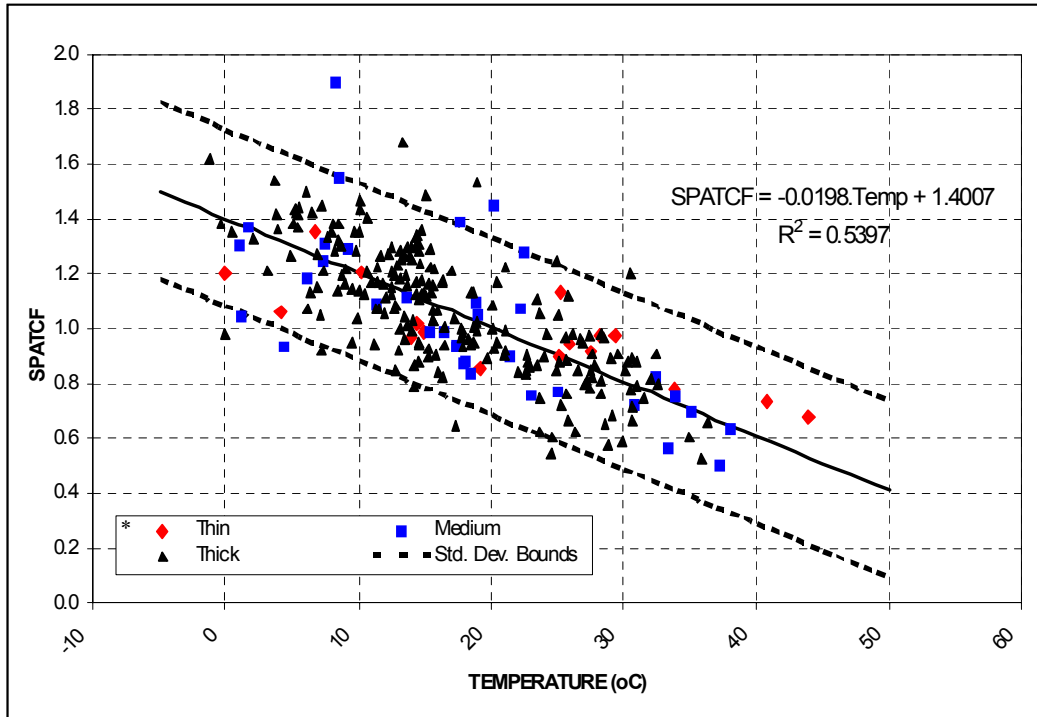


Figure 62b: Typical Asphalt Modulus Variation Obtained through SASW Analysis with Temperature for Test Section No. 3



* As per explanation in Temperature Correction Study Section

Figure 63: SPATCF Values for Asphalt Modulus and Results of Regression Analysis

Based on the statistical analysis, the SASW analysis temperature correction factor (SPATCF) can be presented by the following equations:

$$SPATCF = a * T + b \quad (E16)$$

Where:

SPATCF= Correction factor for Modulus of Flexible Pavements,
 T = Average AC Temperature, °C
 a and b= Regression Coefficients (a=-0.0198 and b=1.4007)

Rigid Pavements

Backcalculated SPA moduli obtained through SASW analysis for rigid pavements suggest that there is no significant change of modulus with seasonal and daily temperature changes for rigid pavements. This result was expected, as the modulus of concrete is not strongly dependent on temperature in the range of the seasonal and daily temperature changes considered in this study. Typical backcalculated concrete modulus variation with date and temperature for two rigid test sections is presented in Figure 64. As presented in the figure, backcalculated concrete modulus does not have a significant relationship with the measured concrete temperature. Consequently, the SPATCF for rigid pavements is 1.0.

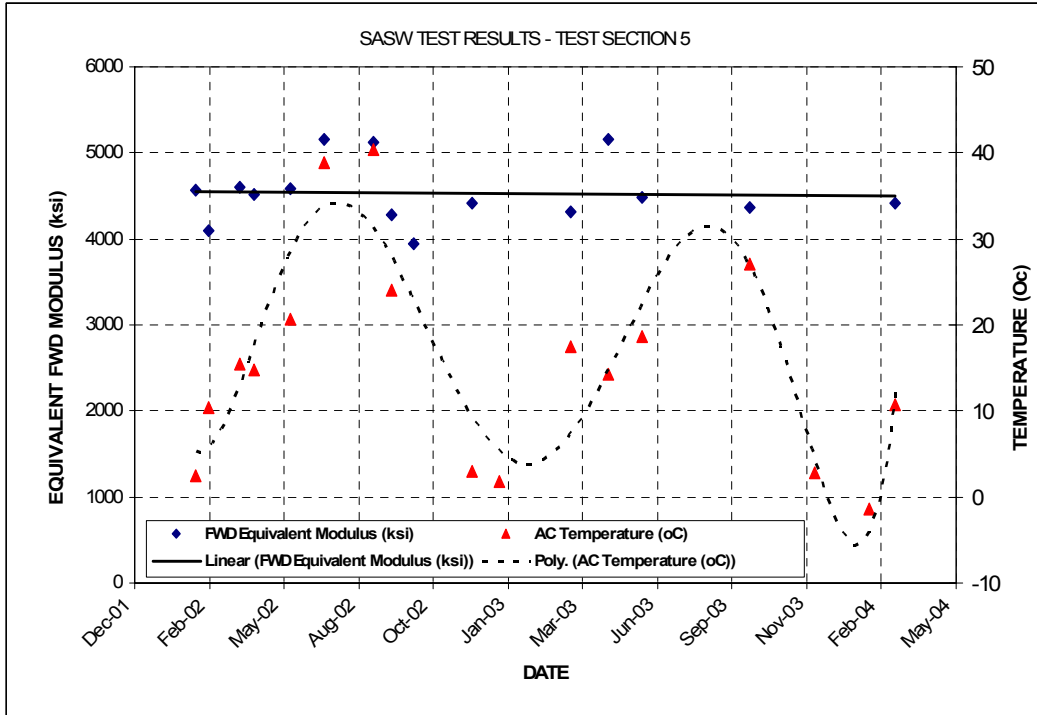


Figure 64a: Typical Asphalt Modulus Variation Obtained through SASW Analysis with Date - Test Section No. 5

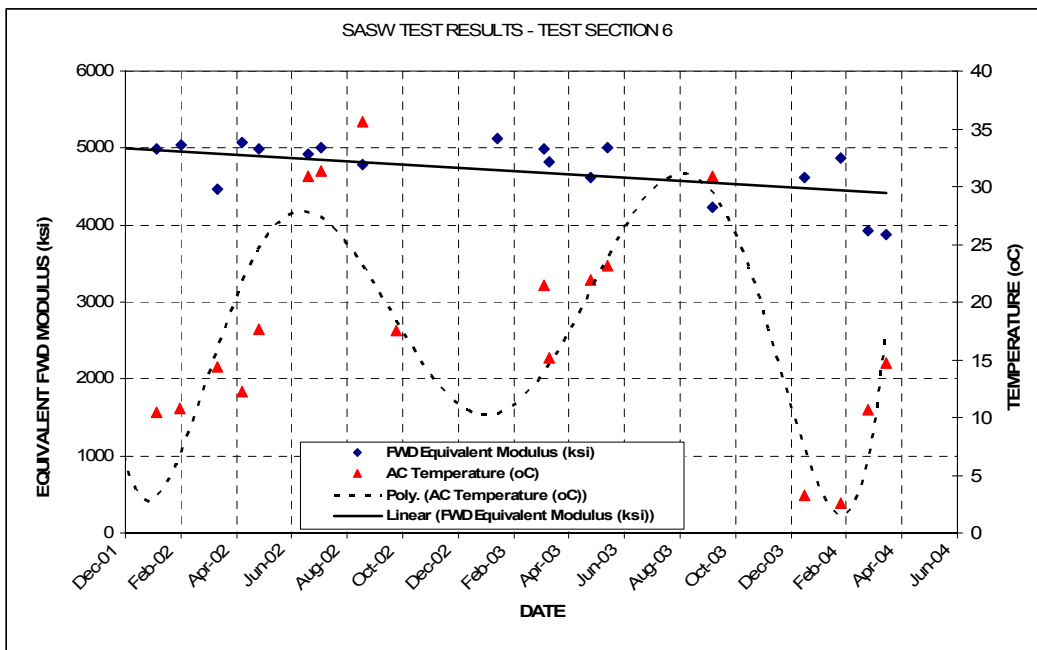


Figure 64b: Typical Asphalt Modulus Variation Obtained through SASW Analysis with Date - Test Section No. 6

Development of Layer Moduli Temperature Correction Factors for SPA based on USW Analysis Results (SPATCF)

Flexible Pavements

Similar to the regression analysis of the SASW results, an analysis was performed to develop Ultrasonic Waves (USW) Temperature Correction Factors for SPA (SPATCF-USW). These factors account for the impact of temperature changes on the backcalculated paving layer moduli obtained from the USW analysis. The developed SPATCF-USW is used in the following formula:

$$\text{Standard Modulus} = \frac{\text{Measured Modulus}}{\text{SPATCF-USW}} \quad (\text{E17})$$

Where:

Standard Modulus is the temperature-corrected modulus (i.e. estimated modulus at 20°C/68 °F).

Measured Modulus is the temperature-uncorrected modulus.

The regression analysis performed on the USW results is identical to the analysis performed for the SASW results, except that instead of using an average measured temperature of the asphalt layer, the near surface asphalt temperatures were used to develop SPATCF-USW. Typical backcalculated asphalt modulus variations with date and temperature are depicted in Figure 64. Results of the analysis in developing SPATCF-USW are presented in Figure 65.

Based on the statistical analysis, the USW analysis temperature correction factor (SPATCF-USW) can be presented by the following equations:

$$\text{SPATCF-USW} = a * T + b \quad (\text{E18})$$

Where:

SPATCF= Correction factor for Modulus of Flexible Pavements

T = Average near surface AC Temperature, °C

a and b= Regression Coefficients (a=-0.0143 and b=1.2812)

Rigid Pavements

Paving layer moduli obtained through USW analysis on rigid pavements follow similar trends as the moduli obtained through SASW analysis. Typical backcalculated concrete modulus variation with date and temperature for two rigid test sections is presented in Figure 67. As presented in the figure, backcalculated concrete modulus does not have a significant relationship with the measured concrete temperature. Consequently, the SPATCF-USW for rigid pavements is 1.0.

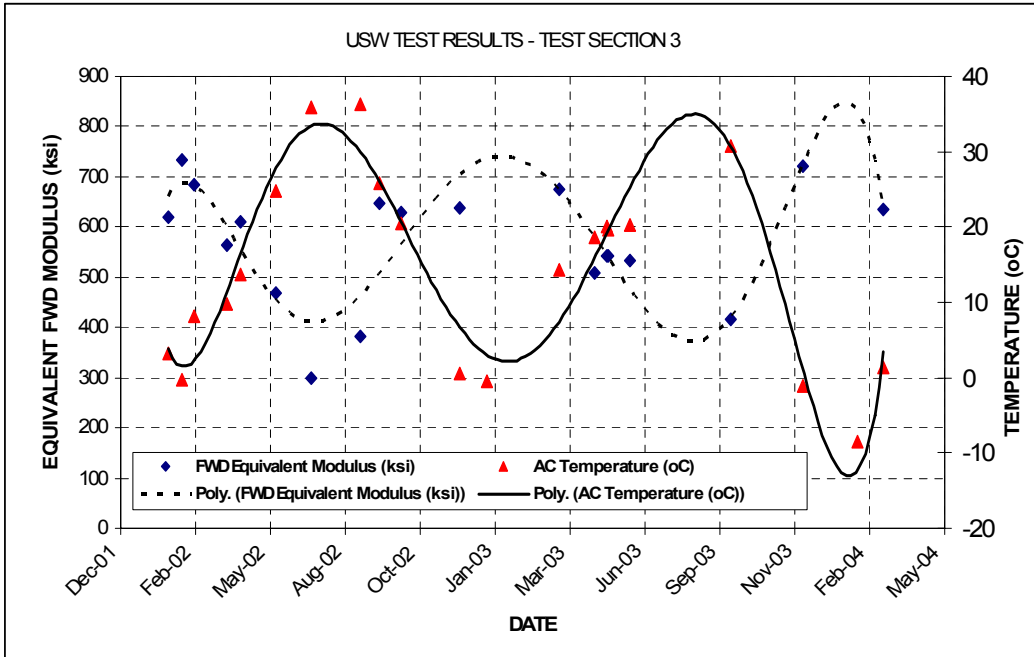


Figure 65a: Typical Asphalt Modulus Variation Obtained through USW Analysis with Date for Test Section No. 3

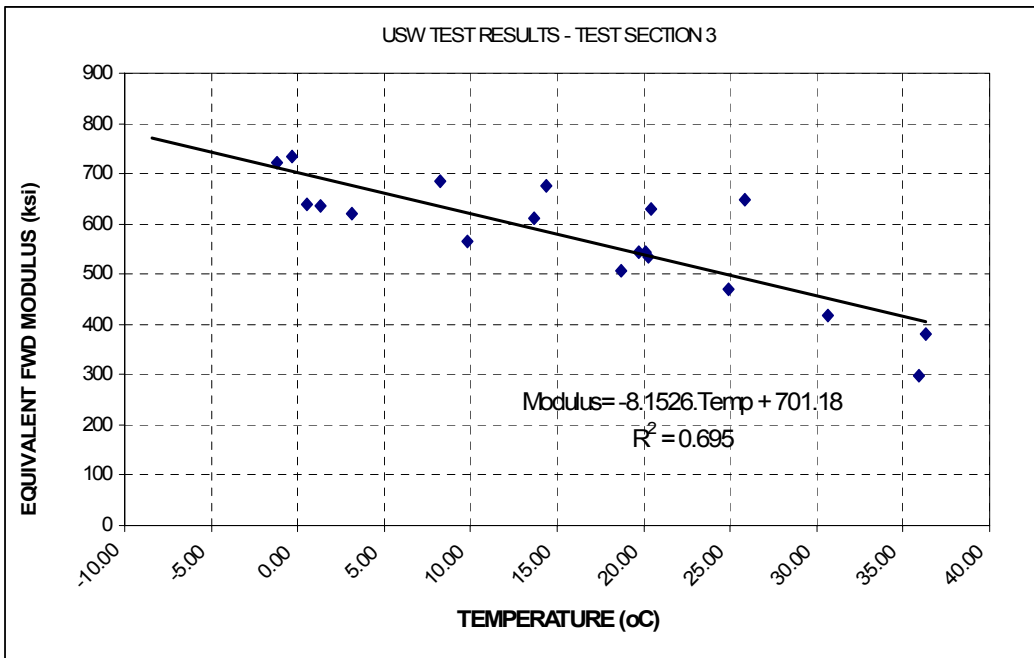


Figure 65b: Typical Asphalt Modulus Variation Obtained through USW Analysis with Temperature for Test Section No. 3

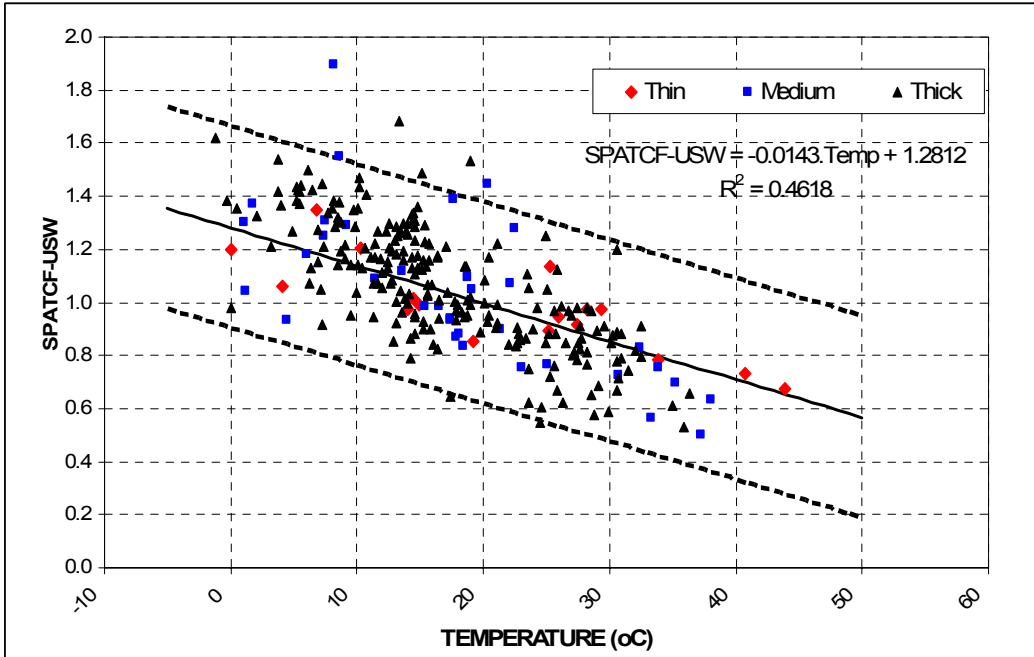


Figure 66: SPATCF-USW Values for Asphalt Modulus and Results of Regression Analysis

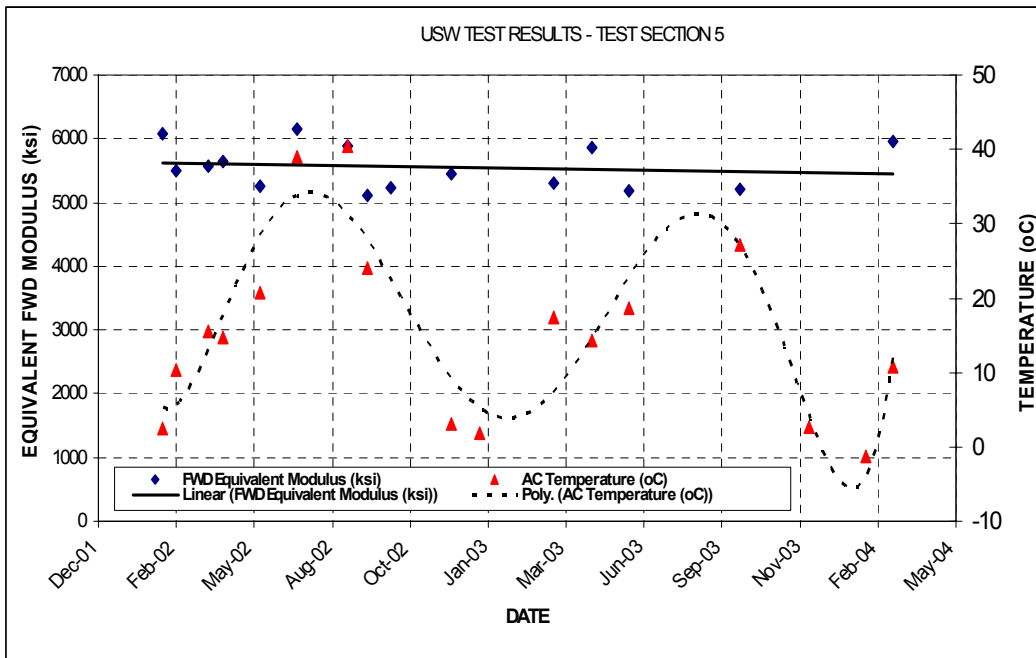


Figure 67a: Typical Asphalt Modulus Variation Obtained through USW Analysis with Date - Test Section No. 5

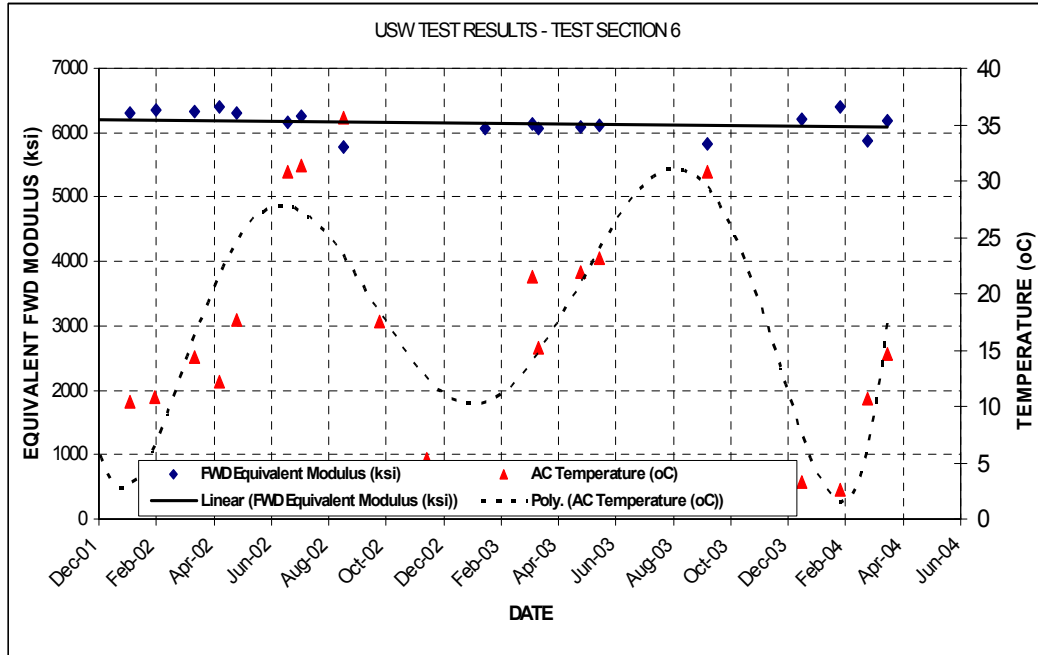


Figure 67b: Typical Asphalt Modulus Variation Obtained through USW Analysis with Date - Test Section No. 6

Variation of Layer Moduli with Moisture based on SPA Results

Backcalculated composite modulus, based on the IR analysis, represents the modulus of subgrade reaction for rigid pavements, or the modulus of the overall system for flexible pavements. Backcalculated composite moduli have a general decreasing trend as the subgrade layer moisture content increases. However, no strong correlation can be identified based on these results.

For presentation purposes, the backcalculated composite modulus for all the test sections are plotted in Figure 68 against the subgrade moisture content, and for both flexible and rigid test sections. It should be mentioned that combining all test results together, without some form of normalization, can be misleading. The reason is that the data presentation does not take into account the differences in subgrade materials between the test sections. As presented in the figure, although the modulus has a general decreasing trend as the subgrade moisture content increases, this trend is not strong enough for individual sections to develop a stronger correlation.

Summary and Conclusions

Empirical seasonal and temperature models were developed to account for the impact of climatic changes on New Jersey pavements. These included TCFs that account for temperature changes on the measured deflections and backcalculated layer moduli, and SCFs that account for seasonal variations other than temperature. The SCFs should be applied to the temperature corrected deflections, and the resulting backcalculated moduli.

OCFs that account for all seasonal variations were also developed. Results of the sample implementation of the seasonal adjustment models indicate that there is a significant difference

between the OCFs and the SCFs. Combining the temperature change with the seasonal change, as in case of the Overall Correction Factors, ignores the rapid change in temperature. Therefore, it is recommended that the Temperature Adjustment Model followed by the Seasonal Correction Model be used, instead of the Overall Correction Factors.

Also, enhanced seasonal correction models were developed to correct for parameters other than temperature and moisture content. The use of the enhanced seasonal correction models depends on the availability of moisture content for different pavement layers.

Results from SPA (SASW) testing show a strong correlation between the AC temperature and modulus. Small differences are observed in this relationship for pavements with different thickness and in different geographical regions. While there is a clear general trend of decrease of the subgrade modulus (from IR) with moisture content, no strong relationship could be defined, as shown in Figures 68a and 68b.

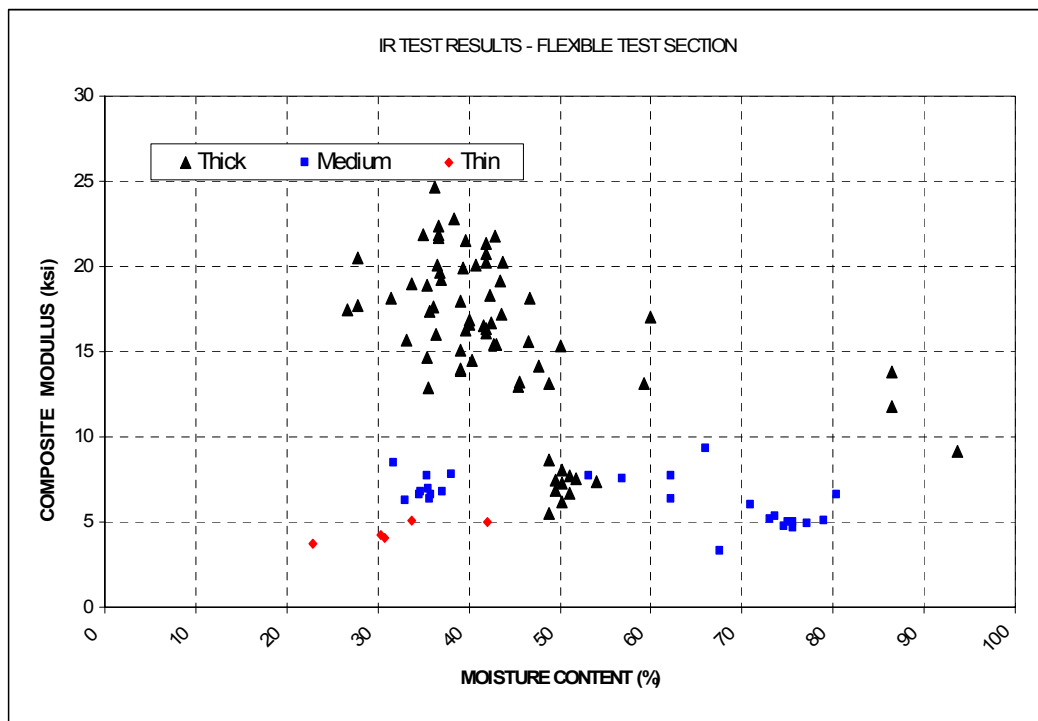


Figure 68a: Typical Variation of Composite Modulus with Moisture Content for Flexible Test Sections

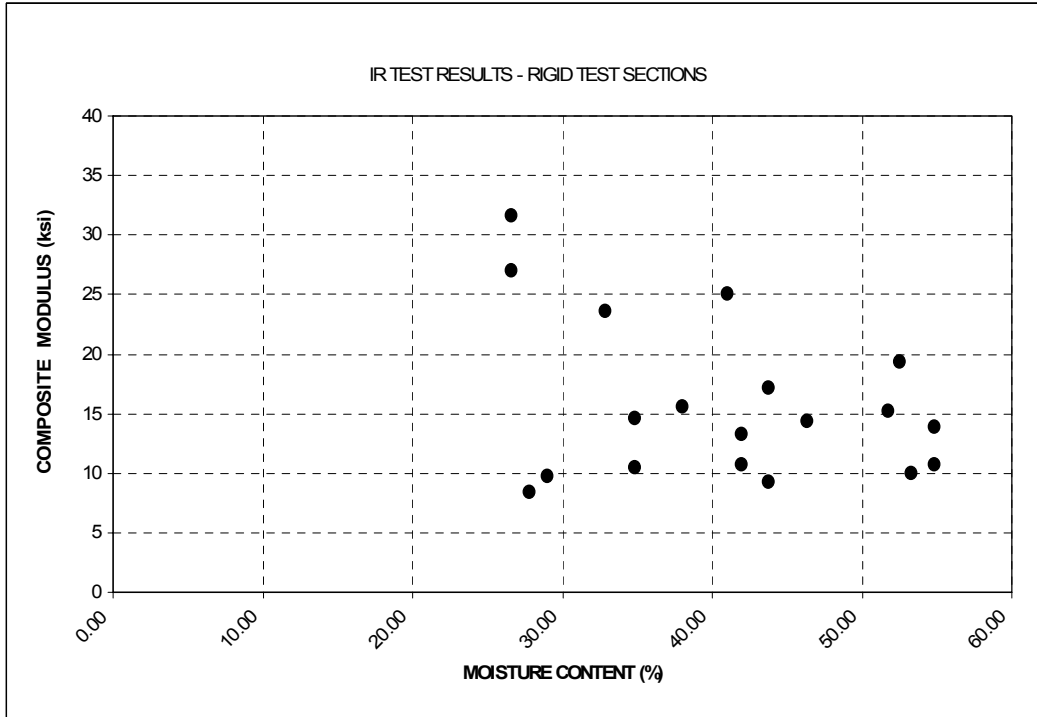
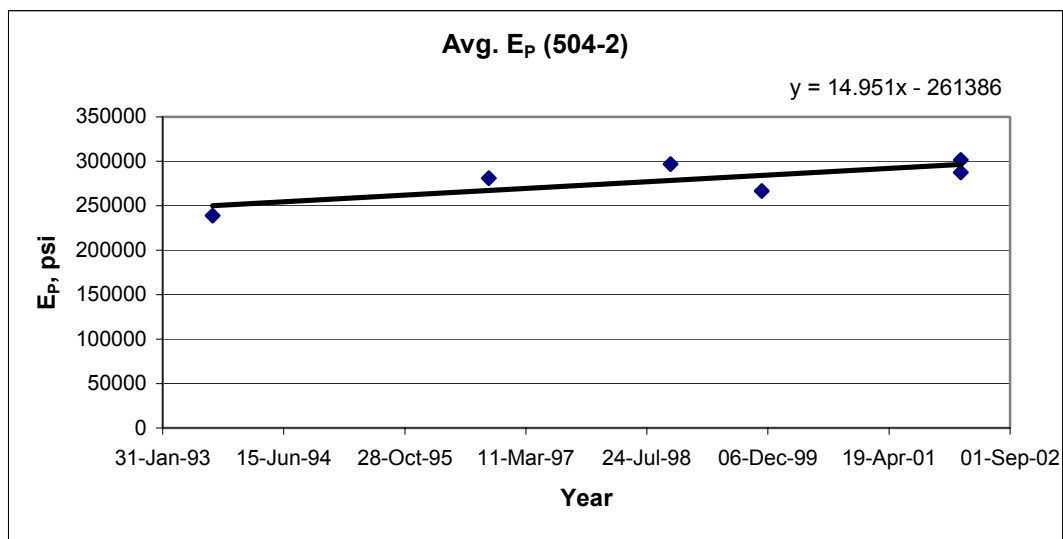


Figure 68b: Typical Variation of Composite Modulus with Moisture Content for Rigid Test Sections

VALIDATION OF NEW JERSEY TEMPERATURE AND SEASONAL MODELS ON NEW JERSEY LTPP DATA

Background

One of the main objectives of the LTPP study is to provide high quality data to the pavement community that can be used to develop performance prediction models. This goal has been partially achieved because the data available in the LTPP database has been collected using a best practice approach and has passed an intensive quality control procedure. However, for some LTPP test sections, the historic deflection data available in the LTPP database shows reverse trends. The observed trends contradict the fact that pavements deteriorate with time and traffic. Figure 69 shows an example of these trends. In this figure, the Effective Pavement Modulus (E_p) was backcalculated from the historic FWD data of Section 340504, one of the sections from the SPS-5 site in New Jersey. The backcalculation procedure of the 1993 AASHTO Design Guide was used in this analysis. As can be seen, the value of E_p was at 238,000 psi in 1993 and continued increasing until it reached over 300,000 psi in 2002. This trend shows a reversal from the common trend of decrease of pavement modulus with time, and implies that the *in-situ* structural capacity of the pavement increases with time and traffic, and that, therefore, no structural improvement will be needed in the future.



**Figure 69: Historic Data for SPS-5 in New Jersey (SPS 340504)
Based on 1993 AASHTO Analysis**

A more detailed study of this section's data indicated that the 1993 test was performed in August, while the 2002 test was performed in February. Although the 1993 AASHTO temperature models were used in the backcalculation analysis presented in Figure 69, two important issues should be investigated to determine the reasons for the reversed trend shown in Figure 69. These two issues are:

- How reliable and consistent are the 1993 AASHTO temperature correction models?
- Is temperature the only factor that has to be accounted for?

It has been reported several times that the 1993 AASHTO temperature correction models have several limitations, especially with high temperatures.^(34,35,25) Figure 70 shows one of the limitations of the 1993 AASHTO temperature correction models. In this figure, the before and after temperature correction deflection basins are shown. This deflection basin was measured in August. As can be seen, the deflection at the center of the load plate (D_1) is significantly reduced when the AASHTO temperature correction models are applied. The corrected D_1 is less than the deflection measured at 12 in from the center of the load plate (D_2), which is not realistic.

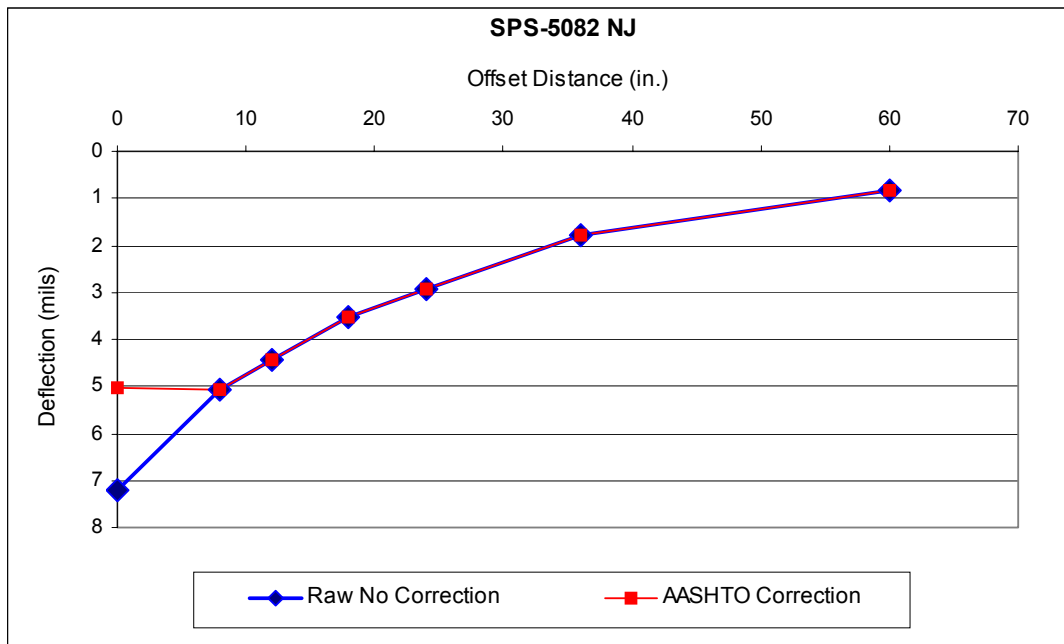


Figure 70: Example of the Limitations of the 1993 AASHTO Temperature Correction Factors

Although temperature has a significant impact on flexible pavements, it is only one of the seasonal parameters that impact flexible pavements. Results of the Analysis of Variance (ANOVA) performed to investigate the significance of different environmental parameters on FWD measurements indicated that in addition to pavement temperature, moisture content, ground water table, and rainfall have significant impact on FWD deflections.⁽³⁶⁾

Therefore, the historic FWD data in the LTPP database must be adjusted for temperature and seasonal variations. These adjustments will enhance the LTPP deflection data, adding value to it and making it more useable. This section of the report presents the results of implementing the New Jersey temperature and seasonal adjustment models, as described earlier, on the historic FWD data of the two New Jersey LTPP-SPS sections (SPS-5 and SPS-9A).

Implementation of the Models to LTPP Data and Results

Pavement deterioration is indicated by the FWD measurements and analysis in the form of higher deflections and lower backcalculated layer moduli. Since there is a general agreement that pavements deteriorate with time, the sign of the deterioration curve, backcalculated pavement modulus (E_p) with time, is expected to be negative (positive means improvement and

negative means deterioration). Therefore, the sign of the E_p deterioration curve is used to evaluate the success of the developed temperature and seasonal adjustment models.

Recalling Figure 69, the sign of the deterioration curve is positive, i.e. E_p is increasing with time or in other words the pavement strength and structural capacity is increasing with time. In this figure, the 1993 AASHTO procedure was used to backcalculate E_p from the historic FWD deflection data of Section 340504. The New Jersey temperature and seasonal models were implemented on the same historic FWD deflection data of Section 340504, and the 1993 AASHTO backcalculation procedure was then used to backcalculate E_p and M_r , but without the AASHTO temperature correction factors.

Figure 71 shows the results of implementing the New Jersey temperature and seasonal adjustment models. As can be seen, the sign of the E_p deterioration curve did change to be negative to match the expectation that pavements deteriorate with time.

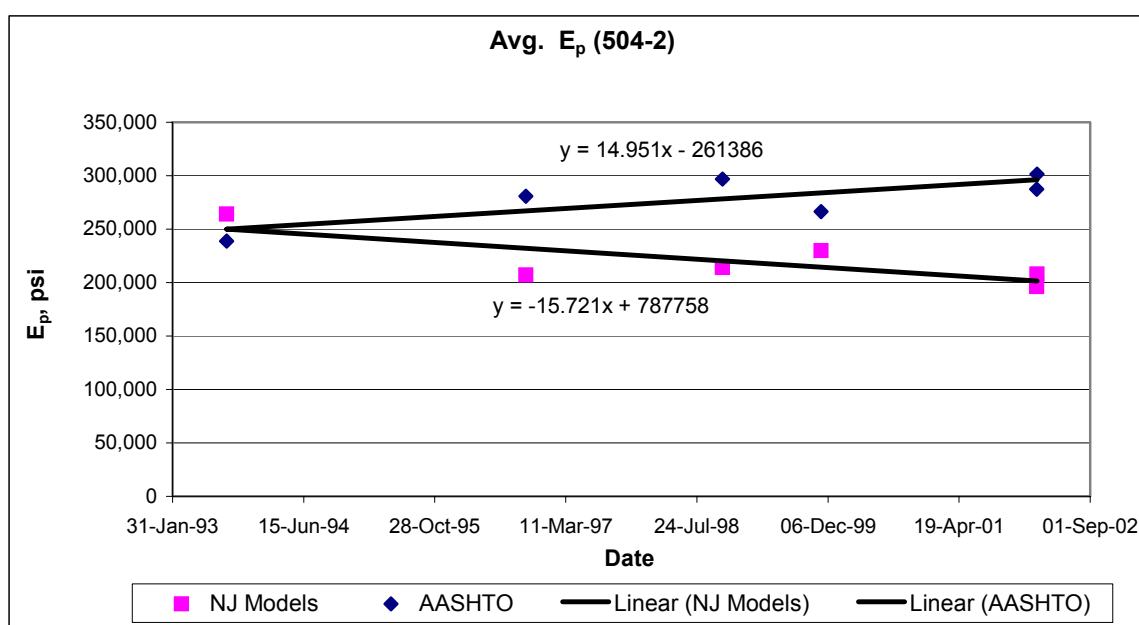


Figure 71: Historic Data for SPS-5 in New Jersey (SPS 340504) – E_p

In Figure 71, the data of Figure 69 was repeated to allow the comparison between implementing the 1993 AASHTO temperature correction factors (labeled as AASHTO) and implementing the New Jersey temperature and seasonal adjustment models (labeled New Jersey Models). It should be noted that in both cases, the same 1993 AASHTO backcalculation procedure was used.

The New Jersey temperature and seasonal adjustment models were then applied to the historic data of all the test sections of the SPS-5 and SPS-9A sites (17 sections) in New Jersey and the sign of the E_p and M_r deterioration curves were determined for each test section. Table 21 shows a summary of the results of implementing the New Jersey temperature and seasonal adjustment models on the historic FWD deflection data of these test sections. In the same table, the results of implementing the 1993 AASHTO temperature correction factors are also shown. In this table, a positive (+ve) sign indicates the wrong trend, i.e. the pavement is improving with

time, while the negative (-ve) sign indicates the expected trend, i.e. the pavement is deteriorating with time.

Table 21: Results of Implementing the New Jersey Models on SPS-5 and SPS-9A

LTPP Section Number	AASHTO		New Jersey Models	
	M_r	E_p	M_r	E_p
5012	+	-	-	-
5022	-	-	-	-
5032	+	-	-	-
5042	-	+	-	-
5052	-	+	-	-
5062	+	+	-	-
5072	+	+	-	-
5082	-	+	-	-
5092	+	+	-	-
5592	-	+	-	-
5602	-	-	-	-
9012	-	+	-	-
9022	-	+	-	-
9032	+	+	-	-
9602	-	+	-	-
9612	-	+	-	+
9622	-	+	-	+
*Total	6	13	0	2

* Total represents the number of cells with positive sign in column

Also, Figures 72 to 77 show samples of the results of implementing the New Jersey temperature and seasonal adjustment models on the historic FWD data of the SPS-5 and SPS-9A test sections. It should be noted that the backcalculation analysis for all sections/cases was performed using the 1993 AASHTO backcalculation procedure.

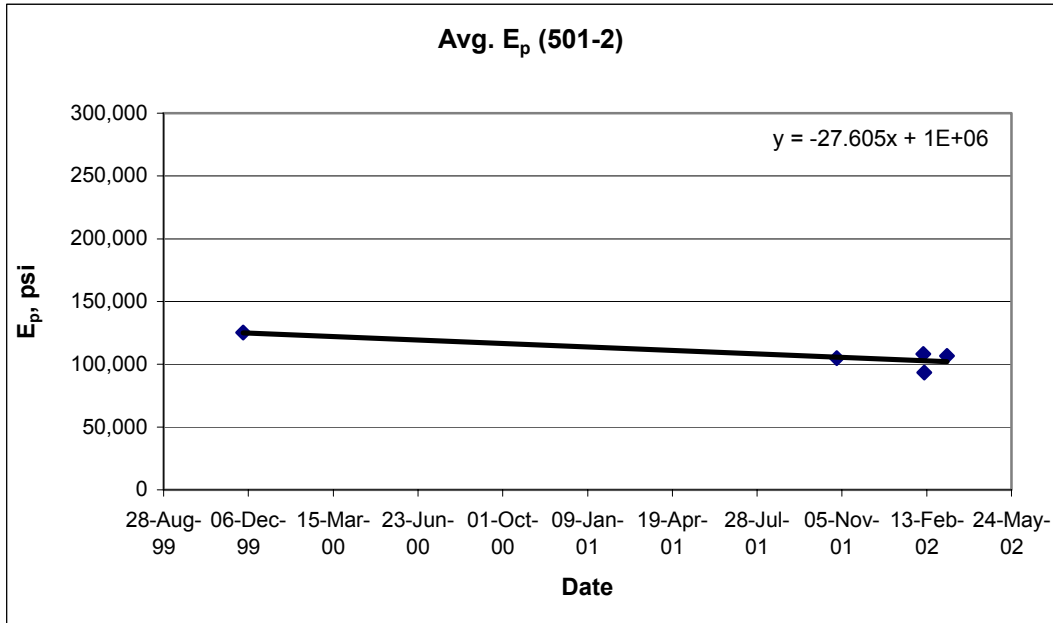


Figure 72: Historic Data for SPS-5 in New Jersey (SPS 340501) – E_p

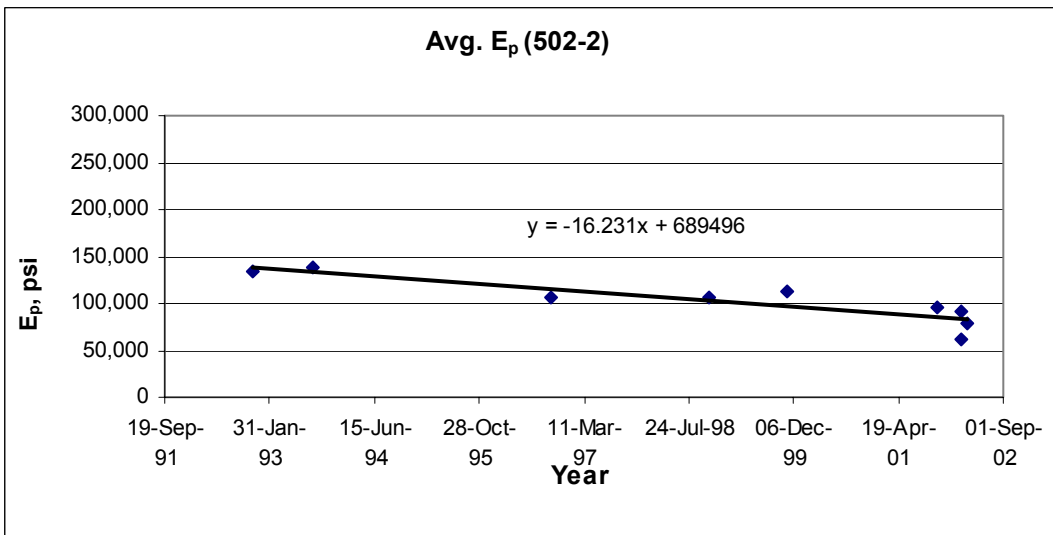


Figure 73: Historic Data for SPS-5 in New Jersey (SPS 340502) – E_p

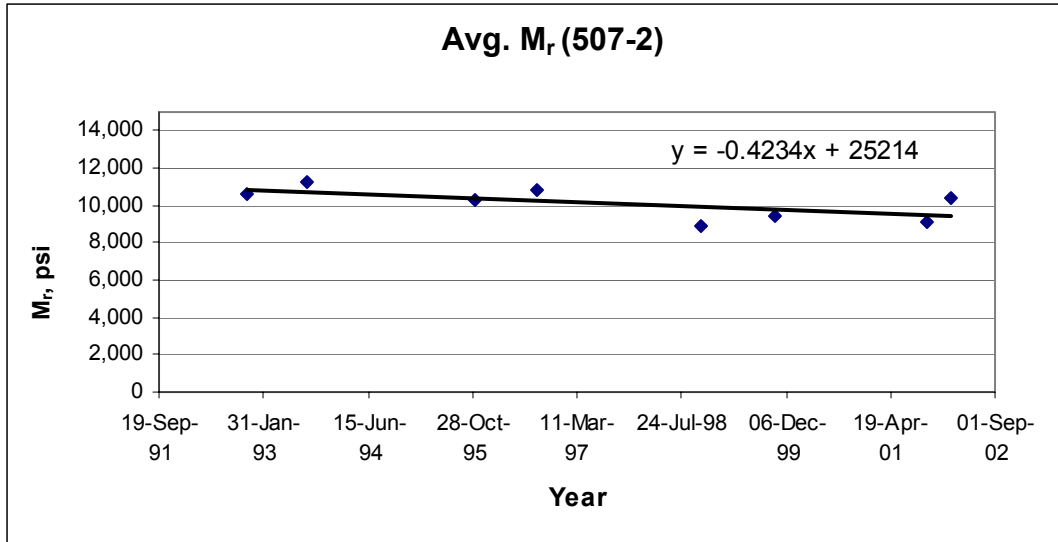


Figure 74: Historic Data for SPS-5 in New Jersey (SPS 340507) – M_r

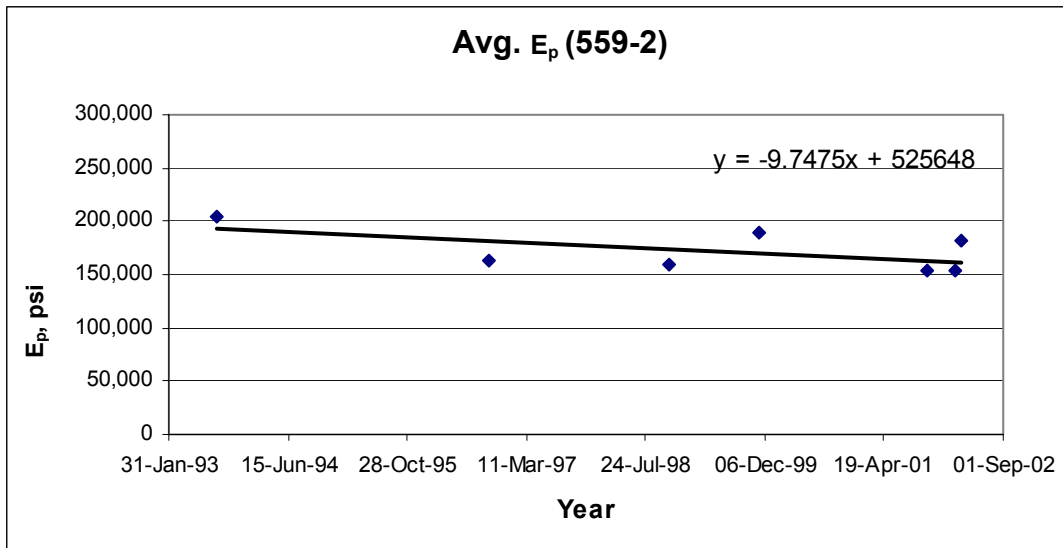


Figure 75: Historic Data for SPS-5 in New Jersey (SPS 340559) – E_p

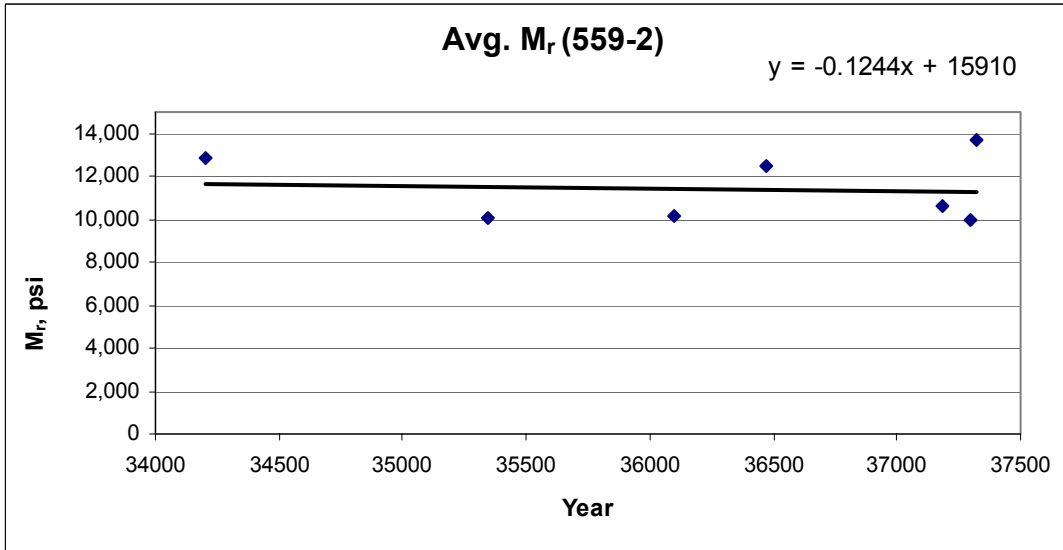


Figure 76: Historic Data for SPS-5 in New Jersey (SPS 340559) – M_r

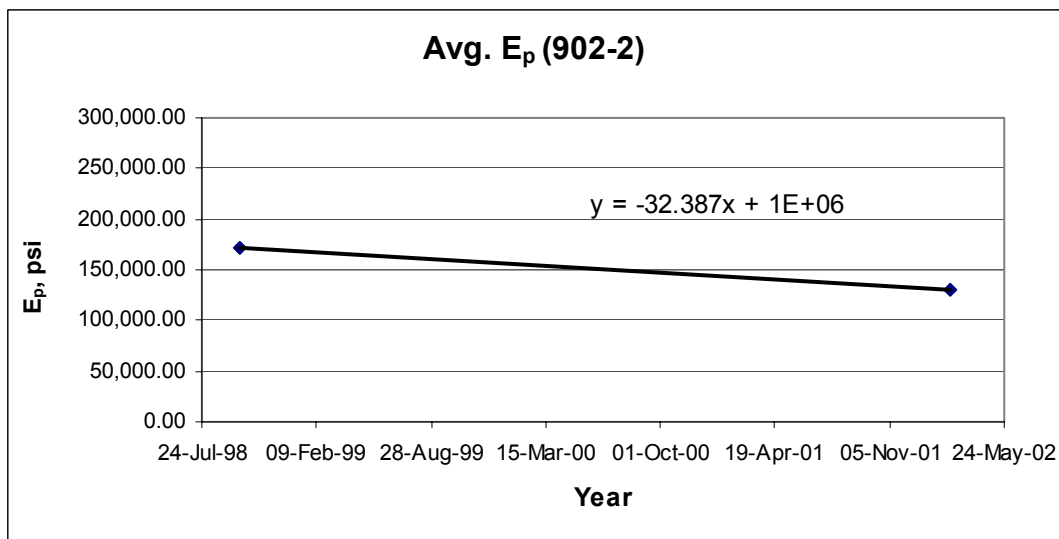


Figure 77: Historic Data for SPS-9A in New Jersey (SPS 340902) – E_p

The results are summarized as follows:

- When the 1993 AASHTO Pavement Design Guide was followed, 13 sections of the 17 sections indicated the wrong trend (+ve) for E_p and 6 for M_r .
- When New Jersey temperature and seasonal adjustment models were applied, and then backcalculation analysis was performed using the 1993 AASHTO Procedure (with no temperature correction), only 2 sections indicated the wrong trend (+ve) for E_p and 0 for M_r .

As can be seen, the New Jersey temperature and seasonal models provide superior results.

The two sections that showed a reverse trend when the New Jersey temperature and seasonal models were applied are Sections 340962 and 340961, shown in Figures 78 and 79. These two sections are supplemental sections that are not tested as frequently as the core sections and only two data points were available, measured in 1998 and 2002. Also, the data for the supplemental sections has not gone through a strict QA/QC procedure, as has the data for the core sections.

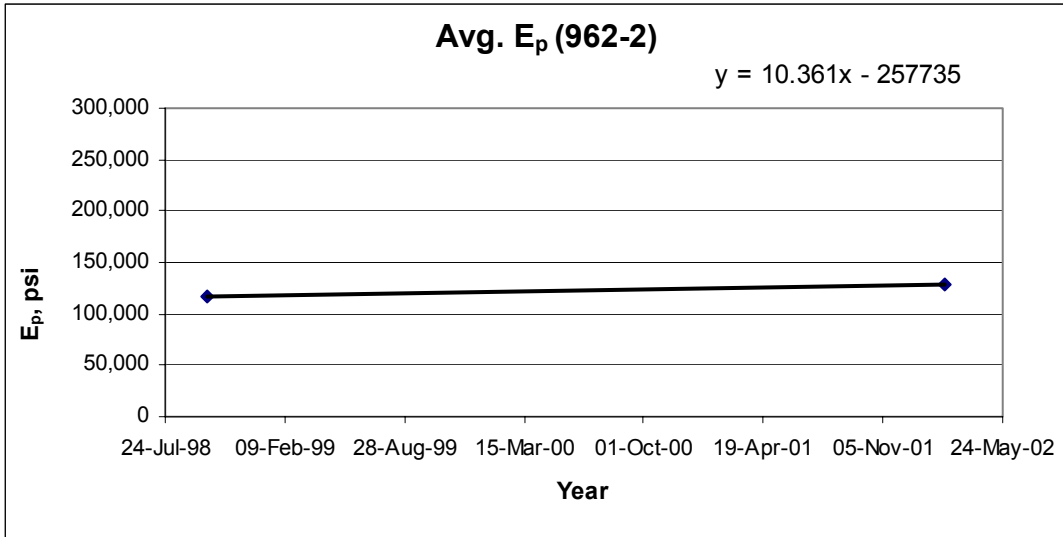


Figure 78: Historic Data for SPS-9A in New Jersey (SPS 340962) – E_p

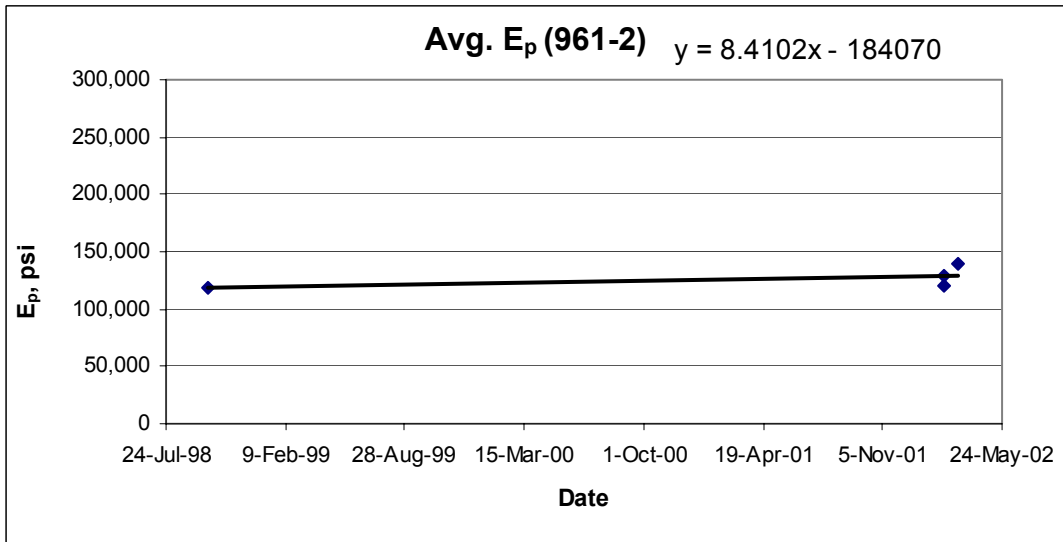


Figure 79: Historic Data for SPS-9A in New Jersey (SPS 340961) – E_p

More investigations were conducted to find out the reasons why these two sections demonstrated a reversed (wrong) trend. One possibility is that the 1998 testing was performed only a few days after completing the rehabilitation construction, which resulted in higher deflections. It has been reported before that testing shortly after construction results in higher than expected deflection, and hence lower modulus.⁽³⁷⁾

Summary of Findings

When New Jersey Temperature and Seasonal Correction Models were applied to the SPS-5 and SPS-9A historic FWD data, the reversed trends that had previously been observed for 13 sections out of the 17 were corrected for 11 out of these 13 sections. The final results of all sections have the anticipated trend, except for the 2 supplemental sections. The New Jersey temperature and seasonal adjustment models enhance the quality of the historic FWD deflection data in the LTPP database by compensating for inadequacies in the simplified AASHTO 1993 temperature correction model. Also, as can be seen from Figures 78 and 79, the backcalculated pavement moduli (E_p) from deflections of 2002 are marginally higher than those of 1998.

EVALUATION OF NSOG BASE LAYERS

Moisture is a fundamental variable in all problems of soil and material behavior. It has special significance in highway pavements. Highways are thin structures built on soils. Their foundation, subbase, and base layers are made of soil aggregate material. The stiffness response of these soils changes when subjected to large variations in moisture content.⁽³⁸⁾ Moisture, therefore, has an adverse effect on pavements, and its rapid removal from pavement layers is a necessity. The impact of poor drainage on the performance and service life of rigid pavement is well documented.^(39,40) Some of the factors that could lead to the intrusion of water and poor drainage in rigid pavements are cracked slabs, bad joint sealant, deteriorated shoulder joints, poor draining material in various layers, inadequate cross-slope, and a high water table. Entrapped water in the pavement can result in detrimental effects such as pumping/water bleeding, voids, frost penetration, differential heaving or faulting, and, ultimately, premature failure of the pavement due to loss of load bearing capacity. AASHTO recorded up to 40 times faster reduction in pavement life due to moisture-related problems.⁽⁴⁰⁾

Construction of a base/subbase course with good drainage characteristics aids in maintaining the pavement in a dry condition. The use of open graded drainage layers (OGDLs) has gained acceptance as means of rapidly draining infiltrated water from the pavement structure, and represents a careful balance of permeability and stability of the base material. These types of base and subbase layers have limited fines. The range of permeability of OGDLs is quite wide, with permeability ranging from 1000 ft/day (305 m/day) to about 22965 ft/day (7,000 m/day).⁽⁴¹⁾ Climate, geologic location and other environmental factors have a considerable impact on pavement performance in general and on moisture movement within base and subbase layers.⁽³⁸⁾ The practice is to provide positive drainage in the form of permeable base/subbase, thereby reducing the moisture retention time within the pavement structure. In this regard, field data collection becomes vital in establishing any possible trends between pavement performance and seasonal factors such as moisture content and rainfall.

Study Background

One of the three objectives of the study reported herein, as stated earlier, was to evaluate the performance of non-stabilized open graded (NSOG) base/subbase layers for rigid pavements under different moisture and temperature conditions. As a part of this study, two rigid pavement sections with different base drainage layers were investigated to assess the effectiveness of NSOG base as a drainage layer compared to the typical soil aggregate base layer. The evaluation was carried out in terms of the effect of moisture presence within the two base types on the pavement strength. FWD testing was carried out on the two sections to determine deflections and consequently the effect of the base layers on pavement strength. This section presents the methodology for carrying out the evaluation and subsequent results and findings.

Test Sites

Two test sites having rigid pavement structure were selected in New Jersey for the study. One having an NSOG base and the other having a conventional dense-graded aggregate base. The test sites are hereafter referred to as Site 5 (S5) and Site 6 (S6) respectively.

Site 5 (S5)

This test section is a weigh station located on the eastbound section of Route 78 near Milepost 4. The weigh station consists of a unidirectional single lane rigid pavement with gravel shoulders. The PCC slabs are 12 ft wide with joints at approximate 78 ft intervals. The pavement structure of S5 consists of 9.75 inch of reinforced concrete over 4 in of NSOG

aggregate base, followed by a thin geotextile sheet and 8 in of sandy gravel subbase. Using the Textural Classification System, the subgrade is classified as sandy loam subgrade. The pavement cross section is shown in Figure 80. The NSOG base is a 50-50 blend of #57 and #8 stone with an average permeability of 790 ft/day (457 m/day). FWD testing is carried out on a monthly basis at the test sites along mid-slab and wheel paths, pavement-shoulder edge, slab corners, and the approach and leave sides of the joints and cracks for all slab panels within the test section. In total, S5 has 20 different test locations.

Material	Depth inch (mm)		TDR Depth inch (mm)	Comments
PCC	9.75 (248)			
Non-Stabilized Open Graded Aggregate Base	13.75 (349)	TDR 1	11 (279)	Thermistor Probe Depth 9 in (229 mm) Resistivity Probe Depth 9.5 in (241 mm)
Sandy Gravel	21.75 (552)	TDR 2	15 (406)	
Sandy Loam (Clayey Silty Sand)		TDR 3	48 (1219)	

Figure 80: Pavement Profile and Location of Probes at S5

Site 6 (S6)

This test section is also a weigh station located at milepost 3.5 on the northbound section of interstate route I-295. The test site represents a rigid pavement section with an AC shoulder and an NJDOT crushed aggregate base layer. The PCC slab panels are 15 ft (4.6 m) wide and 78 ft (23.8 m) long (joint spacing). The rigid pavement structure consists of 10 in (254 mm) of jointed reinforced concrete on a 3 in (76 mm) traditional granular soil aggregate base material and 3 in (76 mm) of sandy gravel subbase underlain by a clayey silty sand subgrade as shown in Figure 81. The clayey silty sand subgrade is very similar in composition to the sandy loam of Site S5. The FWD testing locations (22 test locations) on the rigid slab panels include mid-lane, left wheel path, pavement-shoulder edge of concrete slab, and the AC shoulder.

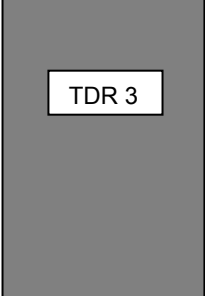
Material	Depth Inch (mm)		TDR Depth Inch(mm)	Comments
PCC	10 (254)			
Crushed Aggregate Base	13 (330)		12 (305)	Thermistor Probe Depth 10 in (254 mm) Resistivity Probe Depth 10 in (254mm)
Sandy Gravel	47 (1194)		26.5 (673)	
Clayey Silty Sand			51.5 (1308)	

Figure 81: Pavement Profile and Location of Probes at S6

Characteristics of Study Sites

A comparison of the site characteristics for the two rigid pavement sites S5 and S6 revealed the following key features:

- The PCC thickness variation between the two sites is minimal (6 mm/0.25 inch).
- Site S5 has a 4 in (102 mm) thick NSOG base whereas Site 6 has a 3 in (76 mm) granular soil aggregate base.
- Both sites have a sandy gravel subbase and a clayey silty sand subgrade underlying the base layer, therefore providing a common platform for evaluating the drainability of the two base types.
- Site 5 is a newer constructed and controlled site (age of 4 years), whereas Site 6 has a pavement structure with an age of 14 years.
- Both sites show some degree of distress in the form of mid-slab transverse cracking.

Graphical presentation of as-sampled gradation for the NSOG material from S5 and the crushed aggregate base layer used at S6 is shown in Figure 82. The gradation of the S6 base layer was obtained from NJDOT Specifications for base material and correspond to designation I-3. It was observed that the NSOG had a coarser gradation as compared to the crushed aggregate base layer.

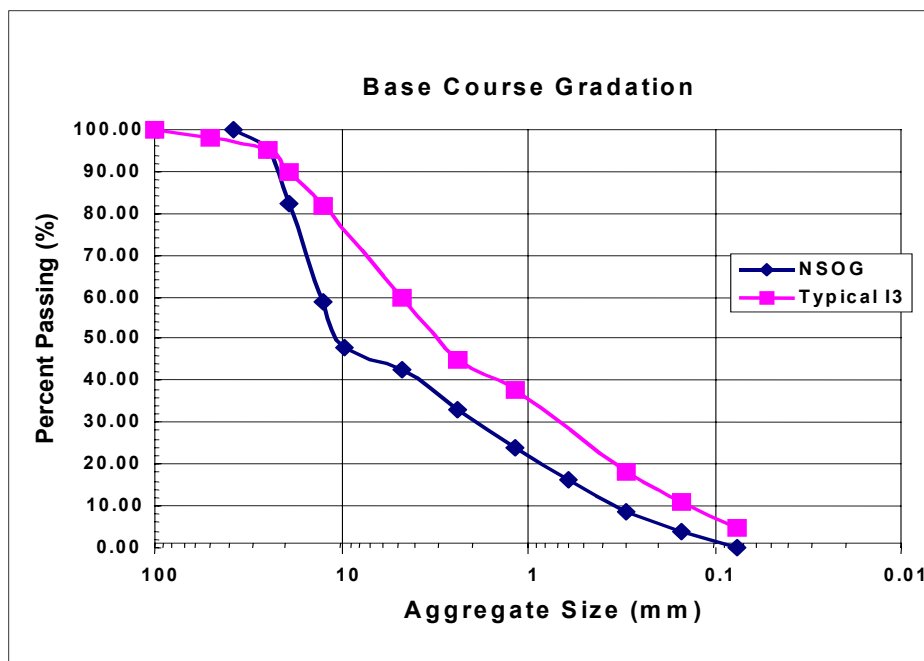


Figure 82: Gradations of NSOG (S5) and Crushed Aggregate Bases (S6)

Selection of only two case study sites may not be statistically adequate to compare the performance of base layers in terms of drainability. However, selecting the test sites having the same climatic environment in terms of location, knowing the material properties of the base drainage layers, and testing and collecting data from the two sites for a two year period compensated this constraint to some extent. This allowed the study to collect sufficient data on rainfall and moisture content, spanning all climatic seasons, to arrive at meaningful conclusions.

Instrumentation and Data Collection

The equipment installed at these test sites included instrumentation for measuring subsurface volumetric moisture content (TDR Probes), pavement and subsurface temperatures (MRC temperature probes), frost depth (resistivity probes), and water table (vibrating wire piezometer). In addition, weather stations were installed to monitor air temperature and rainfall. Equipment cabinets were also installed at the instrumented sites to hold the data logger, battery pack, and all electrical connections from the instrumentation. The monitoring program involved monthly FWD testing and downloads of daily air temperature, moisture, water table, pavement temperature, and rainfall data.

The collected data went through a comprehensive QC/QA process to ensure that only reliable data was loaded into the database. The FWD deflection data was backcalculated using the standard 1993 AASHTO Pavement Design Guide procedure to determine pavement response parameters such as modulus of elasticity of a rigid pavement (E_{PCC}).

Analysis of Data

Rainfall And Volumetric Moisture Content Trends

Rainfall and moisture content data collected from the two sites on a daily basis during the period of March 2002 and March 2003 was used to determine rainfall and moisture trends. During this period, rainfall ranged from 0 in (0 mm) to 2.65 (67.4 mm) for S5 and 0 in (0 mm) to 2.25 in (57.2 mm) for S6, as shown in Figure 83. A review of the figure indicates that rainfall intensity at both sites is mostly less than 0.78 (20 mm) with some high precipitation recorded at both sites.

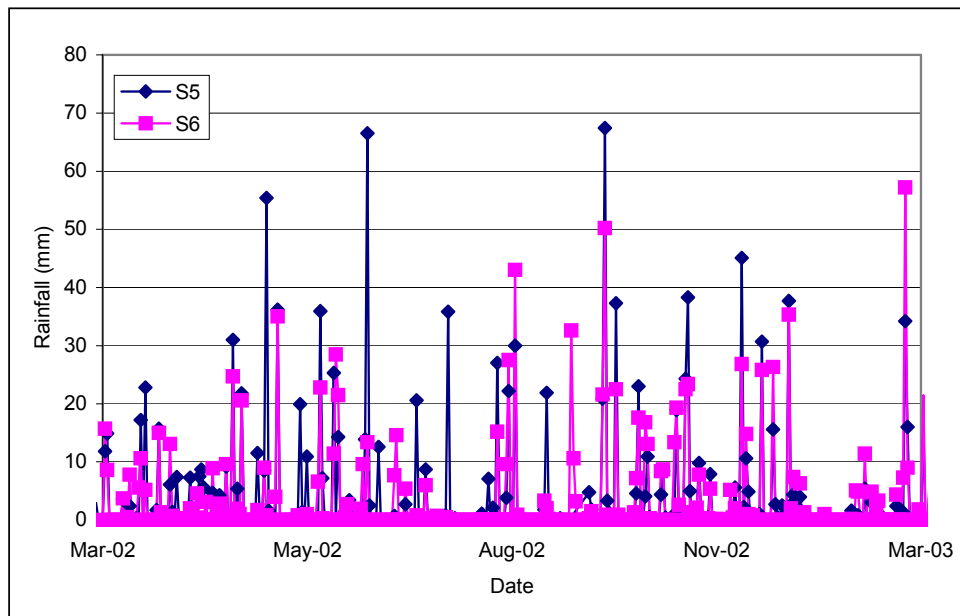


Figure 83: Rainfall Distribution at Case Study Sites

To determine whether a meaningful evaluation of the base course performance could be made, a statistical analysis was carried out on the rainfall data from the two sites to find out whether there was any significant difference between the rainfalls. The hypothesis for testing was:

$$H_0: \text{Rainfall}_{S5} = \text{Rainfall}_{S6}$$

$$H_1: \text{Rainfall}_{S5} \neq \text{Rainfall}_{S6}$$

Results of the statistical analysis shown in Table 22 indicate that there is no significant difference in terms of rainfall between the two sites.

Table 22: Statistical Analysis Results of Rainfall at Sites S-5 and S-6

Comparison of Rainfall (S5 and S6)		
	S5	S6
Mean	3.18	2.63
Variance	71.68	48.85
Observations	496	579
Hypothesized Mean	0	
df	1073	
t stat	1.172	
P(T<=t) two-tail	0.242	
t Critical two-tail	1.962	

The average daily moisture content within the base course ranged from approximately 1 percent to 53 percent for S5 and 11 percent to 99 percent for S6 as depicted in Figure 84. A review of the figure indicates that moisture content for S5 (having an NSOG base) is mostly within 30 percent, whereas for S6 (having the typical soil aggregate base) it reaches the point of saturation on numerous occasions. This indicates that moisture is retained in the soil aggregate base layer whereas the NSOG layer is performing its intended drainage function by not letting the moisture exceed a certain limit (30 percent).

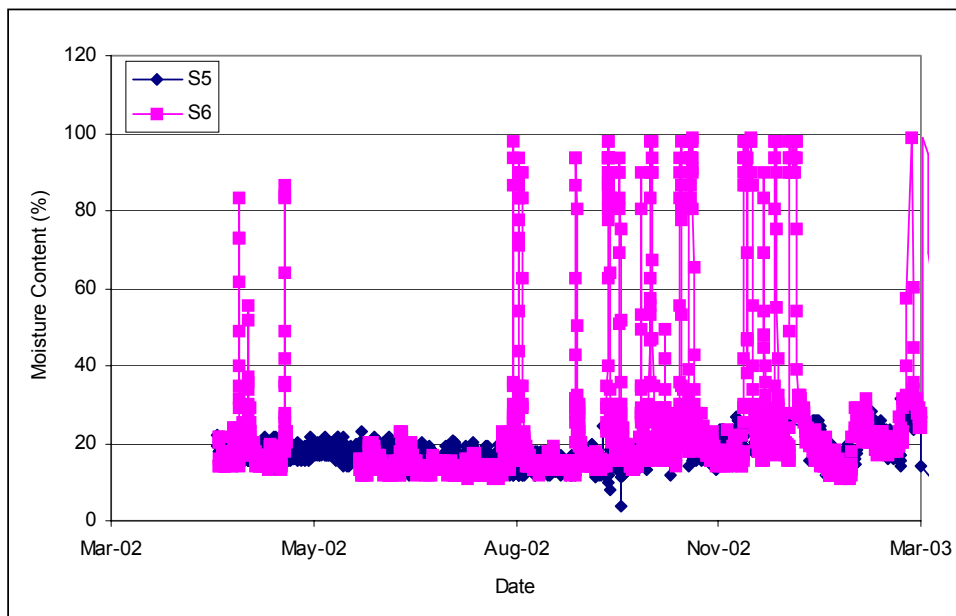


Figure 84: Moisture Content Distribution at Case Study Sites

A review of both Figures 83 and 84 in tandem indicates that even when the rainfall intensity was high at S5, the corresponding moisture content did not exceed the limit, whereas for S6, high rainfall intensities resulted in moisture content reaching saturation levels. To prove the conclusion, a statistical test was carried out on the moisture content data from the two sites with the following hypotheses:

H₀: Moisture Content_{S5} = Moisture Content_{S6}

H₁: Moisture Content_{S5} ≠ Moisture Content_{S6}

The statistical analysis results shown in Table 23 indicate that significant difference exists between the two sites in terms of moisture content. This reinforces the finding arrived at earlier that the NSOG base at S5 was performing its intended function as a drainage layer by not allowing the moisture contents to reach saturation level.

Table 23: Statistical Analysis Results of Rainfall at Sites S-5 and S-6

Comparison of Moisture Content (S5 and S6)		
	S5	S6
Mean	17.61	25.09
Variance	14.83	426.32
Observations	1836	2149
Hypothesized Mean	0	
df	3983	
t stat	15.307	
P(T<=t) two-tail	0.000	
t Critical two-tail	1.961	

Drainage Layer Influence on Pavement Performance

Deflection testing at the two sites was conducted using FWD equipment on a monthly basis and the climatic data was collected daily through the previously listed instrumentation. The variation of average daily volumetric moisture content for both S5 and S6 during the monthly FWD testing days is shown in Figure 85.

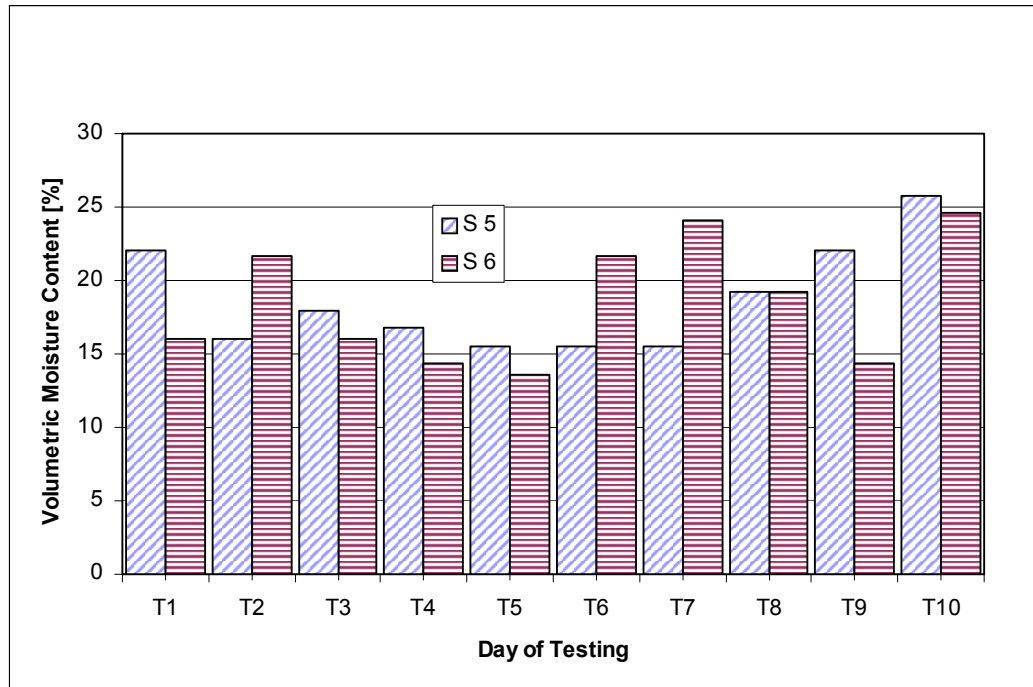


Figure 85: Moisture Content in Base Courses on FWD Testing Days

As the testing days for both sites in each month were very close, the testing days have therefore been designated as T1, T2, T3, etc., as shown in Table 24.

Table 24: Designation of FWD Test Days

Designation	Dates for S5	Dates for S6
T1	4/18/02	4/19/02
T2	5/21/02	5/19/02
T3	6/20/02	6/21/02
T4	7/25/02	7/24/02
T5	8/15/02	8/16/02
T6	9/26/02	9/27/02
T7	10/30/02	-
T8	11/17/02	11/22/02
T9	12/8/02	12/6/02
T10	2/3/03	2/1/03

There was no substantial difference in the moisture content between the base courses of the two sections on the testing dates. To get a better understanding of the reason for this lack of difference, rainfall on the days of testing at both sites (S5 and S6) is shown in Figure 86. This figure shows rainfall only on three days of FWD testing on S5 and five days on S6. No rainfall was recorded on the other FWD testing days.

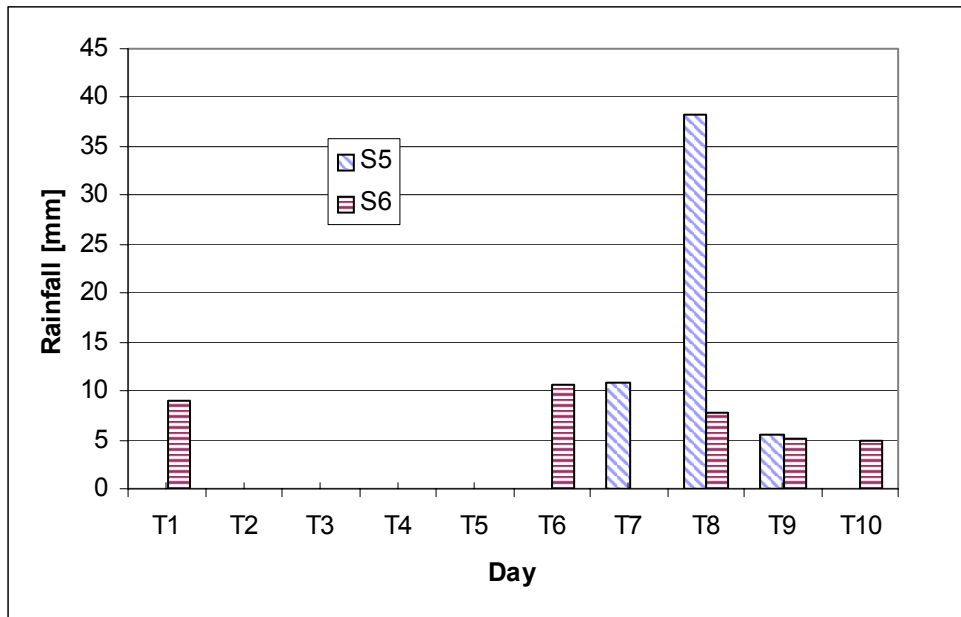


Figure 86: Rainfall on FWD Testing Days

In order to consider the effects of accumulated moisture within the base layer on previous rain days that might affect the amount of moisture content on FWD testing days, an average rainfall is required. The average daily rainfall (ADR) was calculated for the previous fourteen days inclusive of the day of testing. ADR ranges from 0.04 in (1.1 mm) to 0.32 in (8.1 mm) at S5, and 0 in (0 mm) to 0.26 in (6.6 mm) at S6, as shown in Figure 87. In general, there was more accumulated rainfall at S5 compared to S6, but the ranges of moisture content for both sites remain the same.

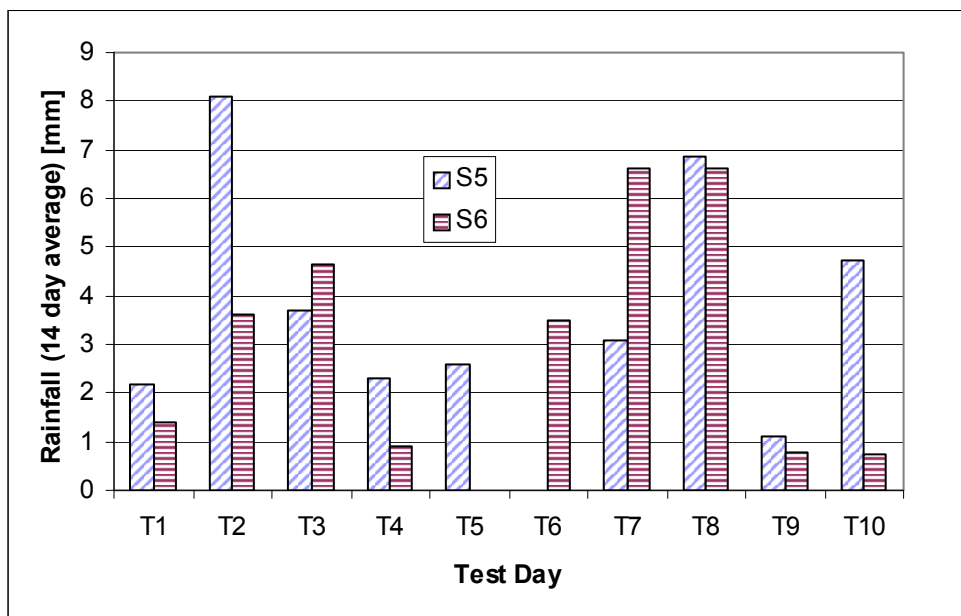


Figure 87: Average 14-Day Rainfall

The trend in moisture content in the base layers for Sites S5 and S6, with 14-day average rainfall is shown in Figures 88 and 90, respectively.

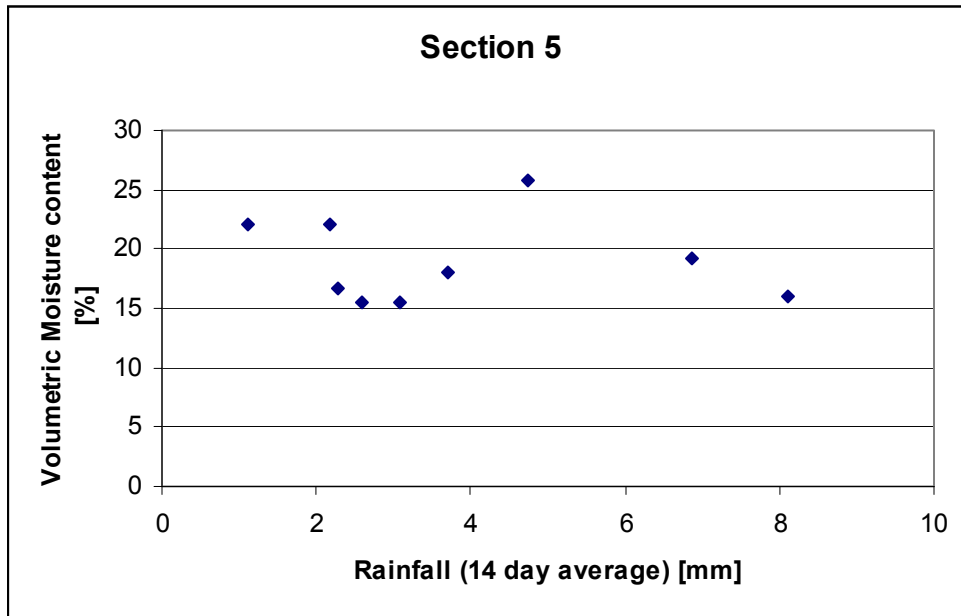


Figure 88: Variation of Base Layer Moisture Content with Average Rainfall for S5

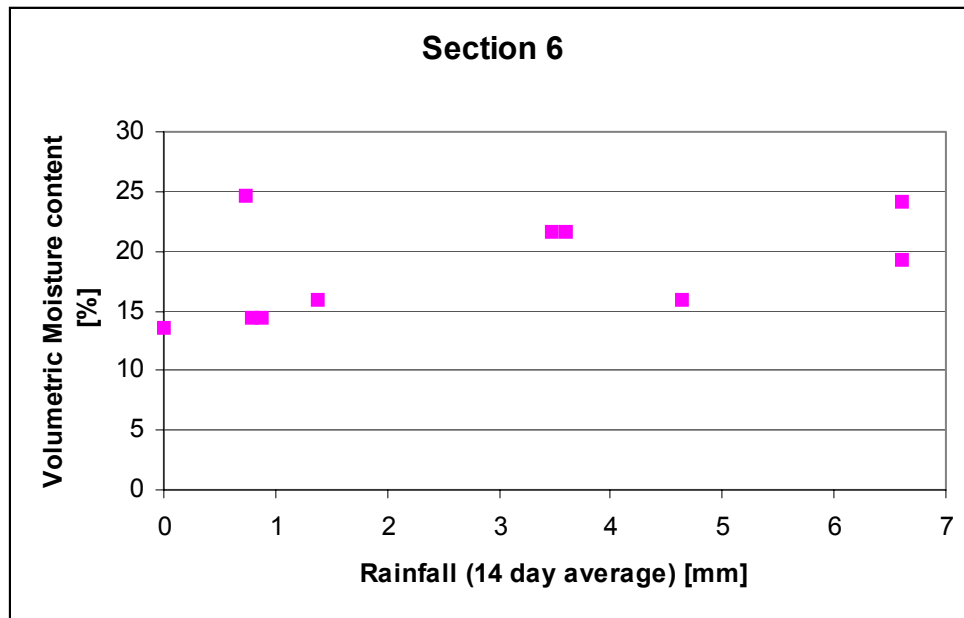


Figure 89: Variation of Base Layer Moisture Content with Average Rainfall for S6

To investigate the influence of moisture on pavement strength, pavement deflections at the mid-slab locations at S5 and S6 obtained through FWD testing were normalized to a load of 9 kips, and plotted against the date of testing. However, a direct comparison of deflection and backcalculated properties between S5 and S6 is difficult because of the differences in pavement age, layer thickness, material type, and other pavement structure characteristics. An approach was therefore used to normalize the FWD data and backcalculation results and hence the structural capacity of each section. The structural capacity normalization was done through the use of the NJDOT SAI, which provides a measure of structural capacity of the pavement on a scale of 0 to 5. An SAI value of five represents a pavement in excellent structural condition – as in the case of a new pavement. SAI is a function of the backcalculated effective thickness (D_{eff}) of the PCC slab, the as-built slab thickness ($D_{as-built}$), and the required thickness (D_{req}), which is the thickness required to carry future traffic. An SAI value of 2.5 is used as a trigger value indicating that the pavement section is approaching the end of its structural life and is in need of structural improvement. SAI, as developed for the NJDOT, is determined using the following formula:

$$SAI = 5 * \tanh(2.812943 * DR^2 - 0.083425 * DR + (-0.89774 * DR^3)) \quad (E19)$$

Where:

$$DR = \text{Depth Ratio} = x_1 * (D_{eff} / D_{as-built}) + x_2 * (D_{eff} / D_{req}) \quad (E20)$$

Where: $x_1 = 0.3$
 $x_2 = 0.7$

The SAI was calculated using the above equations for the FWD data from both sites and plotted against corresponding moisture contents recorded for the test dates, as shown in Figures 90 and 91, for S5 and S6, respectively. A review of the figures shows that the SAI values range between 4.0 and 5.0 for both sections at all moisture content levels. This therefore indicates that at present, there is no influence of the base material on the structural capacity of the pavement sections.

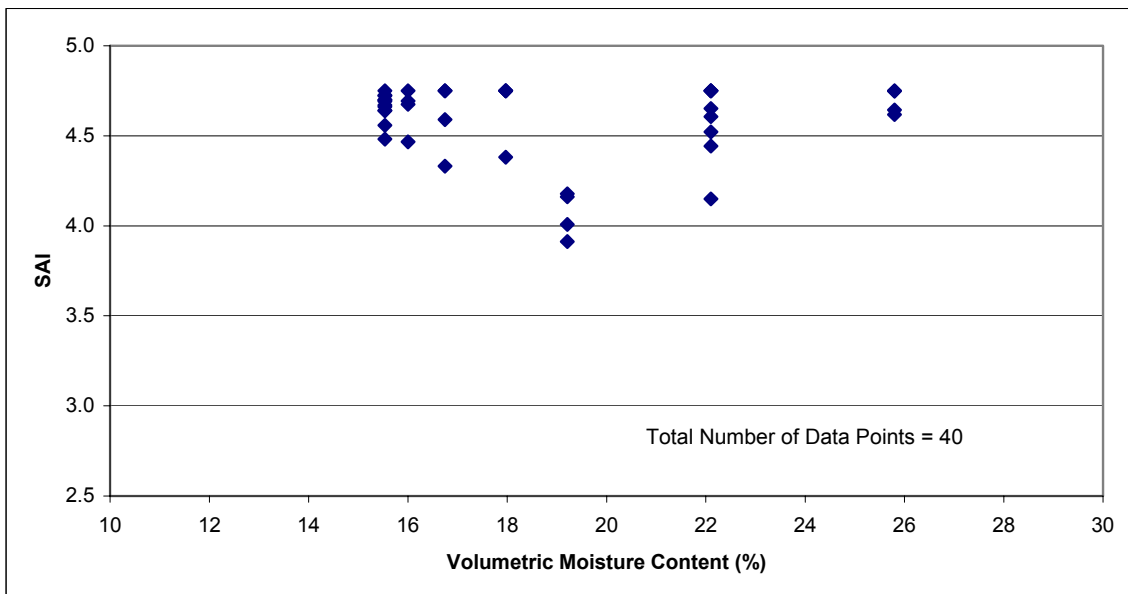


Figure 90: Variation of SAI with Base Layer Moisture Content for S5

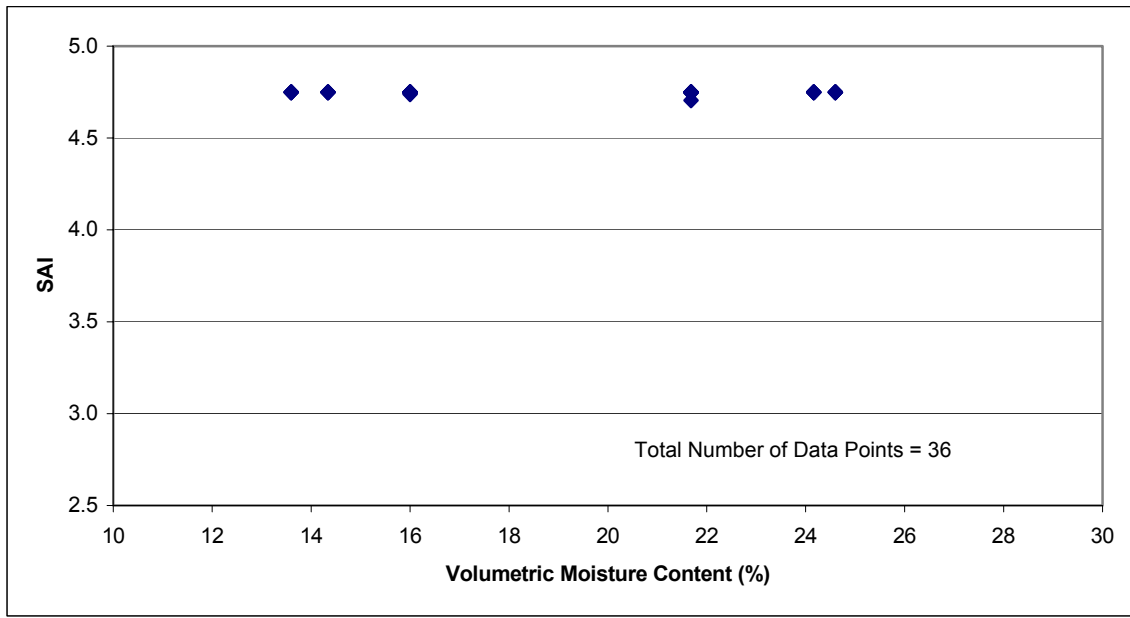


Figure 91: Variation of SAI with Base Layer Moisture Content for S6

In order to further investigate whether there was any significant difference between S5 and S6 in terms of structural performance, an ANOVA test was carried out applying the following hypothesis:

H₀: SAI_{S5} = SAI_{S6} for all moisture content ranges

H₁: SAI_{S5} ≠ SAI_{S6} for all moisture content ranges

To test the hypothesis, an average SAI was calculated for each moisture content range (<5, 5-10, 11-15, etc.) from each of the two sites. A t-test statistic was used at a 95 percent confidence level. Results are summarized in Table 25.

Table 25: Results of Hypotheses Test on SAI for S5 and S6

Comparison of SAI (S5 and S6)		
	S5	S6
Mean	4.58	4.75
Variance	0.04933	0.00006
Observations	40	36
Hypothesized Mean	0	
df	74	
t stat	4.520	
P(T<=t) two-tail	0.000	
t Critical two-tail	1.993	

The results indicate that there is no significant difference between the two sites S5 and S6. The slab thickness, period of testing, subbase/subgrade characteristics, and environment of testing

are identical for the two sites. The only difference between S5 and S6 is in terms of the base layers with one having an NSOG base intended to promote subsurface drainage and the other, a conventional soil aggregate base.

The results imply that the base material, whether drainable or otherwise, presently does not have an influence on the pavement structural capacity. However, this condition could change in the future. As stated earlier, both sites showed minor distresses in the form of transverse cracking. Poor subsurface drainage through the continued presence of high moisture contents in the soil aggregate base layer can result in the development of additional distresses at higher severity levels. This can lead to the pavement section reaching a lower or trigger SAI value much faster, with corresponding deterioration in pavement performance. In such a case, the results are expected to be different than those arrived at for present conditions.

Summary and Conclusions

Presence of water in any part of a pavement structure leads to early deterioration, and therefore early removal of water is essential. As a part of an ongoing large-scale research study in New Jersey, a study was carried out on the effectiveness of drainable base material placed under rigid pavements and the effects of moisture in the base layer on pavement response. Two in-service rigid pavements, one with an NSOG base (S5) and another having a crushed aggregate base layer (S6) were investigated. Rainfall and moisture content data recorded and measured at the two sites on a daily basis and for a one-year period was used in the analysis. Results from the study indicate that for identical rainfall conditions, the base layer with the NSOG material (S5) retains less moisture than a typical soil aggregate base (S6). This was further confirmed through statistical analysis carried out on the rainfall and moisture content data from both sites. It is therefore concluded that the base layer using NSOG material does provide better subsurface drainage under rigid pavements and can therefore facilitate flow of moisture out of the pavement system. This will reduce the potential of pumping and in the long run benefit the NJDOT highway system through reduced cost of maintenance and longer service life.

FWD testing was carried out at the two sites for a period of one year encompassing all climatic seasons. No significant trend in moisture content variation due to rainfall was observed within the base layer types at either site during the FWD test days. To provide a direct comparison of the effects of moisture on the structural capacity of two pavements having different base materials, but almost identical slab thickness and material type in the subbase and subgrade, a Structural Adequacy Index (SAI) was employed. SAI values were calculated from normalized FWD data collected from each site and plotted against moisture content recorded within the FWD testing period. Results indicated that both pavements were in good to excellent condition at all moisture content levels. A statistical analysis was carried out to determine whether there was any significant difference between the two sites in terms of gain in structural strength due to variation in moisture. The results indicate that at present, there is no effect of moisture content on structural capacity. This conclusion is valid for the investigated New Jersey pavement sections with their present distress conditions. However, poor subsurface drainage and the continued presence of high moisture contents can lead to an early deterioration of the pavement structure. This will lead to lower structural capacities in terms of lower SAI values. Correspondingly, future analysis results are expected to differ from those arrived at for the present conditions.

EFFECT OF SUBSURFACE DRAINAGE ON FLEXIBLE PAVEMENT LIFE CYCLE COST

Introduction

It has been well documented in previous studies and literature that improving the subsurface drainage characteristics has a positive impact on pavement performance. Long-term pavement performance is directly related to the amount, extent, and duration of moisture in pavements. In flexible pavements, the continued presence of moisture in conjunction with heavy vehicle loads may result in the stripping of asphalt from aggregate, potholes, and alligator cracking, as well as significant reduction in the unbound materials strength. Also, the freeze-thaw negative impact on the pavement performance is much higher when water exists (higher moisture content) within the pavement structure and is not drained out due to the absence of subsurface drainage systems.

The effect of moisture on the strength and durability of the pavement system and subgrade soils has been a focus of a number of studies in recent years.^(42,43) It is a fundamental variable in all problems of pavement material behavior and has special significance in highway pavements. Though soil physicists have been dealing with moisture movement in soils for quite sometime, work on understanding and quantifying moisture movement profiles of pavement layers is limited. This is due to the fact that field boundary conditions of pavement subgrade soils and base/subbase materials are different from agricultural soils.⁽⁴³⁾ The Organization for Economic Co-operation and Development has summarized research work carried out in participating countries to predict the moisture content of road subgrade.⁽⁴⁴⁾

Most water found in pavement sections is a result of infiltration through the pavement. A number of simulation studies have been made to assess pavement performance due to variation of infiltrated moisture in pavement layers.^(45,46) The models based on these studies tend to incorporate assumed parameter values for evaluation. These complex evaluation procedures for moisture movement have underscored the need for accurately determined moisture conditions in pavements. Data from on-site instrumentation can be used to validate analytical models as well as to calibrate model response variables.

The nature of the base/subbase layer has a major effect on the drainage characteristics of pavement structures. For identical pavement geometry, sections with more permeable base layers exhibit higher outflow volumes, and less pore pressure buildup.⁽⁴⁷⁾ Prolonged head buildup in pavement layers can lead to the development of distresses, and ultimately to the failure of the pavement structure. The severity of the problem increases in areas where frost penetration or freeze-thaw cycles occur.

Impact of Subsurface Drainage Quality on the *In-Situ* Structural Capacity

The 21 flexible pavement test sections considered in this study varied significantly with respect to layer thickness and type base, subbase, and subgrade material, as shown in Table 26. These test sections did not have collector systems/edge drains and subsurface drainage is achieved only through daylighted base layers.

Table 26: Details of the Instrumented Flexible Pavement Sections

Section Number	AC Thickness (in.)	Base Thickness (in.)	Subbase Thickness (in.)	Base Course Type	Subbase Type and Properties	Subgrade Type and Properties
LTPP TEST SITES						
340507 (5A)	14.2	10.8	17	Dark brown sand with stone	Brown sand with stone	Brown sand over clayey sand
340503 (5B)	13.7	11.3	19	Gravel (uncrushed)	Soil Aggr. Mix	Coarse grained clayey sand
340508 (5C)	14.9	11.3	22	Gravel (uncrushed)	Soil Aggr. Mix	Coarse grained clayey sand
340509 (5D)	11.5	11.3	22	Gravel (uncrushed)	Soil Aggr. Mix	Coarse grained clayey sand
340506 (5E)	11.7	3.8	13.5	Coarse stone with sand mix	Coarse sandy gravel	Silty sand
340502 (5F)	10.8	10.4	19	Gravel (uncrushed)	Soil Aggr. Mix	Coarse grained clayey sand
340560 (5G)	10.5	10.5	4	Gravel (uncrushed)	Soil Aggr. Mix	Coarse grained clayey sand
341559 (5H)	10.2	10.5	30	Gravel (uncrushed)	Soil Aggr. Mix	Coarse grained clayey sand
340504 (5I)	13	15	10	Sandy gravel with stone	Brown silty sand	Clean sand
340505 (5J)	10.8	22.7	9.5	Brown sandy gravel	Silt sand mix with some stone	Sand
340501 (5K)	9.5	10	20	Gravel (uncrushed)	Soil Aggregate Mix (Predominantly coarse-grained)	Coarse Grained clayey sand
340901 (9A)	11	6.5	10	Bituminous Base Course	Soil Aggr. Mix	Coarse grained silty sand
340903 (9B)	11	7.4	10	Bituminous Base Course	Soil Aggr. Mix	Coarse grained silty sand
340902 (9C)	11.5	7.5	26	Sandy gravel with large granite	Brown silty sand with small stone	Sandy silt with traces of clay
340960 (9D)	11.5	6.4	10	Bituminous Base Course	Other	Coarse grained silty sand
340961 (9E)	11.5	5.6	10	Bituminous Base Course	Soil Aggr. Mix	Coarse grained silty sand w/gravel
340962 (9F)	11	6.6	10	Bituminous Base Course	Soil Aggr. Mix	Coarse grained silty sand w/gravel
NON-LTPP TEST SITES						
NJ - 1	7.5	7	15.75	Crushed stone w/sand	7 in. of sand w/crushed aggr. over 8.75 of sand and gravel w/large boulders	Brown sand and gravel w/large boulders
NJ - 2	4	6	14	Recycled aggregate mix	Old 2 in. AC layer over sandy gravel	Sand and stone
NJ - 3	10	4	13	Crushed stone w/sand	Med gray-brown sandy gravel w/some cobbles	Dark brown silty sand w/sand stone and decomposed root material
NJ - 4	10	10.5	No subbase	Crushed aggr. limestone	N/A	Sandy clay and silt

The volumetric moisture content of different layers at the listed test sections was continuously monitored. However, as the purpose of this analysis is to study the impact of moisture content on pavement response in terms of FWD deflection, only the moisture content data recorded during the FWD testing has been considered in the analysis. Table 27 shows a summary of the measured moisture from different sections during the regular FWD testing.

Table 27: Max. and Min. Moisture Contents for Instrumented Test Sections at Different Pavement Depths

Section	Maximum Moisture Content (%)				Minimum Moisture Content (%)			
	MC1 (Base)	MC2 (Base or Subbase)	MC3 (Subbase or Subgrade)	MC4 (Subgrade)	MC1 (Base)	MC2 (Base or Subbase)	MC3 (Subbase or Subgrade)	MC4 (Subgrade)
5A	50.2	40.2	45.6		27	34.81	43	
5B	50.2	40.2	45.6		21.68	34.81	43	
5C	44.8	34.81	41.2		33.69	17.97	36.98	
5D	44.8	34.81	41.2		33.69	17.97	36.98	
5E	44.8	38.03	41.2		33.69	17.97	36.98	
5F	44.8	30.6	41.2		33.69	17.97	36.98	
5G	24.6	37.2	32.55	42.1	11.98	32.55	28.2	40.2
5H	24.6	37.2	32.55	42.1	11.98	32.55	28.2	40.2
5I	24.6	37.2	32.55	42.1	14.34	32.55	28.2	40.2
5J	30.22	44.8	44.68	28.2	17.97	42.9	38.03	22.92
5K	30.22	44.8	44.68	28.2	17.97	42.9	38.03	22.92
9A	22.1	38.03	51.01		17.97	33.69	47.96	
9B	22.1	38.03	51.01		17.97	33.69	47.96	
9C	22.1	38.03	51.01		17.97	33.69	47.96	
9D	22.1	38.03	51.01		17.97	33.69	47.96	
9E	20.44	38.03	51.01		17.97	33.69	47.96	
9F	22.1	38.03	51.01		17.97	33.69	47.96	
NJ-1	11.3	56.4	54.7	60.4	6.9	38.2	21.68	31.6
NJ-2	40.05	42.9	39.4		29.03	19.21	15.54	
NJ-3	45.53	41.03	54.83		16.75	21.68	47.17	
NJ-4	39.3	98.8	58.2		35.1	67.3	52.4	

An effort was made to correlate the deflection measurements and/or the backcalculation results of all sections with the moisture contents measured during the FWD testing. However, this effort was not successful because of the large variability in the pavement structure of the sections in terms of layer thickness. For example, the AC thickness varies from 4 in to 14.9 in. This variation in layer thickness is reflected in the measured deflection, regardless of the moisture content. For example, although the moisture content is expected to cause some increase on the measured deflection, the measured deflection of a thick pavement section will have lower deflection than that of a thinner pavement section, even when higher moisture content is recorded for the thicker pavement section. Therefore, trying to combine the data from all sections for a correlation analysis was not successful.

Another trial was made to correlate the moisture content and FWD data of each individual section. However, each section had a limited range of moisture content and limited number of data points. Therefore, the results of this analysis were also not satisfactory.

An approach was therefore used to normalize the FWD data and backcalculation results and hence the structural capacity of each section. This will allow the use of data from all sections at once, which will provide a wide range of moisture content information. The structural capacity normalization was done through the use of the NJDOT SAI. SAI uses a scale of 0 to 5 (0 is for a failed pavement, whereas 5 is for new pavements). SAI is a function of the backcalculated effective structural number (SN_{eff}), the as-built structural number ($SN_{as-built}$), and the required structural number (SN_{req}) for future traffic based on the FWD analysis. It is expressed in terms of structural number ratio (SNR), which is a weighted average of $SN_{eff}/SN_{as-built}$, and SN_{eff}/SN_{req} with thirty percent of weight assigned to $SN_{eff}/SN_{as-built}$ and seventy percent to SN_{eff}/SN_{req} .

An SAI value of 2.5 is used as a trigger value indicating that the pavement section is approaching the end of its structural life and is in need of structural improvement. SAI was calculated from the FWD measurements performed on each test section. Correlation analysis was then performed on the calculated SAI. Results of this analysis are shown in Figure 92. In this figure, the base course moisture content is correlated with SAI for different sections. Similar analysis was performed to correlate the subbase and subgrade moisture contents with SAI. However, the results of these analyses are not presented because the impact of subsurface drainage will be more visible on the base course moisture content.

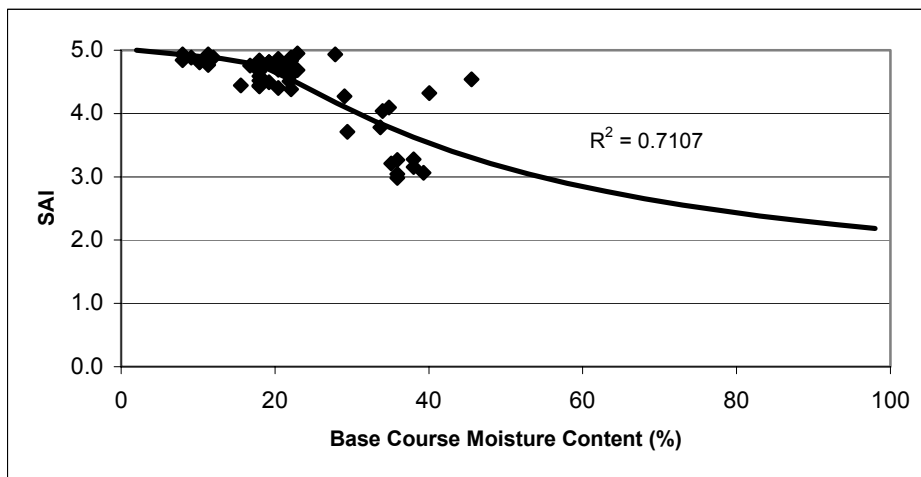


Figure 92: Correlation between Base Course Moisture Content and SAI

Impact of Subsurface Drainage Quality on Pavement Performance

The model shown in Figure 92, which correlates the base course moisture content and SAI, was then used to illustrate the impact of high moisture content (poor subsurface drainage) on the pavement structural capacity in terms of SAI. The data from the non-LTPP site NJ-3 was used for this purpose. The recorded base course moisture content of NJ-3 during the regular monthly FWD testing ranged from 16.75 percent to 45.53 percent. These moisture contents correspond to SAI values of 4.82 and 3.30, respectively.

Figure 93 shows the SAI-Age model adopted by NJDOT PMS. NJDOT PMS SAI-Age model has 3 activity classes, which are functional improvement (thin overlay), structural improvement (thick

overlay) and reconstruction. The model shown in Figure 93 is for the thick overlay pavement structure class. Using this model, the effective pavement ages corresponding to SAI values of 4.82 and 3.30 are 2 and 9 years, respectively. In other words, the pavement structural capacity, as measured in terms of SAI and based on FWD data, shows a reduction of 7 years in the pavement service life because of the increase in the base course moisture content. The model shown in Figure 93 indicates that the structural service life of this class (thick overlay) of pavements is 15 years (SAI = 2.5). Therefore, the remaining structural lives of section NJ-3 for the high and low moisture contents are 6 and 13 years, respectively.

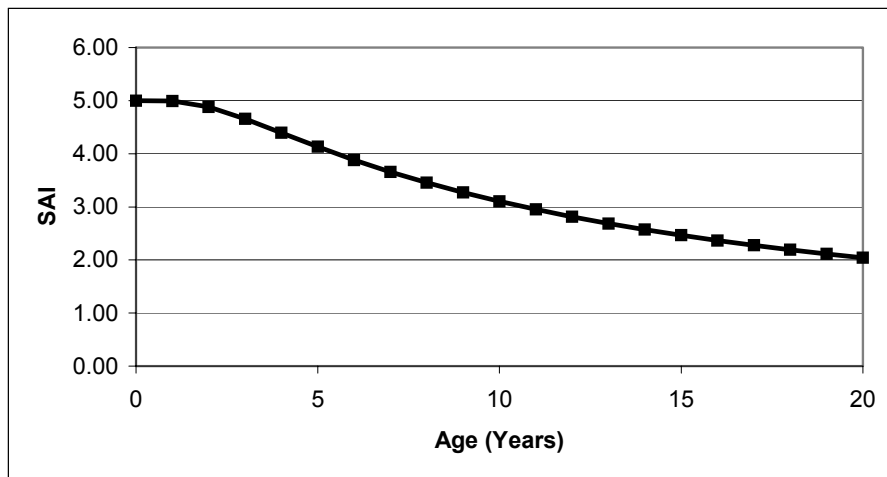


Figure 93: SAI Performance Prediction Model

Since the actual age of section NJ-3 is the same regardless of the base course moisture content, a modification to Figure 93 is required to reflect the impact of moisture content on the remaining structural life. Section NJ-3 was constructed in 2001, i.e. the actual age of this section is only 2 years. Therefore, the SAI-Age model shown in Figure 94 represents the performance of this section if the base course moisture content is kept at its lowest level (16.75 percent). However, if the base course moisture content is kept at its highest level (45.53 percent), the pavement structural performance will follow another curve, as shown in Figure 94. In this figure, the original SAI curve, representing the expected performance at low-level base course moisture content, and the revised SAI curve, representing the expected performance at high-level base course moisture content, are superimposed. As can be observed, the section with high moisture content will reach the trigger level (SAI = 2.5) at age 9 years compared to the section with low moisture content, which will reach the same trigger level at age 15 years. Considering the present age of the section to be 2 years, it will have only 7 years left in its remaining structural service life for the high-level moisture scenario.

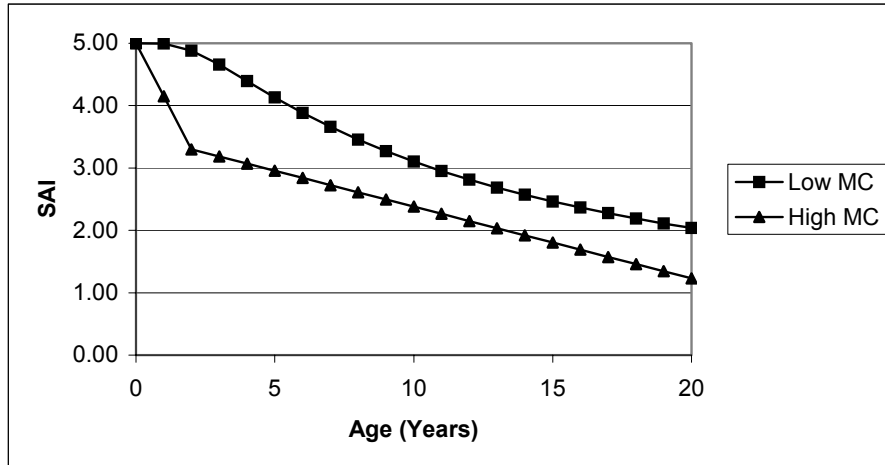


Figure 94: SAI Performance with Low and High Base Course Moisture Contents

Life Cycle Cost Analysis (LCCA)

To demonstrate the impact of poor subsurface drainage on the life cycle of the pavement, section NJ-3 was considered for the LCCA. Two cases were considered: Case 1 where poor subsurface drainage (constant presence of high moisture content) was applied to the pavement; and Case 2 where an enhanced subsurface drainage system (constant presence of low moisture content) was considered. The study section is a truck rest area located on the northbound section of Interstate route I-287 near milepost 32.5. The test section is a curved shape with a width of 50 ft at mid section and a total length of 250 ft. For simplicity of life cycle calculations, the section width was assumed to be 45 ft. An analysis period of 40 years was considered to investigate the differences between the two cases of subsurface drainage systems, as shown in Figure 95. As explained earlier, the structure service life of this section will be 9 years with poor subsurface drainage system. However, when the subsurface drainage system is improved, the structure service life will go up to 15 years.

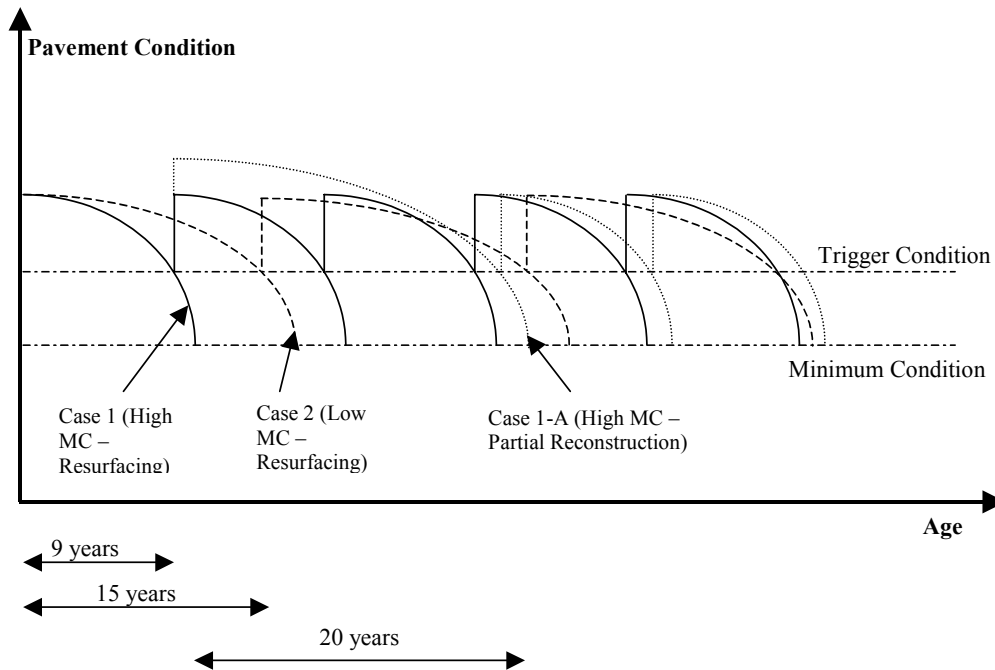


Figure 95: Case Studies of Pavement Performance for a 40-year Analysis Period

The pavement condition before applying both drainage alternatives was assumed to be the same. Also, a typical resurfacing maintenance activity of milling the existing AC surface to a 2 in. depth followed by an overlay of 4 in. thickness was considered for both alternatives whenever the pavement condition reaches its trigger value. The maintenance activity was kept the same for both cases over the analysis period, so that it could be shown that variation in costs is due to the two moisture content scenarios. However, for Case 1 (high moisture content), regular maintenance activity in the form of resurfacing (mill 2 in., overlay 4 in.) was carried out at every 9-year interval, whereas for Case 2 (low moisture content) the resurfacing was carried out at every 15-year interval.

A sub-case was also considered within Case 1 and referred to as Case 1-A, whereby partial reconstruction of the pavement (removal of asphalt concrete layer to its full depth and replacement with new 10 in. asphalt concrete) was considered as a treatment activity for the poor drainage (high moisture content) conditions. For this sub-case, it was assumed that the pavement would have an initial service life of 9 years prior to reconstruction, followed by 20 years of service life, and then resurfacing at every 9 years thereafter.

An inflation rate of 0 percent and discount rate of 6 percent was used for the LCCA. The present worth cost (PWC) was calculated at each scheduled activity using the following formula:

$$PWC = FW \times \left(\frac{1}{(1+i)^n} \right) \quad (\text{E21})$$

Where:

- PWC = Present Worth Cost
- FW = Future Worth
- i = discount Rate
- n = year in which maintenance cost applied

The maintenance activity is always considered whenever the pavement reaches its trigger conditions. In the LCCA, the unit cost for the resurfacing maintenance activity (Mill 2 in. Overlay 4 in.) was taken as \$35.96/sq.yd. For partial reconstruction (placement of a 10 in. AC layer over base and subbase), the assumed unit cost was \$87.53/sq.yd. In comparing the PWC, the base/subbase cost was kept constant for all three cases.

A typical calculation for LCCA for Case 1 for the NJ-3 (45 ft x 250 ft) section is shown in Table 28. The PWC for the three cases is calculated to be \$55,250 (Case 1, high moisture content - resurfacing), \$76,996 (Case 1-A, high moisture content - partial reconstruction), and \$23,669 (Case 2, low moisture content – resurfacing).

Table 28: Sample LCCA Analysis for Case 1 - High Moisture Content

Year	Treatment	Unit Cost/yard ²	Total Cost (\$)	PW Cost (\$)
9	1st Resurfacing Mill 2" Overlay 4"	35.96	44,950	26,606
18	2nd Resurfacing Mill 2" Overlay 4"	35.96	44,950	15,748
27	3rd Resurfacing Mill 2" Overlay 4"	35.96	44,950	9,321
36	4th Resurfacing Mill 2" Overlay 4"	35.96	44,950	5,517
40	Residual Value			-1,942
Total Life Cycle Cost for a 250 ft by 45 ft section				\$55,250

The results of the LCCA for all 3 cases of NJ-3 section, extrapolated in terms of PWC/lane mile, are shown in Table 29. As can be seen, when a good drainage system was applied to the pavement (Case 2), the life cycle cost dropped to almost half of the cost compared to when a poor drainage system was considered (Case 1). Also, in case of poor drainage, resurfacing (Case 1) was a better alternative than partial reconstruction (Case 1-A) in terms of PWC. Applying the results to a typical 4-lane five-mile long road section, the savings in PWC through improving the drainage quality equal approximately \$3.6 million.

Table 29: Results of LCCA Analysis

Analysis Case	Present Worth Cost/Lane Mile (\$)
Case 1 High Moisture Content (Resurfacing)	311,168
Case 1-A High Moisture Content (Partial Reconstruction)	433,641
Case-2 Low Moisture Content	133,303

Summary and Conclusions

It is a well-known fact that moisture due to poor subsurface drainage is one of the principal causes of failure of pavement systems. Most water found in pavement sections is a result of infiltration through the pavement. Consequently, base/subbase moisture control is of prime importance in pavement design, construction, behavior, and performance. This section presented a methodology to quantify the effect of moisture infiltration on pavement service life. It was shown that pavement instrumentation could be used effectively in monitoring response of subsurface drainage systems to moisture infiltration. The successful instrumentation of the test sections for monitoring climatic data and subsequent development of a database has given a better understanding of the moisture retention within a pavement system and its profound effect on the cost and service life of a highway network. Data collected through TDR probes from one of the study's 24 instrumented sites were used to develop relationships between the moisture content at the base course and pavement structural capacity expressed in terms of the SAI. The analysis has shown that pavement service life decreases with an increase in the base course moisture content as a result of poor subsurface drainage. Instrumentation placed for measuring frost/thaw depths did not yield any data due to non-freezing conditions at the NJ-3 site during the 2002 monitoring period. However, it would have further compounded the pavement performance due to moisture.

To demonstrate the potential economic impact of using a subsurface drainage system that will reduce the moisture retention time within the pavement structure, three case studies were investigated. The first case assumed poor subsurface drainage was applied to the pavement and resulted in higher moisture content within the base layer, while the second assumed good subsurface drainage system was used. A third case was considered where carrying out partial pavement reconstruction for the poor subsurface drainage conditions resulted in a longer service life. A life cycle cost analysis was performed using the three alternatives on an Interstate route section in New Jersey, which was instrumented to acquire climatic data including moisture content. The analysis showed that when a good quality subsurface drainage system is applied to a pavement structure, resulting in lowering the retained moisture content within the pavement base layers, corresponding life cycle costs can be reduced by more than 50 percent as compared to the same structure with poor subsurface drainage systems. Also, a significant increase in the structural service life of the pavement is observed. The analysis also showed that in the case of poor subsurface drainage conditions (high moisture content), the resurfacing alternative was more cost-effective as compared to partial reconstruction.

It is concluded that substantial long-term savings can be achieved by improving the subsurface drainage quality of flexible pavements. This section has addressed only the impact on service life and cost-savings that can be achieved due to lower moisture content on a pavement section having a daylighted base. These savings can be enhanced by a more rapid lowering of the moisture content through the use of other subsurface drainage elements such as collector systems in conjunction with permeable base/subbase layers.

FWD VS. SPA CORRELATION ANALYSIS

Non-destructive testing (NDT) is one of the most commonly used approaches in structural condition evaluation and monitoring of in-service pavements. Some of the advantages of NDT are that it does not disturb the underlying pavement layers, it does not require any removal of the pavement material to be taken to a lab for testing, and it is relatively quick and inexpensive, resulting in fewer traffic delays or disruptions. State Highway Agencies and DOTs most commonly use the deflection-based FWD device. Another NDT device that is gaining usage is the seismic-based SPA, as shown in Figure 96. Each testing device (FWD and SPA) uses its own methods and characteristics for determining the *in-situ* strength and moduli of a pavement.

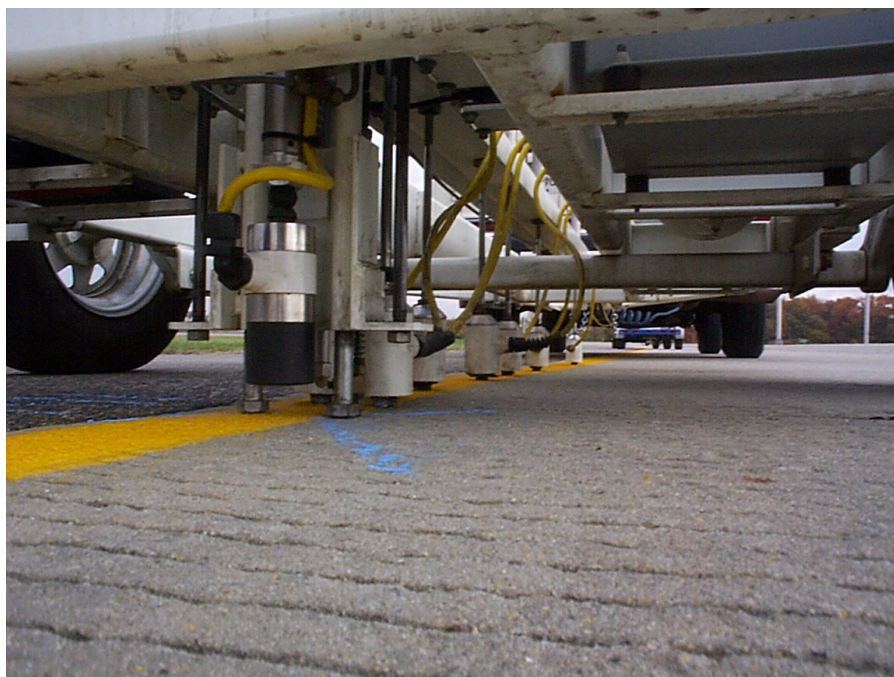


Figure 96: Seismic Pavement Analyzer (SPA)

One of the objectives of the study was to compare the results of the FWD and the SPA analyses and perform correlation analysis between the two pieces of non-destructive pavement response testing equipment. Deflection testing using the FWD was carried out on a monthly basis, and bi-monthly during the recovery period on the test sections. In addition two 24-hour testing cycles (FWD) were performed on two sites. SPA testing was carried out on the same basis, with a few tests missed during the coldest test days due to the equipment's more limited operational temperature range.

This section details the results of the correlation analysis carried out on data collected by the FWD and SPA for flexible and rigid pavement sections of selected test sites.

SPA Seismic Methods

The theory behind testing by seismic methods is based on generation, detection, and measurement of different properties of stress waves, such as velocity of propagation and various wave propagation phenomena: reflections, refractions, dispersion, etc. The raw data collected on the surface of a pavement by seismic methods are simply time histories of an

impact source and surface deformation. For pavement applications, these time records are generally processed and analyzed using three different techniques: SASW Method, USW Method, and IR Method. For this comparison study, the SPA and corresponding FWD parameters are listed in Table 30, while the seismic techniques implemented in the SPA are described below.

Table 30: SPA and FWD Comparison Parameters

SPA Parameter	FWD Parameter	Characteristic
SASW E_p	E_p	Pavement Modulus
SASW $E_{Subgrade}$	M_r	Subgrade Modulus
SASW E_{AC} Avg.	E_{AC}	AC Modulus
IR composite modulus	E_p	Pavement Modulus
IR subgrade modulus	K_{static}	Subgrade (PCC)
USW E_{AC}	E_{AC}	AC Modulus

Spectral Analysis of Surface Waves (SASW)

The SASW test is one of the most commonly used seismic tests for shallow explorations of pavement and soil systems. The SASW method utilizes the dispersive characteristic of surface waves propagating in a layered media. It is used in delineation of the modulus profile of a pavement section. The SASW test consists of two major steps: determination of a dispersion curve, i.e. surface wave velocity vs. frequency relationship, and derivation of a modulus profile from the dispersion curve through a backcalculation procedure. Similar to the FWD deflection bowl, the shape of the dispersion curve depends on the modulus and thickness of each layer.

The SASW test elastic modulus profile backcalculation is typically done on either a three- or four-layer pavement model. If the model was assumed to be a four-layer in the backcalculation, with the AC divided into two layers, the given modulus is an average of the two. Results from the SASW method are compared in three ways to the FWD results. The first comparison is between the SASW “overall” pavement modulus and the FWD backcalculated pavement modulus (E_p). The second comparison is between the SASW and FWD backcalculated subgrade moduli (M_r). Finally, the SASW and FWD asphalt pavement moduli (E_{AC}) are compared.

Impulse Response (IR)

The IR method is generally used to determine the modulus of subgrade reaction (k) of rigid pavement foundation. It is also defined as an index test providing the overall modulus or stiffness of a pavement structure for flexible pavements. The method is similar to the FWD-based methods in which the surface bending of a pavement under mechanic impact is measured. In the case of a rigid pavement, the results correspond to the shear modulus of the subgrade. Sometimes it is expressed as a modulus of subgrade reaction. The results from the IR method were compared to the FWD backcalculated, FWD K_{static} , and E_{pcc} from the rigid pavements.

Ultrasonic Surface Waves (USW)

The USW method can be described as a high frequency SASW method. It is used to directly measure an average modulus of the top layer of a pavement. However, the USW method allows for evaluation of modulus variation within the surface layer.

Spectral Analysis of Surface Waves (SASW) Results

This section covers results based on the Seismic Analysis of Surface Waves testing method. It contains three sub-sections that compare the pavement modulus, subgrade modulus, and AC modulus from FWD and SPA testing. It should be noted that to account for the difference in testing frequency ranges, AC layer moduli from SPA testing are divided by a factor, usually around 3.0, to convert them to values typical for FWD.

FWD and SPA (SASW) Pavement Modulus (E_p)

To compare the pavement moduli of a flexible pavement obtained from the FWD and SPA (SASW) methods, it was necessary to determine an equivalent pavement modulus from the SASW method. This was achieved by using an Odemark weighted transformation that considers the thickness and moduli for each layer obtained from the SASW results (excluding the subgrade). The equivalent pavement modulus is calculated from:

$$E_p = \frac{\sum (E_{ACi} * h_i^3) + E_{base} * h_b^3}{h_{total}^3} \quad (E22)$$

Where:

- E_p is the overall pavement elastic modulus of the layer above the subgrade
- E_{ACi} is the elastic modulus of the asphalt layer(s)
- h_i is the thickness of the asphalt layer(s)
- E_{base} is the elastic modulus of the base and subbase (granular layers)
- h_b is the thickness of the base and subbase (granular layers)

Presented in Table 31 are the average pavement moduli values for each test section for the 2-year testing period. The pavement moduli represent an average or overall pavement moduli for the two years of testing. It is observed that the magnitude of the SPA pavement moduli was consistently lower than the FWD pavement moduli for each test section.

The FWD and SPA pavement moduli showed a reasonable correlation, as shown in Figure 97, with an R^2 value of 0.4943. The test sections were then split into two classes based on the pavement thickness (greater or less than 20 in).

The result of grouping the test sections into two pavement classes (thin and thick) had no significant effect on the R^2 for thin pavements (0.4641), and had a small increase in R^2 for the thick pavements (0.535). Correlation plots are shown in Figures 98 and 99.

Table 31: Average FWD and SPA Pavement Moduli

Test Section	FWD	SPA (SASW)
	E_p (psi)	E_p (psi)
S1	135,164	23,267
S2	92,218	42,161
S3	220,799	46,027
S4	87,041	38,002
SPS-5-1	248,355	37,350
SPS-5-2	232,204	31,154
SPS-5-3	296,971	44,738
SPS-5-4	215,289	78,232
SPS-5-5	248,493	70,107
SPS-5-6	101,522	40,639
SPS-5-7	234,199	44,273
SPS-5-8	225,145	66,732
SPS-5-9	314,144	43,651
SPS-5-10	208,411	46,801
SPS-5-11	117,213	67,311
SPS-901	225,888	66,129
SPS-902	188,803	34,131
SPS-903	159,403	44,860
SPS-960	160,592	35,479
SPS-961	174,631	34,148
SPS-963	159,874	47,081

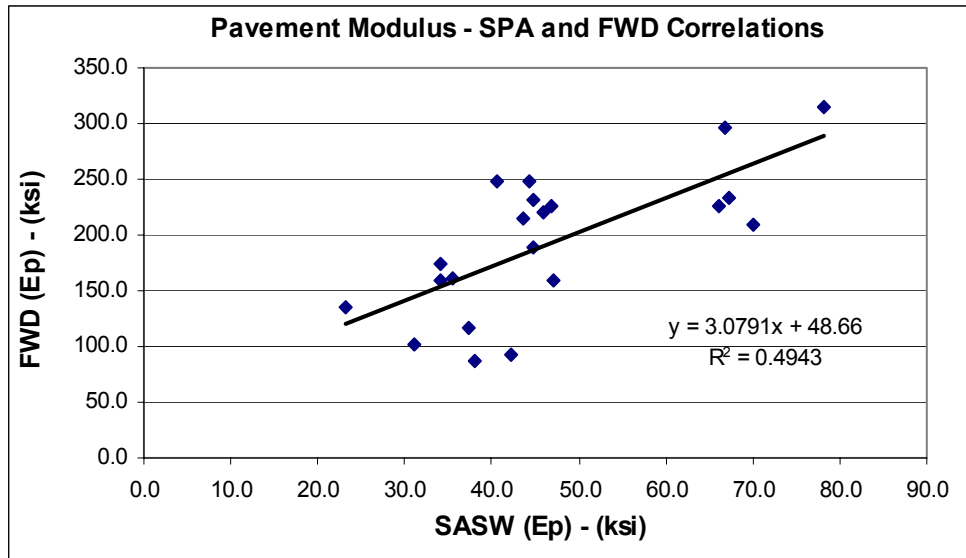


Figure 97: Overall Correlation of Pavement Modulus

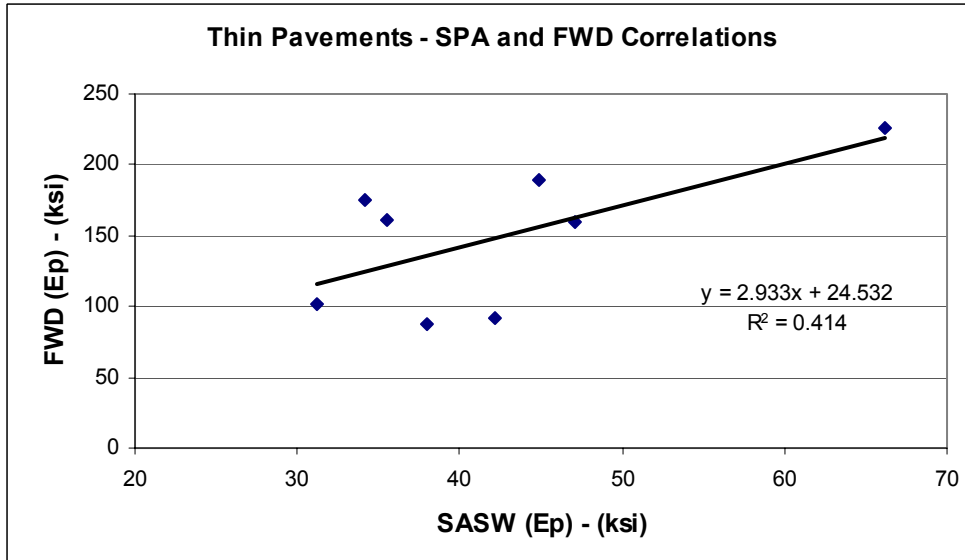


Figure 98: Correlation of Pavement Modulus – Thin Pavements

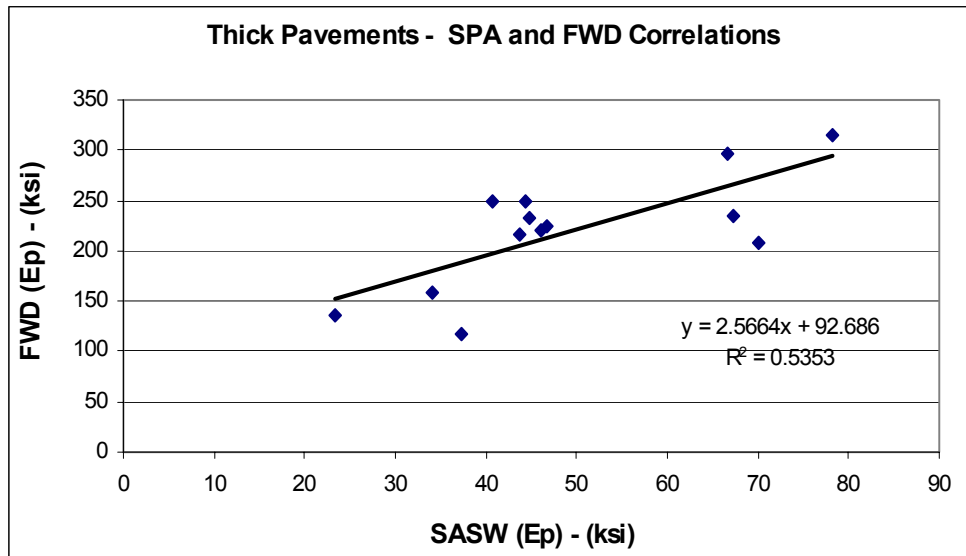


Figure 99: Correlation of Pavement Modulus - Thin Pavements

SASW Variation in Equivalent Pavement Modulus With Time

To investigate the variation in the equivalent pavement modulus from the SASW analysis methods for the SPA and pavement modulus (E_p) for the FWD, it was necessary to plot the normal distributions for the pavement moduli over the 2 years of testing. Also, the mean and standard deviation of the pavement moduli over the approximate 2 years of testing was evaluated and compared (Table 32).

Table 32: Averages and Standard Deviation of Pavement Modulus (E_p) for SPA and FWD

Test Type		E_p (PSI)
FWD	Avg	197,653
	Std. Dev	85,931
SPA (SASW)	Avg	36,675
	Std. Dev	22,847

For the SPA testing, the average equivalent pavement modulus for the SASW method was 36,675 psi over a time period of 2 years, with a standard deviation of 22,847psi. For the FWD testing, the pavement modulus (E_p) was 197,653 psi, with a standard deviation of 85,931 psi. The normal distribution for the FWD and SPA pavement moduli are presented in Figure 100.

The FWD pavement moduli show a greater variability than those from the SPA over the 2-year cycle (Figure 100). This could be due to the fact that FWD testing is highly affected by temperature and environmental parameters and was conducted under all climatic conditions, while SPA testing could not be carried out during extreme cold weather conditions over the 2-year testing period.

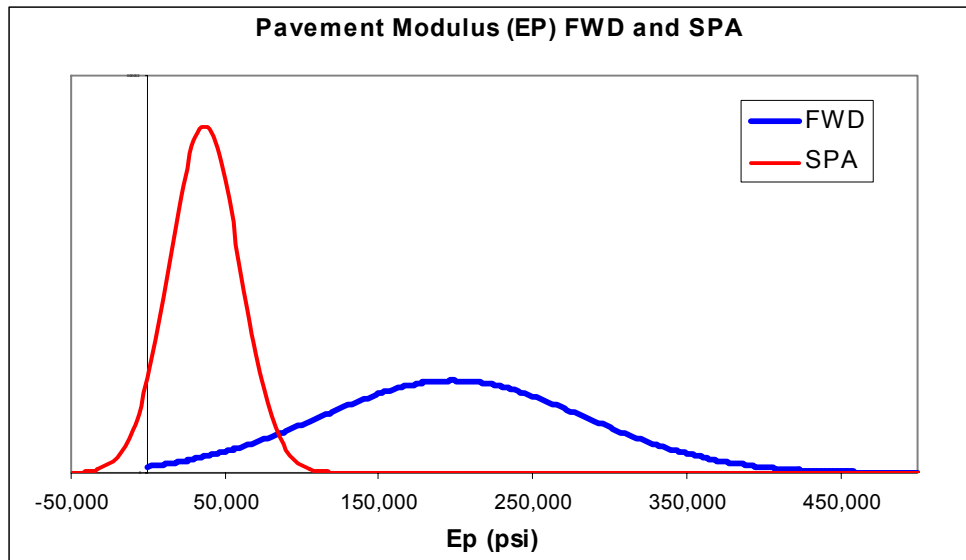


Figure 100: Normal Distributions SPA and FWD Pavement Moduli

Due to the variation in the pavement moduli, the New Jersey seasonal corrections factors were applied to the FWD deflections. The resulting backcalculated E_p distributions were compared to the SPA distributions for each environment zone (north and south) and thickness class (thin and thick).

After applying the temperature and seasonal correction models, the variation in the FWD pavement moduli was reduced for each environment and thickness class. Results are shown in Figures 101 to 104.

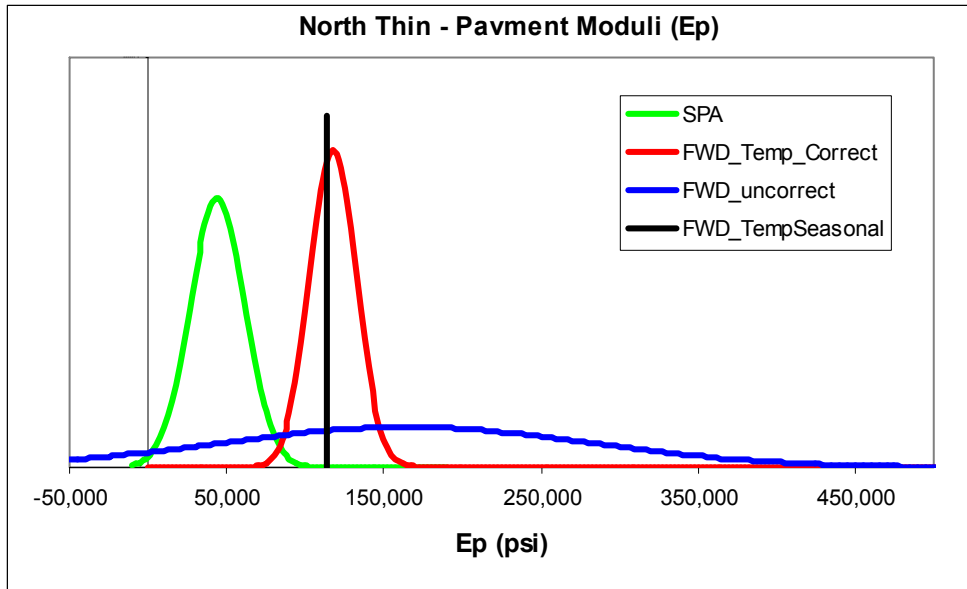


Figure 101: Normal Distributions SPA and FWD – North Thin

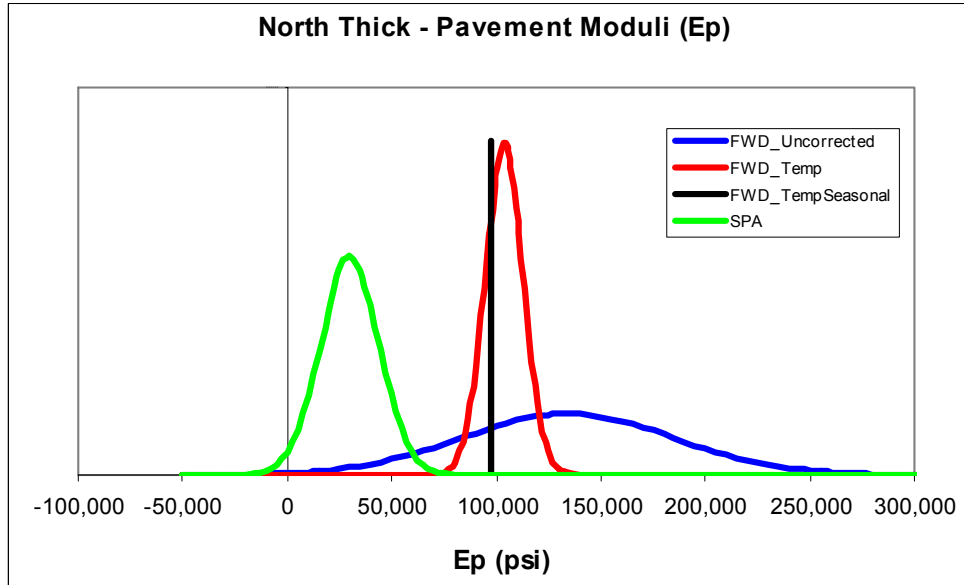


Figure 102: Normal Distributions SPA and FWD – North Thick

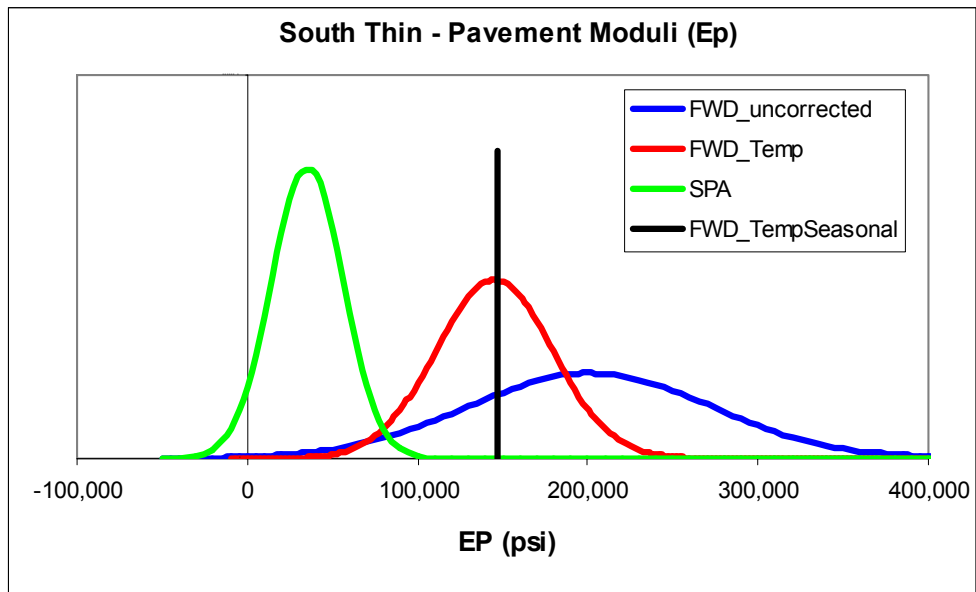


Figure 103: Normal Distributions SPA and FWD – South Thin

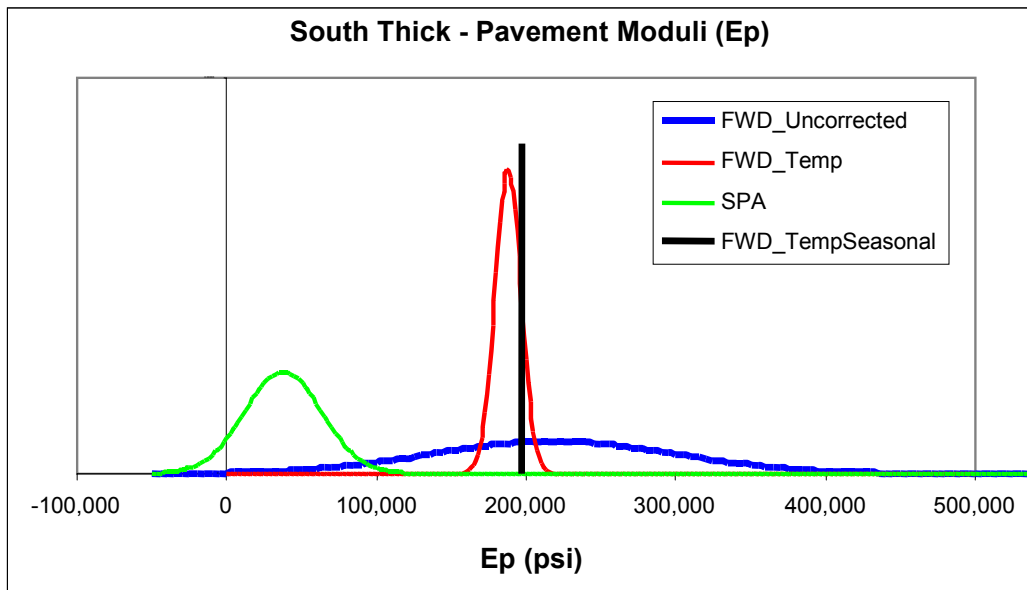


Figure 104: Normal Distributions SPA and FWD – South Thick

FWD and SPA (SASW) Subgrade Modulus (M_r)

To compare the subgrade modulus of flexible pavements for the FWD and SPA methods, it was necessary to compare the Resilient Modulus (M_r) with the subgrade modulus from the SASW testing method.

Presented in Table 33 are the average subgrade moduli values for each test section for the 2-year testing period. It is observed that the magnitudes of the SPA (SASW) subgrade moduli were consistently higher than the corresponding FWD subgrade moduli for each test section.

Table 33: Average FWD and SPA Subgrade Moduli

Test Section	FWD	SPA (SASW)
	Mr (psi)	Subgrade Modulus (psi)
S1	19,752	33,625
S2	6,309	11,489
S3	10,548	34,605
S4	7,659	29,849
SPS-5-1	12,476	68,109
SPS-5-2	11,904	84,735
SPS-5-3	11,955	64,910
SPS-5-4	12,412	38,792
SPS-5-5	14,324	28,065
SPS-5-6	6,310	35,463
SPS-5-7	8,561	42,853
SPS-5-8	11,964	30,944
SPS-5-9	12,851	48,533
SPS-5-10	10,577	59,130
SPS-5-11	11,535	66,041
SPS-901	10,027	27,160
SPS-902	10,826	37,501
SPS-903	11,244	33,716
SPS-960	10,166	62,248
SPS-961	8,440	52,572
SPS-963	13,722	52,229

The FWD and SPA subgrade moduli showed a low correlation, with an R² value of 0.0319 (Figure 105). The test sections were then split into two classes based on the pavement thickness (greater or less than 20 in.).

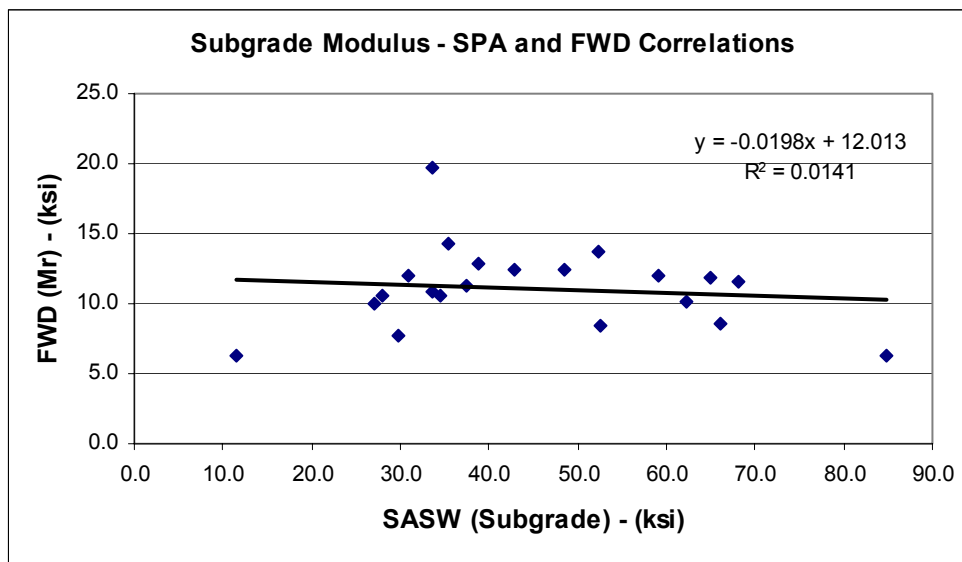


Figure 105: Overall Correlation of Subgrade Modulus

As shown in Figures 106 and 107, grouping the results into the two pavement classes did not lead to significant improvement on the correlation.

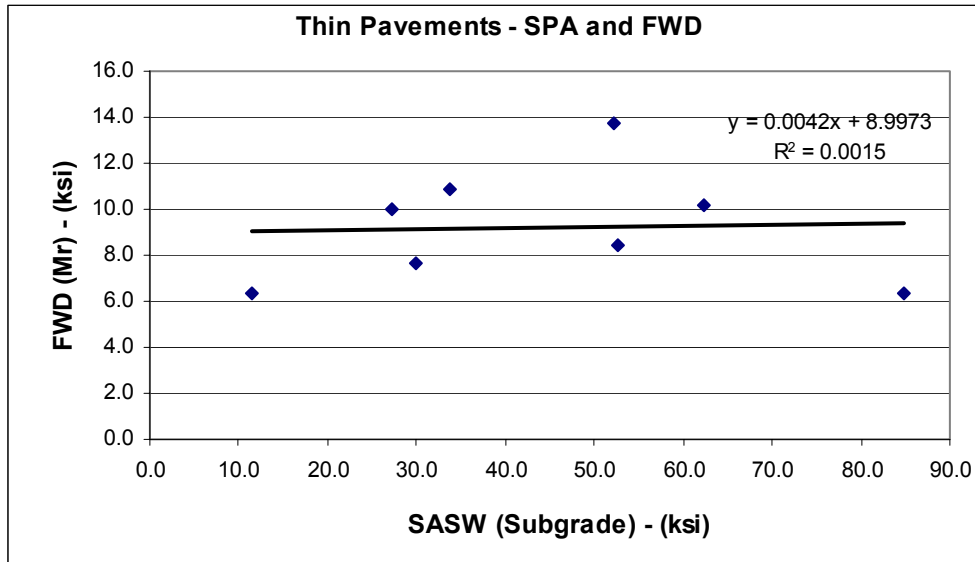


Figure 106: Correlation of Subgrade Modulus – Thin Pavements

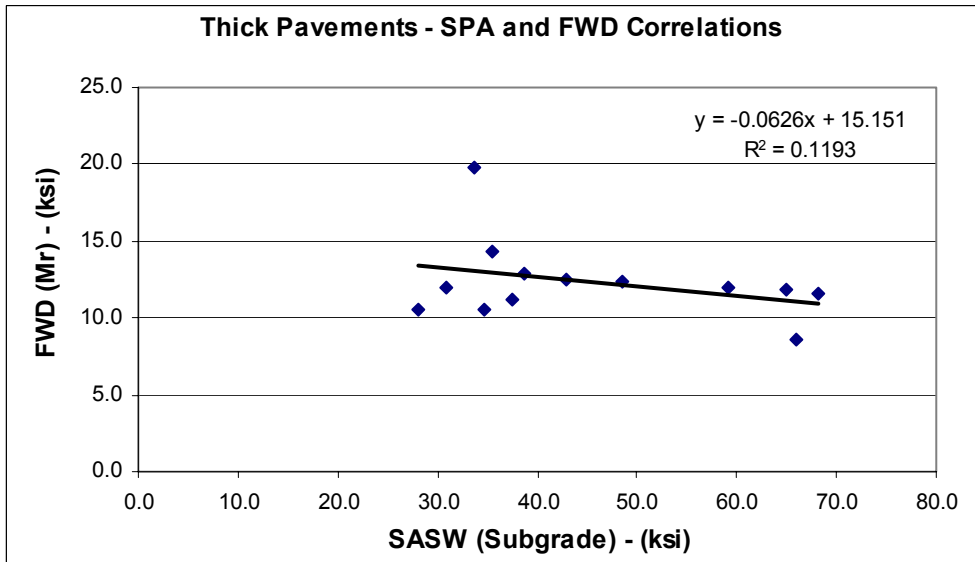


Figure 107: Correlation of Subgrade Modulus – Thick Pavements

Variation in Subgrade Modulus With Time

To investigate the variation in the subgrade modulus from the SASW method and the Resilient Modulus (M_r) for the FWD, normal distributions for the subgrade moduli over the 2-year period of testing were evaluated. Also, the mean and standard deviation of the subgrade moduli over the approximate 2 years of testing were evaluated and compared (Table 34).

Table 34: Averages and Standard Deviation of Subgrade Moduli (M_r) for SPA and FWD

Test Type		M_r (PSI)
FWD	Avg	11,354
	Std. Dev	3,729
SPA (SASW)	Avg	44,085
	Std. Dev	35,372

For the SPA testing, the average subgrade modulus for the SASW method was 44,085 psi over a time period of 2 years, with a standard deviation of 35,372 psi. For the FWD testing, the Resilient Modulus (M_r) was 11,354 psi, with a standard deviation of 3,729 psi. The normal distributions for the FWD and SPA pavement moduli are presented in Figure 108.

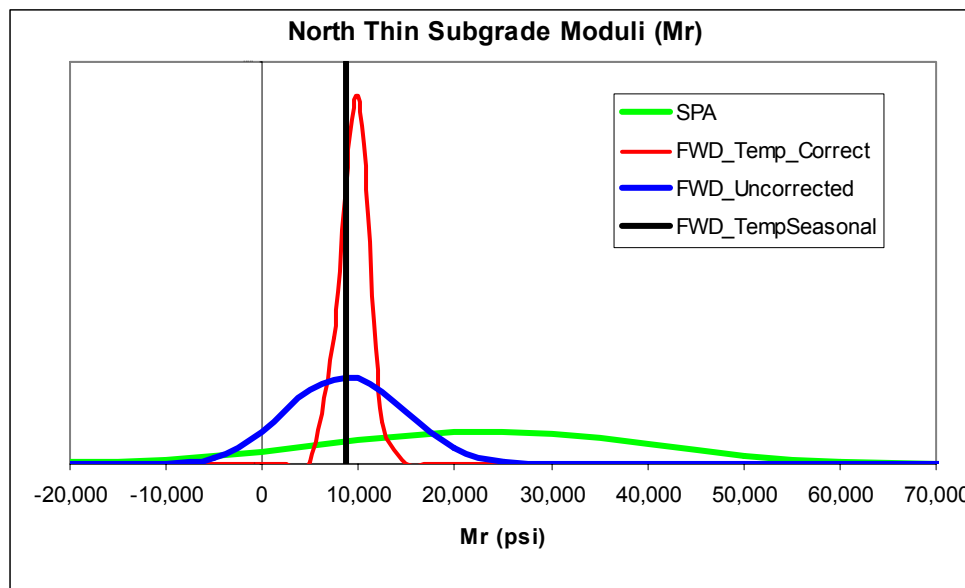


Figure 108: Normal Distributions SPA and FWD – North Thin

Due to the variation in the subgrade moduli, the New Jersey seasonal corrections were applied to the FWD deflections. The resulting backcalculated M_r distributions were compared with the SPA distributions for each environment zone (north and south) and thickness class (thin and thick). After applying the temperature and seasonal correction models, the variation in the FWD subgrade moduli was reduced for each environment and thickness class, as shown in Figures 109 to 111.

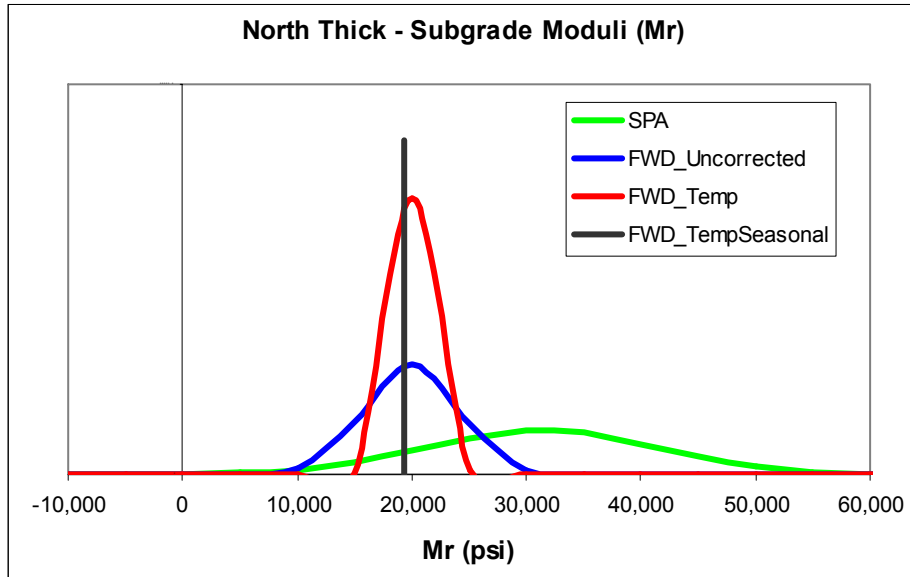


Figure 109: Normal Distributions SPA and FWD – North Thick

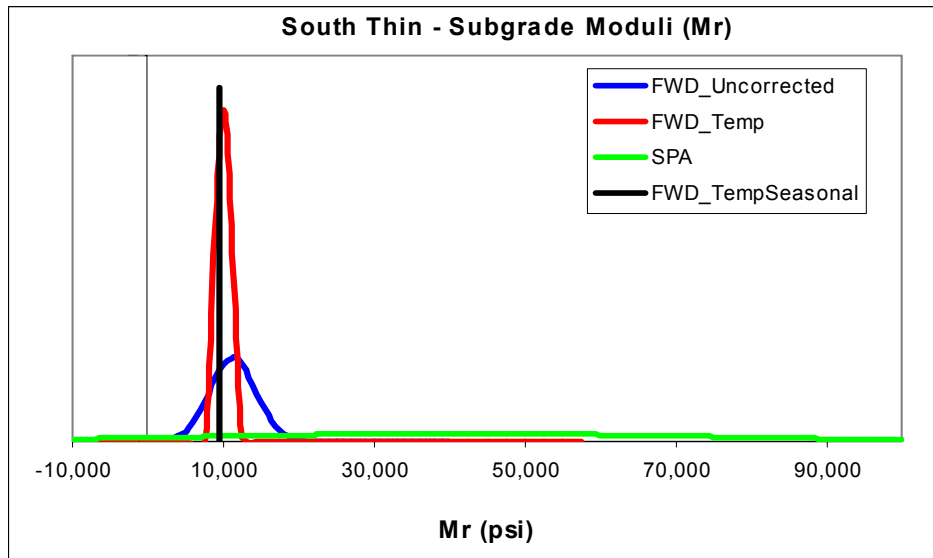


Figure 110: Normal Distributions SPA and FWD – South Thin

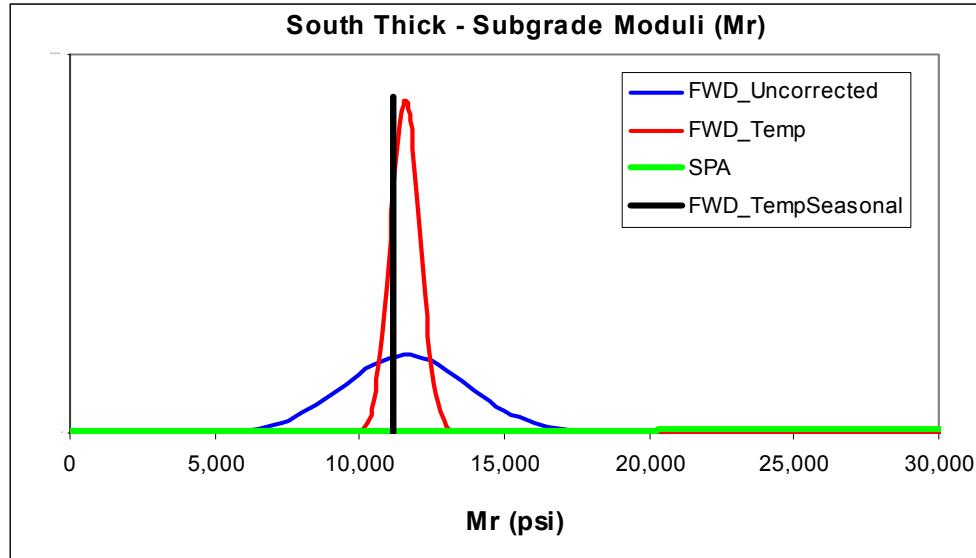


Figure 111: Normal Distributions SPA and FWD – South Thick

SASW Results of FWD and SPA AC Modulus (E_{AC})

To compare the AC modulus of flexible pavements for the FWD and SPA methods, it was necessary to compare the AC Modulus (E_{AC}) with the average AC modulus from the SASW testing method. Presented in Table 35 are the average AC moduli values for each test section for the 2-year testing period.

Table 35: Average FWD and SPA Subgrade Moduli

Test Section	FWD	SPA
	E_{AC} (psi)	SASW AC Avg (psi)
S1	685269.52	289565.58
S2	899397.51	670877.90
S3	890213.38	424909.70
S4	215241.40	215962.38
SPS-5-1	504969.13	324947.30
SPS-5-2	518002.44	232652.51
SPS-5-3	665916.39	453880.87
SPS-5-4	729058.78	609411.21
SPS-5-5	638858.20	433610.31
SPS-5-6	344713.86	451195.91
SPS-5-7	731916.06	504094.18
SPS-5-8	972752.95	499121.16
SPS-5-9	815818.81	413359.88
SPS-5-10	762115.43	394447.19
SPS-5-11	433312.86	576847.72
SPS-901	588211.69	508235.93
SPS-902	486568.08	394288.10
SPS-903	459586.33	363649.68
SPS-960	389301.50	331687.28
SPS-961	412767.52	317641.94
SPS-963	418775.49	375742.69

The FWD and SPA AC moduli showed a fair correlation, with an R^2 value of 0.423. The test sections were again grouped into two classes based on the pavement thickness (greater or less than 20 in.). The resulting correlations based on the pavement thickness are shown in Figures 113 and 114 for thin and thick pavements, respectively. The correlation between the FWD and SPA parameters improved significantly for thin pavements ($R^2=0.948$), and decreased for thick pavements ($R^2 = 0.0384$).

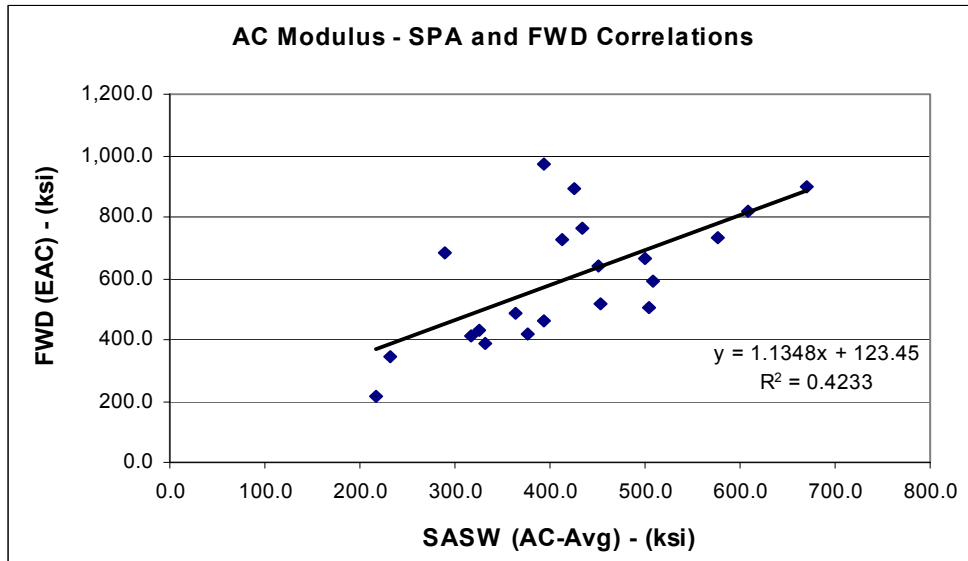


Figure 112: Overall Correlation of AC Modulus

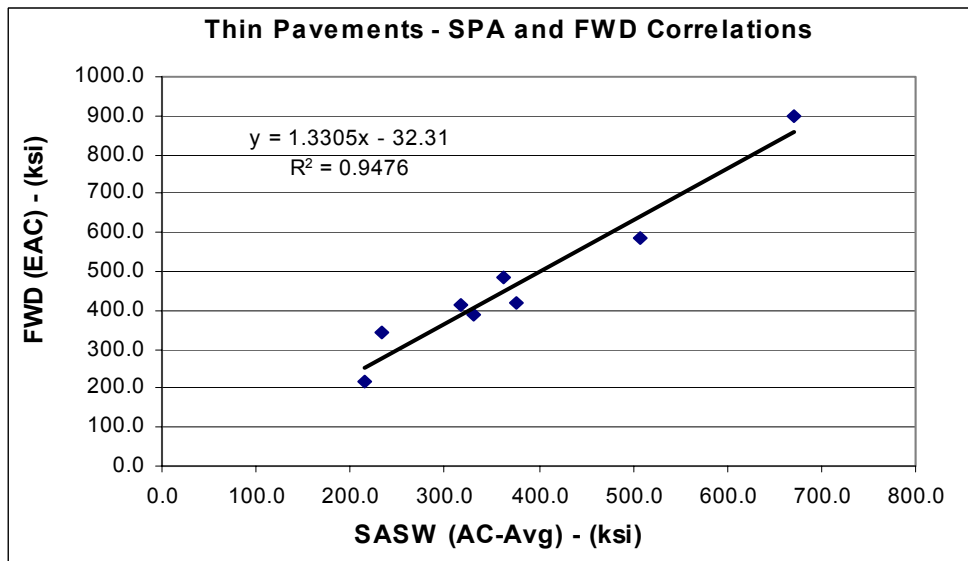


Figure 113: Correlation of AC Modulus – Thin Pavements

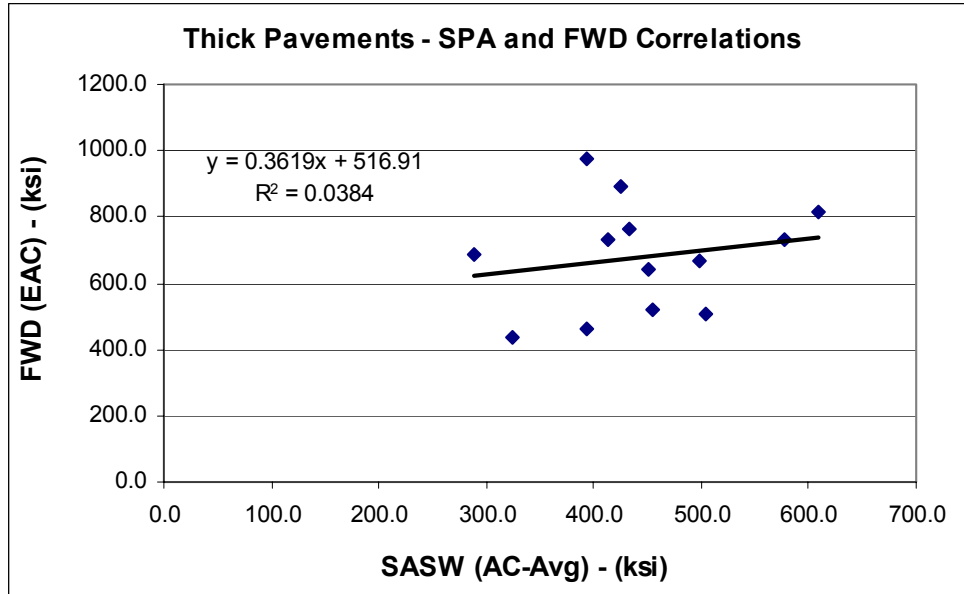


Figure 114: Correlation of AC Modulus – Thick Pavements

SASW Variation in AC Modulus With Time

To investigate the variation in the AC modulus from the SPA SASW analysis and AC Modulus (E_{AC}) for the FWD, it was necessary to plot the normal distributions for the AC moduli over the 2 years of testing. Also, the mean and standard deviations of the AC moduli over the approximate 2 years of testing were evaluated and compared (Table 36).

Table 36: Averages and Standard Deviation of AC Moduli (E_{AC}) for SPA and FWD

Test Type		E_{AC} (psi)
FWD	Avg	606,209
	Std. Dev	356,633
SPA (SASW)	Avg	419,382
	Std. Dev	152,881

For the SPA testing, the average AC modulus for the SASW method was 419,382 psi over a time period of 2 years, with a standard deviation of 152,881 psi. For the FWD testing, the AC modulus (E_p) was 606,209 psi, with a standard deviation of 356,633 psi. The normal distributions for the FWD and SPA AC moduli are presented in Figure 115.

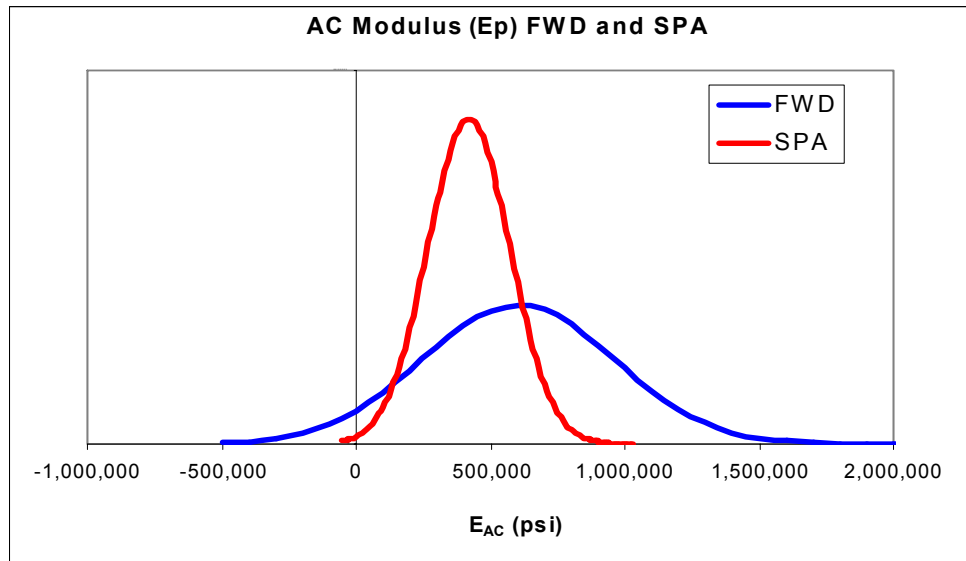


Figure 115: Normal Distributions SPA and FWD Pavement Moduli

Impulse Response (IR) Results

The IR method is generally used to determine the modulus of subgrade reaction (k) of rigid pavement foundation.⁽⁴⁸⁾ The IR method is also defined as an index test that provides the overall modulus or stiffness of a pavement structure for flexible pavements. This section covers the correlation of the IR composite modulus of SPA with the FWD subgrade modulus (k_{static}) for the rigid pavement sections.

To compare the subgrade modulus of rigid pavements for the FWD and SPA, the subgrade modulus (in psi) from the IR method has to be converted to a k (in pci) value. The approximation for a slab placed directly on a subgrade in the 1993 AASHTO design guide was used to estimate the resulting modulus of subgrade reaction k_{IR} from the SPA subgrade modulus.

Presented in Table 37 are the average subgrade moduli values for each test section for the 2-year testing period. It is observed that the magnitudes of the SPA (IR) subgrade moduli were consistently higher than the corresponding FWD subgrade moduli for each test section.

Table 37: Average Subgrade Moduli in ksi for Rigid Sections

Test Section	FWD k_{FWD} (pci)	SPA IR Subgrade Modulus (psi)	SPA IR ¹ K_{IR} (pci)
S5	104	15,000	773.2
S6	121	17,000	876.3

Since only two rigid pavements sections were included in the study, the monthly averages over the 2 years of testing were used to compare the FWD and SPA test results. The average monthly k_{FWD} and k_{IR} over the 2-year testing period are presented in Table 38.

Table 38: Monthly Averages for Modulus of Subgrade Reaction

RoutelD	Month	Year	FWD k_{FWD} (pci)	SPA - IR (Sub) (psi)	SPA - IR (k_{IR}) ¹
S5	2	2002	116.2	15,600	803.6
S5	2	2002	116.2	24,100	1241.2
S5	4	2002	87.2	17,300	893.3
S5	5	2002	101.6	15,200	785.1
S5	6	2002	103.6	10,700	550.5
S5	8	2002	129.4	10,000	513.4
S5	9	2002	112.5	13,900	716.0
S5	9	2002	112.5	18,300	941.8
S5	12	2002	102.9	19,300	994.3
S5	3	2003	93.1	10,900	560.8
S5	4	2003	86.1	10,100	518.6
S5	9	2003	141.0	14,300	737.6
S5	2	2004	73.4	17,800	917.0
S6	1	2002	78.7	23,300	1200.0
S6	2	2002	81.9	11,000	568.0
S6	4	2002	92.9	9,500	489.7
S6	4	2002	92.9	14,500	749.5
S6	5	2002	88.1	27,000	1390.7
S6	7	2002	65.6	9,700	501.0
S6	7	2002	65.6	31,600	1627.8
S6	9	2002	83.8	8,400	432.0
S6	2	2003	102.2	23,600	1214.9
S6	3	2003	79.7	8,600	444.8
S6	3	2003	79.7	9,700	501.0
S6	5	2003	74.1	15,500	800.0
S6	5	2003	74.1	25,100	1293.3
S6	9	2003	60.6	10,700	549.5
S6	12	2003	66.3	13,200	680.4
S6	2	2004	60.6	14,300	736.6
S6	3	2004	44.1	9,200	474.7
S6	3	2004	44.1	17,200	884.0

¹Converted to equivalent k using AASHTO approximation

As shown in Figure 116, FWD and SPA subgrade moduli for the rigid pavement sections showed a poor correlation or no correlation, with an R^2 value of 0.001.

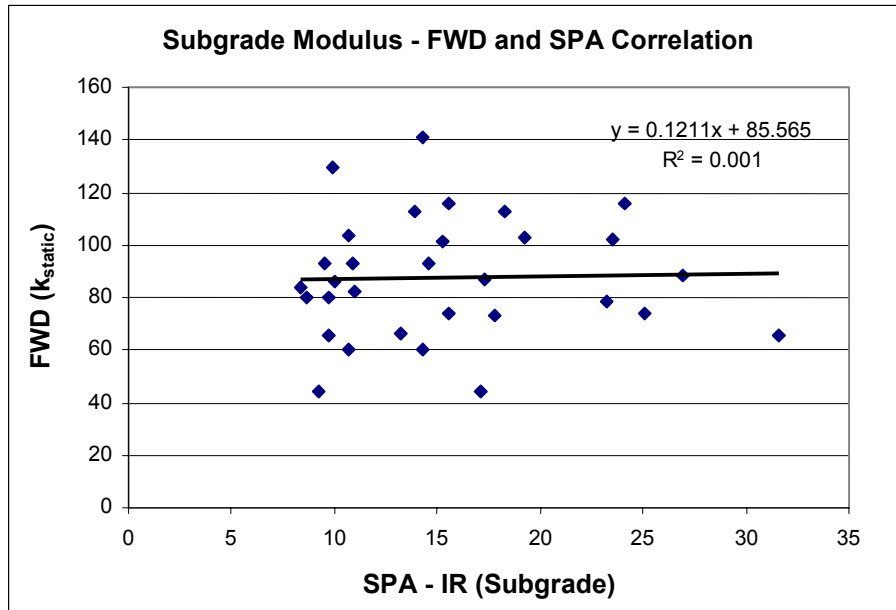


Figure 116: Correlation of Subgrade Modulus for Rigid Pavements

IR Results of FWD and SPA Pavement Modulus (E_p)

For the flexible test sections, the backcalculated FWD pavement moduli were compared with the IR composite moduli. Average pavement moduli values for each test section for the 2-year testing period are presented in Table 39. The pavement moduli represent average or “overall” pavement moduli for the two years of testing. It is observed that the magnitudes of the FWD pavement moduli were significantly higher than the SPA composite moduli for each test section.

Table 39: Average FWD and SPA Pavement Moduli

Test Section	FWD - E_p (ksi)	SPA - IR (Composite Modulus, ksi)
S1	135.2	7.3
S2	92.2	4.7
S3	220.8	8.0
S4	87.0	5.8
SPS-5-1	117.2	10.2
SPS-5-2	101.5	11.0
SPS-5-3	232.2	16.2
SPS-5-4	314.1	20.2
SPS-5-5	208.4	15.9
SPS-5-6	248.5	16.1
SPS-5-7	248.4	18.5
SPS-5-8	297.0	21.1
SPS-5-9	215.3	16.3
SPS-5-10	225.1	14.9
SPS-5-11	234.2	14.3
SPS-901	225.9	16.5
SPS-902	159.4	16.0

Test Section	FWD - E _p (ksi)	SPA - IR (Composite Modulus, ksi)
SPS-903	188.8	15.9
SPS-960	160.6	12.7
SPS-961	174.6	12.9
SPS-963	159.9	12.7

The FWD and SPA pavement moduli showed a good correlation, with an R² value of 0.698 (Figure 117). The test sections were grouped into two classes based on the pavement thickness (greater or less than 20 in.).

The results for both pavement classes are shown in Figures 118 and 119. The R² increased for thin pavements (0.842) and decreased R² for thick pavements (0.568).

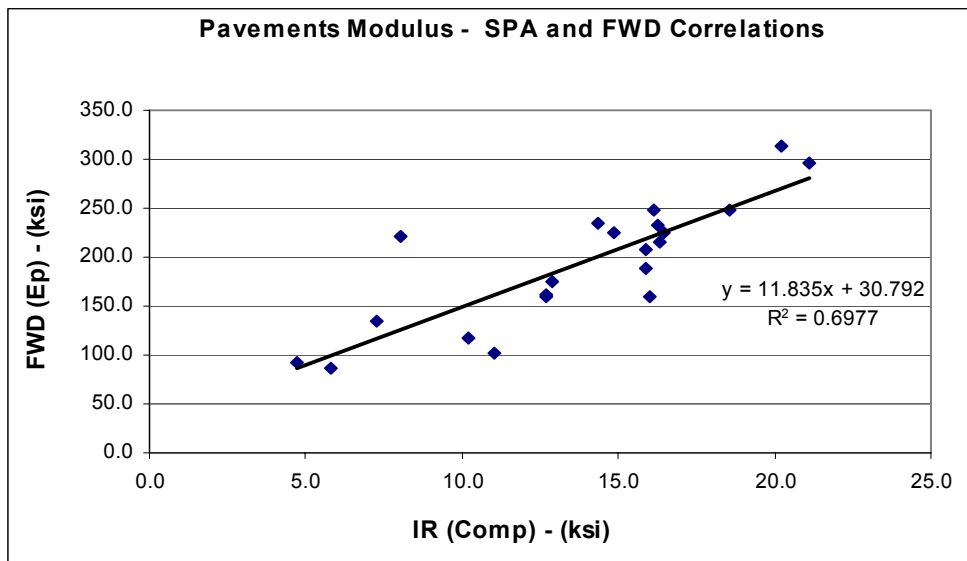


Figure 117: Correlation of Pavement Modulus and Composite Modulus

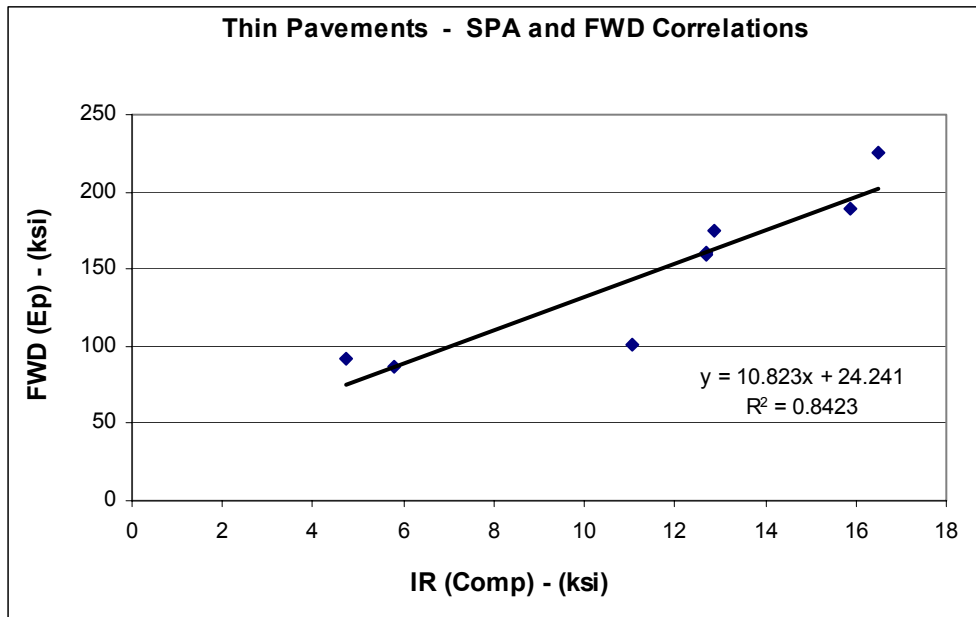


Figure 118: Correlation of Pavement Modulus and Composite Modulus – Thin Pavements

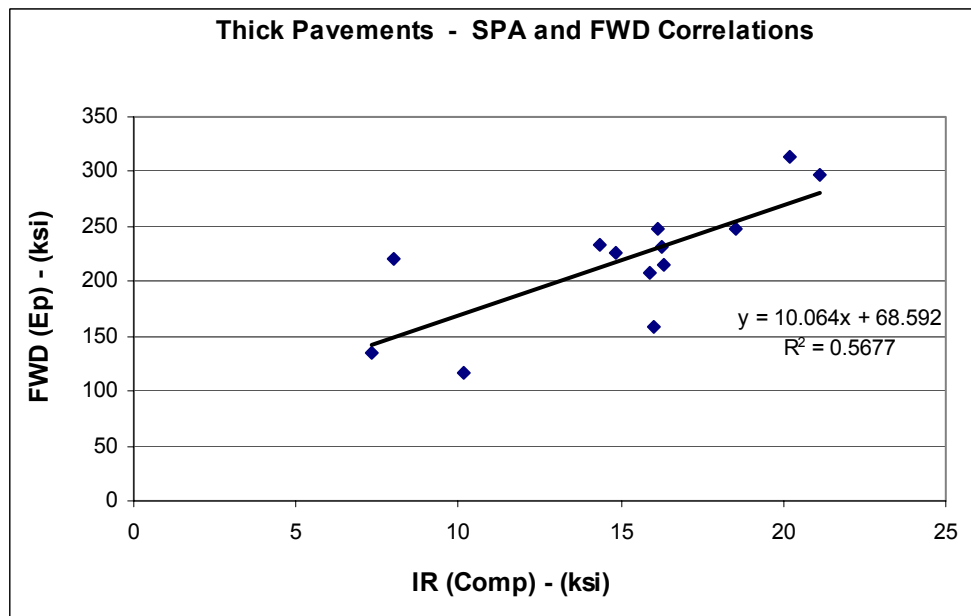


Figure 119: Correlation of Pavement Modulus and Composite Modulus – Thick Pavements

Ultrasonic Surface Waves (USW) results

The USW method is related to the SASW method, and is used to measure directly the average modulus of the top layer of a pavement.⁽⁵⁴⁾ It can also be used to measure the PCC strength for rigid pavements. This section contains results for the two rigid pavement sections.

USW Results of FWD and SPA PCC Modulus for Rigid Pavements

To compare the PCC modulus of rigid pavements for the FWD and SPA methods, it was necessary to compare the backcalculated FWD E_{pcc} value with Young's Modulus from the USW test.

Average PCC strength values for each test section for the 2-year testing period are presented in Table 40. It is observed that the magnitudes of the SPA (USW) moduli were consistently higher than the corresponding FWD PCC moduli for each test section.

Table 40: Average Subgrade Moduli for Rigid Sections

Test Section	FWD E_{pcc} (ksi)	SPA E_{pcc} (ksi)
S5	3,726	5,586
S6	3,107	6,158

Since only two rigid pavement sections existed in the study, the monthly averages over the 2 years of testing were used to compare the FWD and SPA testing methods. The average monthly FWD E_{pcc} and Young's Modulus from the USW testing method over the 2-year testing period are presented in Table 41.

Table 41: Average FWD and SPA PCC Modulus

RouteID	Month	Year	E_{pcc} (ksi)	Youngs (ksi)
S5	2	2002	3,937	6,076
S5	2	2002	3,937	5,497
S5	4	2002	4,213	5,641
S5	5	2002	3,766	5,258
S5	6	2002	3,887	6,150
S5	8	2002	4,434	5,884
S5	9	2002	3,117	5,101
S5	9	2002	3,117	5,228
S5	12	2002	3,522	5,451
S5	3	2003	3,651	5,301
S5	4	2003	3,711	5,867
S5	9	2003	4,343	5,218
S5	2	2004	2,804	5,949
S6	1	2002	3,179	6,311
S6	2	2002	3,382	6,351
S6	4	2002	2,961	6,335
S6	4	2002	2,961	6,410
S6	5	2002	3,086	6,298
S6	7	2002	3,613	6,155
S6	7	2002	3,613	6,266
S6	9	2002	3,033	5,771
S6	2	2003	3,598	6,059
S6	3	2003	3,035	6,132
S6	3	2003	3,035	6,068

RoutelD	Month	Year	E _{pcc} (ksi)	Youngs (ksi)
S6	5	2003	3,046	6,097
S6	5	2003	3,046	6,124
S6	9	2003	3,230	5,820
S6	12	2003	2,842	6,211
S6	2	2004	2,892	6,389
S6	3	2004	2,684	5,875
S6	3	2004	2,684	6,175

The FWD and SPA PCC moduli for the rigid pavement sections showed a poor correlation, with an R² value of 0.1486.

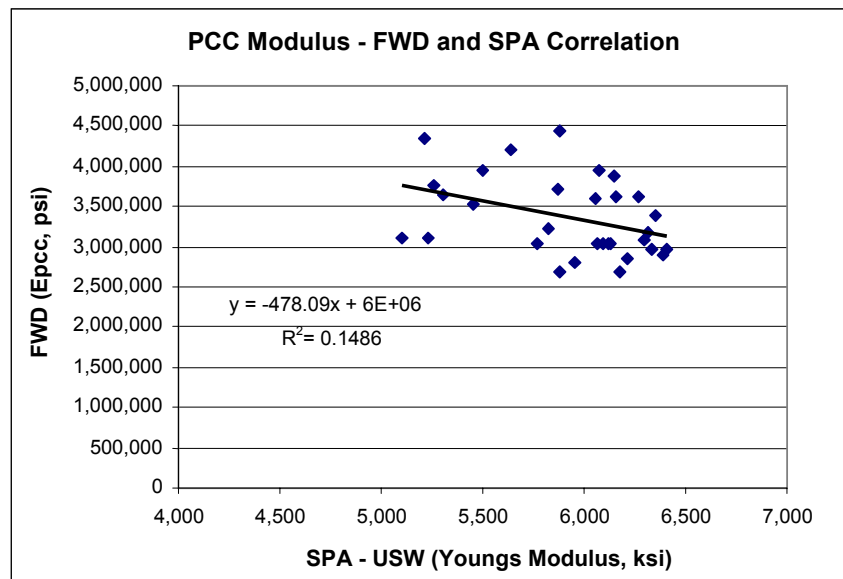


Figure 120: Correlation of PCC Modulus – Thick Pavements

Summary

Pavement moduli values obtained from the FWD and SPA testing were compared. Since the two devices do not utilize the same principles of operation and in some cases do not measure the same set of properties, it was necessary for the comparison to be sometimes made using comparable or adjusted parameters. The SPA AC modulus values used in the correlation analysis were initially corrected by dividing them by a factor of 3.0 to account for the difference in operational frequency ranges of the SPA and FWD tests. In general, correlations between pavement parameters obtained from the two devices ranged from weak to strong. Poor correlations were obtained for: 1) resilient modulus of the subgrade from FWD and SASW, and from FWD and IR for rigid pavements, 2) AC modulus for thick pavements from FWD and SASW, and 3) PCC modulus from FWD and PCC. Good correlations were established for: 1) AC modulus for thin pavements, and 2) Composite modulus for flexible pavements from IR and equivalent pavement modulus from FWD, especially for thin pavements. The rest of the correlations were moderately strong: 1) Equivalent pavement modulus from SASW and FWD, 2) AC modulus in general, and 3) Composite modulus for thick flexible pavements from IR and equivalent pavement modulus from FWD. The uncorrected FWD pavement moduli showed a greater variability due to seasonal changes than those from SPA. It is uncertain whether this is the case, or simply a result of reduced SPA testing during the cold winter periods, because of which higher moduli values were not captured.

ENVIRONMENTAL ANALYSIS

The environmental data collected from the instrumented sections were reviewed and analyzed to produce general trends for New Jersey (e.g. frost/thaw penetration depth with time for different climatic regions in New Jersey, fluctuation in the moisture content with time for unbound layers, etc.). Since the pavement instrumentation has been permanently installed, the environmental data can still be continuously collected after the completion of this project.

One component of this research study was to observe the relationship between surface and subsurface environmental parameters. Some examples of the surface parameters that were measured as a part of the study are rainfall, air temperature, and pavement surface temperature. Examples of subsurface parameters are moisture content (base, subbase, and subgrade), and pavement and mid-depth asphalt temperatures.

Rainfall and Moisture Content

Rainfall has a profound effect on pavement strength and performance. For flexible pavements, the in-place moisture content is influenced by the amount of rainfall. Long periods of low intensity rainfall can be more severe than concentrated periods of high intensity rainfall since the amount of moisture absorbed by the soil is greatest under the former conditions.⁽⁴⁹⁾

To observe the effect of rainfall on the moisture content of a pavement structure, the base, subbase, and subgrade moisture contents of the pavement were plotted against the amount of rainfall at 2, 4, 6, and 8 hours after the start of the rain event.

Rainfall and Base Moisture Content

For the base moisture content, it was observed that as the amount of rainfall increased, the base moisture content also increased, as noted in Figure 121. Furthermore, as the time increased from the initial start of the rain event (e.g. 2, 4, 6 hours), the slope of the line also increased, as shown in Figure 122. Beyond 6 hours after the initial rainfall, there was a reversal in trend with a decrease in slope with time (see Figure 123).

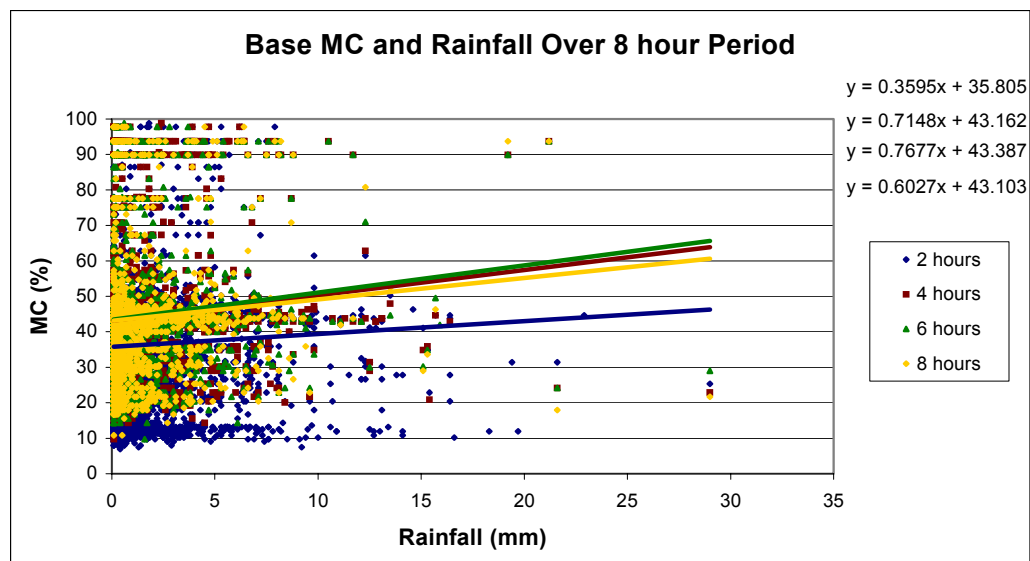


Figure 121: Base Moisture Content (M/C) and Rainfall Over an 8-hour Period

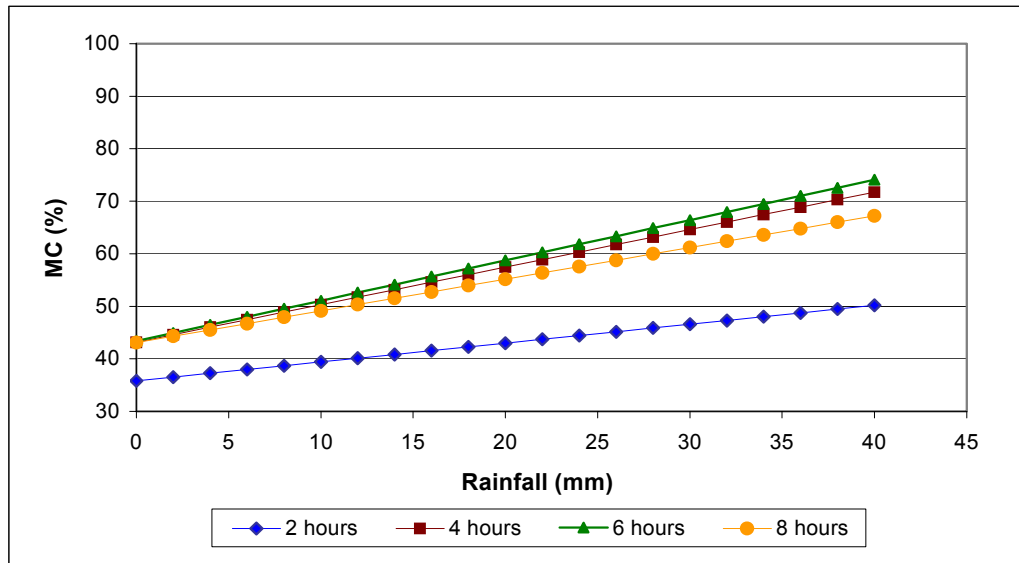


Figure 122: Slope of the Base M/C and Rainfall Trends Over an 8-hour Period

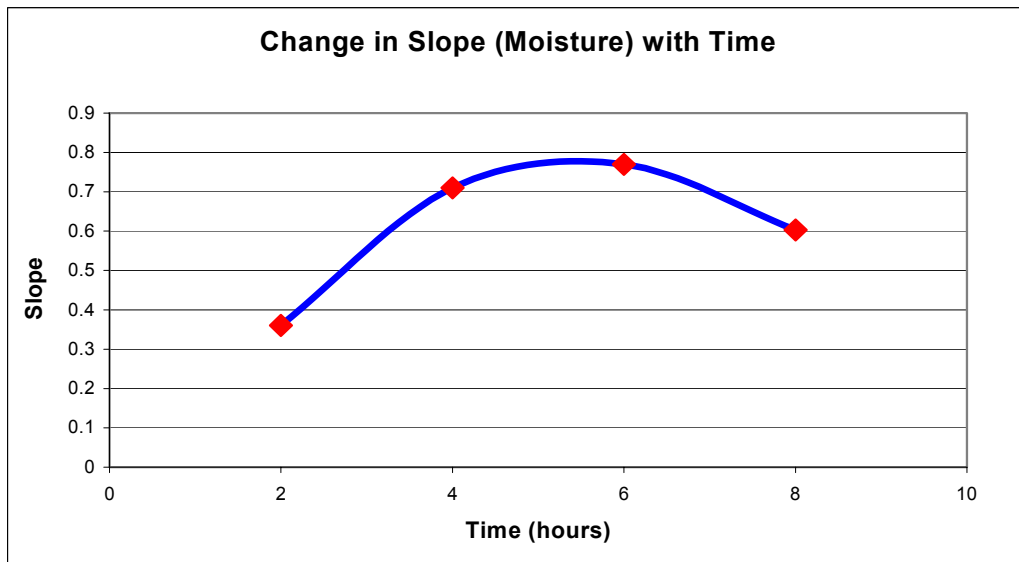


Figure 123: Change in Slope with Time Over an 8-hour Period

Rainfall and Subbase Moisture Content

For the subbase moisture content, it was observed that as the amount of rainfall increased, the subbase moisture content also increased. Furthermore, as the time increased from the initial start of the rain event (e.g. 2, 4, 6 hours), the slope of the line increased until 6 hours, after which the trend was reversed, and the slope started to decrease (Figure 124).

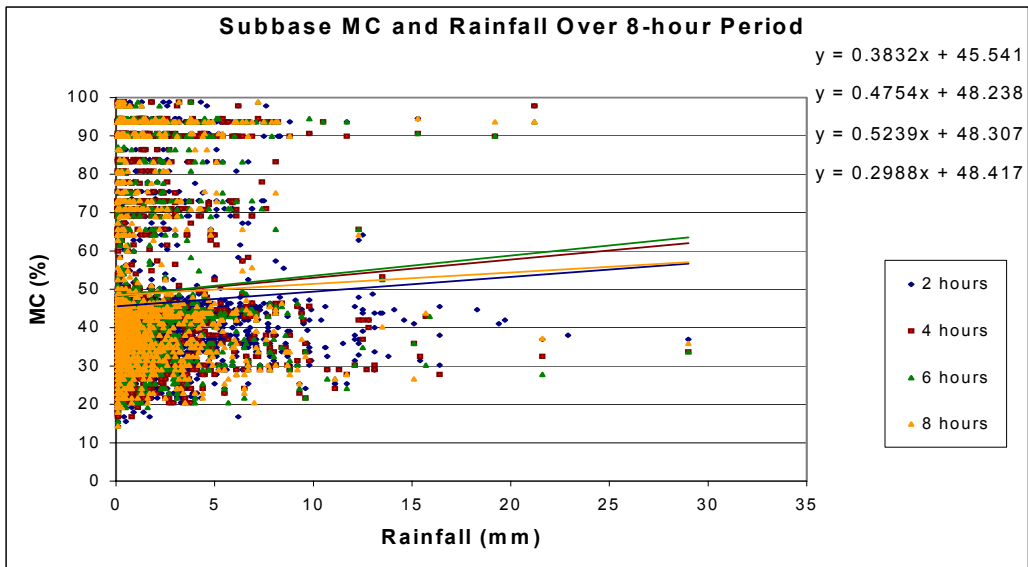


Figure 124: Subbase Moisture Content and Rainfall Over an 8-hour Period

The magnitude of the slopes for the subbase-rainfall curves was observed to be generally lower than those for the base-rainfall curves (Figures 125 and 126).

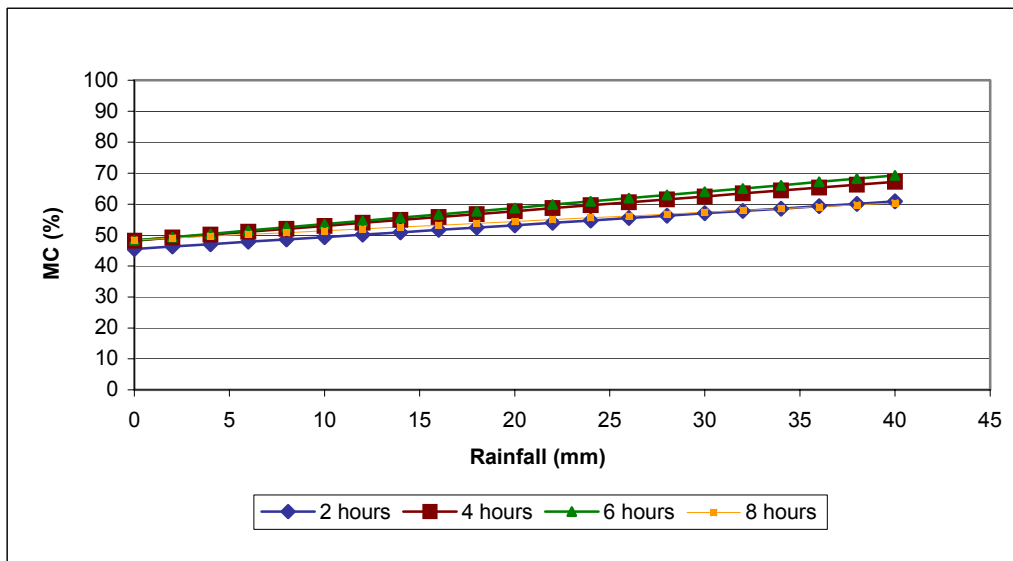


Figure 125: Slope of the Subbase M/C and Rainfall Trends Over an 8-hour Period

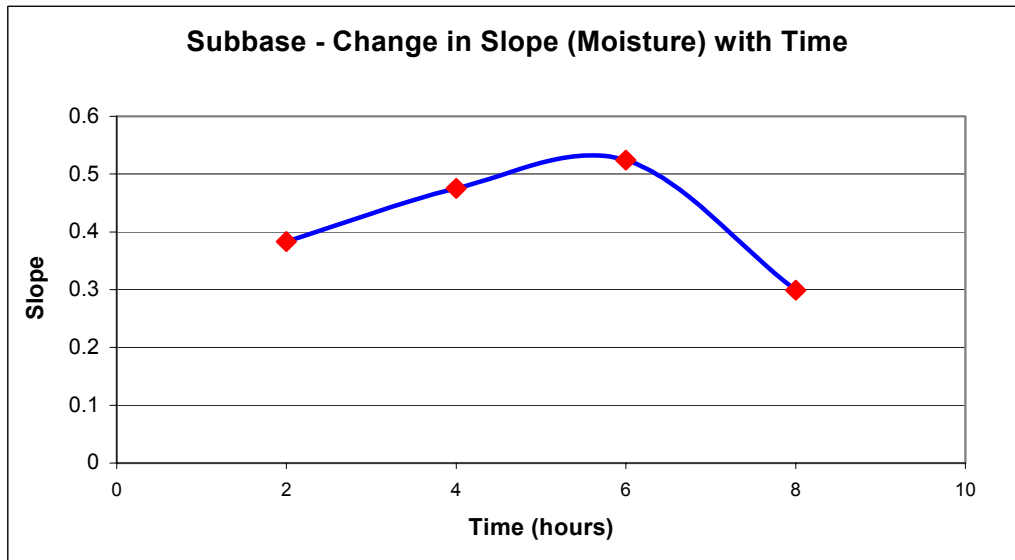


Figure 126: Change in Slope with Time Over an 8-hour Period

Rainfall and Subgrade Moisture Content

During a rainfall event lasting 2 to 4 hours, the subgrade moisture content increased with an increase in rainfall. Beyond 4 hours after the rain event, the subgrade moisture content was observed to decrease with increasing rainfall. However the slope was observed to be quite flat.

As the time increased from the initial start of the rain event (e.g. 2, 4, hours), the slope of the line increased until 6 hours, where the trend reversed and started to decrease (Figure 127). The magnitudes of the slopes for the subgrade-rainfall curves were observed to be generally lower than those for the base and subbase moisture-rainfall curves (Figures 128 and 129).

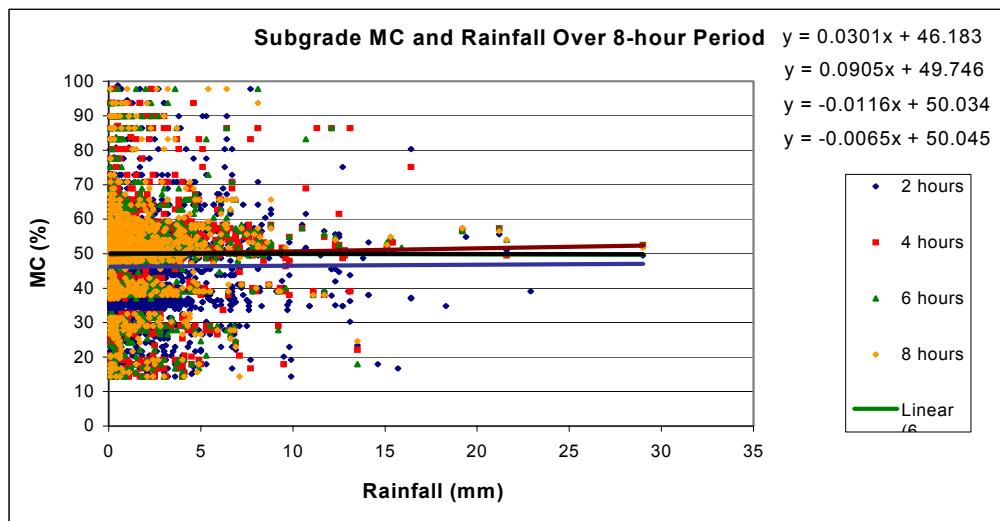


Figure 127: Subgrade Moisture Content and Rainfall Over an 8-hour Period

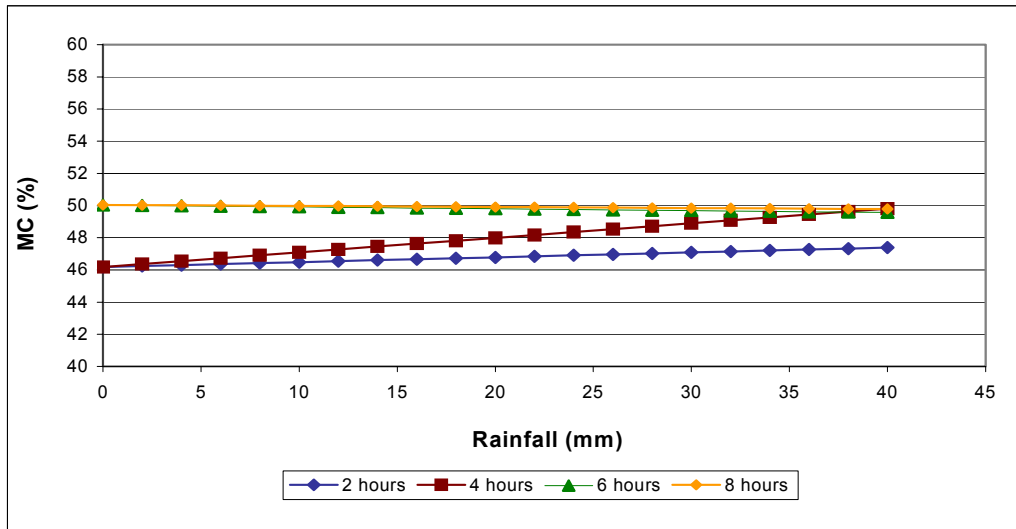


Figure 128: Slope of the Subgrade M/C and Rainfall Trends Over an 8-hour Period

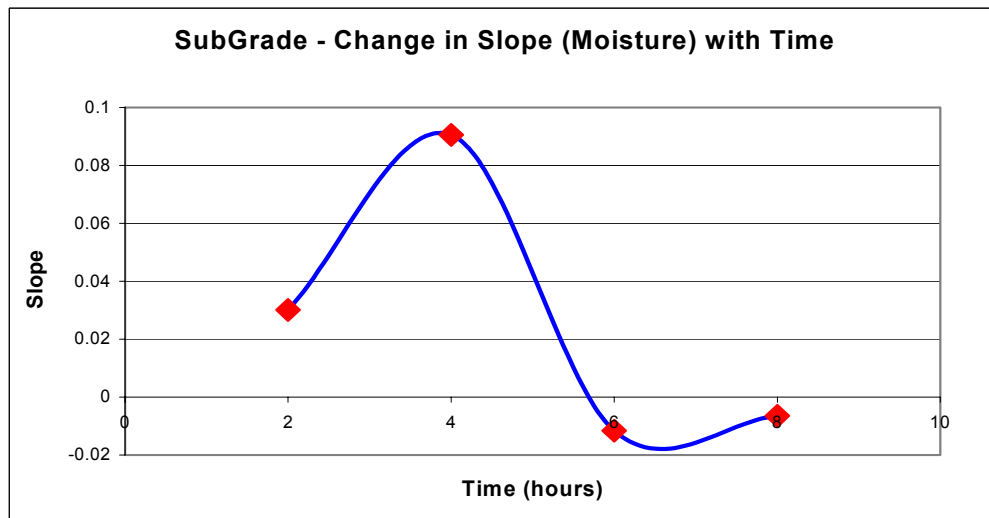


Figure 129: Change in Slope with Time Over an 8-hour Period

Air Temperature and Pavement Temperature (Surface and Mid Depth)

The models for air and pavement temperature were developed using data from the 21 test sites forming part of this study. In each pavement section, 11 sensors were placed to collect a temperature profile of the pavement. The mid-depth temperature was calculated as the average of the first three sensors located typically in the surface layer. The pavement surface temperature was defined as the first (top) sensor located closest to the surface (Figure 130).

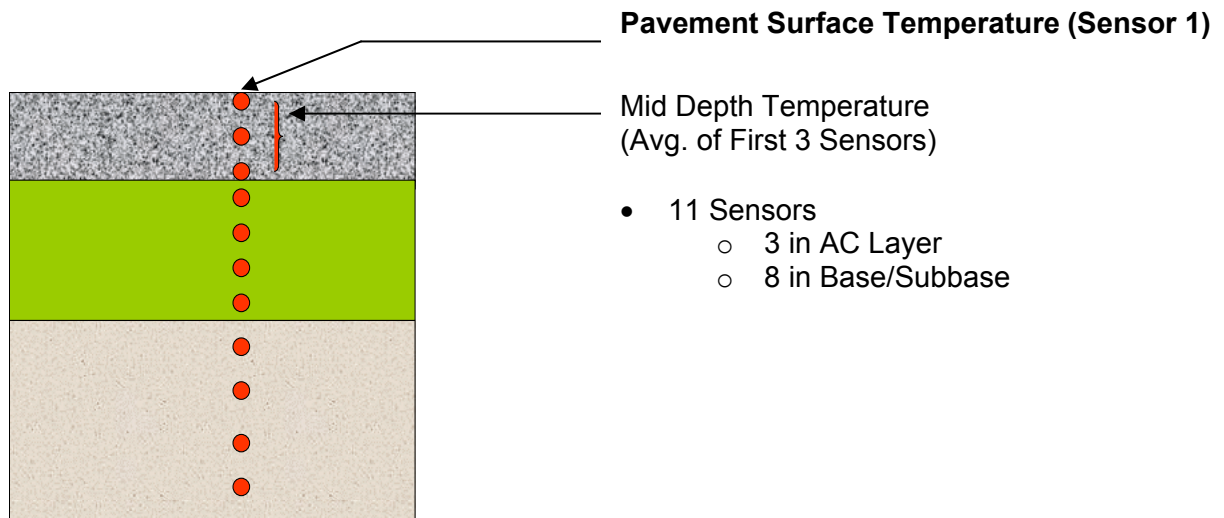


Figure 130: Sensor Locations in Pavement Structure

The seasonal test sites were characterized as being thin or thick pavement sections (AC). A thin pavement section was defined as a section having an AC layer of less than 10 in. A thick pavement section was defined as a site having an AC layer greater than or equal to 10 in. Models were developed for thin and thick pavement sections, and for the temperature at different times of the day. Air temperature readings were recorded at 1-hour intervals throughout the day, while pavement temperature readings were recorded at 4-hour intervals.

For all pavement sections (thin and thick), and irrespective of the time of day, the model resulted in a relatively high R^2 value. Despite the high R^2 value, some spread/dispersion around the regression line was evident. As a result of the spread/dispersion, models were developed for different times of the day. Models based on the time of day were developed using the following three time ranges:

- 2:00 am to 10:00 am
- 10:00 am to 6:00 pm
- 6:00 pm to 2:00 am

Multiple Regression models were developed that relate the mid-depth pavement temperature to the air temperature and the AC thickness, as well as pavement surface temperature to the air temperature and the AC thickness. These models were found to be statistically significant at the 95 percent Confidence Interval, and all had relatively high R^2 values.

Air Temperature and Pavement Temperature Models

The developed models for air and pavement temperatures for thin and thick pavements at different times of the day are presented within this subsection. All models were found to have a good correlation, with R^2 values greater than 0.83. Multiple regression models are also presented which relate the mid-depth and pavement surface temperatures to two independent variables, namely, AC thickness and air temperature.

Thin Pavements Sections (AC < 10")

(1) Air & Mid-Depth Pavement Temperature (Average of Sensor 1, 2, 3)

- For Time 2:00 am to 10:00 am
Mid_Temp = 1.0858 * Air_Temp + 4.0976, R² = 0.8962
- For Time 10:00 am to 6:00 pm
Mid_Temp = 1.1813 * Air_Temp + 2.0277, R² = 0.8562
- For Time 6:00 pm to 2:00 am
Mid_Temp = 1.2751 * Air_Temp + 4.9777, R² = 0.8883

(2) Air & Pavement Surface Temperature (Sensor 1)

- For Time 2:00 am to 10:00 am
Pave_Temp = 1.0854 * Air_Temp + 3.2344, R² = .9195
- For Time 10:00 am to 6:00 pm
Pave_Temp = 1.2659 * Air_Temp + 2.934, R² = 0.8364
- For Time 6:00 pm to 2:00 am
Pave_Temp = 1.3218 * Air_Temp + 4.4324, R² = 0.8871

Thick Pavement Sections (AC > 10")

(3) Air & Mid-Depth Pavement Temperature (Average of Sensor 1, 2, 3)

- For Time 2:00 am to 10:00 am
Mid_Temp = 1.0541 * Air_Temp + 5.0656, R² = 0.8546
- For Time 10:00 am to 6:00 pm
Mid_Temp = 1.0489 * Air_Temp + 1.7568, R² = 0.86
- For Time 6:00 pm to 2:00 am
Mid_Temp = 1.1558 * Air_Temp + 5.1889, R² = 0.8609

(4) Air and Pavement Surface Temperature (Sensor 1)

- For Time 2:00 am to 10:00 am
Pave_Temp = 1.0489 * Air_Temp + 3.0536 R² = 0.8947
- For Time 10:00 am to 6:00 pm
Pave_Temp = 1.1881 * Air_Temp + 1.6057, R² = 0.8453
- For Time 6:00 pm to 2:00 am
Pave_Temp = 1.3218 * Air_Temp + 4.4324, R² = 0.8871

Multiple Regression Models

5) Air and Pavement Temperature and AC Thickness for all Data

- Model 1: Mid Depth Temperature: Average of Sensors 1, 2, & 3
Mid_Temp = 1.084 * Air_Temp – 0.197 * AC_Thick + 6.084 R² = 0.842
- Model 2: Pavement Surface Temperature: Sensor 1
Pave_Temp = 1.181 * Air_Temp – 0.268 * AC_Thick + 5.655 R² = 0.864

(6) Air and Mid-Depth Temperature and AC Thickness (Avg. of Sensor 1, 2, & 3)

- For Time 2:00 am to 10:00 am
Mid_Temp = 1.065 * Air_Temp – 0.168 * AC_Thick + 3.203 R² = 0.868
- For Time 10:00 am to 6:00 pm
Mid_Temp = 1.09 * Air_Temp – 0.537 * AC_Thick + 6.782 R² = 0.860
- For Time 6:00 pm to 2:00 am
Mid_Temp = 1.19 * Air_Temp – 0.218 * AC_Thick + 7.133 R² = 0.869

(7) Air and Pavement Surface Temperature and AC Thickness (Sensor 1)

- For Time 2:00 am to 10:00 am
Pave_Temp = 1.060 * Air_Temp – 0.0723 * AC_Thick + 3.780 R² = 0.902
- For Time 10:00 am to 6:00 pm
Pave_Temp = 1.212 * Air_Temp – 0.499 * AC_Thick + 6.617 R² = 0.845
- For Time 6:00 pm to 2:00 am
Pave_Temp = 1.263 * Air_Temp – 0.243 * AC_Thick + 6.353 R² = 0.879

Mid-Depth and Pavement Temperature Relationships

The models for the mid-depth and pavement surface temperatures were developed using data from 21 New Jersey Seasonal test sites. In each pavement section, 11 sensors were placed to collect a temperature profile of the pavement. The mid-depth temperature was calculated as the average of the first three sensors located typically in the surface (AC) layer. The pavement surface temperature was defined as the first sensor located closest to the surface.

From the 21 sites, 3 sites were characterized as having thin pavement sections, and 18 sites were classified as thick sections. A thin pavement section was defined as a section having an AC layer of less than 10 in. A thick pavement section was defined as a section having an AC layer greater than or equal to 10 in. Models were developed for thin and thick pavement sections, and for the temperature at different times of the day. Pavement temperature readings were recorded at 4-hour intervals.

For all pavement sections (thin and thick), and irrespective of the time of day, the models resulted in high R² values (R² > 0.93). Despite the high R², some spread/dispersion around the regression lines were evident, as well as some fanning.

Thin Pavements Sections (AC < 10")

- For Time 2:00 am to 10:00 am
Mid_Temp = 1.0131 * Surf_Temp + 0.7479, R² = 0.994
- For Time 10:00 am to 6:00 pm
Mid_Temp = 0.9167 * Surf_Temp – 0.159, R² = 0.9897
- For Time 6:00 pm to 2:00 am
Mid_Temp = 0.9624 * Surf_Temp + 0.6978, R² = 0.9913

Thick Pavements Sections (AC > 10")

- For Time 2:00 am to 10:00 am
Mid_Temp = 1.0018 * Surf_Temp + 2.0287, R2 = 0.9825
- For Time 10:00 am to 6:00 pm
Mid_Temp = 0.8427 * Surf_Temp + 0.5527, R2 = 0.9571
- For Time 6:00 pm to 2:00 am
Mid_Temp = 0.9169 * Surf_Temp + 1.2683, R2 = 0.9763

All Pavement Sections (Thin and Thick)

- For Time 2:00 am to 10:00 am
Mid_Temp = 1.0023 * Surf_Temp + 1.7809 R2 = 0.9832
- For Time 10:00 am to 6:00 pm
Mid_Temp = 0.8168 * Surf_Temp + 0.3528, R2 = 0.9639
- For Time 6:00 pm to 2:00 am
Mid_Temp = 0.9261 * Surf_Temp + 1.1496, R2 = 0.9791

Multiple Regression Models

(1) Mid-Depth Temperature & Pavement Surface Temperature & AC Thickness

- For All Times of The Day
Mid_Temp = 0.893794 * Surf_Temp - 0.0534 * AC_THICK + 2.089, R2 = 0.980

(2) Mid-Depth Temperature & Pavement Surface Temperature & AC Thickness for Different Times of the day.

- For Time 2:00 am to 10:00 am
Mid_Temp = 1.0034 * Surf_Temp + 0.14633 * AC_THICK + 0.2588, R2 = 0.985
- For Time 10:00 am to 6:00 pm
Mid_Temp = 0.8600 * Surf_Temp - 0.21204 * AC_THICK + 2.5758, R2 = 0.9665
- For Time 6:00 pm to 2:00 am
Mid_Temp = 0.9255 * Surf_Temp - 0.08834 * AC_THICK + 2.102, R2 = 0.979

Frost Damage

In seasonal frost areas, pavements experience freeze-thaw cycles that expose the pavement structure to significant moisture and temperature changes. These changes subject the pavement to environmental fatigue in addition to the permanent fatigue caused by traveling vehicles. The structural damage of pavements during the spring thaw may result in very high maintenance costs and in some cases, lead to posting the road and prohibiting the use of heavy loads during the period. The economic loss to the public resulting from road closures may be significant.⁽⁵⁵⁾

Freeze/thaw cycles have two major effects on pavement: thaw weakening and frost heaving. AASHTO provides guideline procedures for calculating the damage during various seasons of the year as a function of these two factors. The AASHTO guideline shows that the thaw-weakening period can range from a few weeks to a few months, with varying degrees in structural capacity. Even though a well-defined methodology is introduced to calculate the frost

penetration depth using the air-freezing index, AASHTO encourages users of the guide to develop their own relationships based on site-specific measurements within their area and compare such experiences with both AASHTO and other agencies nationally.

Frost/Thaw Depth Measurement

Temperature gradients have traditionally been used to determine depth of frost/thaw penetration into a soil. Since de-icing chemicals can depress the freezing point, the temperature gradient method can be unreliable.

Presently, measuring the electrical resistance and resistivity is the most reliable method of determining depth of frost/thaw penetration. Therefore, electrical resistivity probes permanently installed in the pavement were used to measure frost/thaw depth.

FROST Software

FROST is an interactive program that displays freeze-state data in a graphical form.⁽⁵⁰⁾ In order to determine the maximum depth of frost penetration, it is necessary to input the three electrical resistivity (ER) parameters – resistivity, resistance, and voltage measurements – into the FROST software. The program includes a set of built-in logical statements that will define the freeze state of a soil, given the user-defined threshold line for the three ER measurements.

The FROST software outputs the data into a graphical form or database (.mdb), which can then be further processed or analyzed. Presented in Figure 131 is an example of frost penetration output from the FROST software for New Jersey seasonal site S5I.

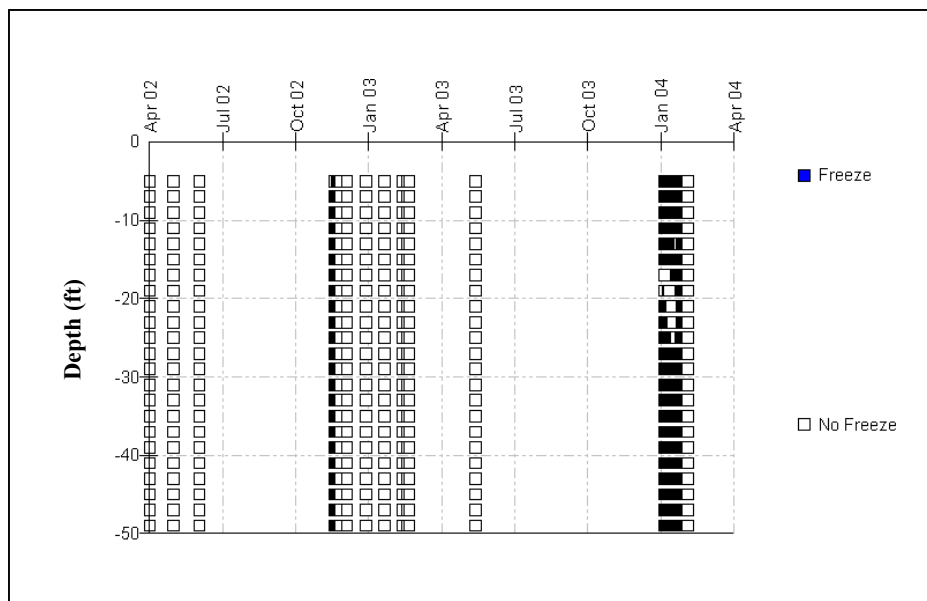


Figure 131: Frost Penetration Graph for New Jersey Seasonal Site S5I

Freezing Index Calculations

Soil freezing depends to a large extent upon the duration of depressed air temperatures. It is popular to measure time and temperature by degree-days. A 'one-degree day' represents one day with a mean air temperature one degree below freezing. Therefore, a '10-degree day'

results when the air temperature is 31°F for 10 days or when the air temperature is 22°F for 1 day.⁽⁴⁹⁾

To determine the freezing index and freeze period at a site, a cumulative plot of degree-days versus time must be produced. The difference between the maximum and minimum points on the cumulative degree-day plot represents the freezing index. The freeze period is the distance (x-axis) from the maximum to the minimum peak. An example of a cumulative degree-day plot is presented in Figure 132. The freezing index has been correlated with depth of frost penetration.

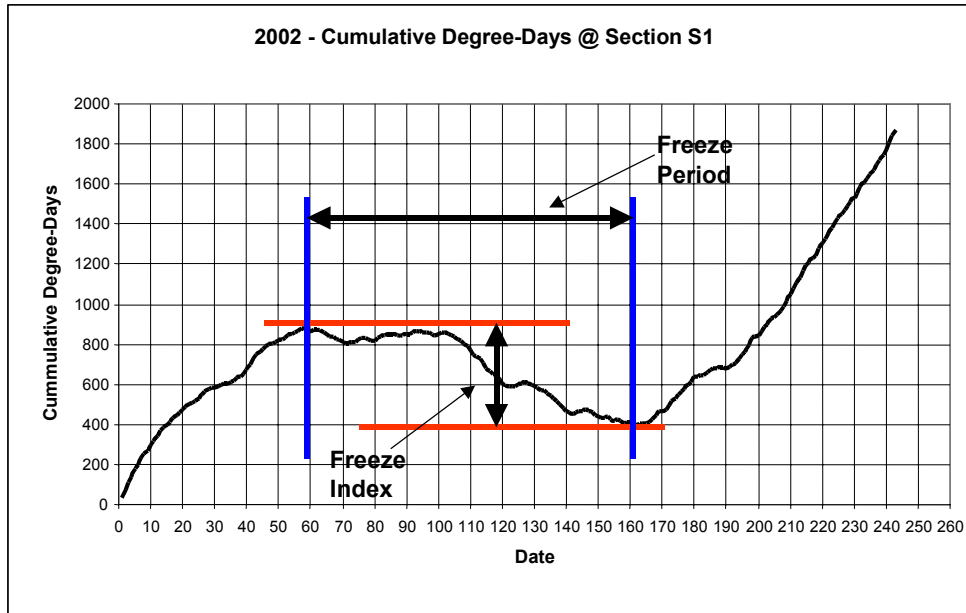


Figure 132: Cumulative Degree-Day Plot for Section S1 in New Jersey

Frost Penetration Depths

The performance of pavements in frost-affected areas is highly dependent on the depth of frost penetration. The maximum depth of frost can be predicted in several ways, including field penetration data with temperature data, and theoretical formulas and charts. The Corps of Engineers has determined an empirical curve that relates depth of frost penetration to the freezing index for a well-drained, non-frost susceptible base course. The freezing index and frost penetration empirical curve developed by the Corps of Engineers is presented in Figure 133.⁽⁵¹⁾

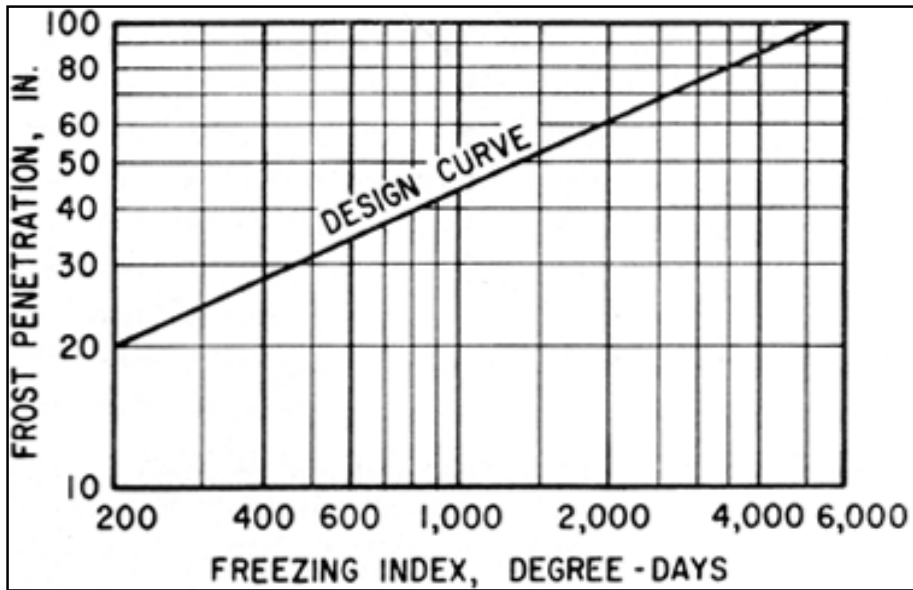


Figure 133: Freezing Index and Frost Penetration Curve ⁽⁵⁷⁾

Since the data for this curve was determined from only a few winters, some deviation of true measured values from the curve is to be expected.⁽⁴⁹⁾ From the cumulative degree-day plots for New Jersey seasonal sites, the depth of frost penetration was correlated with the Corps of Engineers curve and is presented in Table 42. The average freeze index was calculated for 2003 and 2004; and the frost penetration depth was obtained from the Corps of Engineers frost penetration curve shown in Figure 133. The empirical and measured frost depths for 2003 and 2004 are presented and compared in Table 43. The correlation between the empirical and measured frost depths was found to be weak (Figure 134). This could be explained since the empirical curve (Corps of Engineers) does not accurately represent New Jersey's environment or pavement conditions.

Table 42: Frost Penetration Depths Based on Empirical Curve

Site	Freeze Index (Degree Days)	Freeze Period (Days)	Frost Penetration Depth (in)
S1	346.75	69.5	26
S2	227.5	35	22
S3	357.255	49.5	26
S4	264.6605	33.5	23
S5	409.92	72.5	28
S5E	205.9423	38	20
S6	233.75	33.5	23
S7	272.1	27	24
S9C	294.85	38	25

Table 43: Comparison of Empirical and Measured Data for Flexible Sections

Seasonal Site	Freeze Index	Frost Penetration Empirical Curve	Measured Frost Penetration Depths
2003			
S2	266.6	22.5	15
S3	328.51	26	35.5
S4	264.4	23	19
S5A	274.5	23.5	-
S5E	274.5	23.5	14.685
S5I	274.5	23.5	14.016
S9C	299	24.5	22.362
2004			
S2	188.4	19	25
S3	386	28	41.5
S4	264.921	23	21
S5A	137.846	16	15.945
S5E	137.846	16	16.654
S5I	137.846	16	14.016
S5J	137.846	16	16.063
S9C	290.7	24.4	23.3465

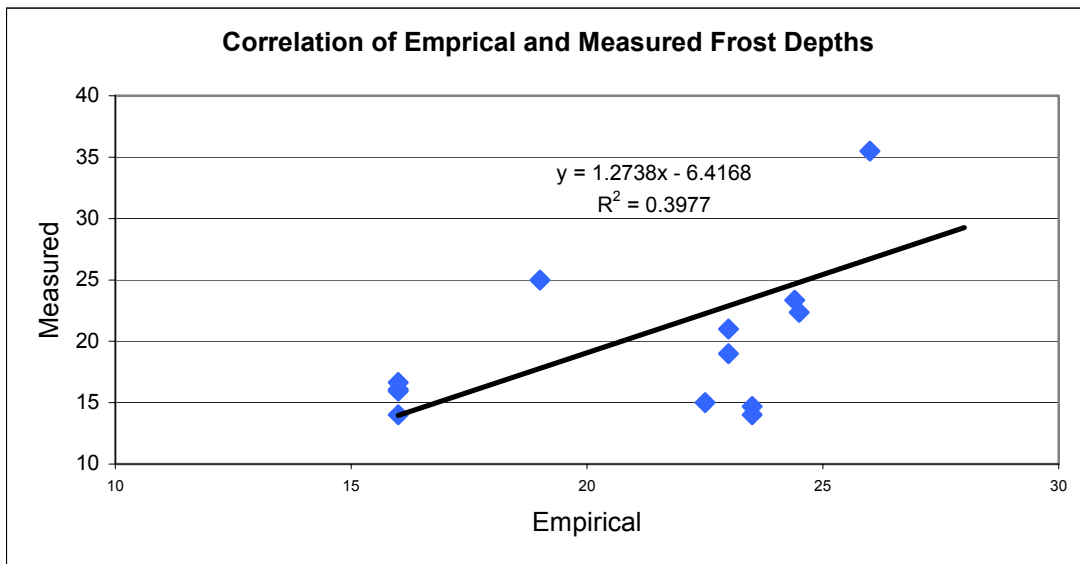


Figure 134: Empirical and Measured Frost Depth Correlation

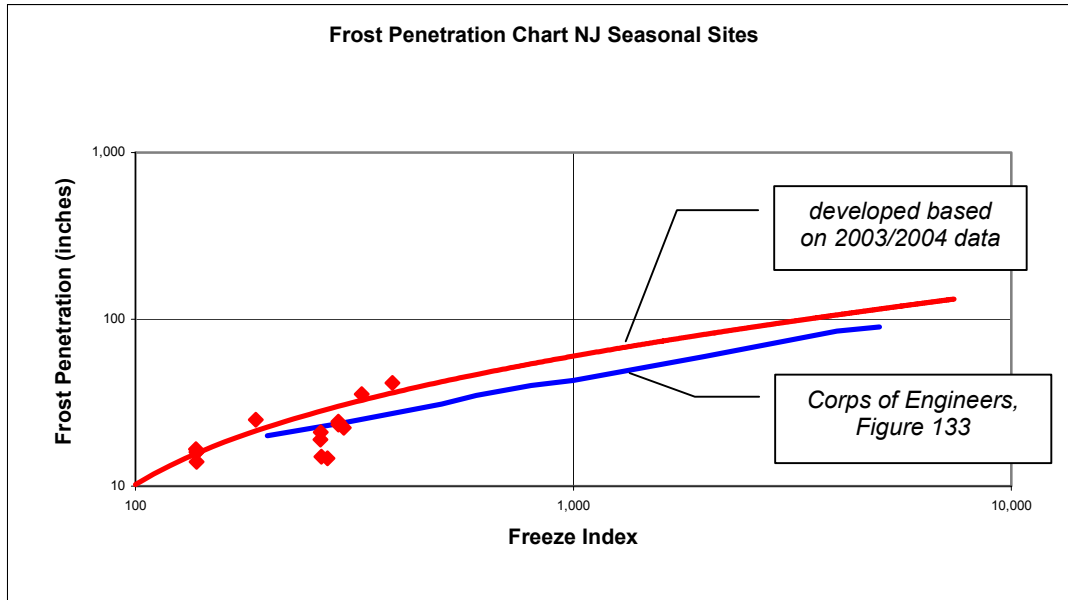


Figure 135: Sigmoidal Model and Empirical Frost Penetration Curves

The empirical frost penetration curve (Corps of Engineers) was plotted against the measured New Jersey frost data. A Sigmoidal model was generated to represent the relationship between the frost penetration depth and the freeze index for New Jersey conditions. This model shows reasonable results for a freeze index between 100 and 1000 (Figure 135).

Summary of Findings

One major component of the New Jersey Seasonal study is to observe the relationship between surface and subsurface environmental parameters. Some examples of the surface parameters that were measured as a part of the study are rainfall, air temperature, and pavement surface temperature.

The effect of rainfall on the base, subbase, and subgrade moisture contents was observed over the course of an 8-hour period after the initial start of a rain event. It was observed that the moisture content would initially increase as the rainwater entered the pavement, and then decrease with time, as rainwater moved through the pavement layers.

Environment data collected from the 21 seasonal test sites were used to develop models relating air, pavement surface, and mid-depth pavement temperatures. Models were developed for thin and thick pavements for different periods of the day. These models can be used for predicting the mid-depth temperatures, and for temperature correction of FWD data.

Frost data was collected from the New Jersey seasonal sites and the FROST software was used to determine the frost penetration depths. The measured frost penetration depths were compared to the empirical frost penetration depths developed by the Corps of Engineers. This relationship between the empirical and measured data showed a fairly weak relationship.

PROJECT CONCLUSIONS AND RECOMMENDATIONS FOR FURTHER STUDIES

This research study funded by the NJDOT and the FHWA investigated the influence and seasonal fluctuation of environmental factors on pavement performance in New Jersey. The objectives of the study were thoroughly addressed through a comprehensive pavement instrumentation program on selected sites representing different environmental zones and pavement types. Data was collected on the various climatic and seasonal factors. The effect of these factors on long-term pavement performance was evaluated by studying the response of pavement structures with different thicknesses and material properties under different environmental conditions. Available seasonal and temperature adjustment models were evaluated. New models were developed specific to New Jersey conditions. Conclusions from this research effort are described herein.

Conclusions

The successful instrumentation of the test sections to monitor climatic data and the subsequent development of a database have given a better understanding of moisture retention within a pavement system and its profound effect on the cost and service life of a highway network.

The trends of the mean air temperature, average pavement temperature, average soil temperature, and total rainfall are very similar to that of the pavement moduli. The backcalculated subgrade and pavement moduli are found to follow the same trend. This trend shows a reduction in the moduli in the spring. However, the reduction in the pavement modulus happens earlier than that of the subgrade modulus.

Temperature and moisture data from the Seasonal Monitoring Program testing at two locations from LTPP test sites were analyzed to evaluate the EICM for its applicability to New Jersey conditions. It was shown that EICM-predicted and field-measured temperature data do not exhibit a strong consistent correlation, especially for the surface layers. For some sites/hours an acceptable correlation was found for the subgrade. However, the correlation varies significantly by site and time. In addition to temperature, the capability of the EICM to predict pavement moisture variation was also evaluated. A wide discrepancy was observed between predicted and measured moisture contents, and no reasonable correlation was found. Therefore, because of the inconsistent model output results, EICM cannot be utilized in its present form to account for seasonal adjustment on pavement sections within New Jersey. As such, adjustments to the EICM model are required.

Analysis Of Variance (ANOVA) performed on the pavement parameters (deflections and backcalculated moduli) and environmental parameters (base course moisture content, average AC, temperature, GWT, rainfall, and air temperature) to investigate the impact of the environmental parameters on pavement response to FWD and SPA loads. In the ANOVA analysis, the pavement parameters D_1 , (D_1-D_7) , D_7 , E_p and M_r were considered individually as the independent parameter, while the environmental parameters (GWT, pavement temperature, air temperature, ...) were considered as to depth parameters. Also, two-way interactions were considered in this analysis. Results of the analysis indicated that all main effects have significant impact on the overall pavement deflection (D_1), difference in pavement deflections (D_1-D_7), and the Effective Pavement Modulus (E_p), which is expected. However, GWT and pavement temperature were found to have no significant impact on the subgrade deflection (D_7). This finding does not agree with the common assumption made in backcalculation analysis that GWT acts as a rigid layer.

Results of the sample implementation of the seasonal adjustment models indicate that there is a significant difference between the Overall Correction Factors and the Seasonal Correction

Factors. Combining the temperature change with the seasonal change, as in case of the Overall Correction Factors, ignores the rapid change in temperature. Therefore, it is recommended that the Temperature Adjustment Model followed by the Seasonal Correction Model be used, instead of the Overall Correction Factors.

A comparison of trends on temperature-corrected historic FWD data for NJ LTPP-SPS sections using the developed NJDOT temperature and seasonal models and the current AASHTO temperature correction model indicated that more realistic trends are obtained when NJDOT models are used.

Pavement service life decreases with an increase in the base course moisture content as a result of poor subsurface drainage. Substantial long-term savings can be achieved by improving the subsurface drainage quality of flexible pavements. These savings can be enhanced by a more rapid lowering of the moisture content through the use of other subsurface drainage elements, such as collector systems, in conjunction with permeable base/subbase layers.

FWD and SPA testing was carried out for a period of one year at two rigid pavement sites having subbase materials with different drainage capabilities and encompassing all climatic seasons. Analyses of the FWD data have indicated that the subbase layer using NSOG material provides better subsurface drainage under rigid pavements and can therefore facilitate flow of moisture out of the pavement system. The results also indicate that at present, there is no effect of moisture content on structural capacity. This conclusion is valid for the investigated New Jersey pavement sections with their present distress conditions. However, poor subsurface drainage through the continued presence of high moisture contents can lead to an early deterioration of the pavement structure. This will lead to lower structural capacities in terms of lower SAI values.

Recommendations for Further Studies

During the course of the research study, the following areas were identified for further research:

- Continued monitoring of the environmental parameters at the present sites with working instruments and equipment. This will help in further refining the developed temperature and seasonal adjustment models through additional data.
- A major limitation of the study was the presence of a limited number of sections for certain combinations of environmental region (north or south) and asphalt concrete thickness (thick or thin). Only one section for north-thick and one section for south-thin were present in the study for developing temperature and seasonal correction models. It is recommended that to make the models more robust at least 2 more sections from each of the above two combinations should be identified and instrumented in any future study.
- The 24-hour testing carried out at the two rigid pavement sections provided a deeper insight into the effects of curling and warping due to temperature variation within the pavement slab during the period. Similar investigations are recommended on additional rigid pavement sections on the NJ highways to reinforce the findings from the present study.
- A targeted pilot study is recommended for developing better testing protocols for studying the effects of slab curling.
- This study included only one composite section. Most rehabilitation activities on rigid pavements involve an asphalt concrete overlay. Future studies should include more composite sections to study the effects of climatic changes on this pavement type.

REFERENCES

1. Hanek, G., et al., **“Update on Seasonal Variations in Pavement Strength and Moisture”** 2000 FWD Users Group Meeting, Ithaca, NY, 2000.
2. Janoo, V., et al., **“Seasonal Variation of Moisture and Subsurface Layer Moduli”** Transportation Research Record, Transportation Research Board, National Research Council, Washington, D.C., 2000.
3. Ksaibati, K., et al., **“Effect of Moisture on the Modulus Values of Base and Subgrade Materials”**. Annual Meeting of Transportation Research Board, 2000.
4. Ovik, J.M., et al., **“Seasonal Variation in Backcalculated Pavement Layer Moduli in Minnesota”**, The 3rd International Symposium on Non-Destructive Testing of Pavements and Backcalculation of Moduli, 3rd volume, Seattle, Washington, ASTM, STP 1375, 1999.
5. Chen, D., et al., **“Temperature Correction on FWD Measurements”**. Annual Meeting of Transportation Research Board, 2000.
6. Long, B., et al., **“Seasonal Variation of Backcalculated Subgrade Moduli”**, Transportation Research Record 1577, pp. 70 - 80, Transportation Research Board, National Research Council, Washington, D.C.
7. Kim, Y.R., et al., **“Temperature Correction of Deflections and Backcalculated Asphalt Concrete Moduli”**, Transportation Research Record 1473, pp. 55 - 62, Transportation Research Board, National Research Council, Washington, D.C.
8. AASHTO Guide for Design of Pavement Structure, American Association of State Highway and Transportation Officials, Washington, D.C., U.S.A. 1993.
9. ITX Stanley Ltd, **“NJDOT Project Scoping using FWD Testing – FWD Analysis and Pavement Rehabilitation”**, March 1998.
10. Lukanen, Erland O., et al., **“Temperature Predictions and Adjustment Factors for Asphalt Pavements”**. Report FHWA-RD-98-085. Federal Highway Administration, 2000.
11. Stubstad, R. N., et al., **“Calculation of AC Layer Temperatures From FWD Field Data”**. Proceedings, Fifth International Conference on the Bearing Capacity of Roads and Airfields, Trondheim, 1998, pp.919-928.
12. SHRP Procedure for Temperature Correction of Maximum Deflections, Strategic Highway Research Program, Washington, D.C., U.S.A. 1993.
13. Asphalt Overlays for Highway and Street Rehabilitation, MS Series No. 17, Asphalt Institute, Lexington, KY, U.S.A., June 1983 Edition.
14. Larson, G. et al., **“Enhanced Integrated Climatic Model”**, Version 2.0, Final Report, Contract DTFA MN/DOT 72114, Department of Civil Engineering, University of Illinois at Urbana-Champaign, Urbana, Illinois. 1997.
15. Richter, C. A., et al., **“Application of LTPP Seasonal Monitoring Data to Evaluate Volumetric Moisture Predictions From The Integrated Climatic Model”**. Paper presented at 80th Annual Meeting, Transportation Research Board, Washington D.C., 2001.
16. Salem, H.M., et al., **“Prediction of Seasonal Variation of Subgrade Resilient Modulus Using LTPP Data”**, Paper presented at 83rd Annual Meeting, Transportation Research Board, Washington D.C., 2003.

17. Birgisson, B., et al., "**Analytical Predictions of Seasonal Variations in Flexible Pavements at the Mn/Road Site**", Transportation Research Record 1730, pp.81-90, Transportation Research Board, National Research Council, Washington, D.C., 2000.
18. Lytton, R.L., et al., "**An Integrated Model of the Climatic Effects on Pavements**". Federal Highway Administration Final Report No. FHWA-RD-90-033, McLean, Virginia, 1993.
19. Jin, M.S., et al., "**Seasonal Variation of Resilient Modulus of Subgrade Soils**", Journal of Transportation Engineering, ASCE, Vol.120, No.4, 1994.
20. Marshall, C., et al., "**Seasonal Temperature Effects on Flexible Pavements in Tennessee**", Transportation Research Record, Transportation Research Board, National Research Council, Washington, D.C., 2001.
21. Park, D., et al., "**Development of Effective Layer Temperature Prediction Model and Temperature Correction using FWD Deflections**", Transportation Research Record, Transportation Research Board, National Research Council, Washington, D.C., 2000.
22. Kennedy, C.K., et al., "**Prediction of Pavement Performance and the Design of Overlays**", TRRL Laboratory Report 833, 1978.
23. Shaat, A.A., "**Evaluation of Highways and Airport Pavement Life Based on Nondestructive Structural Assessment Techniques**", Ph.D. Thesis Submitted to the Queen's University of Belfast, Northern Ireland. 1989.
24. Bergstedt, B., "**Temperature Correction of Falling Weight Deflectometer**", Proc. 3rd Int. Conf. on Bearing Capacity of Roads and Airfields, vol. 1, p. 291-304, Trondheim, Norway, 1990.
25. Baltzer, S., et al., "**Temperature Correction of Asphalt-Moduli for FWD-Measurements**", The 4th International Conference on the Bearing Capacity of Roads and Airfields, Minnesota, USA, 1994.
26. Carson, A.M., et al., "**Factors Affecting Measured Deflection in Shropshire, England**", Proc. of 3rd Int. Conf. On Bearing Capacity of Roads and Airfields, Vol. 1, p. 281-290, Trondheim, Norway, 1990.
27. Shaat, A.A., et al., "**Relationships Between Climatic Conditions and the Structural Parameters of Flexible Pavements**", Proc. 7th Int. Conf. on Asphalt Pavements, Nottingham, Vol. 3, p. 326-340, 1992.
28. Nazarian, S. et al., "**A New Nondestructive Testing Device for Comprehensive Pavement Evaluation**", Journal: Proceedings Nondestructive Evaluation of Civil Structures and Materials, FHWA and National Science Foundation, 1992, 437-452.
29. Gucunski, N., et al., "**Evaluation of Seismic Pavement Analyzer for Pavement Condition Monitoring**", FHWA-NJ 2002-11 Final Report, May 2002.
30. Nazarian S., et al., "**Development and Testing of a Seismic Pavement Analyzer**", Report SHRP-H-375, Strategic Highway Research Program, National Research Council, Washington, D.C., 1993.
31. Zaghoul, S., et al., "**Dynamic Analysis of FWD Loading and Pavement Response Using a Three-Dimensional Dynamic Finite Element Program**", Nondestructive Testing of Pavements and Backcalculation of Moduli (Second Volume), STP 1198, Harold L. Von Quintas, Albert J. Bush, and Gilbert Baladi, Eds., American Society for Testing and Materials, Philadelphia, 1994, pp. 125-138.

32. Everstress – Version 5, Washington State Department of Transportation, Seattle, Washington, 1995.
33. Farrington, S.P., et al., “**Frost Penetration Prediction Using Simulation With GIS**”, Proc., of the 22nd Annual ESRI International User Conference, Environmental Systems Research Institute, San Diego, California, July 8–12, 2002.
34. Kim, Y. R., et al., “**New Temperature Correction Procedure for FWD Deflections of Flexible Pavements**”, Proceedings of the Fourth International Conference on Bearing Capacity of Roads and Airfields, MN, 1994.
35. Johnson, A. M., et al., “**Alternative Method for Temperature Correction of Backcalculated Equivalent Pavement Moduli**”, Transportation Research Record (TRR) 1355, Transportation Research Board, Washington, D.C., 1992, pp. 75-81.
36. Zaghoul, S.M., et al, “**Development of Seasonal Adjustment Models for Flexible Pavements**”, presented at the 84th Annual Meeting of the Transportation Research Board (TRB) and submitted for publication in the Transportation Research Record (TRR), TRB, Washington DC, 2005.
37. Zaghoul, S.M., et al., “**The Use of Falling Weight Deflectometer in Asphalt Pavement Construction Quality Control**”, Quality Management of Hot Mix Asphalt, ASTM 1299, Dale S. Decker, Ed., American Society for Testing and Materials, 1996.
38. Ahmed, Z., et al., “**Soil-Moisture Characteristics of Pavement Subgrades and Subbases**”, NED University Journal of Engineering Research Vol. 1, No. 2, Karachi, Pakistan.1994, pp. 13-26.
39. Cedergren, H.R., et al., “**Water: Key Cause of Pavement Failure**”, Civil Engineering, ASCE, Vol. 44, No. 9, 1974, pp. 78-83.
40. Macmaster, J.B., et al., “**Pavement Drainage in Seasonal Frost Area, Ontario, A Report in Symposium on Aspects of Subsurface Drainage Related to Pavement Design and Performance**”, Transportation Research Record 849, Transportation Research Board, National Research Council, Washington, D.C. 1982, pp. 18-24.
41. Mathis, D. M., “**Permeable Base Design and Construction**”, Proceedings of the Fourth International conference on Concrete Pavement Design and Rehabilitation, Purdue University, U.S.A.1989, pp. 662-670.
42. Raad, L., et al., “**Characterization of Saturated Granular Bases under Repeated Loads**”, Transportation Research Record 1369, Transportation Research Board, Washington D.C., 1992, pp 73-82.
43. Werkmeister, S., et al., “**Design of Granular Pavement Layers Considering Climatic Conditions**”, Paper presented at 82nd Annual Meeting, Transportation Research Board, Washington D.C., 2003.
44. Organization for Economic Co-Operation and Development, “**Water in Roads: Prediction of Moisture Content of Road Subgrades**”, OECD, Paris, France, 1973.
45. Markow, M.J., “**Simulating Pavement Performance Under Various Moisture Conditions**”, Transportation Research Record 849, TRB, Washington D.C., 1982, pp 24-29.
46. Topp, G. C., et al., “**Electromagnetic Determination of Soil Water Content: Measurements in Coaxial Transmission Lines**”, Water Resources Research, Vol. 16, No: 3, 1980, pp 574-582.

47. Ahmed, Z., et al., "**Pavement Drainage and Pavement-Shoulder Joint Evaluation and Rehabilitation**", Report No. FHWA/IN/JHRP-93-2, Federal Highway Administration, Washington, D.C., March 1993.
48. Yuan, D., et al., "**Use Of Seismic Pavement Analyzer To Monitor Degradation Of Flexible Pavements Under Texas Mobile Load Simulator**", Transportation Research Record, Issue 1615, pp 3-10, 1998
49. Yoder, E.J., et al., "**Principles of Pavement Design**", 2nd Edition. John Wiley & Sons, Inc., 1975.
50. Freeze/Thaw Monograph for LTPP, Publication No. FHWA-RD-98-177, 1998.
51. Corps of Engineers, "**Engineering and Design, Pavement Design for Frost Conditions**", EM- 1110-345-306. 1959.

APPENDIX A



Stantec

**Material Characterization and Seasonal
Variation in Material Properties**

Instrumentation Installation

**Test Section 4, Rest Area Route 295,
New Jersey**

For:

New Jersey Department of Transportation

Prepared by:

Stantec Consulting Ltd.
415 Lawrence Bell Drive, Suite 3
Amherst, NY 14221
Tel: (716) 632-0804
Fax: (716) 632-4808

Copyright © Stantec Consulting Ltd., 2002

MATERIAL CHARACTERIZATION AND SEASONAL VARIATION IN MATERIAL PROPERTIES – INSTRUMENTATION INSTALLATION

Table of Contents

	Page
1.0 INTRODUCTION 1.199	
2.0 INSTRUMENTATION INSTALLATION	200
2.1 SITE INSPECTION AND MEETING WITH HIGHWAY AGENCY	200
2.2 EQUIPMENT INSTALLED	200
2.3 EQUIPMENT CHECK/CALIBRATION	201
2.4 EQUIPMENT INSTALLATION	202
2.5 SITE REPAIR AND CLEANUP	202
2.6 PATCH/REPAIR AREA ASSESSMENT	202
3.0 INITIAL DATA COLLECTION	202
3.1 AIR TEMPERATURE, SUBSURFACE TEMPERATURE, RAIN-FALL DATA	202
3.2 TDR MEASUREMENTS	202
3.3 RESISTANCE MEASUREMENT DATA	202
3.4 DEFLECTION MEASUREMENT DATA	202
3.5 ELEVATION SURVEY	202
3.6 WATER DEPTH	202
4.0 SUMMARY	202
APPENDIX A – TEST SECTION BACKGROUND INFORMATION	202
APPENDIX B – SUPPORTING SITE VISIT AND INSTALLED INSTRUMENT INFORMATION	202
APPENDIX C – SUPPORTING INSTRUMENTATION INSTALLATION INFORMATION	202
APPENDIX D – INITIAL DATA COLLECTION	202
APPENDIX E - PHOTOGRAPHS	202

MATERIAL CHARACTERIZATION AND SEASONAL VARIATION IN MATERIAL PROPERTIES – INSTRUMENTATION INSTALLATION

1.0 Introduction

To study the seasonal variation in pavement strength in the State of New Jersey, several sites across the state were selected for instrumentation to monitor temperature and other climatic factors. The installation of Site 4 instrumentation was performed on October 27 – October 29, 2001. The test section is a rest area truck entrance located at Northbound Route 295 close to mile post 49.5. The test section starts at the truck entrance with a one lane of 26 ft width and the lane is getting wider at station 0+50 to accommodate the existing truck parking lot as shown in Appendix A, Figure A.1.

The Falling Weight Deflectometer (FWD) section starts at station 0+00 and continues up to station 0+200 with a testing station each 25 ft. Based on the initial visual inspection, it was found that it is better to have the instrumentation hole at 0–25 to avoid any interfering with the on-going traffic during the installation. The FWD stations are located at the wheel path 4 ft from the curb.

The pavement structure of Section 4, which is a flexible pavement, consists of 10 in. of asphalt concrete on 10.5 in. of crushed aggregate base. The subgrade consists of sandy clay and silty soil and the clay content increases with depth. Pavement structure information from the material drilling logs during installation is presented in Appendix A, Figure A.2.

Figure A.3 in Appendix A summarizes the FWD deflections as measured during the installation. The backcalculated subgrade modulus and structural number are summarized in Table A.1, Appendix A.

The site is located at the northern climatic zone. The site is considered as a thin pavement (<24 in.) in depth on a non-cohesive subgrade soil (Type II).

Installation of the instrumentation was primarily done by Stantec. Personnel from the New Jersey Department of Transportation (NJDOT) and the Center for Advanced Infrastructure and Transportation (CAIT) Rutgers University attended the installation. The following personnel participated in the instrumentation installation:

Tony Chmiel	NJDOT	Sameh Zaghloul	Stantec Consulting
Nenad Gucunski	Rutgers University-CAIT	Rafael Olejniczak	Stantec Consulting
Rambod Haidi	Rutgers University	Brock Smith	Stantec Consulting
Jack Norton	Jersey Boring and Drilling	Amr Ayed	Stantec Consulting
Paul McCarthy	Semcor Equipment	Ben Walker	Stantec Consulting-NARO
Brandt Henderson	Stantec Consulting-NARO	Steve Allen	Stantec Consulting

MATERIAL CHARACTERIZATION AND SEASONAL VARIATION IN MATERIAL PROPERTIES – INSTRUMENTATION INSTALLATION

2.0 Instrumentation Installation

2.1 SITE INSPECTION AND MEETING WITH HIGHWAY AGENCY

Several preliminary meetings were held at the Research Division of NJDOT during the spring and summer of 2001. The attendees at each meeting varied among the following members:

Nicholas Vitillo	NJDOT Research
Tony Chmiel	NJDOT Research
Nenad Gucunski	Rutgers University-CAIT
Sameh Zaghoul	Stantec
Frank Meyer	Stantec-NARO
Brandt Henderson	Stantec-NARO
Frank Palise	NJDOT-LTPP State Coordinator
Raj Chawla	NJDOT-QMS
Jack Springer	FHWA LTPP
Rich Shaw	NJDOT
Dennis Moniani	NJDOT
Richard Eng	NJDOT

Several demonstrations and presentations on the seasonal monitoring instrumentation were provided by Sameh Zaghoul and Brandt Henderson of Stantec on different occasions. Plans for the installation on October 27 and October 29, 2001 including the tasks to be covered by all parties involved were discussed during such meetings.

The site was visited on October 4 and 5, 2001 by Stantec personnel, Brandt Henderson, Sameh Zaghoul and Frank Meyer to select the location for instrumentation installation. Following this, the site was marked with paint and stakes to identify the utility locations. In addition, the site was reviewed for potential installation problems.

2.2 EQUIPMENT INSTALLED

The equipment installed at the test site included instrumentation for measuring air, pavement and subsurface temperature, subsurface moisture content, frost depth, precipitation, and water table. An equipment cabinet was also installed to hold the datalogger, battery pack, and all electrical connections from the instrumentation. A list of the equipment installed is shown in Table 2.1.

MATERIAL CHARACTERIZATION AND SEASONAL VARIATION IN MATERIAL PROPERTIES– INSTRUMENTATION INSTALLATION
 INSTRUMENTATION INSTALLED

Table 2.1
 Equipment Installed

Equipment	Quantity	Serial Number
Instrumentation Hole		
TDR Probes (CS610)	3	4-1 to 4-3
MRC Temperature Probe (TP101)	1	101001-NJ-4
ABF Resistivity Probe	1	4
Equipment Cabinet		
Campbell Scientific Datalogger (CR10X)	1	X27902
Campbell Scientific TDR 100 Time Domain Reflectometer	1	1192
Campbell Scientific Multiplexer (SDMX50SP)	1	3137
ABF-ERB 20 Resistivity Multiplexer	1	R002
HD 12V-19AH Battery	1	HD-NJ-4
Crydom Relay	1	CR-NJ-4
AVW1 Vibrating Wire Interface	1	3514
Datalogger Wiring Panel	1	18013
Weather Pole		
TE525 mm Tipping Bucket (rain gauge)	1	29162-801
CS 107 Air Temp. Probe	1	111001-NJ-4
ATP Radiation Shield	1	RS-NJ-4
MSX20R Solar Panel	1	I0101231693522
Other Equipment		
Observation well/benchmark	1	

2.3 EQUIPMENT CHECK/CALIBRATION

Prior to the installation, each measurement instrument was checked or calibrated. The tipping bucket rain gauge was connected to the CR10X datalogger for calibration. A plastic container with 16 oz. of water was placed in the tipping bucket. The container had a small hole in the bottom, which allowed all the water to be drained out in 45 minutes. For the 16 oz. of water, the tipping bucket should measure 100 tips \pm 3 tips. The results showed 97 tips, which was within specification.

MATERIAL CHARACTERIZATION AND SEASONAL VARIATION IN MATERIAL PROPERTIES– INSTRUMENTATION INSTALLATION

INSTRUMENTATION INSTALLED

The air temperature and thermistor probes were connected to the CR10X datalogger simultaneously. They were checked by placing the probes in ice, room temperature, and hot water. In order for the probes to pass this check, the temperatures for each probe should correspond to the exact temperature measured with temperature gauge. The check indicated that the air temperature and thermistor probes were working properly. A second check was done where the air temperature and thermistor probes were connected to the datalogger and run, in air, for 24 hours. The minimum, maximum, and mean temperature for each sensor was checked. All 11 thermistors were similar in their minimum, maximum, and mean readings respectively, therefore the probes were considered to be functioning correctly. The results of the air temperature and thermistor probes calibration along with the spacing between the thermistors are presented in Appendix B.

The wiring of the resistivity probe was checked using continuity measurements between each electrode and the corresponding pins on the connector. The distance between each electrode was measured and recorded as shown in Table B.4, Appendix B. The checks on the resistivity probe indicated all electrodes were functioning properly.

The functioning of the TDR probes were checked by performing measurements in air and water, and with the prongs shorted at the circuit board. The traces were taken and the dielectric constant was calculated for water and air. These values were checked against expected dielectric constants for each medium. The test indicated that all probes were functioning properly. Results of the TDR measurements are presented in Appendix B.

2.4 EQUIPMENT INSTALLATION

The pavement surface drilling, augering of the piezometer and instrumentation hole, and the sawing of the trench and cut for the pavement surface temperature probe were done by Jersey drilling and their subcontractor under the supervision of Stantec staff. The installation of the measurement equipment, the observation piezometer, weather station pole, and cabinet was done by Stantec crew. Assistance was provided by Tony Chmiel, NJDOT Research Group, Nenad Gucunski and Rambod Haidi, Rutgers University-CAIT.

The instrumentation hole was installed on the truck entrance of the rest area on the left side at 4 ft from the curb at station 0-25, as shown in Figure A.1. A material sampling hole was augered at station 0-50. The combination bench mark/piezometer was placed at the right side of the entrance in the grass at station 0+22 ft, 6 inches. The cabling from the instrumentation was placed in a 0.42 ft flexible conduit and buried in a trench running from the instrument hole to an equipment cabinet installed on the slope of the roadway embankment, 10 ft 6 in. from the curb. To support the

MATERIAL CHARACTERIZATION AND SEASONAL VARIATION IN MATERIAL PROPERTIES– INSTRUMENTATION INSTALLATION

INSTRUMENTATION INSTALLED

cabinet, existing site materials were spread around the cabinet base. The weather pole was installed next to the equipment cabinet. Figure A.4 provides the location and distances for the various instrumentations and equipment installed.

The combination piezometer/bench mark was installed 44 ft from the weather pole to a depth of 14 ft. A flight auger was used for drilling the hole. An instrumentation core hole was drilled in the pavement surface, located in the left side wheel path, 4 ft from the edge of the curb at station 0-25, using a 14 in. thin wall diamond core barrel, attached to the truck mounted drilling unit. Several 4 in. and 6 in. pavement core samples were drilled for materials testing by Rutgers. These samples were taken 4 ft from the left curb, from station 0-60 to station 0-52. A 0.42 ft wide by 0.72 ft deep saw cut was done between the core hole and the edge of the pavement, using a heavy duty pavement sawing machine. The remainder of the material from the trench was removed with a trencher and shovels.

A 12 in. flight hollow stem auger was used to drill the instrumentation hole. Material was removed in 12 to 16 in. lifts. Care was taken to ensure that the material was stored in the order of excavation. The material removed was stored in buckets with distinct layers separated. The road base consisted of crushed aggregate (dolomite) over a silty, clayey sand of variable consistency over the depth of excavation. The findings from the drilling are presented in Figure A.2. A wet vacuum and sponges were used to remove as much moisture as was possible resulting from the coring machine.

Samples of the material placed around each TDR probe were retained for laboratory moisture determination by CAIT, Rutgers. The equipment cabinet and pole for the rain gauge and air temperature probe was installed as per manual guidelines. The excavation of the extended trench from the edge of pavement to the cabinet proceeded fairly smoothly as the material was generally grass.

To check for breakage of the TDR probes during installation, each probe was connected to the cable tester and its wave form monitored during compaction of the material around it. The TDR traces are included in Appendix C. The TDR probes were placed such that the cables coming out of them were evenly spaced around the perimeter of the hole to avoid water migrating along a bundle of cables. The thermistor and resistivity probes were installed at opposite sides of the instrumentation hole just below the pavement surface. The cables were kept spaced as best as possible until they converged at the opening of the flexible conduit pipe, placed about 2 in. from the edge of the core hole. The cables were then tie wrapped and passed through the conduit to the equipment cabinet. The ends of the conduit were plugged with a mastic pipe sealant. Appendix C, Tables C.1, C.2 and C.3, present installed depths of the TDR probes, thermistor sensors, and the resistivity probe respectively.

MATERIAL CHARACTERIZATION AND SEASONAL VARIATION IN MATERIAL PROPERTIES– INSTRUMENTATION INSTALLATION

INSTRUMENTATION INSTALLED

2.5 SITE REPAIR AND CLEANUP

The instrumentation hole and material sampling location were repaired by reinstalling the 14 in. core. Some juggling was required to get the core level with the existing pavement surface. Once the core was leveled it was removed from the hole and the bottom 4 in. was heavily covered with a two part epoxy (PC-7) and reset into the hole forcing the epoxy against the side and up along the wall of the hole. The holes for the core samples removed for material analysis were filled with cold mix and compacted.

The trench for the cabling from the instrumentation hole to the edge of pavement was leveled with the native base material to the existing bottom of the paved layer and a cold mix was compacted to the level of the existing surface. The remainder of the trench was filled with native material and compacted, followed by a cleanup of loose material from the paved area. The instrument hole was sealed using Corning self-leveling 888 crack sealing compound followed by the removal of the asphalt trench material and other disposable items.

2.6 PATCH/REPAIR AREA ASSESSMENT

The site has been visited one month after the installation and the overall the site was in good condition.

MATERIAL CHARACTERIZATION AND SEASONAL VARIATION IN MATERIAL PROPERTIES – INSTRUMENTATION INSTALLATION

3.0 Initial Data Collection

The second day's activities included wiring the instrumentation to the datalogger, initial data collection on the site, and checks on the functioning of installed equipment. This consisted of examination of the data collected over the day by the onsite datalogger, data collection with the onsite datalogger, deflection testing, water table measurements, manual resistivity measurements, and an elevation survey. The onsite datalogger was downloaded on October 29, 2001, before leaving the area. A sample of initial data collected by the onsite datalogger is presented in Appendix D, Table D.1.

3.1 AIR TEMPERATURE, SUBSURFACE TEMPERATURE, RAIN-FALL DATA

The air temperature, pavement subsurface temperature profile, and rainfall data, collected on October 29 by the CR10X datalogger, were examined. The equipment and datalogger appeared to be functioning properly. The battery voltages were checked and found to be acceptable. The plots of the temperature profiles are presented in Appendix D, Figures D.1 and D.2.

The tipping bucket rain gauge was checked by determining the number of tips recorded from 473 ml of water discharged into the gauge over a 1 hour time period. The rain gauge was found to be operating properly.

3.2 TDR MEASUREMENTS

The TDR data was collected using the TDR100 System and a CR10X datalogger. Figure D.3 shows the initial TDR traces for all 3 sensors. Only the second set of TDR traces are shown in the appendix because the first set of traces were used to fine tune the starting locations of the traces. The figures indicate that the data collecting system and TDR sensors were working properly.

3.3 RESISTANCE MEASUREMENT DATA

Resistance data was collected in two modes, automated and manual. The ABFERB20 data acquisition system automatically performs two point contact resistance measurements and stores the values in terms of millivolts between adjacent electrodes.

Manual contact resistance and resistivity measurements were performed using a Simpson Model 20d function generator, a Fluke Voltmeter, a Fluke Ammeter, and a FHWA switching box. The measured contact resistance and four-point resistivity data are plotted in Figure D.5 and Figure D.6 respectively. Table D.2 and D.3 in

MATERIAL CHARACTERIZATION AND SEASONAL VARIATION IN MATERIAL PROPERTIES– INSTRUMENTATION INSTALLATION

INITIAL DATA COLLECTION

Appendix D shows the raw data for the 2-point and the 4-point resistance respectively.

The general trend of the automated resistance voltage contact resistance, and the four-point resistivity collected are similar. The data appears to be consistent with what could be expected for the materials and conditions at the site.

3.4 DEFLECTION MEASUREMENT DATA

The FWD tests were done following the instrumentation and the analysis results from instrumentation dates are presented in Appendix A.

3.5 ELEVATION SURVEY

A surface elevation survey of the site was performed following the guidelines. It was assumed that the elevation at the top of the piezometer pipe was 1.000 meters (3.28 ft). The survey was conducted on October 29, 2001 and the results are presented in Appendix D.

3.6 WATER DEPTH

The water level on October 29, 2001 was approximately 2.86 m (9.38 ft) below the top of the piezometer.

MATERIAL CHARACTERIZATION AND SEASONAL VARIATION IN MATERIAL PROPERTIES – INSTRUMENTATION INSTALLATION

4.0 Summary

The installation of the seasonal monitoring instrumentation for section 4 at Route 295 rest area, New Jersey, was completed on October 27, 2001. A check of the equipment and initial data collection was completed on October 29, 2001. The instrumentation, permanently installed at the site, were:

- Time domain reflectometer probes for moisture measurements,
- Thermistor probes for pavement and soil gradient temperature measurements,
- Resistivity probe for frost depth measurements,
- Air temperature, thermistor probe, and tipping bucket rain gauge to record local climatic conditions, and
- Combination piezometer (well) and bench mark to determine changes in water level and pavement elevations.

The pavement gradient temperature and local climatic data are to have continuous data collection stored in an on-site datalogger. The moisture and the frost depths are to be collected and sampled based on the triggering conditions shown in Tables 4.1 and 4.2, respectively. The water level and elevation data are to be collected manually during site visits.

Table 4.1
Moisture Data Sampling Cycle

Start Trigger TDR	End Trigger TDR	TDR Probe
Rain < 1.5 mm No Rain for 8 hours	Rain ≥ 1.5 mm Rain ≥ 5.0 mm	Sample every 4 hours continuously
Rain ≥ 1.5 mm	Rain < 1.5 mm Rain ≥ 5.0 mm	Sample every 45 minutes only while rain continues
Rain ≥ 5.0 mm	Rain < 1.5 mm	Sample every 45 minutes continuously
Rain < 1.5 mm	Rain ≥ 5 mm No Rain for ≥ 8 hours	Sample every 2 hours continuously

MATERIAL CHARACTERIZATION AND SEASONAL VARIATION IN MATERIAL PROPERTIES– INSTRUMENTATION INSTALLATION

SUMMARY

Table 4.2
Frost depth Data Sampling Cycle

Start Trigger	End Trigger	Resistance Probe
Min Soil Temp $\geq 4^{\circ}\text{C}$	Min Soil Temp $< 0^{\circ}\text{C}$	Sample every 4 weeks
Min Soil Temp $< 0^{\circ}\text{C}$	Min Soil Temp $< 0^{\circ}\text{C}$ for ≥ 4 hours	Sample hourly
Min Soil Temp $< 0^{\circ}\text{C}$ for ≥ 4 hours	Min Soil Temp $< 0^{\circ}\text{C}$ for ≥ 20 hours	Sample every 4 hours
Min Soil Temp $< 0^{\circ}\text{C}$ for ≥ 20 hours	Min Soil Temp $\geq 4^{\circ}\text{C}$	Sample every 24 hours

The test section is a truck entrance rest area located on Route 295 near mile post 49.5 and of 26 ft lane width. The pavement structure, which is a flexible type pavement, consists of 10 in. of asphalt concrete over 10.5 in. of crushed aggregate base over a sandy clay and silt.

All instrumentation was checked prior to the installation at the Stantec-NARO facility in Amherst, NY. These initial checks indicated that the instrumentation was within specifications, as required for the seasonal monitoring program. Operational checks during installation and the following day indicated that all instrumentation was functioning properly. The air temperature and gradient temperatures measured in the pavement surface compared favorably with the handheld Omega temperature gauge. The temperature profile for the pavement soils appeared reasonable with no outlying sensors. A check of the tipping bucket indicated it was functioning correctly with tips corresponding to amount of water supplied.

MATERIAL CHARACTERIZATION AND SEASONAL VARIATION IN MATERIAL PROPERTIES – INSTRUMENTATION INSTALLATION

Appendix A – Test Section Background Information

Appendix A contains the following supporting information:

FIGURE A.1: SITE LOCATION INFORMATION

FIGURE A.2: PROFILE OF PAVEMENT STRUCTURE AND TDR PROBE DEPTHS FROM SURFACE

FIGURE A.3: DELFECTION PROFILE (TEST DATE OCT. 29, 2001)

FIGURE A.4: LOCATION OF SEASONAL MONITORING INSTRUMENTATION

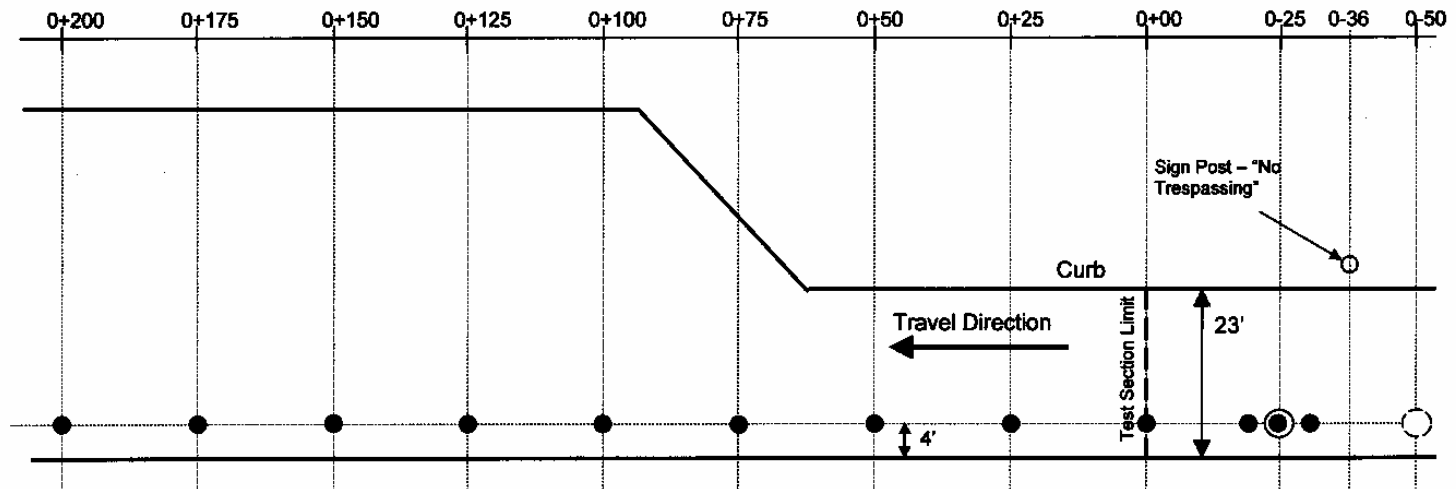
TABLE A.1: SUBGRADE MODULUS AND STRUCTURAL NUMBER

MATERIAL CHARACTERIZATION AND SEASONAL VARIATION IN MATERIAL PROPERTIES- INSTRUMENTATION INSTALLATION

APPENDIX A – TEST SECTION BACKGROUND INFORMATION

Section #4 Route 295 NB Rest Area – Truck Entrance

Test Section Layout



Legend

- HWD Test Location - Permanent
- Instrumentation Hole
- Material Hole

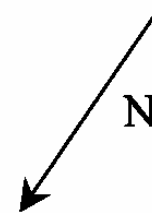


Figure A.1: Site Location Information

June 6, 2002

210

MATERIAL CHARACTERIZATION AND SEASONAL VARIATION IN MATERIAL PROPERTIES– INSTRUMENTATION INSTALLATION

APPENDIX A – TEST SECTION BACKGROUND INFORMATION

Figure A.1: Site Location Information Material	Depth (in)		TDR Depth (in)	Comments
AC	10.0			
Aggr. Base	20.5	TDR 1	13.5	Thermistor Probe Depth 10" Resistivity Probe Depth 10"
Sandy Clay and Silt		TDR 2	25.25	Clay content increases with depth. Layer was interrupted by occasional lenses of silt and sand
		TDR 3	45.25	

Figure A.2: Profile of Pavement Structure and TDR Probe Depths from Surface

MATERIAL CHARACTERIZATION AND SEASONAL VARIATION IN MATERIAL PROPERTIES– INSTRUMENTATION INSTALLATION

APPENDIX A – TEST SECTION BACKGROUND INFORMATION

Table A.1
Subgrade Modulus and Structural Number

Station (ft)	Subgrade Modulus	Effective SN
0.00	6,895.04	6.76
26.25	8,321.14	5.93
49.21	7,594.57	5.92
75.46	8,372.30	6.16
98.43	8,514.51	6.15
124.67	8,864.84	5.85
150.92	8,549.87	5.52
173.88	7,998.14	5.40
200.13	8,571.88	5.44

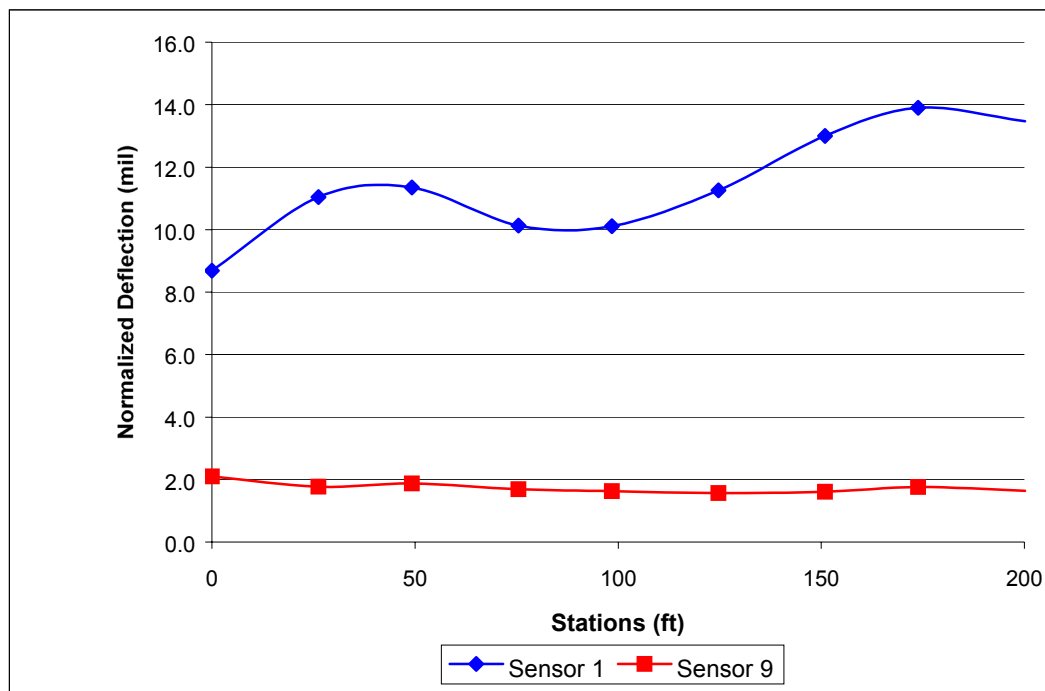


Figure A.3: Deflection Profile (Test Date Oct. 29, 2001)

MATERIAL CHARACTERIZATION AND SEASONAL VARIATION IN MATERIAL PROPERTIES- INSTRUMENTATION INSTALLATION

APPENDIX A – TEST SECTION BACKGROUND INFORMATION

Section #4
Route 295 NB Rest Area – Truck Entrance
Installation Oct 28,29 2001

Instrumentation Detail

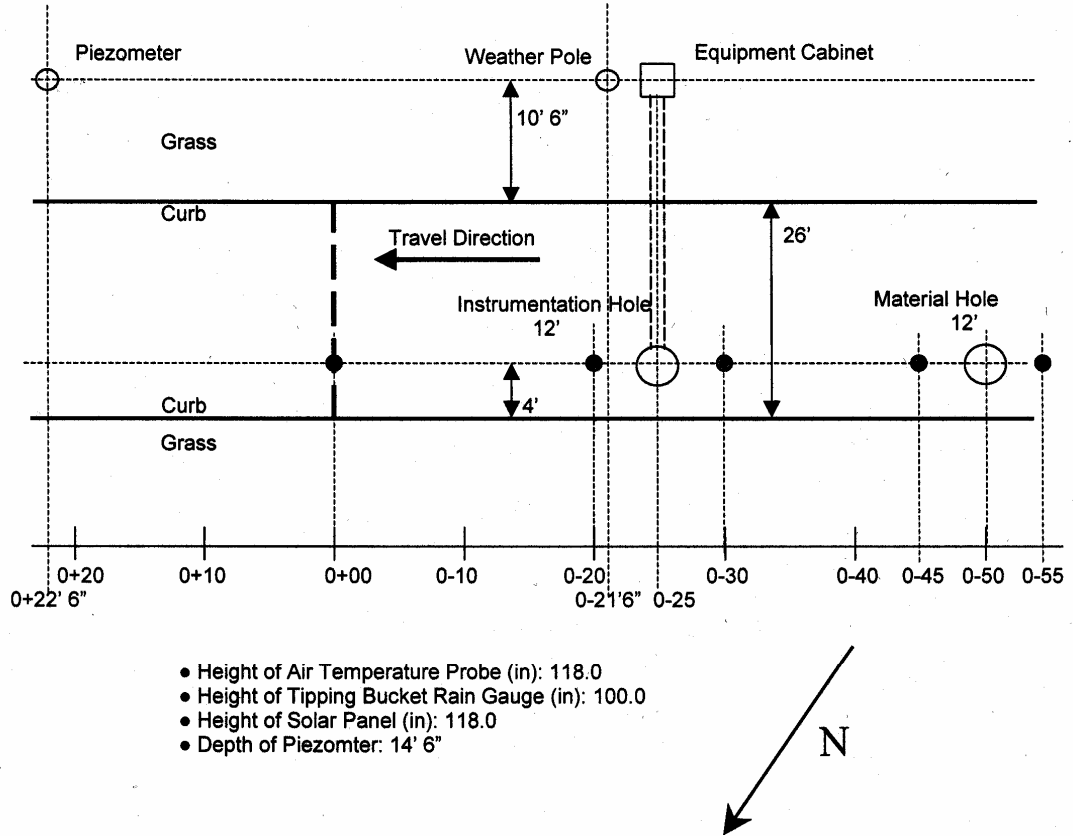


Figure A.4: Location of Seasonal Monitoring Instrumentation

MATERIAL CHARACTERIZATION AND SEASONAL VARIATION IN MATERIAL PROPERTIES – INSTRUMENTATION INSTALLATION

Appendix B – Supporting Site Visit and Installed Instrument Information

Appendix B contains the following supporting information:

TABLE B.1: MRC PROBE CALIBRATION

TABLE B.2: DESCRIPTION OF MRC THERMISTOR PROBE AND SENSOR SPACING

TABLE B.3: RESISTIVITY PROBE AND SENSOR SPACING

TABLE B.4: TDR PROBES CALIBRATION

FIGURE B.1: TDR TRACES OBTAINED DURING CALIBRATION

MATERIAL CHARACTERIZATION AND SEASONAL VARIATION IN MATERIAL PROPERTIES – INSTRUMENTATION INSTALLATION

APPENDIX B – SUPPORTING SITE VISIT AND INSTALLED INSTRUMENT INFORMATION

Table B.1
MRC Probe Calibration

Calibration Date		Oct 11, 2001	
Probe S/N		101001-NJ-4	
Operator		Rafael Olejniczak	
No.	Ice Bath 0° C (+/- 1° C) Reading	Hot Water 37.7° C (+/-) Reading	OK Y/N
1	-0.07	37.67	Y
2	-0.07	37.37	Y
3	-0.07	31.11	Y
4	0.54	37.39	Y
5	-0.03	37.51	Y
6	-0.03	37.75	Y
7	-0.03	37.72	Y
8	0.01	37.64	Y
9	-0.07	38.45	Y
10	0.16	38.53	Y
11	0.54	38.13	Y

Table B.2
Description of MRC Thermistor Probe and Sensor Spacing

Unit	Channel No.	Distance from Top of Unit (in)	Remarks
1	1	-	Three separate probes
	2	-	
	3	-	
2	4	1.00	
	5	3.75	
	6	7.00	
	7	10.00	
	8	12.75	
	9	25.00	
	10	37.00	
	11	49.00	

MATERIAL CHARACTERIZATION AND SEASONAL VARIATION IN MATERIAL PROPERTIES – INSTRUMENTATION INSTALLATION

APPENDIX B – SUPPORTING SITE VISIT AND INSTALLED INSTRUMENT INFORMATION

Table B.3
Resistivity Probe and Sensor Spacing

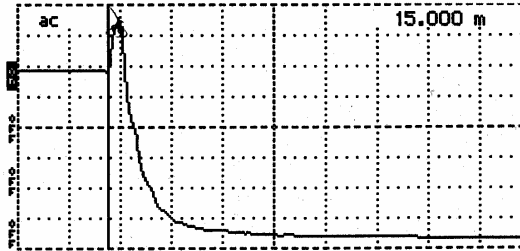
Connector Pin No.	Electrode Number	Distance from Top (in)	Continuity √	Spacing (in)	Comments
36	1	1.00	√	2.00	
35	2	3.00	√	2.00	
34	3	5.00	√	2.00	
33	4	7.00	√	2.00	
32	5	9.00	√	2.00	
31	6	11.00	√	2.00	
30	7	13.00	√	2.00	
29	8	15.00	√	2.00	
28	9	17.00	√	2.00	
27	10	19.00	√	2.00	
26	11	21.00	√	2.00	
25	12	23.00	√	2.00	
24	13	25.00	√	2.00	
23	14	27.00	√	2.00	
22	15	29.00	√	2.00	
21	16	31.00	√	2.00	
20	17	33.00	√	2.00	
19	18	35.00	√	2.00	
18	19	37.00	√	2.00	
17	20	39.00	√	2.00	
16	21	41.00	√	2.00	
15	22	43.00	√	2.00	
14	23	45.00	√	2.00	
13	24	47.00	√	2.00	
12	25	49.00	√	2.00	
11	26	51.00	√	2.00	
10	27	53.00	√	2.00	
9	28	55.00	√	2.00	
8	29	57.00	√	2.00	
7	30	59.00	√	2.00	
6	31	61.00	√	2.00	
5	32	63.00	√	2.00	
4	33	65.00	√	2.00	
3	34	67.00	√	2.00	
2	35	69.00	√	1.75	
1	36	70.75	√		
	Bottom	72.25			

MATERIAL CHARACTERIZATION AND SEASONAL VARIATION IN MATERIAL PROPERTIES – INSTRUMENTATION INSTALLATION

APPENDIX B – SUPPORTING SITE VISIT AND INSTALLED INSTRUMENT INFORMATION

Probe Shorted

Cursor 15.000 m
 Distance/Div 0.5 m/div
 Vertical Scale... 172 m ρ /div
 VP 0.99
 Noise Filter 1 avs
 Power ac

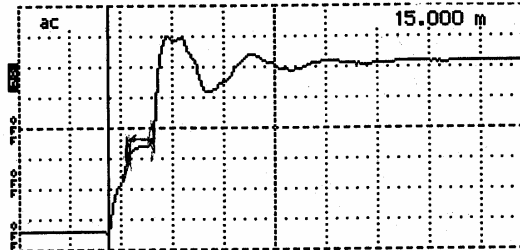


Tektronix 1502C TDR
 Date 10-23-01
 Cable 4-1
 Notes Shorted

Input Trace
 Stored Trace
 Difference Trace

Probe in Air

Cursor 15.000 m
 Distance/Div 0.5 m/div
 Vertical Scale... 172 m ρ /div
 VP 0.99
 Noise Filter 1 avs
 Power ac

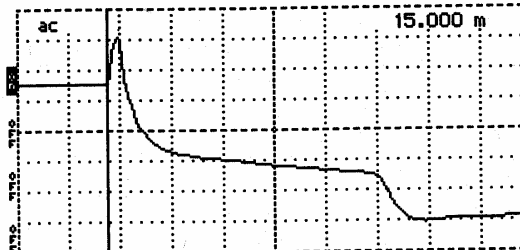


Tektronix 1502C TDR
 Date 10-23-01
 Cable 4-1
 Notes Air

Input Trace
 Stored Trace
 Difference Trace

Probe in Water

Cursor 15.000 m
 Distance/Div 0.5 m/div
 Vertical Scale... 172 m ρ /div
 VP 0.99
 Noise Filter 1 avs
 Power ac



Tektronix 1502C TDR
 Date 10-23-01
 Cable 4-1
 Notes Water

Input Trace
 Stored Trace
 Difference Trace

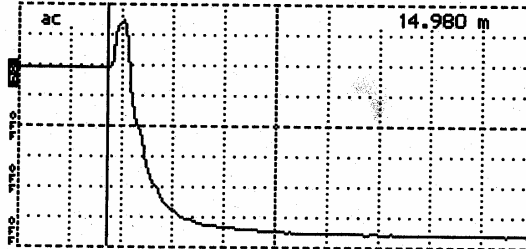
Figure B.1: TDR Traces Obtained During Calibration

MATERIAL CHARACTERIZATION AND SEASONAL VARIATION IN MATERIAL PROPERTIES – INSTRUMENTATION INSTALLATION

APPENDIX B – SUPPORTING SITE VISIT AND INSTALLED INSTRUMENT INFORMATION

Probe Shorted

Cursor 14.980 m
 Distance/Div 0.5 m/div
 Vertical Scale..... 172 m ρ /div
 VP 0.99
 Noise Filter 1 avs
 Power ac

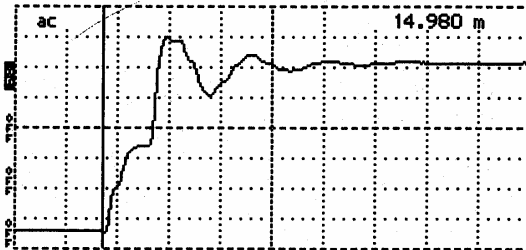


Tektronix 1502C TDR
 Date 10-23-01
 Cable 4-2
 Notes Shorted

Input Trace
 Stored Trace
 Difference Trace

Probe in Air

Cursor 14.980 m
 Distance/Div 0.5 m/div
 Vertical Scale..... 172 m ρ /div
 VP 0.99
 Noise Filter 1 avs
 Power ac

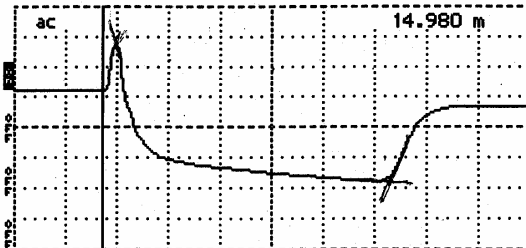


Tektronix 1502C TDR
 Date 10-23-01
 Cable 4-2
 Notes AIR

Input Trace
 Stored Trace
 Difference Trace

Probe in Water

Cursor 14.980 m
 Distance/Div 0.5 m/div
 Vertical Scale..... 172 m ρ /div
 VP 0.99
 Noise Filter 1 avs
 Power ac



Tektronix 1502C TDR
 Date 10-23-01
 Cable 4-2
 Notes Water

Input Trace
 Stored Trace
 Difference Trace

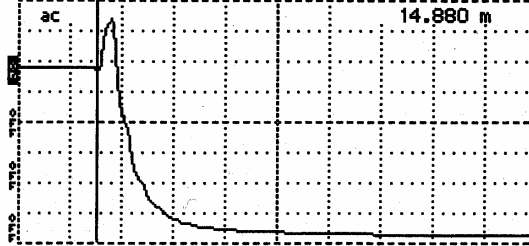
Figure B.1 (cont'd): TDR Traces Obtained During Calibration

MATERIAL CHARACTERIZATION AND SEASONAL VARIATION IN MATERIAL PROPERTIES – INSTRUMENTATION INSTALLATION

APPENDIX B – SUPPORTING SITE VISIT AND INSTALLED INSTRUMENT INFORMATION

Probe Shorted

Cursor 14.880 m
 Distance/Div 0.5 m/div
 Vertical Scale 172 mP/div
 VP 0.99
 Noise Filter 1 avs
 Power ac

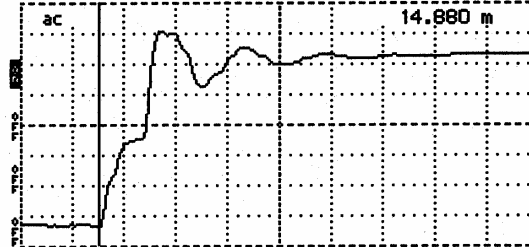


Tektronix 1502C TDR
 Date 10-23-01
 Cable 4-3
 Notes Shorted

Input Trace
 Stored Trace
 Difference Trace

Probe in Air

Cursor 14.880 m
 Distance/Div 0.5 m/div
 Vertical Scale 172 mP/div
 VP 0.99
 Noise Filter 1 avs
 Power ac

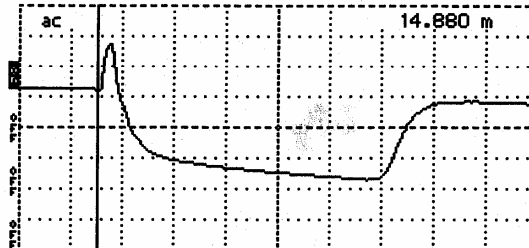


Tektronix 1502C TDR
 Date 10-23-01
 Cable 4-3
 Notes AIR

Input Trace
 Stored Trace
 Difference Trace

Probe in Water

Cursor 14.880 m
 Distance/Div 0.5 m/div
 Vertical Scale 172 mP/div
 VP 0.99
 Noise Filter 1 avs
 Power ac



Tektronix 1502C TDR
 Date 10-23-01
 Cable 4-3
 Notes water

Input Trace
 Stored Trace
 Difference Trace

Figure B.1 (cont'd): TDR Traces Obtained During Calibration

MATERIAL CHARACTERIZATION AND SEASONAL VARIATION IN MATERIAL PROPERTIES – INSTRUMENTATION INSTALLATION

Appendix C – Supporting Instrumentation Installation Information

Appendix C contains the following supporting information:

FIGURE C.1: TDR TRACES MEASURED MANUALLY DURING INSTALLATION

TABLE C.1: INSTALLED DEPTH OF TDR SENSORS

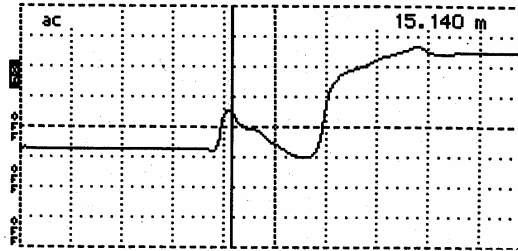
TABLE C.2: INSTALLED LOCATION OF MRC THERMISTOR SENSORS

TABLE C.3: LOCATION OF ELECTRODES OF THE RESISTIVITY PROBE

MATERIAL CHARACTERIZATION AND SEASONAL VARIATION IN MATERIAL PROPERTIES – INSTRUMENTATION INSTALLATION

APPENDIX C – SUPPORTING INSTRUMENTATION INSTALLATION INFORMATION

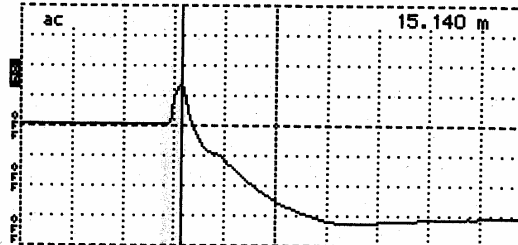
Cursor 15.140 m
 Distance/Div 0.5 m/div
 Vertical Scale.... 172 mP/div
 VP 0.99
 Noise Filter 1 avs
 Power..... ac



Tektronix 1502C TDR
 Date OCT 27/01
 Cable 4-1
 Notes _____

 Input Trace _____
 Stored Trace _____
 Difference Trace _____

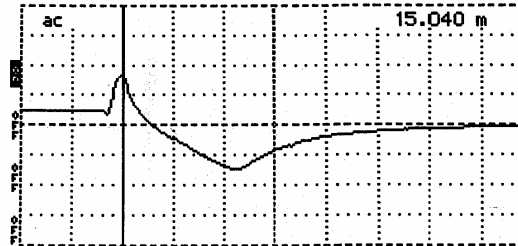
Cursor 15.140 m
 Distance/Div 0.5 m/div
 Vertical Scale.... 172 mP/div
 VP 0.99
 Noise Filter 1 avs
 Power..... ac



Tektronix 1502C TDR
 Date OCT 27/01
 Cable 4-2 (Full Co
 Notes _____

 Input Trace _____
 Stored Trace _____
 Difference Trace _____

Cursor 15.040 m
 Distance/Div 0.5 m/div
 Vertical Scale.... 177 mP/div
 VP 0.99
 Noise Filter 1 avs
 Power..... ac



Tektronix 1502C TDR
 Date OCT 27/01
 Cable 4-3
 Notes _____

 Input Trace _____
 Stored Trace _____
 Difference Trace _____

Figure C.1: TDR Traces Measured Manually During Installation

MATERIAL CHARACTERIZATION AND SEASONAL VARIATION IN MATERIAL PROPERTIES – INSTRUMENTATION INSTALLATION

APPENDIX C – SUPPORTING INSTRUMENTATION INSTALLATION INFORMATION

Table C.1
Installed Depth of TDR Sensors

Sensor #	Depth from Pavement Surface (in)	Layer
4-1	13.5	Base
4-2	25.25	Subgrade
4-3	45.25	

Table C.2
Installed Location of MRC Thermistor Sensors

Unit	Channel Number	Depth from Pavement Surface (in)	Remarks
1	1	1.00	Installed in AC Layer
	2	5.00	
	3	9.00	
2	4	11.00	Installed in Base and in Subgrade
	5	13.75	
	6	17.00	
	7	20.00	
	8	22.75	
	9	35.00	
	10	47.00	
	11	59.00	

MATERIAL CHARACTERIZATION AND SEASONAL VARIATION IN MATERIAL PROPERTIES – INSTRUMENTATION INSTALLATION

APPENDIX C – SUPPORTING INSTRUMENTATION INSTALLATION INFORMATION

Table C.3
Location of Electrodes of the Resistivity Probe

Connector Pin Number	Electrode Number	Depth from Pavement Surface (in)
36	1	11.00
35	2	13.00
34	3	15.00
33	4	17.00
32	5	19.00
31	6	21.00
30	7	23.00
29	8	25.00
28	9	27.00
27	10	29.00
26	11	31.00
25	12	33.00
24	13	35.00
23	14	37.00
22	15	39.00
21	16	41.00
20	17	43.00
19	18	45.00
18	19	47.00
17	20	49.00
16	21	51.00
15	22	53.00
14	23	55.00
13	24	57.00
12	25	59.00
11	26	61.00
10	27	63.00
9	28	65.00
8	29	67.00
7	30	69.00
6	31	71.00
5	32	73.00
4	33	75.00
3	34	77.00
2	35	79.00
1	36	80.75

MATERIAL CHARACTERIZATION AND SEASONAL VARIATION IN MATERIAL PROPERTIES – INSTRUMENTATION INSTALLATION

Appendix D – Initial Data Collection

Appendix D contains the following supporting information:

FIGURE D.1: AIR TEMPERATURE AND FIRST FIVE SUB-SURFACE TEMPERATURES FROM INITIAL DATA COLLECTION, OCTOBER 29, 2001

FIGURE D.2: AVERAGE SUB-SURFACE TEMPERATURE FOR ALL SENSORS FROM INITIAL DATA COLLECTION, OCTOBER 29, 2001

FIGURE D.3: INITIAL SECOND SET OF TDR TRACES

FIGURE D.4: VOLTAGES MEASURED USING THE DATA COLLECTION SYSTEM DURING INITIAL DATA COLLECTION

FIGURE D.5: MANUALLY COLLECTED CONTACT RESISTANCE DURING INSTALLATION

FIGURE D.6: MANUALLY COLLECTED FOUR-POINT RESISTIVITY DURING INSTALLATION

TABLE D.1: SAMPLE DATA FROM THE ONSITE DATALOGGER DURING INITIAL DATA COLLECTION

TABLE D.2: MANUALLY COLLECTED CONTACT RESISTANCE DURING INSTALLATION

TABLE D.3: MANUALLY COLLECTED FOUR-POINT RESISTIVITY DURING INSTALLATION

TABLE D.4: ELEVATION MEASUREMENTS

**MATERIAL CHARACTERIZATION AND SEASONAL VARIATION IN
MATERIAL PROPERTIES – INSTRUMENTATION INSTALLATION**

APPENDIX D – INITIAL DATA COLLECTION

Table D.1
Sample Data from the Onsite Datalogger During Initial Data Collection

5, 2001, 339, 100, 12.95, 10.32, 0
6, 2001, 339, 100, 11.06, 11.69, 12.3, 12.57, 12.65
5, 2001, 339, 200, 12.96, 10.47, 0
6, 2001, 339, 200, 11.05, 11.62, 12.23, 12.51, 12.59
5, 2001, 339, 300, 12.96, 11.27, 0
6, 2001, 339, 300, 11.14, 11.6, 12.18, 12.45, 12.55
2, 2001, 339, 400, 10.98, 11.61, 12.21, 12.49, 12.57, 12.74, 12.86, 13.03, 14.22,
15.28, 15.86
3, 2001, 339, 400, 11.21, 230, 11.76, 4, 12.35, 4, 12.64, 4, 12.7, 2, 12.81, 0, 12.9,
0, 13.07, 157, 14.25, 1, 15.33, 3, 15.89, 1
4, 2001, 339, 400, 10.39, 351, 11.41, 359, 12.09, 345, 12.38, 327, 12.47, 343, 12.6
7, 311, 12.82, 228, 12.99, 4, 14.17, 257, 15.24, 218, 15.82, 230
5, 2001, 339, 400, 12.96, 9.38, 0
6, 2001, 339, 400, 10.66, 11.54, 12.14, 12.41, 12.5
5, 2001, 339, 500, 12.94, 9.2, 0
6, 2001, 339, 500, 10.26, 11.29, 12.06, 12.36, 12.47
5, 2001, 339, 600, 12.95, 10.31, 0
6, 2001, 339, 600, 10.45, 11.13, 11.96, 12.3, 12.42
5, 2001, 339, 700, 12.95, 11.17, 0
6, 2001, 339, 700, 10.74, 11.18, 11.89, 12.23, 12.37
2, 2001, 339, 800, 10.62, 11.22, 11.94, 12.27, 12.4, 12.62, 12.79, 13.03, 14.19, 1
5.25, 15.84
3, 2001, 339, 800, 11.28, 758, 11.42, 401, 12.14, 401, 12.4, 407, 12.51, 401, 12.7,
400, 12.84, 400, 13.07, 411, 14.22, 406, 15.3, 403, 15.89, 410
4, 2001, 339, 800, 10.16, 439, 11.11, 519, 11.85, 636, 12.14, 755, 12.29, 728, 12.5
3, 758, 12.72, 755, 12.98, 718, 14.16, 718, 15.21, 731, 15.8, 701
5, 2001, 339, 800, 13.03, 11.91, 0
6, 2001, 339, 800, 11.03, 11.27, 11.86, 12.18, 12.33
5, 2001, 339, 900, 13.42, 12.82, 0
6, 2001, 339, 900, 11.59, 11.46, 11.87, 12.15, 12.29
5, 2001, 339, 1000, 13.58, 14.04, 0
6, 2001, 339, 1000, 12.27, 11.74, 11.93, 12.16, 12.28
5, 2001, 339, 1100, 13.33, 16.69, 0
6, 2001, 339, 1100, 14.07, 12.34, 12.06, 12.2, 12.28
2, 2001, 339, 1200, 13.27, 12.16, 12.04, 12.2, 12.29, 12.51, 12.7, 12.98, 14.18, 1
5.22, 15.83
3, 2001, 339, 1200, 16.68, 1200, 13.5, 1200, 12.49, 1159, 12.42, 1200, 12.4, 1153,
12.58, 803, 12.78, 808, 13.04, 808, 14.22, 810, 15.27, 802, 15.88, 1113
4, 2001, 339, 1200, 11.27, 800, 11.32, 800, 11.84, 805, 12.11, 844, 12.24, 1033, 12
.44, 1047, 12.64, 1154, 12.91, 1107, 14.14, 1141, 15.16, 1027, 15.78, 1050
5, 2001, 339, 1200, 13.26, 17.81, 0
6, 2001, 339, 1200, 15.17, 13.11, 12.31, 12.31, 12.33
5, 2001, 339, 1300, 13.07, 21.27, 0
6, 2001, 339, 1300, 18.26, 14.21, 12.65, 12.49, 12.43
5, 2001, 339, 1400, 13.04, 22.91, 0
6, 2001, 339, 1400, 20.3, 15.75, 13.2, 12.77, 12.59
5, 2001, 339, 1500, 13.09, 22.35, 0
6, 2001, 339, 1500, 20.76, 16.93, 13.88, 13.18, 12.85

MATERIAL CHARACTERIZATION AND SEASONAL VARIATION IN MATERIAL PROPERTIES – INSTRUMENTATION INSTALLATION

APPENDIX D – INITIAL DATA COLLECTION

2, 2001, 339, 1600, 19.67, 16.06, 13.56, 13.02, 12.76, 12.69, 12.75, 12.96, 14.16, 15.19, 15.81
 3, 2001, 339, 1600, 20.92, 1420, 17.42, 1517, 14.73, 1559, 13.89, 1558, 13.35, 1557, 13.03, 1556, 12.94, 1551, 13.06, 1555, 14.21, 1203, 15.25, 1202, 15.87, 1205
 4, 2001, 339, 1600, 16.71, 1200, 13.46, 1200, 12.44, 1202, 12.36, 1203, 12.34, 1203, 12.46, 1203, 12.64, 1207, 12.91, 1204, 14.11, 1528, 15.14, 1542, 15.76, 1524
 5, 2001, 339, 1600, 13.46, 20.48, 0
 6, 2001, 339, 1600, 19.37, 17.35, 14.49, 13.65, 13.18
 5, 2001, 339, 1700, 13.21, 17.71, 0
 6, 2001, 339, 1700, 17.63, 16.98, 14.84, 14.05, 13.51

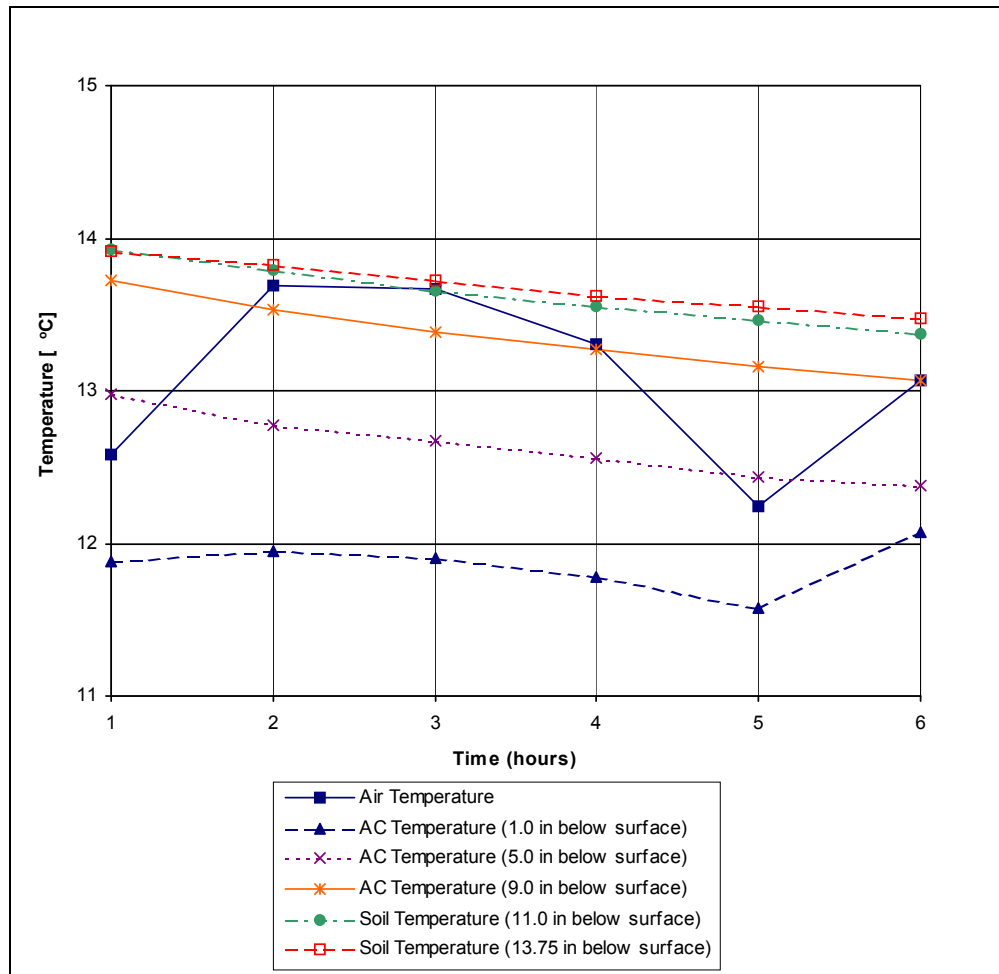


Figure D.1: Air Temperature and First Five Sub-Surface Temperatures from Initial Data Collection, October 29, 2001

MATERIAL CHARACTERIZATION AND SEASONAL VARIATION IN MATERIAL PROPERTIES – INSTRUMENTATION INSTALLATION

APPENDIX D – INITIAL DATA COLLECTION

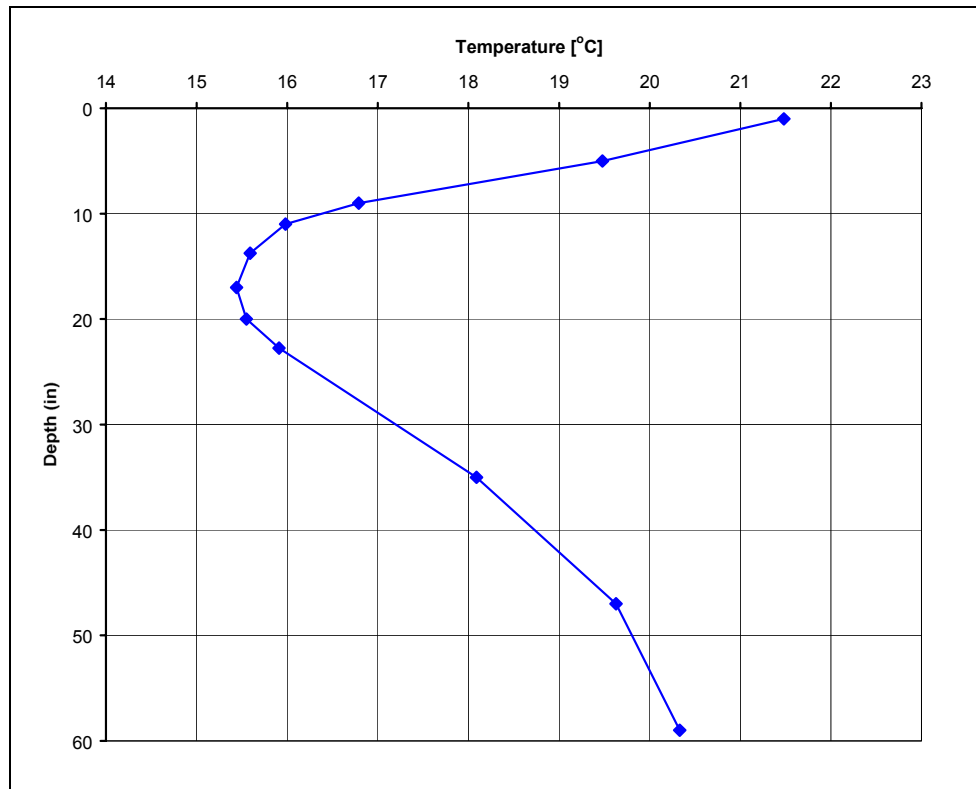


Figure D.2: Average Sub-Surface Temperature for all Sensors from Initial Data Collection, October 29, 2001

**MATERIAL CHARACTERIZATION AND SEASONAL VARIATION IN
MATERIAL PROPERTIES – INSTRUMENTATION INSTALLATION**

APPENDIX D – INITIAL DATA COLLECTION

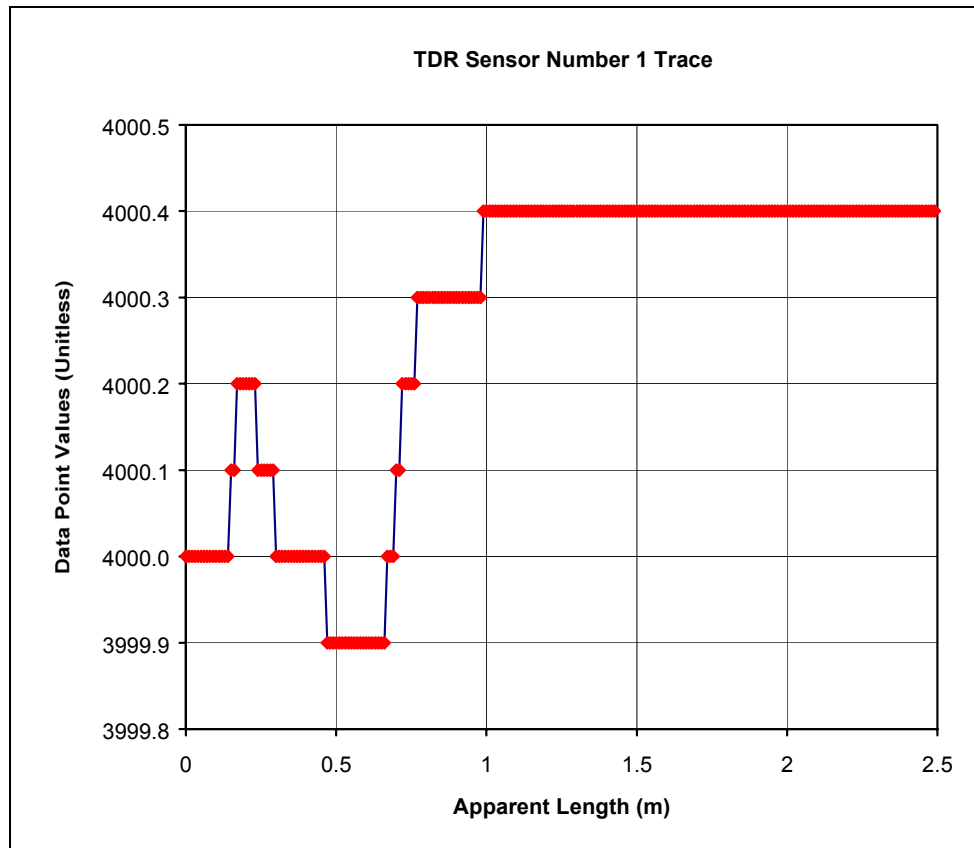


Figure D.3: Initial Second Set of TDR Traces

**MATERIAL CHARACTERIZATION AND SEASONAL VARIATION IN
MATERIAL PROPERTIES – INSTRUMENTATION INSTALLATION**

APPENDIX D – INITIAL DATA COLLECTION

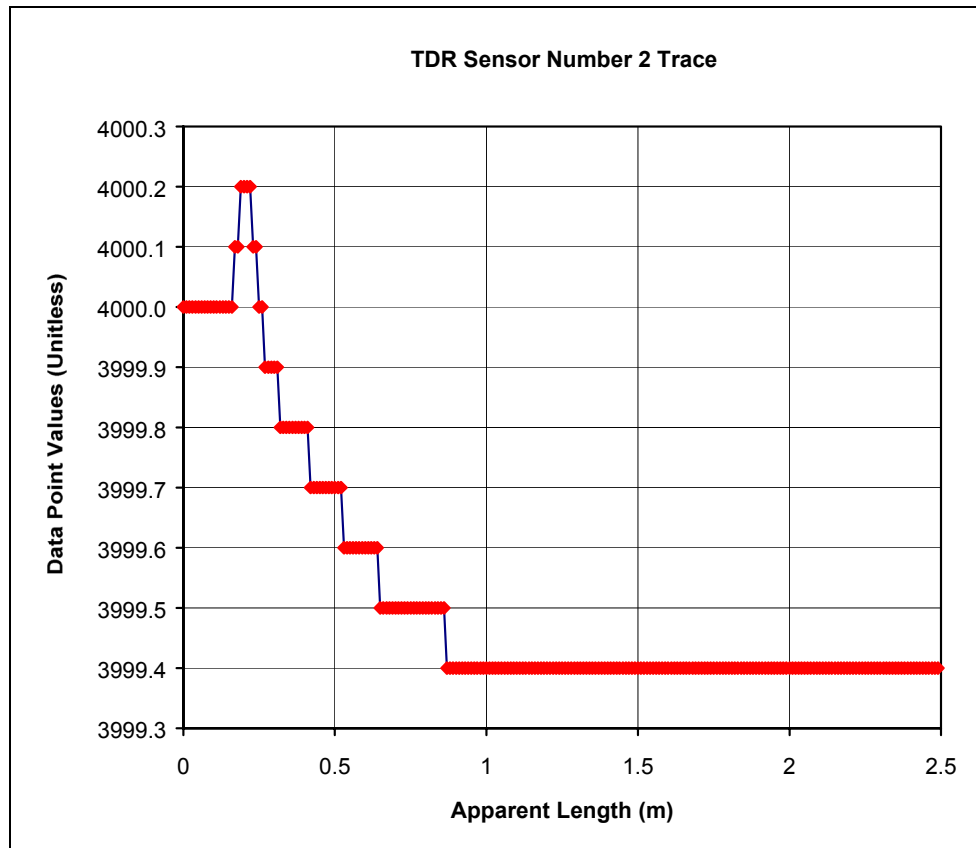


Figure D.3 (cont'd): Initial Second Set of TDR Traces

**MATERIAL CHARACTERIZATION AND SEASONAL VARIATION IN
MATERIAL PROPERTIES – INSTRUMENTATION INSTALLATION**

APPENDIX D – INITIAL DATA COLLECTION

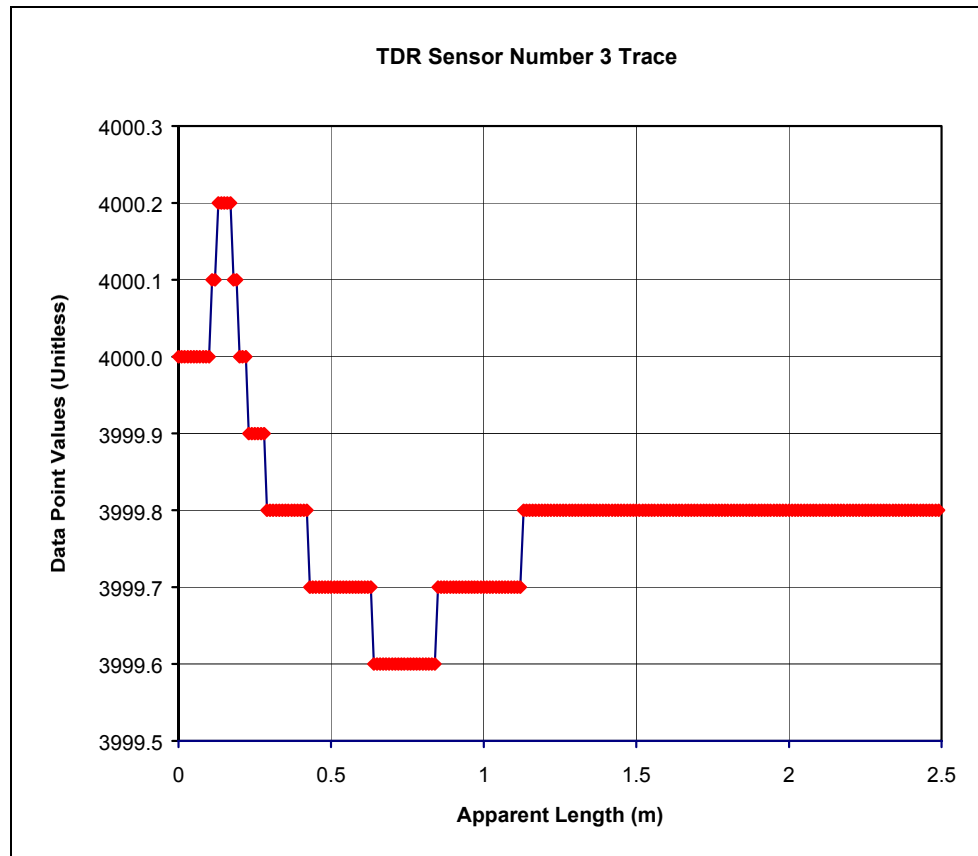


Figure D.3 (cont'd): Initial Second Set of TDR Traces

**MATERIAL CHARACTERIZATION AND SEASONAL VARIATION IN
MATERIAL PROPERTIES – INSTRUMENTATION INSTALLATION**

APPENDIX D – INITIAL DATA COLLECTION

Table D.2
Manually Collected Contact Resistance During Installation

Test Position	Switch Settings		Voltage (ACV)		Current (ACA)		Comments
	I1 V1	I2 V2	Range	Reading	Range	Reading	
1	1	2	mV	141.1	μA	45.1	
2	2	3		190.0		8.7	
3	3	4		189.1		8.0	
4	4	5		176.6		16.2	
5	5	6		170.4		20.4	
6	6	7		182.8		10.4	
7	7	8		185.2		7.8	
8	8	9		186.2		6.4	
9	9	10		184.2		5.2	
10	10	11		183.9		5.3	
11	11	12		182.6		5.8	
12	12	13		179.4		12.9	
13	13	14		177.5		8.1	
14	14	15		177.4		7.7	
15	15	16		157.3		22.9	
16	16	17		138.2		42.9	
17	17	18		54.8		98.1	
18	18	19		68.7		98.0	
19	19	20		68.4		97.5	
20	20	21		37.0		122.6	
21	21	22		177.6		9.2	
22	22	23		178.7		6.0	
23	23	24		178.7		5.8	
24	24	25		177.8		9.1	
25	25	26		33.9		121.7	
26	26	27		33.0		124.1	
27	27	28		56.4		103.8	
28	28	29		62.5		98.0	
29	29	30		48.5		110.3	
30	30	31		51.4		107.5	
31	31	32		80.8		80.8	
32	32	33		108.1		59.7	
33	33	34		116.2		52.8	
34	34	35		121.5		47.6	
35	35	36		127.0		43.2	
36	36	37		2.4		122.1	
37	37	38		17.2		134.9	
38	38	39		79.7		78.1	
39	39	00		175.6		0.6	

**MATERIAL CHARACTERIZATION AND SEASONAL VARIATION IN
MATERIAL PROPERTIES – INSTRUMENTATION INSTALLATION**

APPENDIX D – INITIAL DATA COLLECTION

Table D.3
Manually Collected Four-Point Resistivity During Installation

Test Position	Switch Settings				Voltage (ACV)		Current (ACA)		Comments
	I1	V1	V2	I2	Range	Reading	Range	Reading	
1	1	2	3	4	mV	16.8	μA	23.0	
2	2	3	4	5		7.5		19.1	
3	3	4	5	6		4.2		6.2	
4	4	5	6	7		3.0		7.3	
5	5	6	7	8		12.4		7.5	
6	6	7	8	9		13.4		5.2	
7	7	8	9	10		30.0		3.8	
8	8	9	10	11		24.2		6.1	
9	9	10	11	12		36.6		3.4	
10	10	11	12	13		39.5		4.3	
11	11	12	13	14		6.4		3.1	
12	12	13	14	15		5.2		10.7	
13	13	14	15	16		8.3		23.2	
14	14	15	16	17		4.4		8.1	
15	15	16	17	18		2.9		30.0	
16	16	17	18	19		2.3		39.0	
17	17	18	19	20		2.7		97.9	
18	18	19	20	21		3.5		115.2	
19	19	20	21	22		1.8		7.8	
20	20	21	22	23		21.9		8.7	
21	21	22	23	24		9.8		8.1	
22	22	23	24	25		8.8		8.1	
23	23	24	25	26		25.6		8.6	
24	24	25	26	27		1.8		8.0	
25	25	26	27	28		2.2		97.0	
26	26	27	28	29		2.7		109.4	
27	27	28	29	30		3.1		109.9	
28	28	29	30	31		2.8		89.8	
29	29	30	31	32		3.1		77.9	
30	30	31	32	33		4.2		66.2	
31	31	32	33	34		5.6		62.9	
32	32	33	34	35		6.0		48.6	
33	33	34	35	36		6.7		42.7	
36	36	36	37	37		2.5		127.1	
37	37	37	38	38		16.4		129.1	
38	38	38	39	39		76.3		74.8	
39	39	39	40	40		168.8		0.6	

MATERIAL CHARACTERIZATION AND SEASONAL VARIATION IN MATERIAL PROPERTIES – INSTRUMENTATION INSTALLATION

APPENDIX D – INITIAL DATA COLLECTION

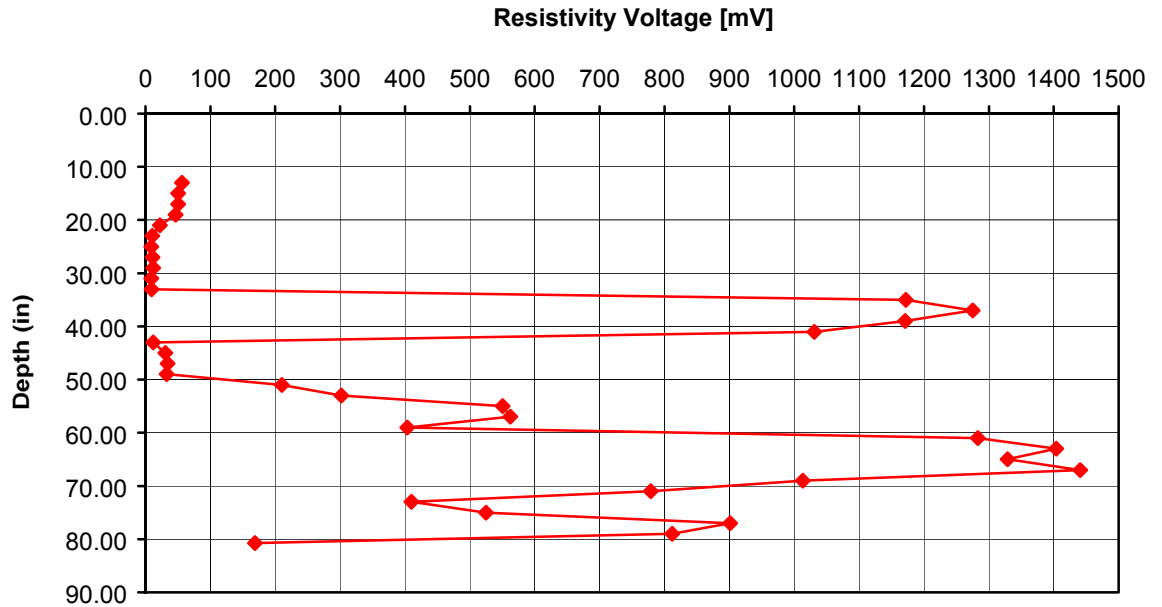


Figure D.4: Voltages Measured Using the Data Collection System During Initial Data Collection

MATERIAL CHARACTERIZATION AND SEASONAL VARIATION IN MATERIAL PROPERTIES – INSTRUMENTATION INSTALLATION

APPENDIX D – INITIAL DATA COLLECTION

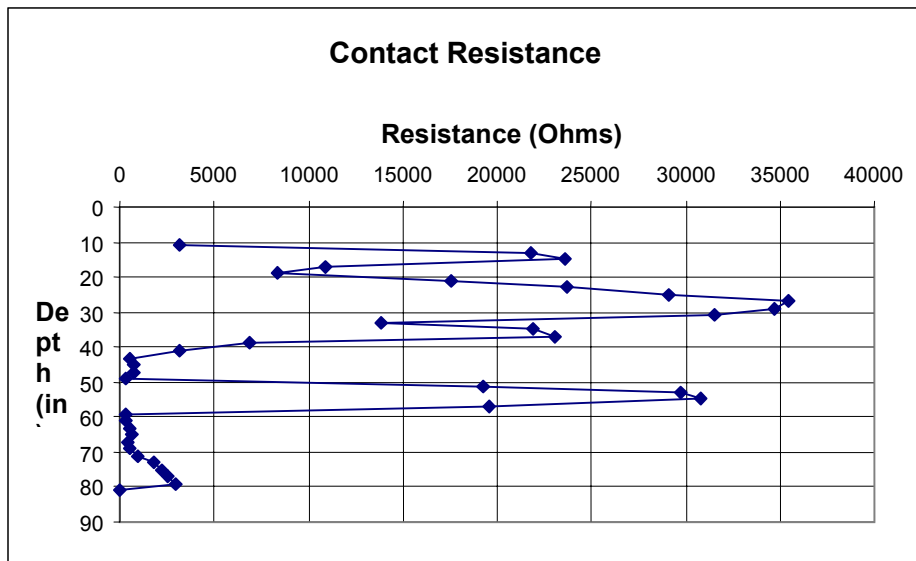


Figure D.5: Manually Collected Contact Resistance During installation

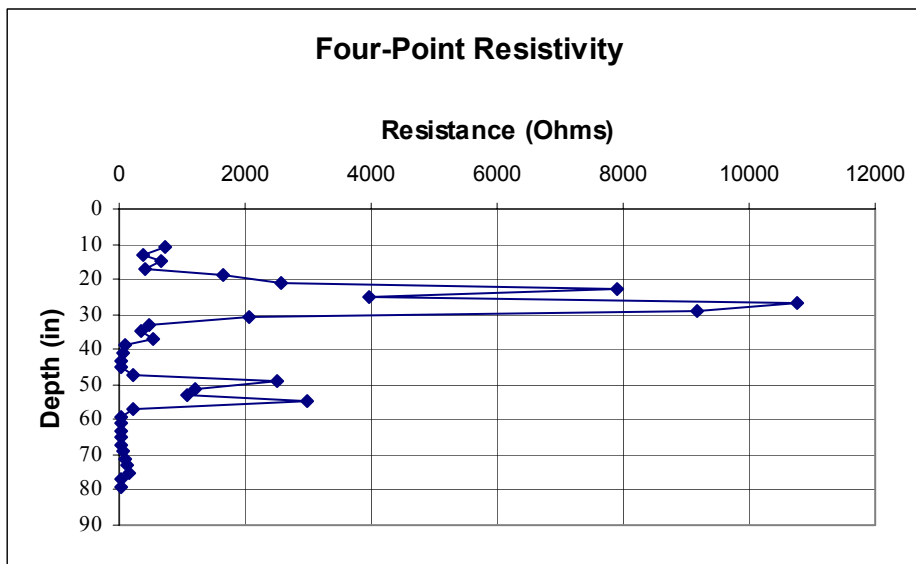


Figure D.6: Manually Collected Four-Point Resistivity During Installation

**MATERIAL CHARACTERIZATION AND SEASONAL VARIATION IN
MATERIAL PROPERTIES – INSTRUMENTATION INSTALLATION**

APPENDIX D – INITIAL DATA COLLECTION

Table D.4
Elevation Measurements

Description	Elevation (m)
Top of Instrumentation Hole	.81
Top of Piezometer	1.00
Water Level	-2.3

MATERIAL CHARACTERIZATION AND SEASONAL VARIATION IN MATERIAL PROPERTIES – INSTRUMENTATION INSTALLATION

Appendix E - Photographs

Appendix E contains the following supporting information:

FIGURE E.1: CORING THE INSTRUMENTATION HOLE

FIGURE E.2: REMOVING THE INSTRUMENTATION HOLE CORE

FIGURE E.3: INSTALLING MRC AND THERMISTOR PROBES

FIGURE E.4. INSTALLED MRC PAVEMENT PROBES

FIGURE E.5. VIEW OF TRENCH WITH EQUIPMENT CABINET HOLE IN FOREGROUND

FIGURE E.6. COMPACTING THE TRENCH BEFORE LAYING THE CONDUIT

FIGURE E.7. REPLACING THE INSTRUMENTATION HOLE CORE

FIGURE E.8. ASSEMBLED WEATHER POLE AND EQUIPMENT CABINET

**MATERIAL CHARACTERIZATION AND SEASONAL VARIATION IN
MATERIAL PROPERTIES – INSTRUMENTATION INSTALLATION**
APPENDIX E - PHOTOGRAPHS



Figure E.1: Coring the Instrumentation Hole



Figure E.2: Removing the Instrumentation Hole Core



Figure E.3: Installing MRC and Thermistor Probes



Figure E.4: Installed MRC Pavement Probes

**MATERIAL CHARACTERIZATION AND SEASONAL VARIATION IN
MATERIAL PROPERTIES – INSTRUMENTATION INSTALLATION**

APPENDIX E - PHOTOGRAPHS



Figure E.5: View of Trench with Equipment Cabinet Hole in Foreground



Figure E.6: Compacting the Trench before Laying the Conduit

**MATERIAL CHARACTERIZATION AND SEASONAL VARIATION IN
MATERIAL PROPERTIES – INSTRUMENTATION INSTALLATION**
APPENDIX E - PHOTOGRAPHS



Figure E.7: Replacing the Instrumentation Hole Core

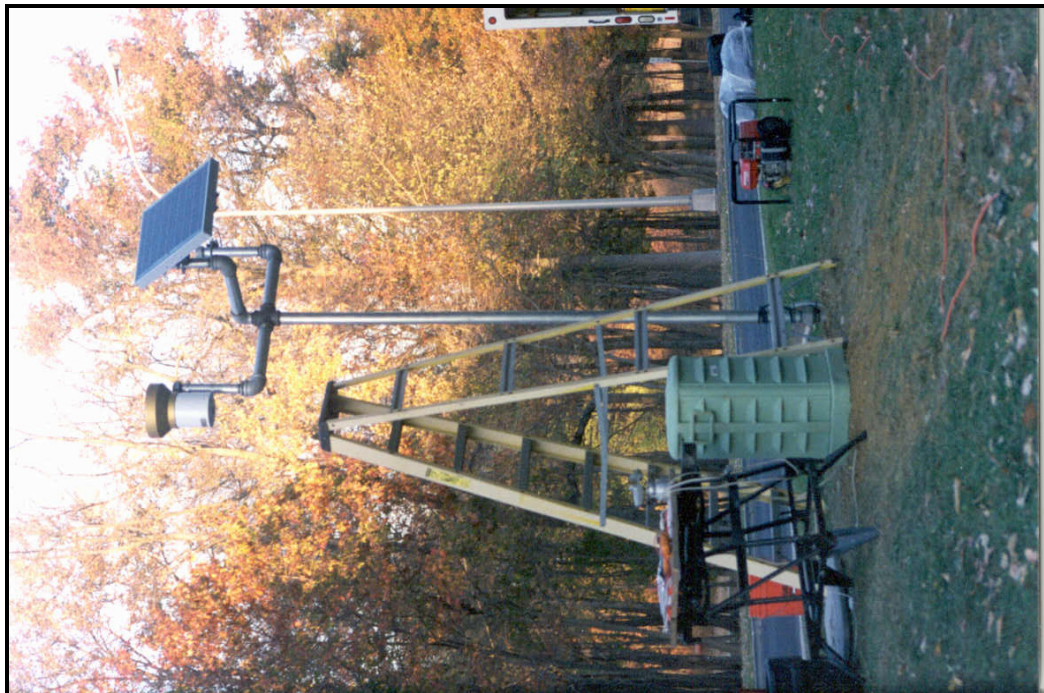


Figure E.8: Assembled Weather Pole and Equipment Cabinet

APPENDIX B

MATERIAL CHARACTERIZATION AND SEASONAL VARIATION IN MATERIAL PROPERTIES

List of Figures

Figure B.1: Variation of Delta Deflection with MC and Pavement Temperature MC=L, PavTemp=L, GWT= L, RF=L.....	B.245
Figure B.2: Variation of Delta Deflection with MC and Pavement Temperature MC=L, PavTemp=L, GWT= L, RF=L.....	B.246
Figure B.3: Variation of Delta Deflection with MC and Pavement Temperature MC=L, PavTemp=L, GWT= L, RF=H.....	B.247
Figure B.4: Variation of Delta Deflection with MC and Pavement Temperature MC=L, PavTemp=L, GWT= L, RF=H.....	B.248
Figure B.5: Variation of Delta Deflection with MC and Pavement Temperature MC=L, PavTemp=L, GWT= H, RF=L.....	B.249
Figure B.6: Variation of Delta Deflection with MC and Pavement Temperature MC=L, PavTemp=L, GWT= H, RF=L.....	B.250
Figure B.7: Variation of Delta Deflection with MC and Pavement Temperature MC=L, PavTemp=L, GWT= H, RF=H.....	B.251
Figure B.8: Variation of Delta Deflection with MC and Pavement Temperature MC=L, PavTemp=L, GWT= H, RF=H.....	B.252
Figure B.9: Variation of Delta Deflection with MC and Pavement Temperature MC=L, PavTemp=H, GWT= L, RF=L.....	B.253
Figure B.10: Variation of Delta Deflection with MC and Pavement Temperature MC=L, PavTemp=H, GWT= L, RF=L.....	B.254
Figure B.11: Variation of Delta Deflection with MC and Pavement Temperature MC=L, PavTemp=H, GWT= L, RF=H.....	B.255
Figure B.12: Variation of Delta Deflection with MC and Pavement Temperature MC=L, PavTemp=H, GWT= L, RF=H.....	B.256
Figure B.13: Variation of Delta Deflection with MC and Pavement Temperature MC=L, PavTemp=H, GWT= H, RF=L.....	B.257
Figure B.14: Variation of Delta Deflection with MC and Pavement Temperature MC=L, PavTemp=H, GWT= H, RF=L.....	B.258
Figure B.15: Variation of Delta Deflection with MC and Pavement Temperature MC=L, PavTemp=H, GWT= H, RF=H.....	B.259
Figure B.16: Variation of Delta Deflection with MC and Pavement Temperature MC=L, PavTemp=H, GWT= H, RF=H.....	B.260
Figure B.17: Variation of Delta Deflection with MC and Pavement Temperature MC=H, PavTemp=L, GWT= L, RF=L.....	B.261
Figure B.18: Variation of Delta Deflection with MC and Pavement Temperature MC=H, PavTemp=L, GWT= L, RF=L.....	B.262
Figure B.19: Variation of Delta Deflection with MC and Pavement Temperature MC=H, PavTemp=L, GWT= H, RF=L.....	B.263
Figure B.20: Variation of Delta Deflection with MC and Pavement Temperature MC=H, PavTemp=L, GWT= H, RF=L.....	B.264
Figure B.21: Variation of Delta Deflection with MC and Pavement Temperature MC=H, PavTemp=L, GWT= H, RF=H.....	B.265
Figure B.22: Variation of Delta Deflection with MC and Pavement Temperature MC=H, PavTemp=H, GWT= L, RF=H.....	B.266
Figure B.23: Variation of Delta Deflection with MC and Pavement Temperature MC=H, PavTemp=H, GWT= L, RF=H.....	B.267

MATERIAL CHARACTERIZATION AND SEASONAL VARIATION IN MATERIAL PROPERTIES

Appendix B: Results of Sensitivity Analysis for Regression Models

July 22, 2005

Figure B.24: Variation of Delta Deflection with MC and Pavement Temperature
MC=H, PavTemp=H, GWT= H, RF=HB.268

Figure B.25: Variation of Delta Deflection with MC and Pavement Temperature
MC=H, PavTemp=H, GWT= H, RF=HB.269

MATERIAL CHARACTERIZATION AND SEASONAL VARIATION IN MATERIAL PROPERTIES

Appendix B: Results of Sensitivity Analysis for Regression Models

July 22, 2005

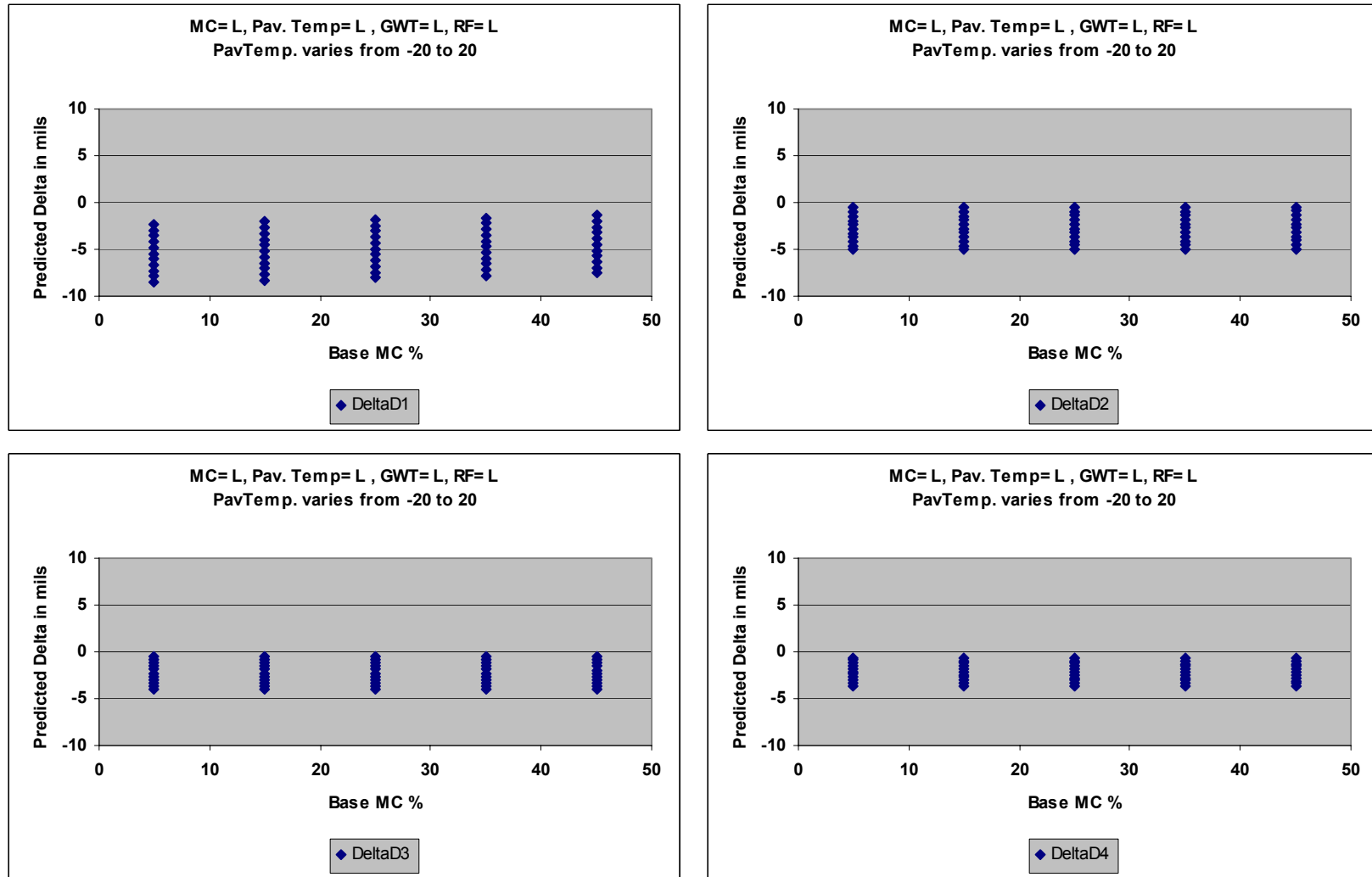


Figure B.1: Variation of Delta Deflection with MC and Pavement Temperature
MC=L, PavTemp=L, GWT=L, RF=L

MATERIAL CHARACTERIZATION AND SEASONAL VARIATION IN MATERIAL PROPERTIES

Appendix B: Results of Sensitivity Analysis for Regression Models

July 22, 2005

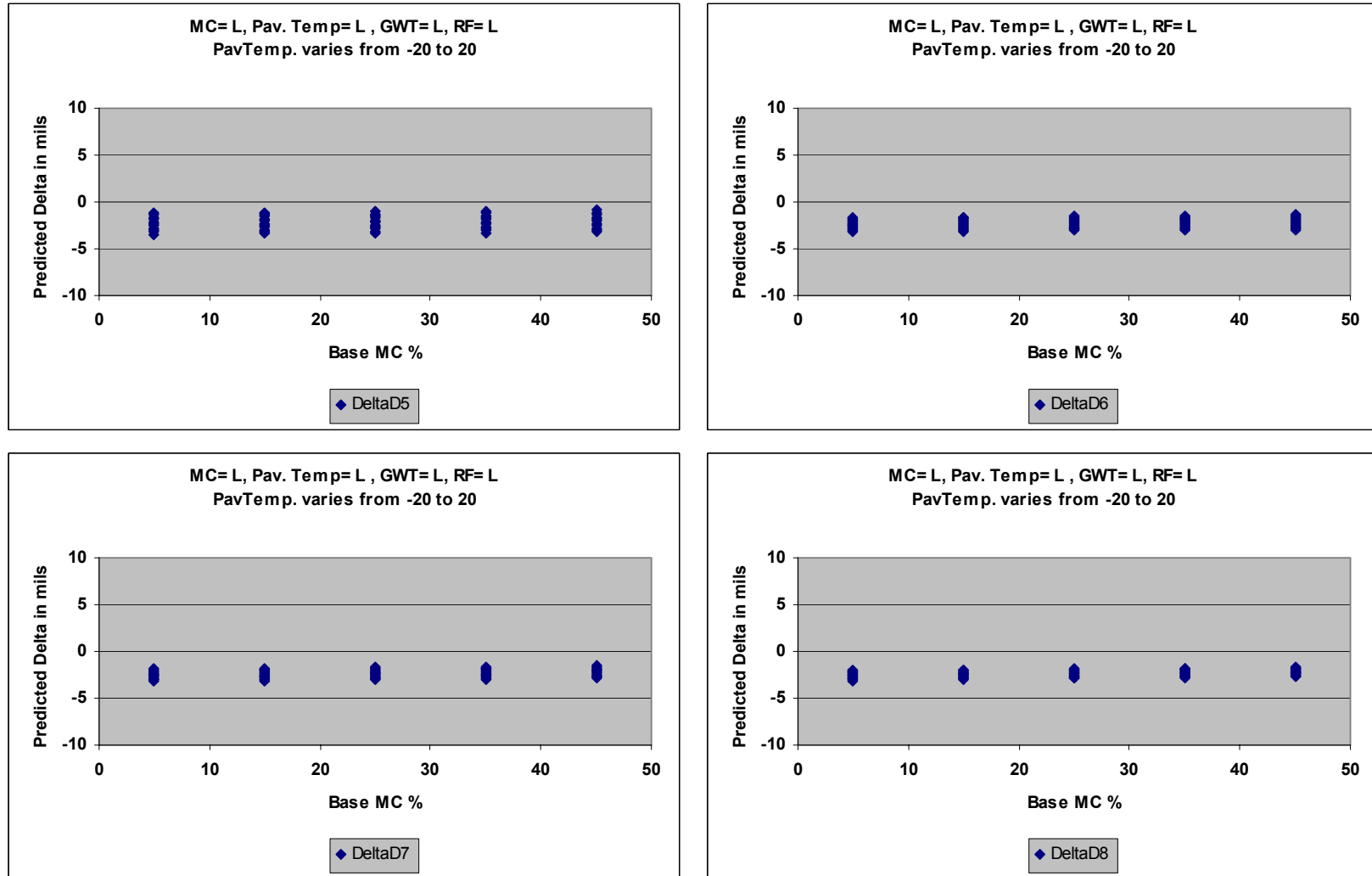


Figure B.2: Variation of Delta Deflection with MC and Pavement Temperature
MC=L, PavTemp=L, GWT=L, RF=L

MATERIAL CHARACTERIZATION AND SEASONAL VARIATION IN MATERIAL PROPERTIES

Appendix B: Results of Sensitivity Analysis for Regression Models

July 22, 2005

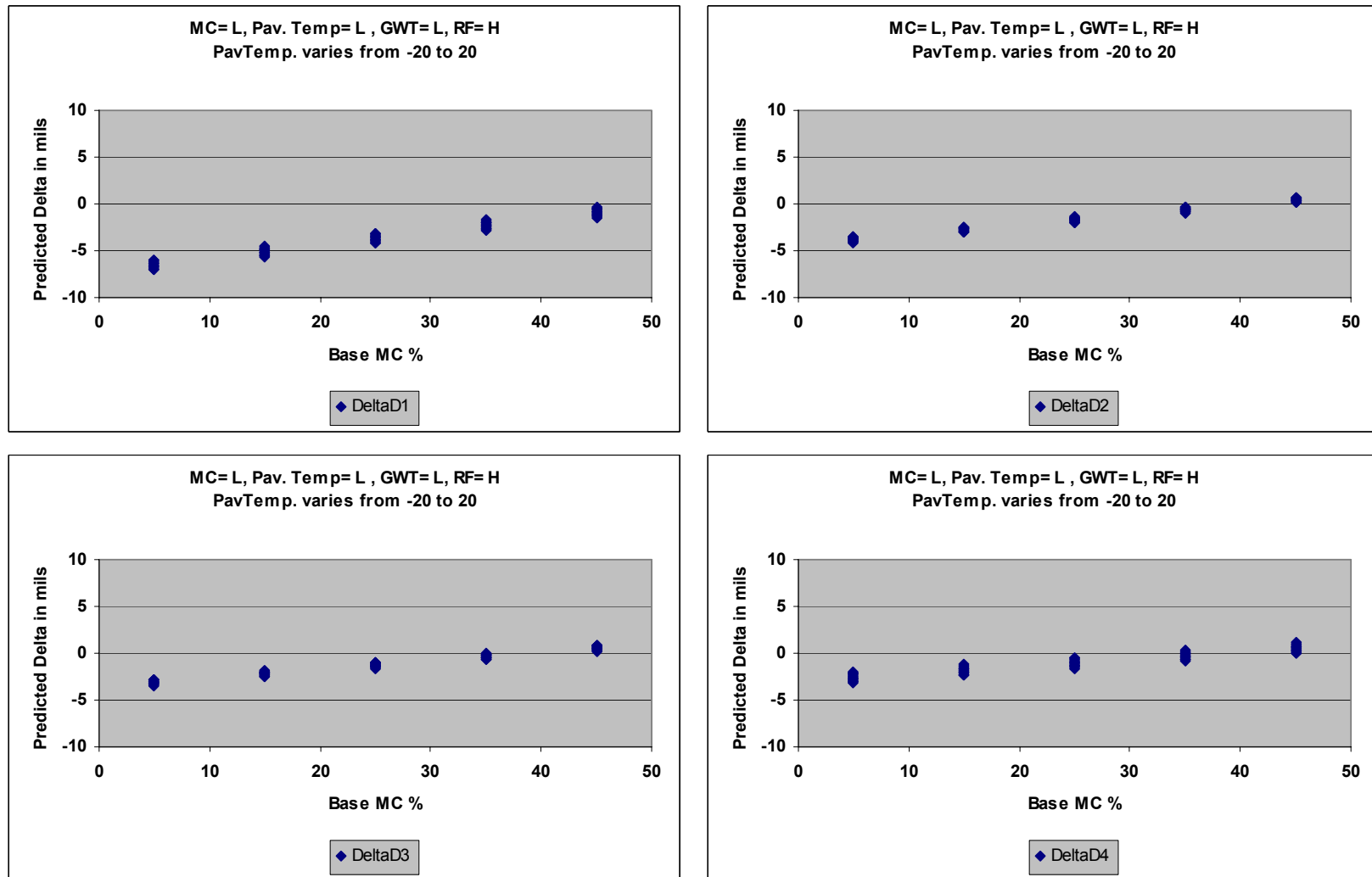


Figure B.3: Variation of Delta Deflection with MC and Pavement Temperature
MC=L, PavTemp=L, GWT=L, RF=H

MATERIAL CHARACTERIZATION AND SEASONAL VARIATION IN MATERIAL PROPERTIES

Appendix B: Results of Sensitivity Analysis for Regression Models

July 22, 2005

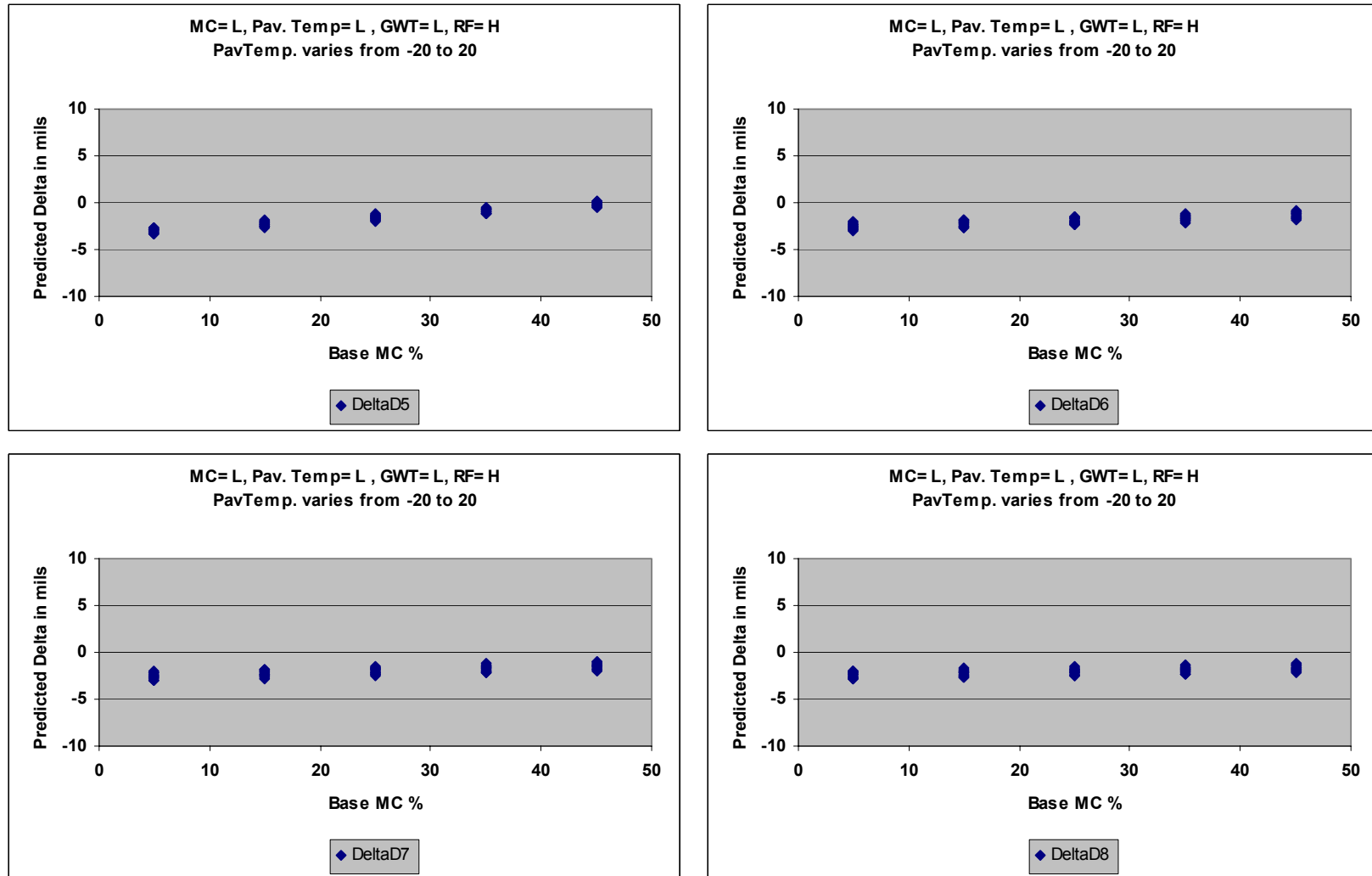


Figure B.4: Variation of Delta Deflection with MC and Pavement Temperature
MC=L, PavTemp=L, GWT=L, RF=H

MATERIAL CHARACTERIZATION AND SEASONAL VARIATION IN MATERIAL PROPERTIES

Appendix B: Results of Sensitivity Analysis for Regression Models

July 22, 2005

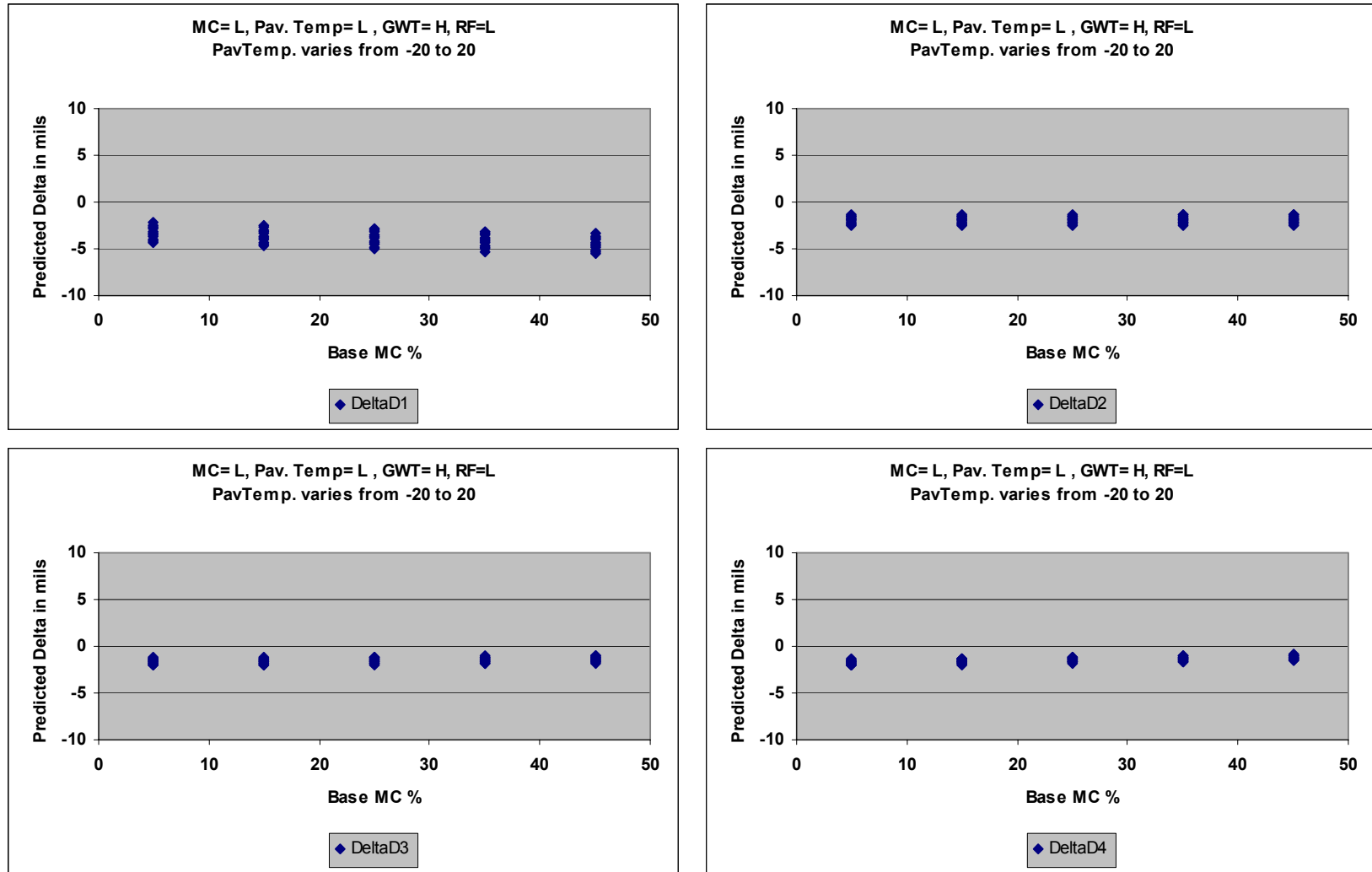


Figure B.5: Variation of Delta Deflection with MC and Pavement Temperature
MC=L, PavTemp=L, GWT= H, RF=L

MATERIAL CHARACTERIZATION AND SEASONAL VARIATION IN MATERIAL PROPERTIES

Appendix B: Results of Sensitivity Analysis for Regression Models

July 22, 2005

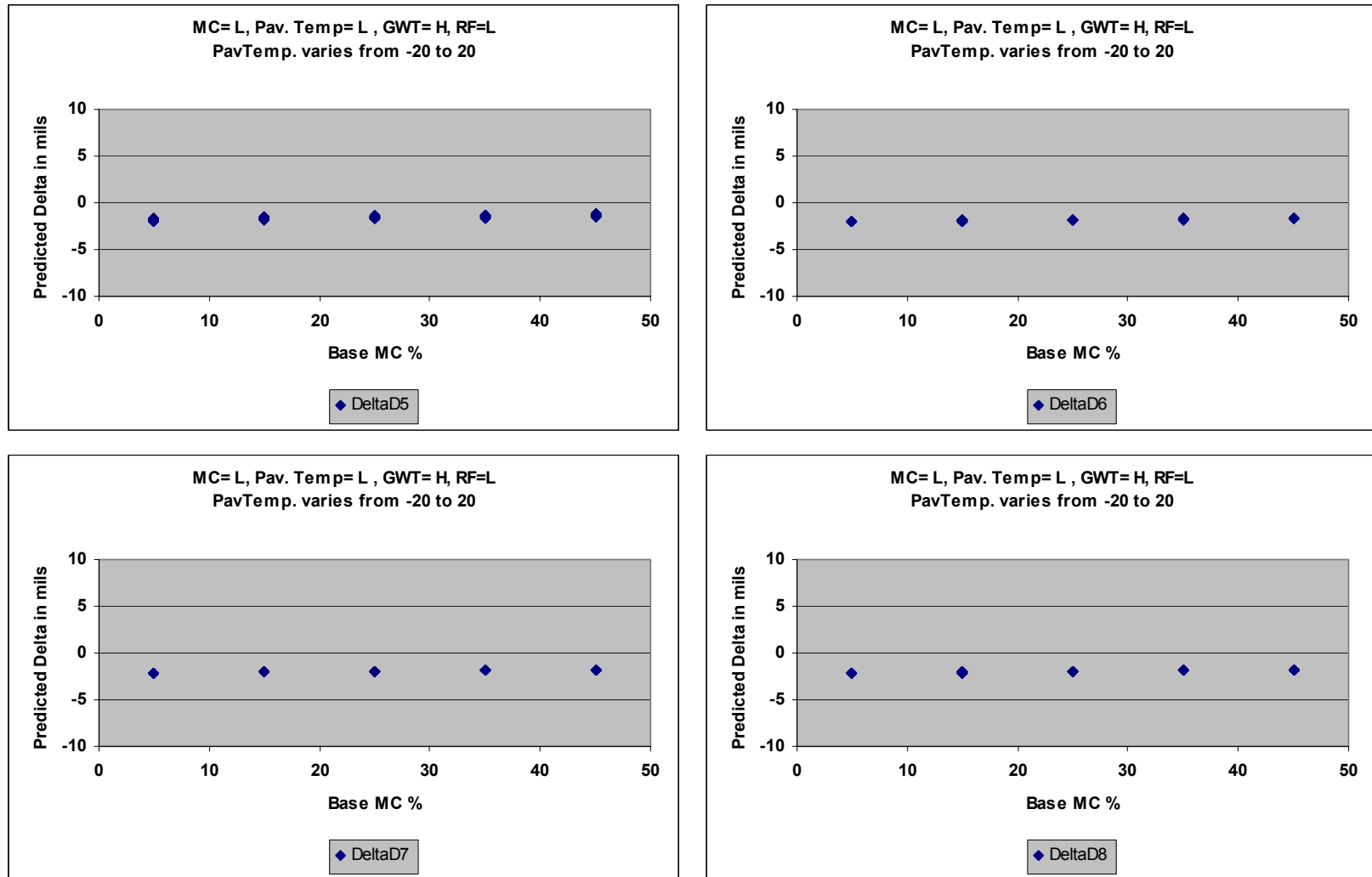


Figure B.6: Variation of Delta Deflection with MC and Pavement Temperature
MC=L, PavTemp=L, GWT= H, RF=L

MATERIAL CHARACTERIZATION AND SEASONAL VARIATION IN MATERIAL PROPERTIES

Appendix B: Results of Sensitivity Analysis for Regression Models

July 22, 2005

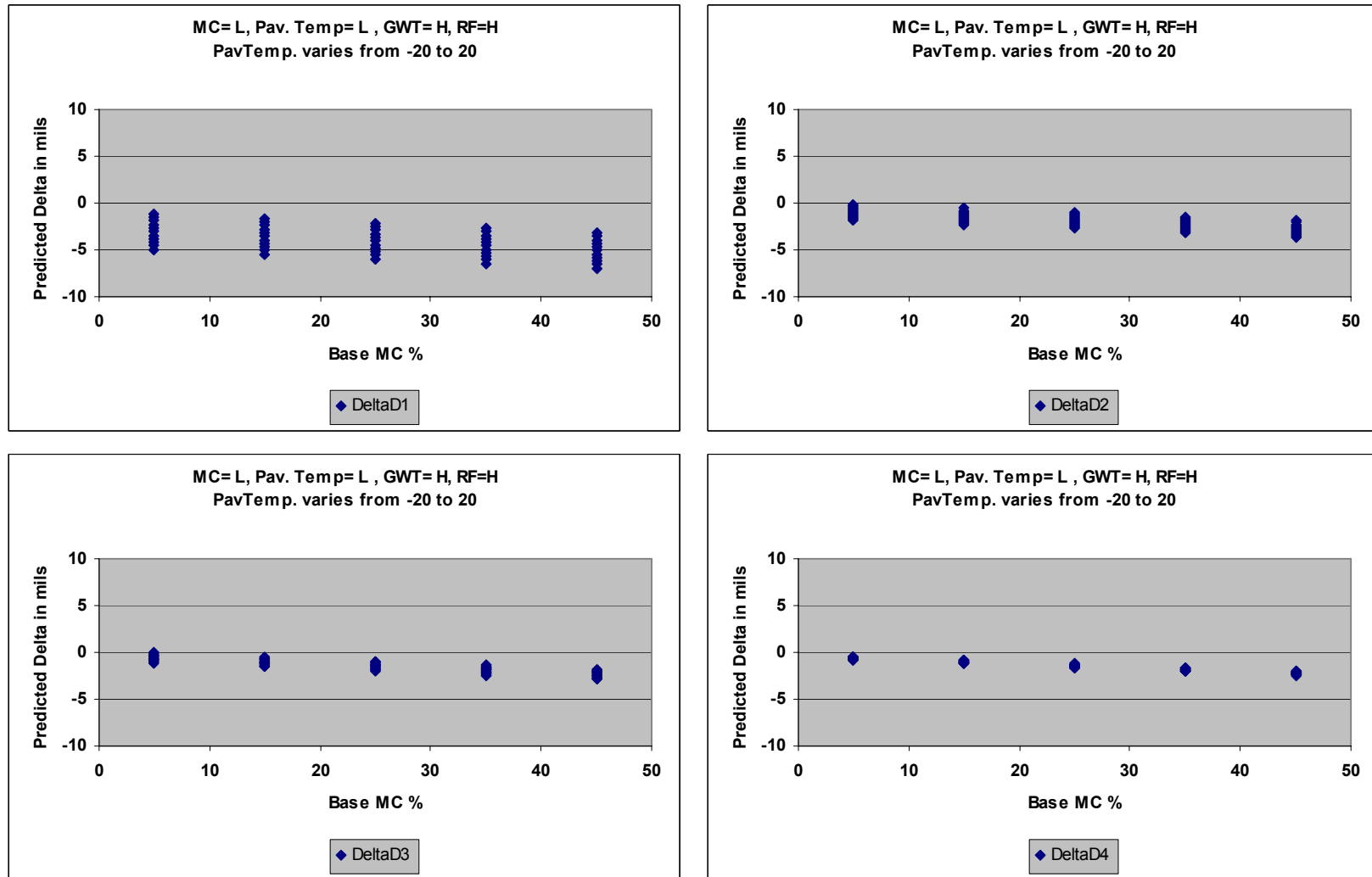


Figure B.7: Variation of Delta Deflection with MC and Pavement Temperature
MC=L, PavTemp=L, GWT=H, RF=H

MATERIAL CHARACTERIZATION AND SEASONAL VARIATION IN MATERIAL PROPERTIES

Appendix B: Results of Sensitivity Analysis for Regression Models

July 22, 2005

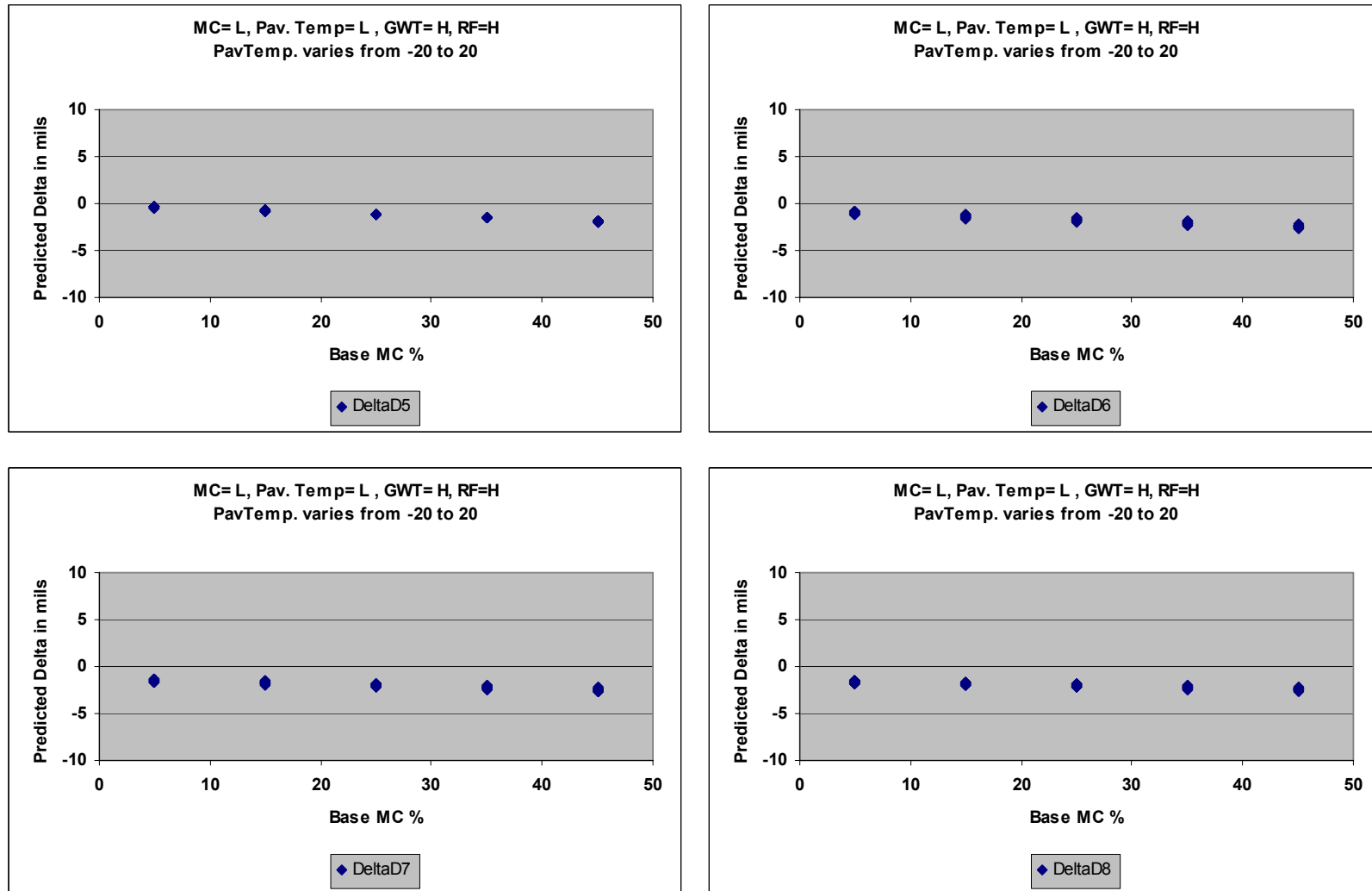


Figure B.8: Variation of Delta Deflection with MC and Pavement Temperature
MC=L, PavTemp=L, GWT= H, RF=H

MATERIAL CHARACTERIZATION AND SEASONAL VARIATION IN MATERIAL PROPERTIES

Appendix B: Results of Sensitivity Analysis for Regression Models

July 22, 2005

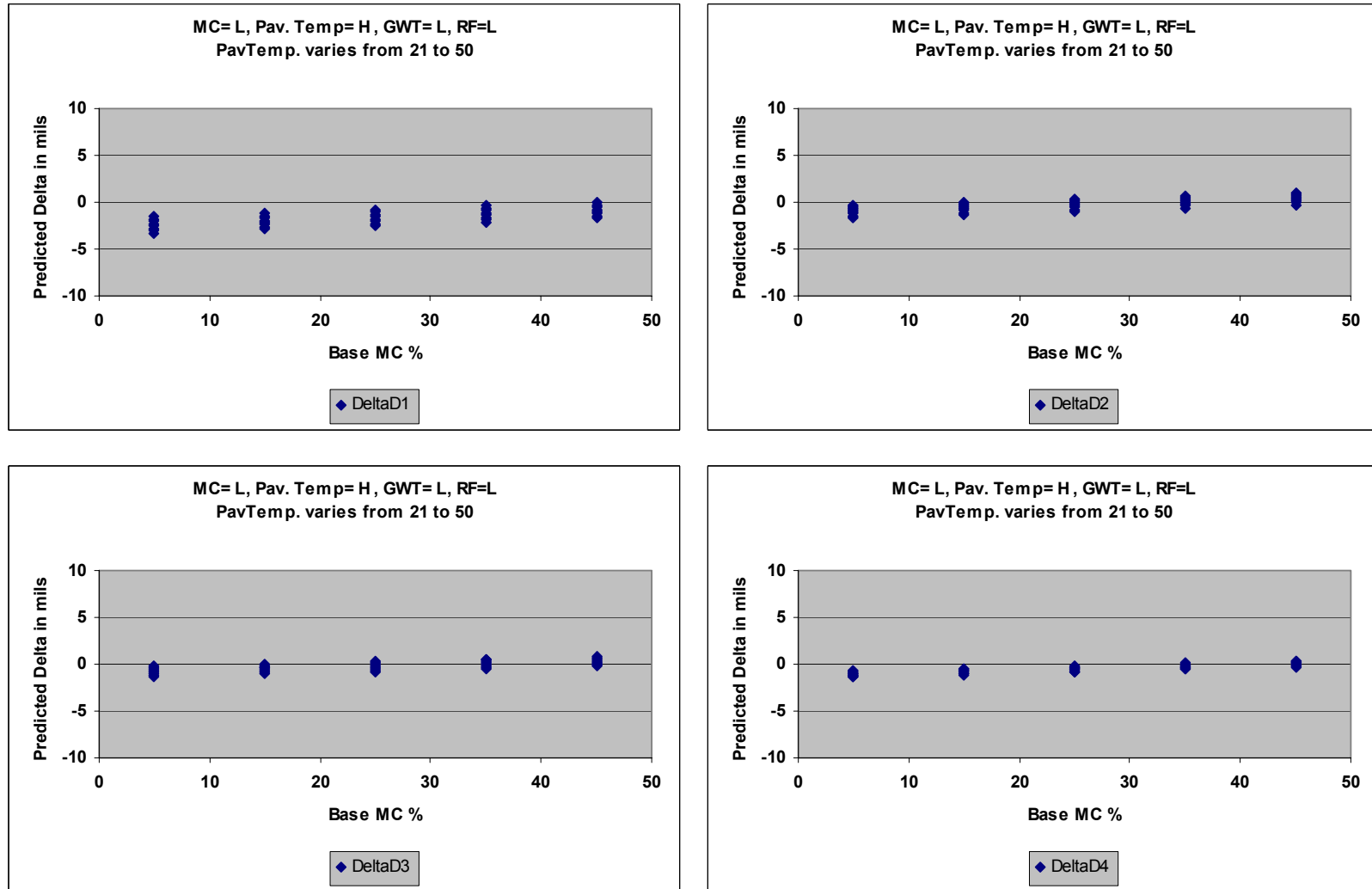


Figure B.9: Variation of Delta Deflection with MC and Pavement Temperature
MC=L, PavTemp=H, GWT= L, RF=L

MATERIAL CHARACTERIZATION AND SEASONAL VARIATION IN MATERIAL PROPERTIES

Appendix B: Results of Sensitivity Analysis for Regression Models

July 22, 2005

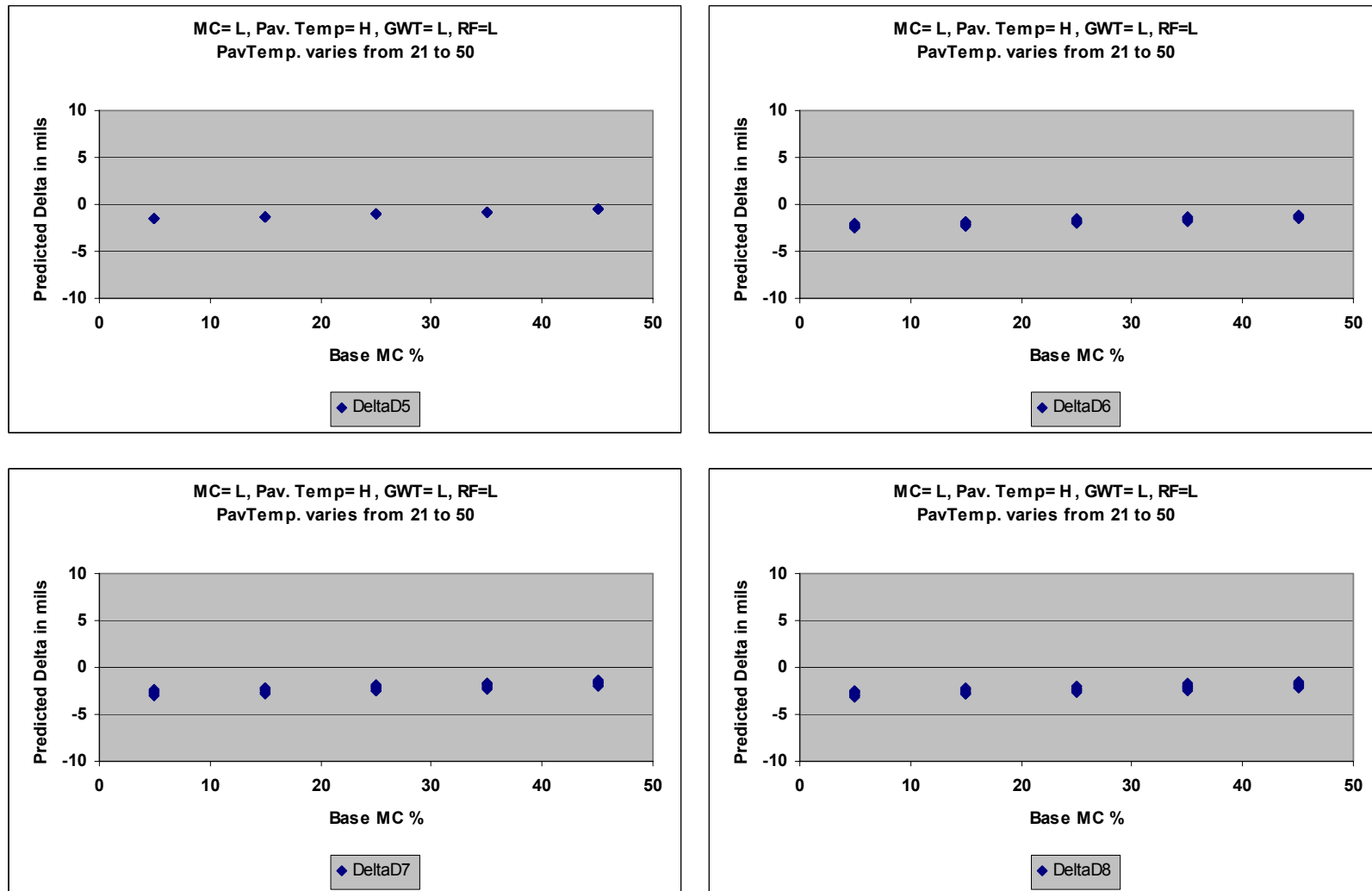


Figure B.10: Variation of Delta Deflection with MC and Pavement Temperature
MC=L, PavTemp=H, GWT= L, RF=L

MATERIAL CHARACTERIZATION AND SEASONAL VARIATION IN MATERIAL PROPERTIES

Appendix B: Results of Sensitivity Analysis for Regression Models

July 22, 2005

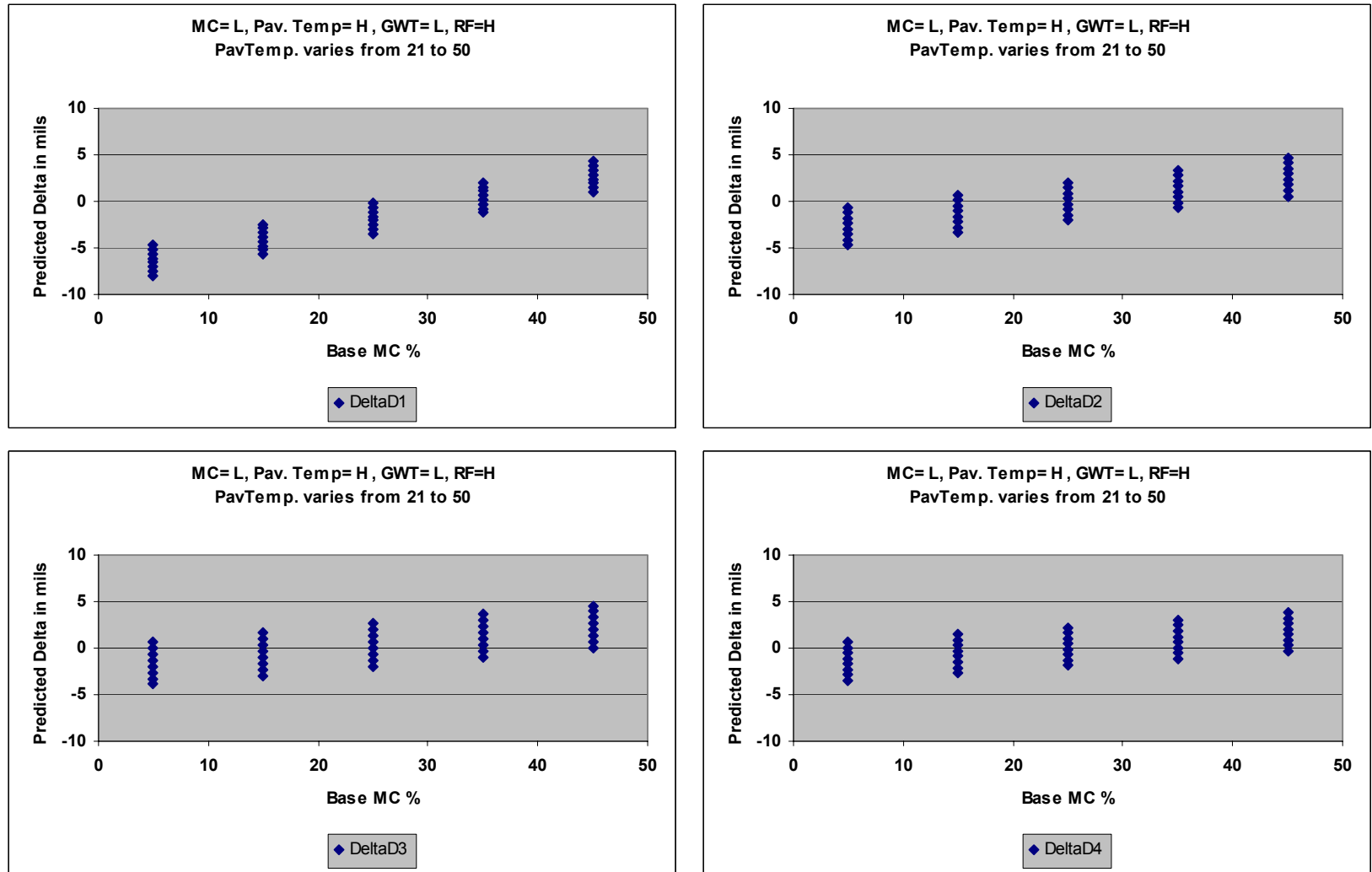


Figure B.11: Variation of Delta Deflection with MC and Pavement Temperature
MC=L, PavTemp=H, GWT= L, RF=H

MATERIAL CHARACTERIZATION AND SEASONAL VARIATION IN MATERIAL PROPERTIES

Appendix B: Results of Sensitivity Analysis for Regression Models

July 22, 2005

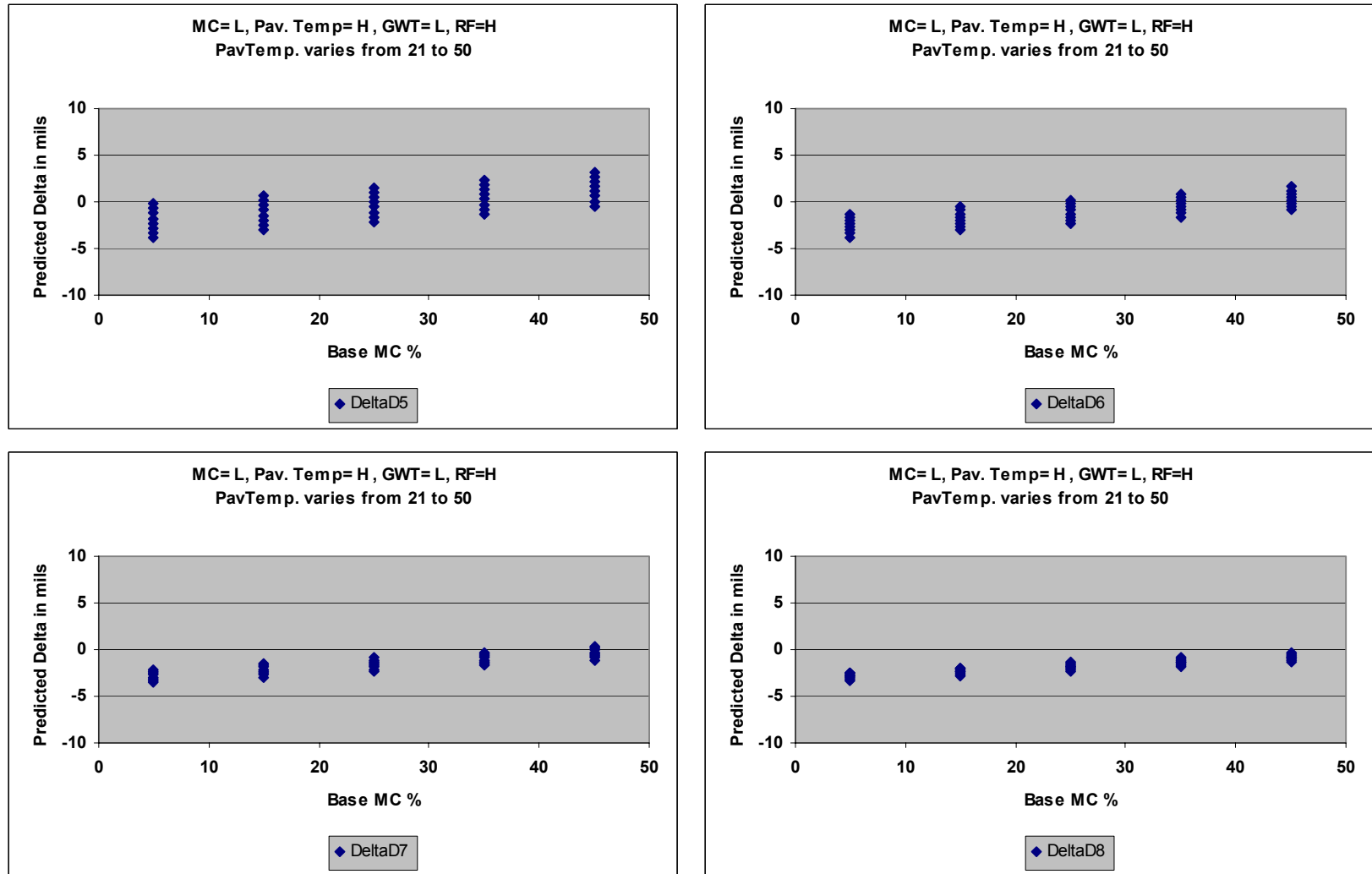


Figure B.12: Variation of Delta Deflection with MC and Pavement Temperature
MC=L, PavTemp=H, GWT= L, RF=H

MATERIAL CHARACTERIZATION AND SEASONAL VARIATION IN MATERIAL PROPERTIES

Appendix B: Results of Sensitivity Analysis for Regression Models

July 22, 2005

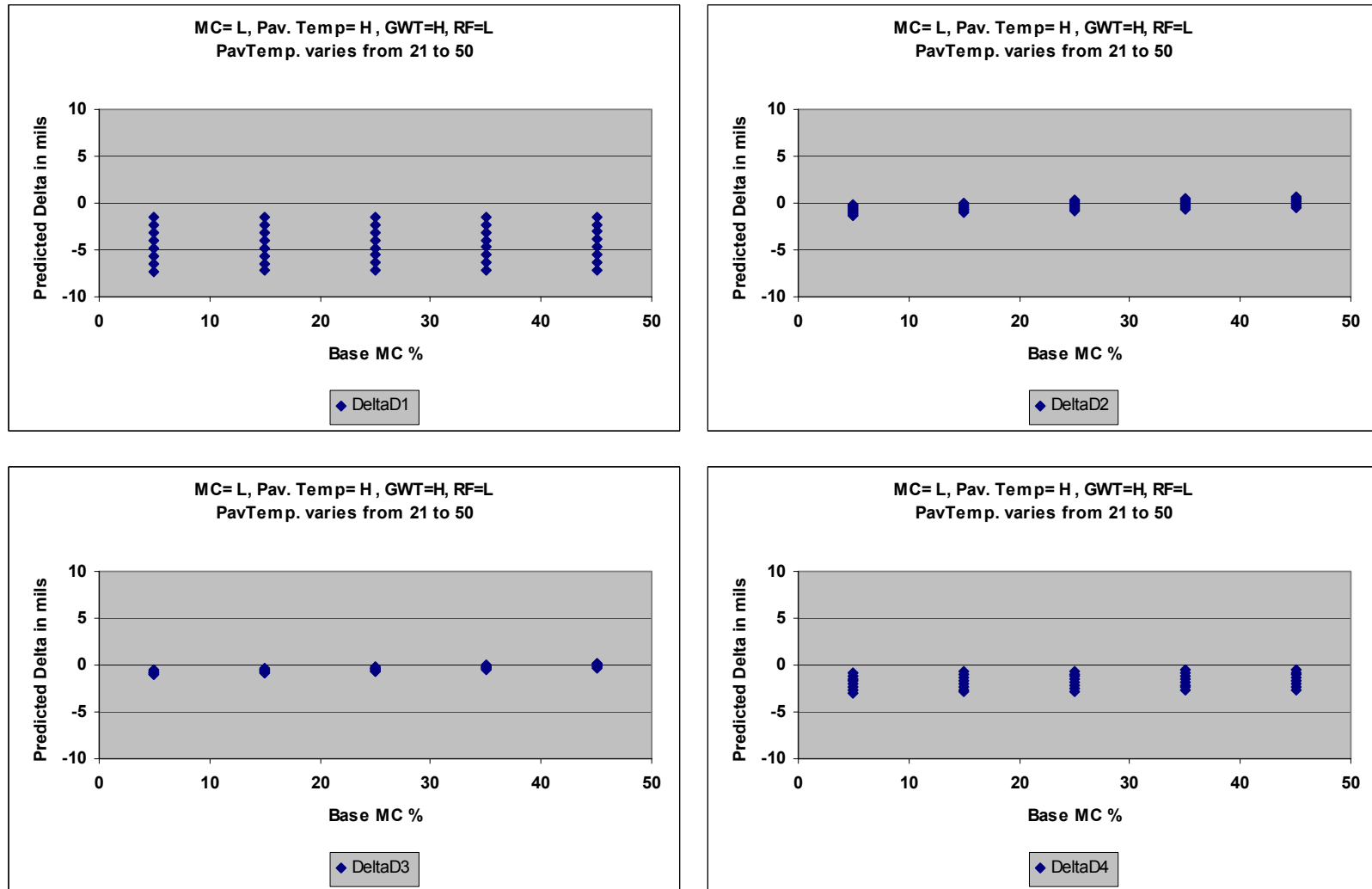


Figure B.13: Variation of Delta Deflection with MC and Pavement Temperature
MC=L, PavTemp=H, GWT= H, RF=L

MATERIAL CHARACTERIZATION AND SEASONAL VARIATION IN MATERIAL PROPERTIES

Appendix B: Results of Sensitivity Analysis for Regression Models

July 22, 2005

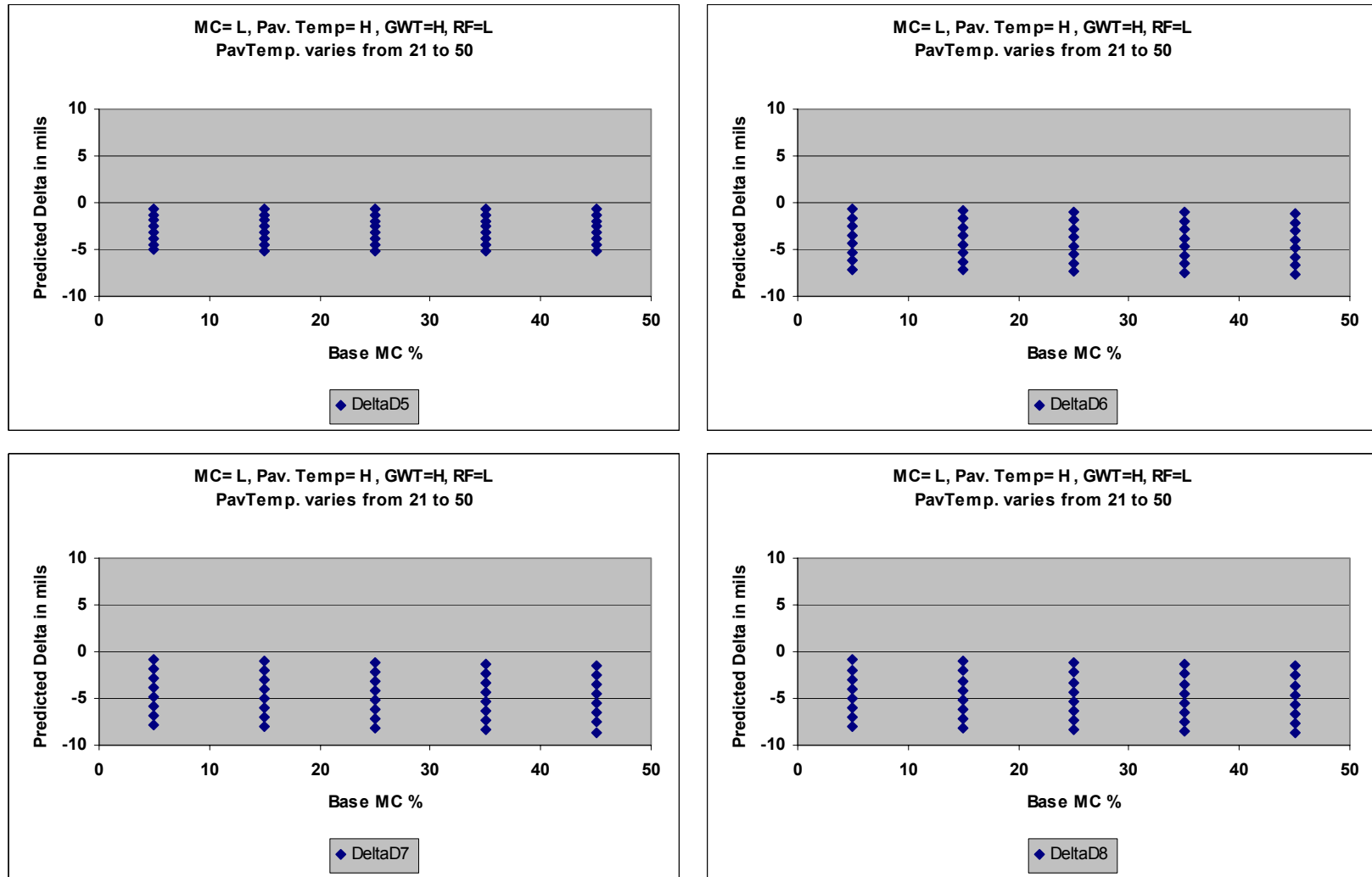


Figure B.14: Variation of Delta Deflection with MC and Pavement Temperature
MC=L, PavTemp=H, GWT= H, RF=L

MATERIAL CHARACTERIZATION AND SEASONAL VARIATION IN MATERIAL PROPERTIES

Appendix B: Results of Sensitivity Analysis for Regression Models

July 22, 2005

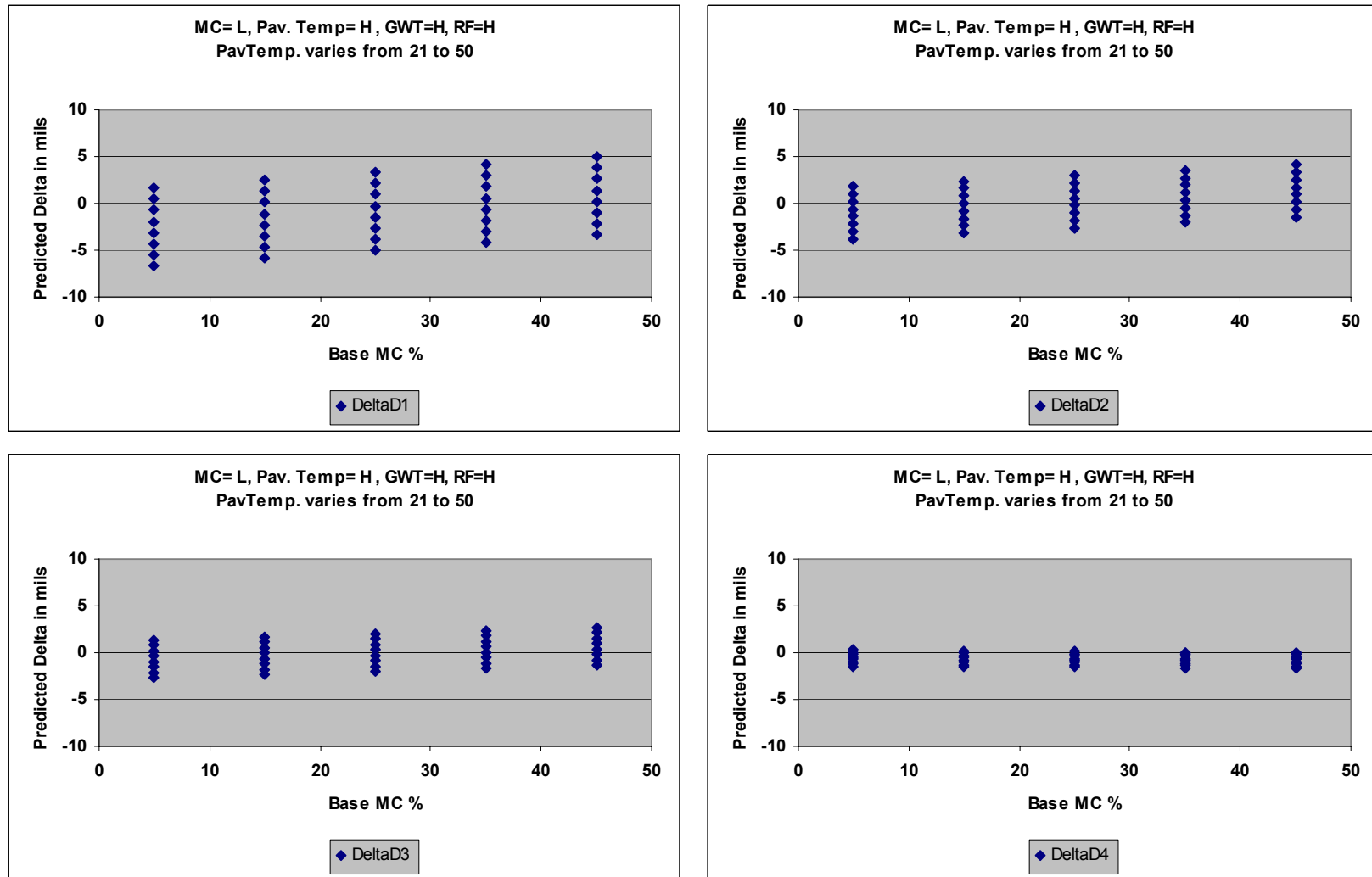


Figure B.15: Variation of Delta Deflection with MC and Pavement Temperature
MC=L, PavTemp=H, GWT= H, RF=H

MATERIAL CHARACTERIZATION AND SEASONAL VARIATION IN MATERIAL PROPERTIES

Appendix B: Results of Sensitivity Analysis for Regression Models

July 22, 2005

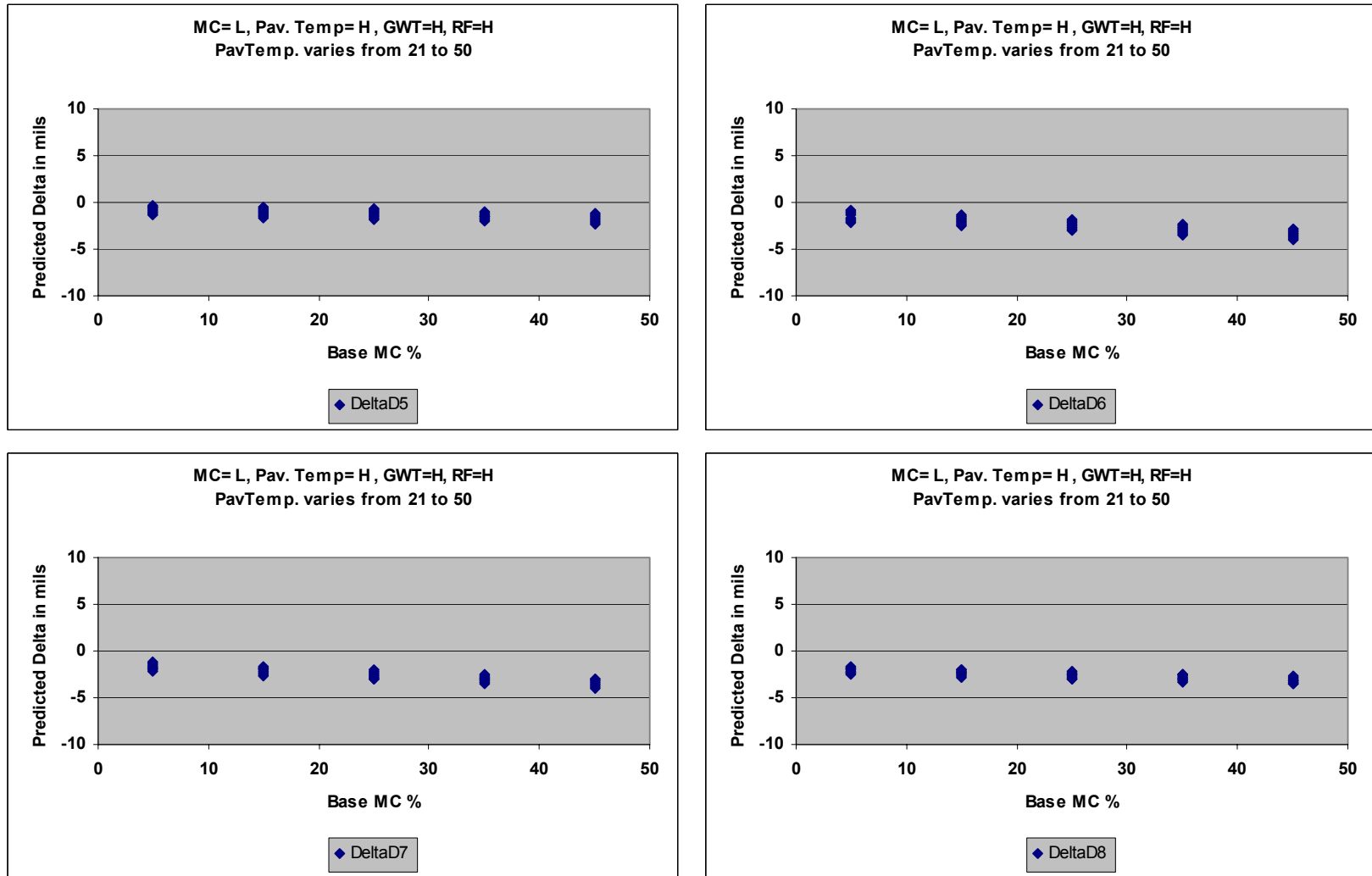


Figure B.16: Variation of Delta Deflection with MC and Pavement Temperature
MC=L, PavTemp=H, GWT= H, RF=H

MATERIAL CHARACTERIZATION AND SEASONAL VARIATION IN MATERIAL PROPERTIES

Appendix B: Results of Sensitivity Analysis for Regression Models

July 22, 2005

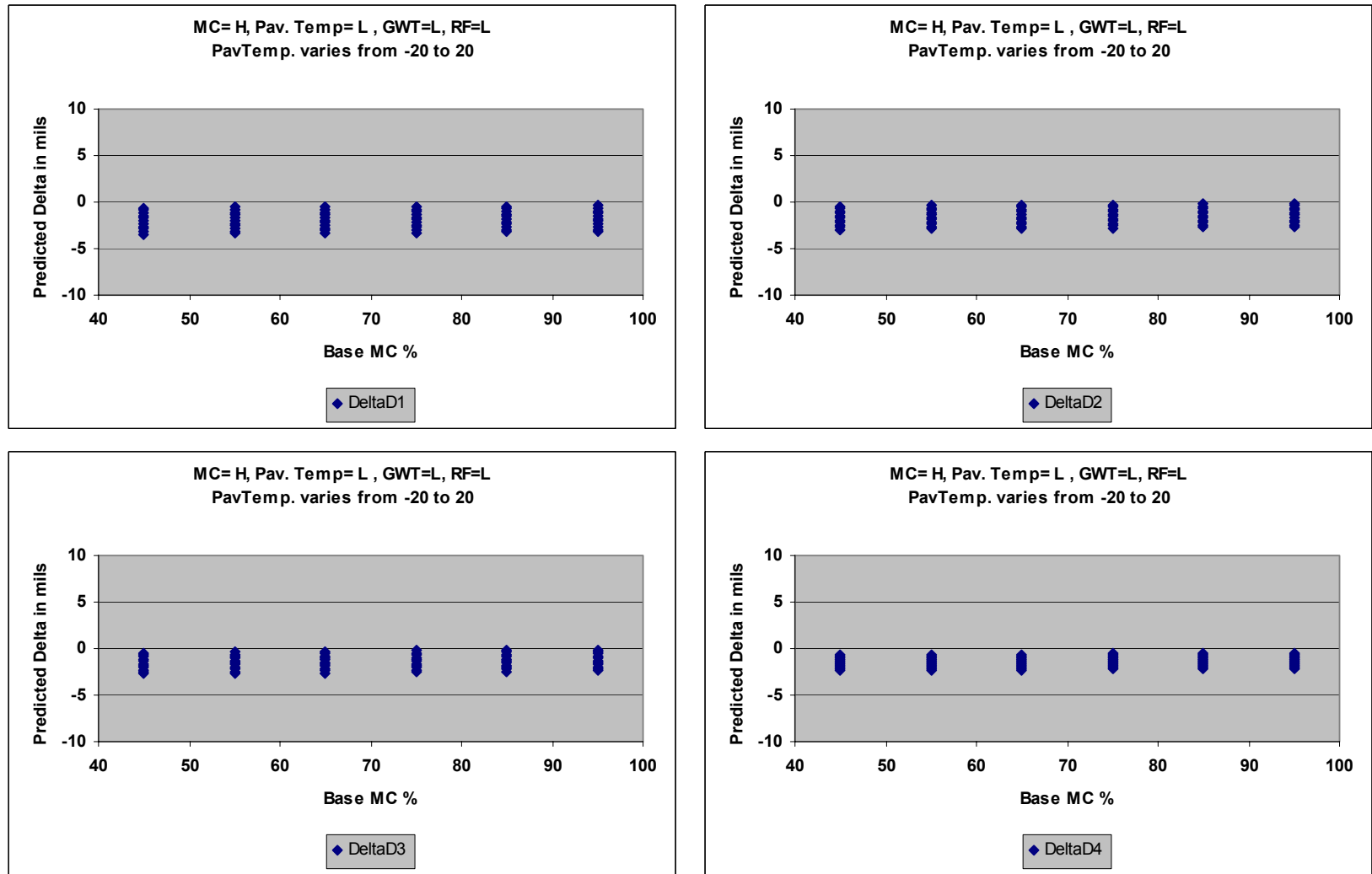


Figure B.17: Variation of Delta Deflection with MC and Pavement Temperature
MC=H, PavTemp=L, GWT= L, RF=L

MATERIAL CHARACTERIZATION AND SEASONAL VARIATION IN MATERIAL PROPERTIES

Appendix B: Results of Sensitivity Analysis for Regression Models

July 22, 2005

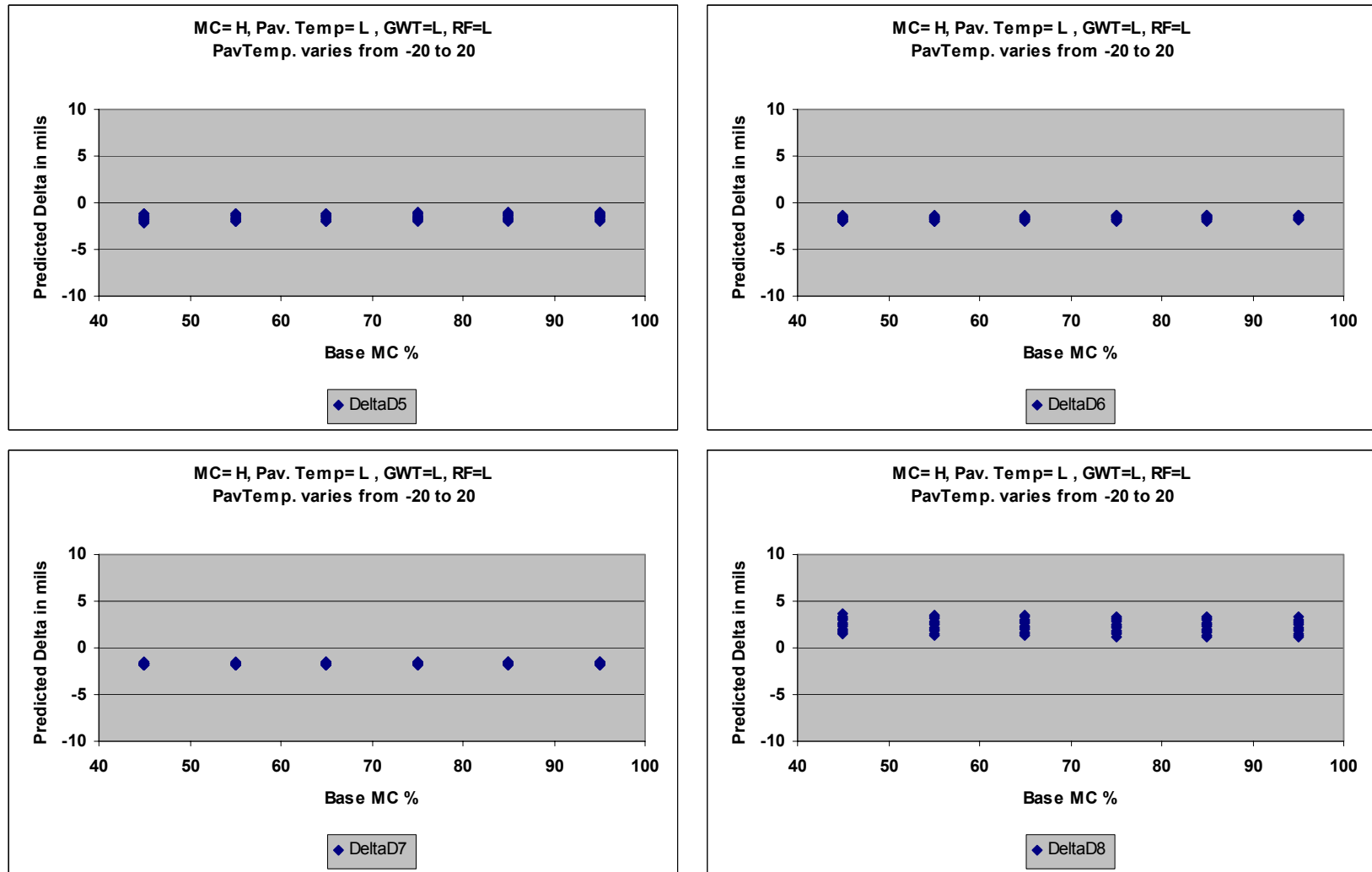


Figure B.18: Variation of Delta Deflection with MC and Pavement Temperature
MC=H, PavTemp=L, GWT= L, RF=L

MATERIAL CHARACTERIZATION AND SEASONAL VARIATION IN MATERIAL PROPERTIES

Appendix B: Results of Sensitivity Analysis for Regression Models

July 22, 2005

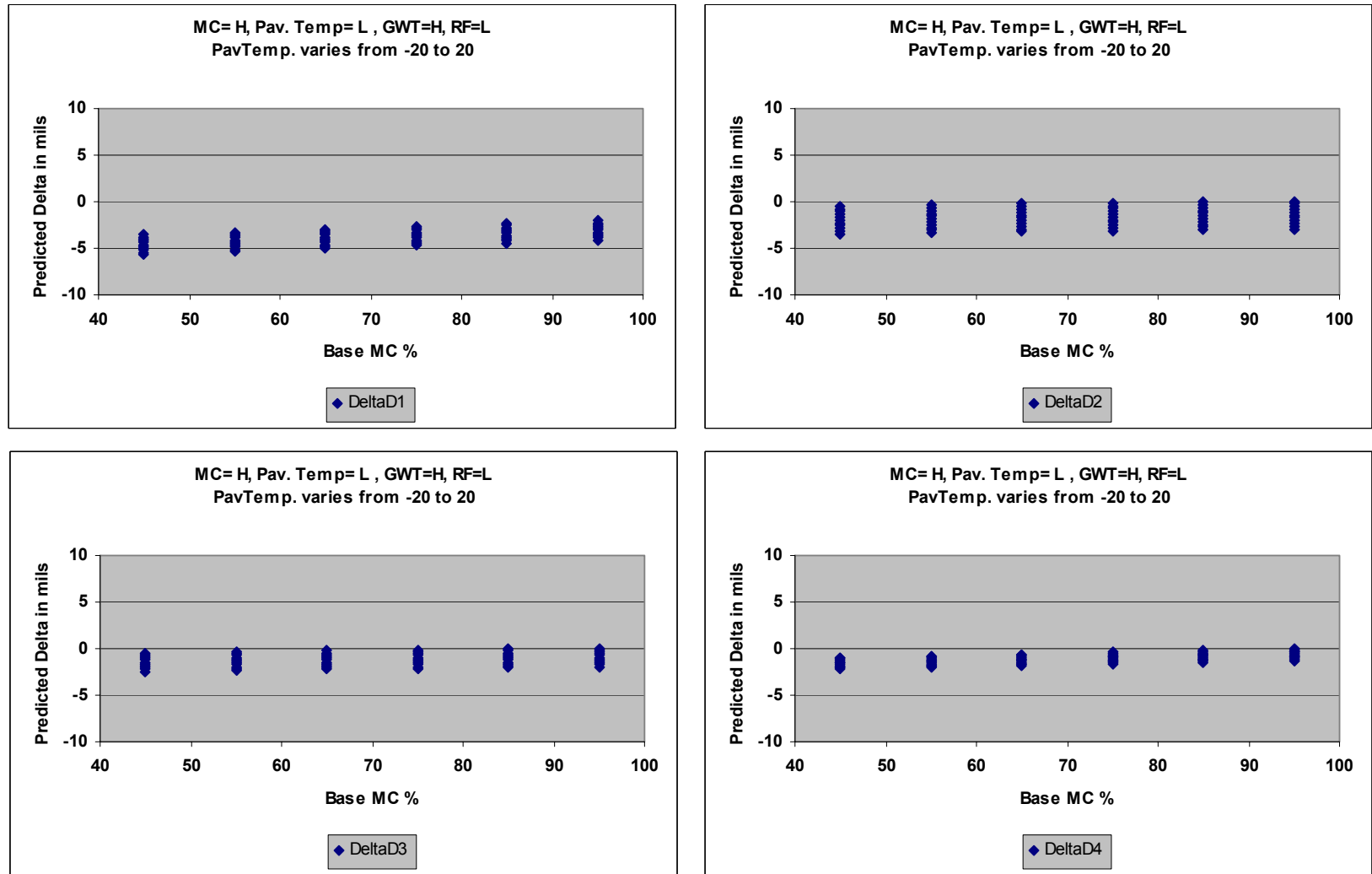


Figure B.19: Variation of Delta Deflection with MC and Pavement Temperature
MC=H, PavTemp=L, GWT= H, RF=L

MATERIAL CHARACTERIZATION AND SEASONAL VARIATION IN MATERIAL PROPERTIES

Appendix B: Results of Sensitivity Analysis for Regression Models

July 22, 2005

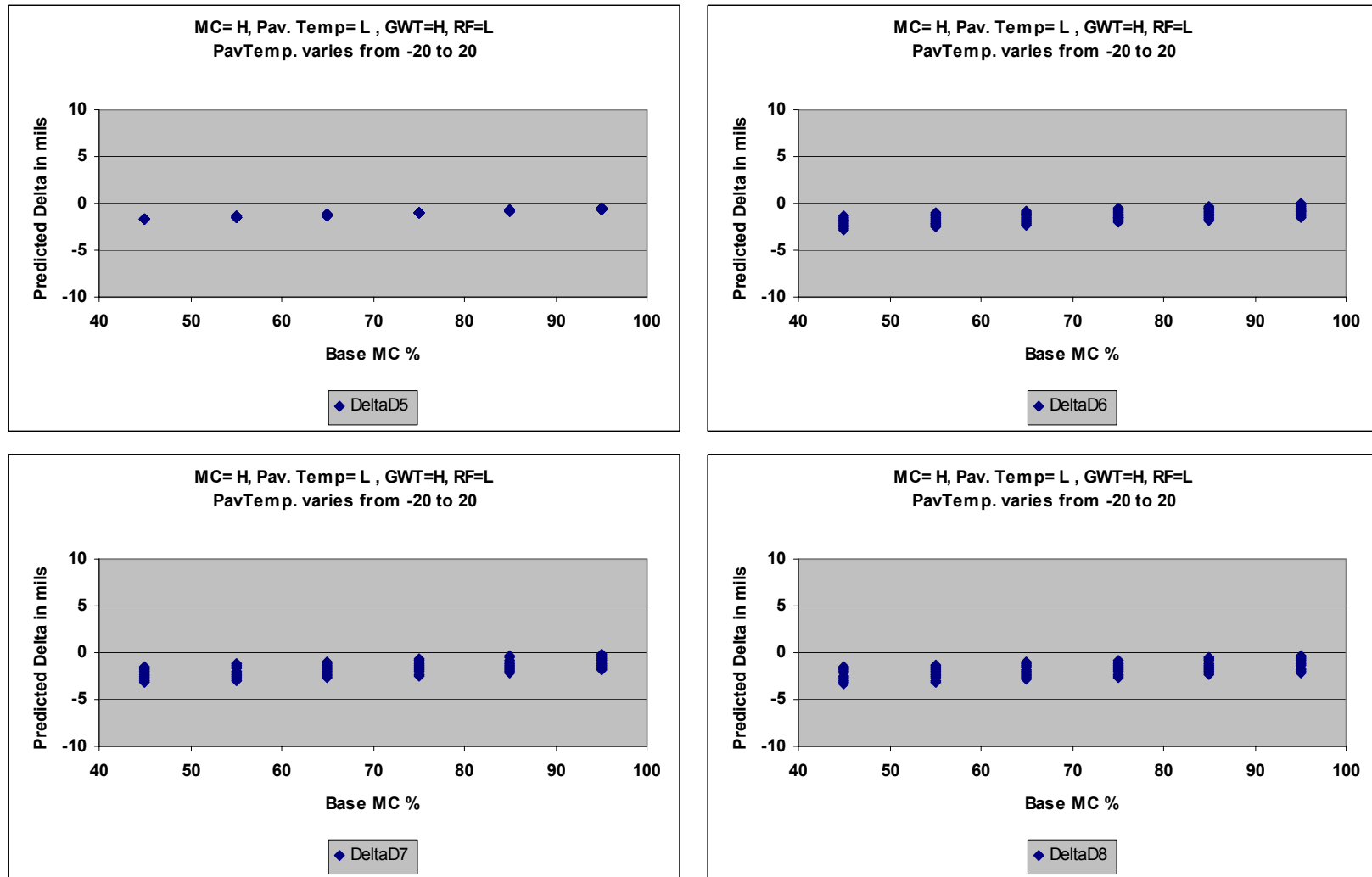


Figure B.20: Variation of Delta Deflection with MC and Pavement Temperature
MC=H, PavTemp=L, GWT= H, RF=L

MATERIAL CHARACTERIZATION AND SEASONAL VARIATION IN MATERIAL PROPERTIES

Appendix B: Results of Sensitivity Analysis for Regression Models

July 22, 2005

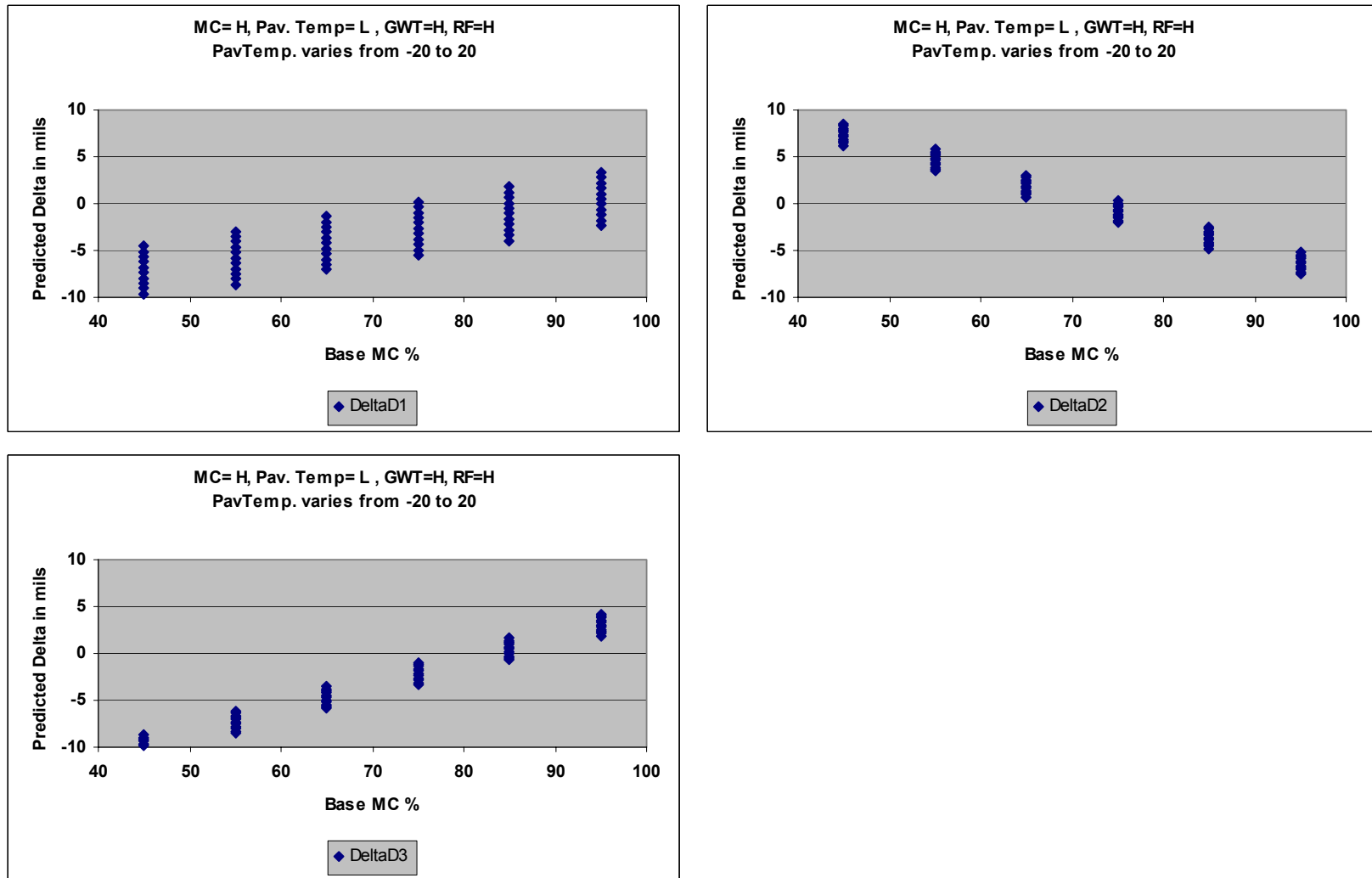


Figure B.21: Variation of Delta Deflection with MC and Pavement Temperature
MC=H, PavTemp=L, GWT= H, RF=H

MATERIAL CHARACTERIZATION AND SEASONAL VARIATION IN MATERIAL PROPERTIES

Appendix B: Results of Sensitivity Analysis for Regression Models

July 22, 2005

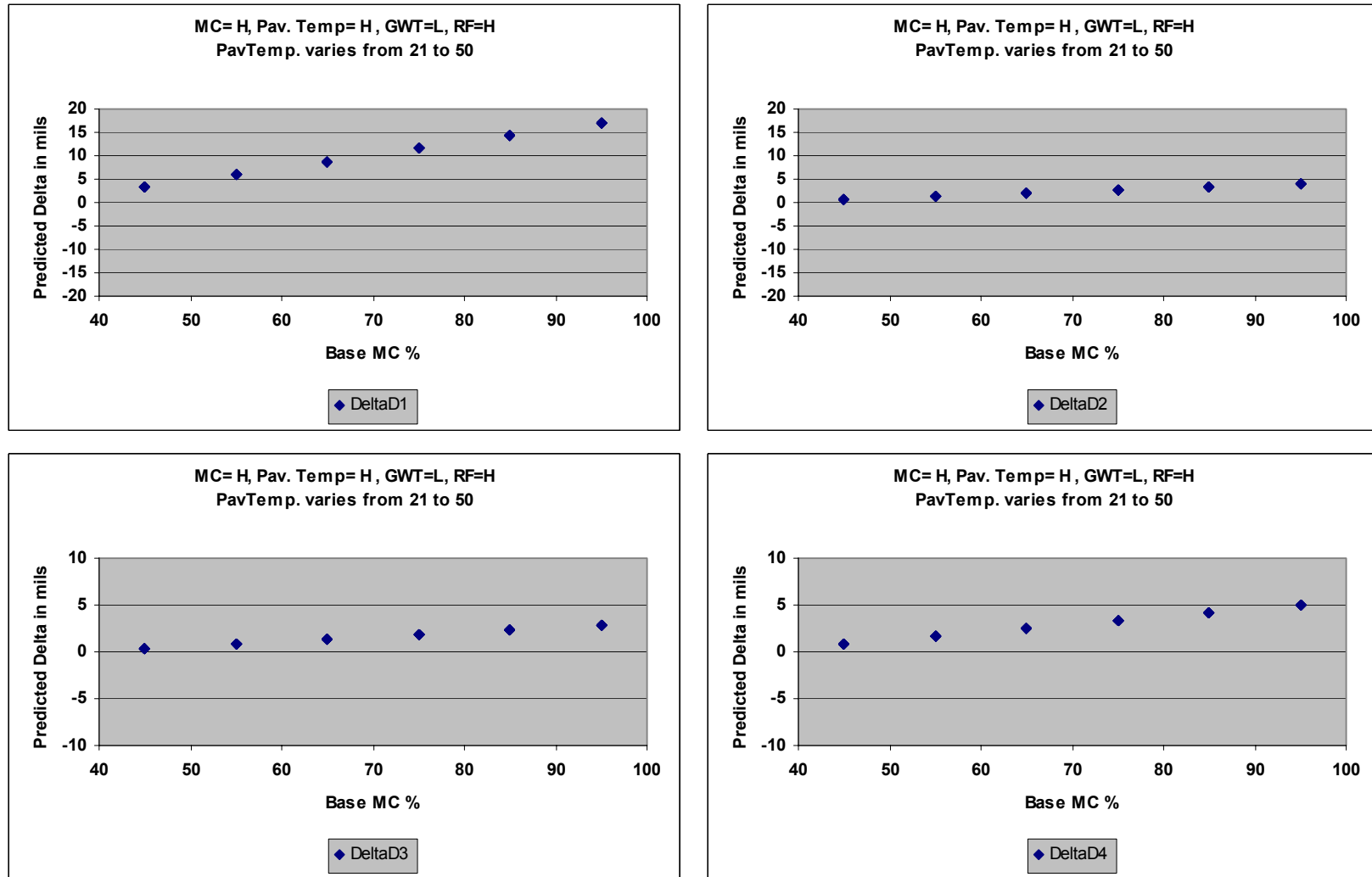


Figure B.22: Variation of Delta Deflection with MC and Pavement Temperature
MC=H, PavTemp=H, GWT= L, RF=H

MATERIAL CHARACTERIZATION AND SEASONAL VARIATION IN MATERIAL PROPERTIES

Appendix B: Results of Sensitivity Analysis for Regression Models

July 22, 2005

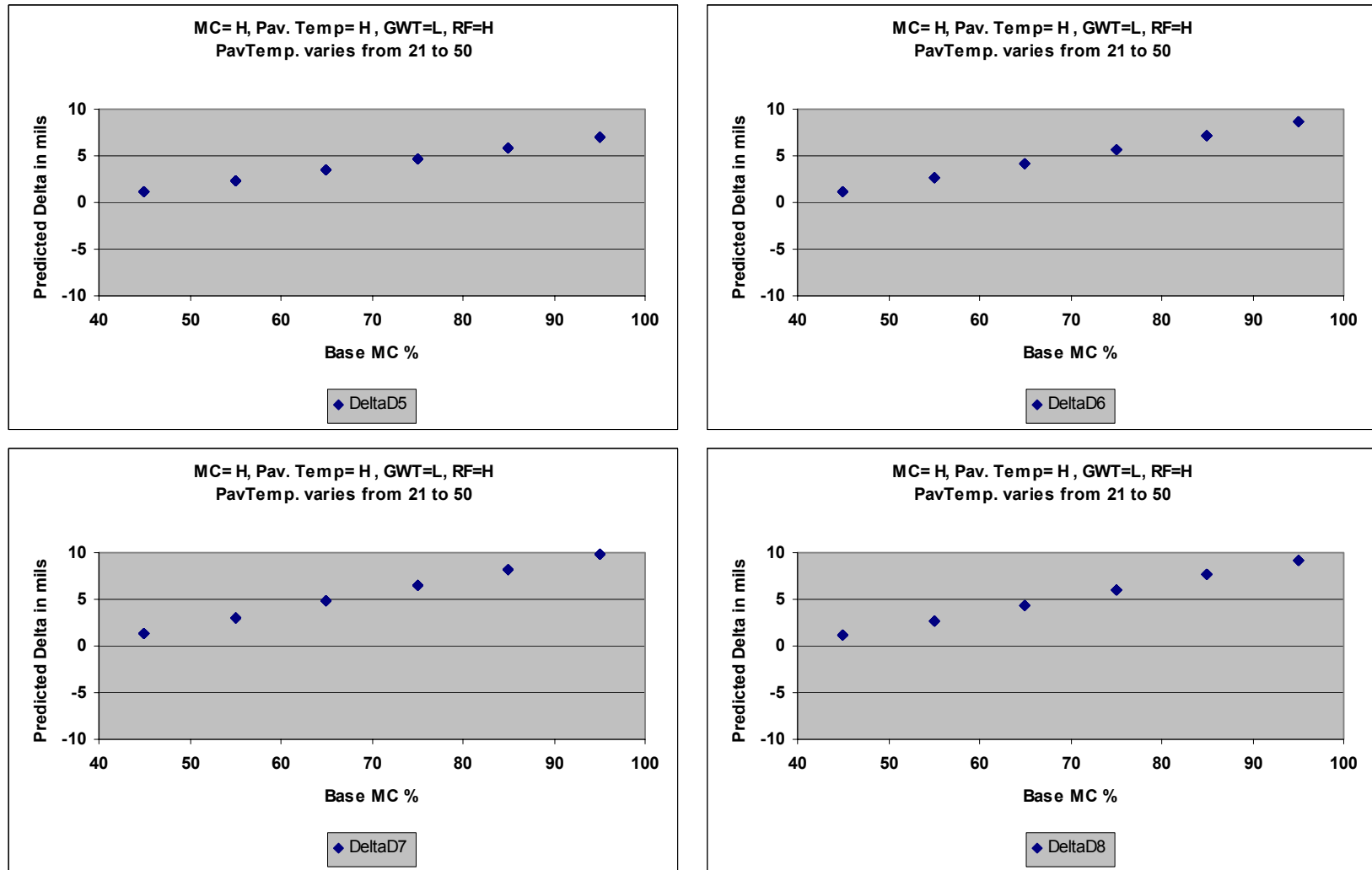


Figure B.23: Variation of Delta Deflection with MC and Pavement Temperature
MC=H, PavTemp=H, GWT= L, RF=H

MATERIAL CHARACTERIZATION AND SEASONAL VARIATION IN MATERIAL PROPERTIES

Appendix B: Results of Sensitivity Analysis for Regression Models

July 22, 2005

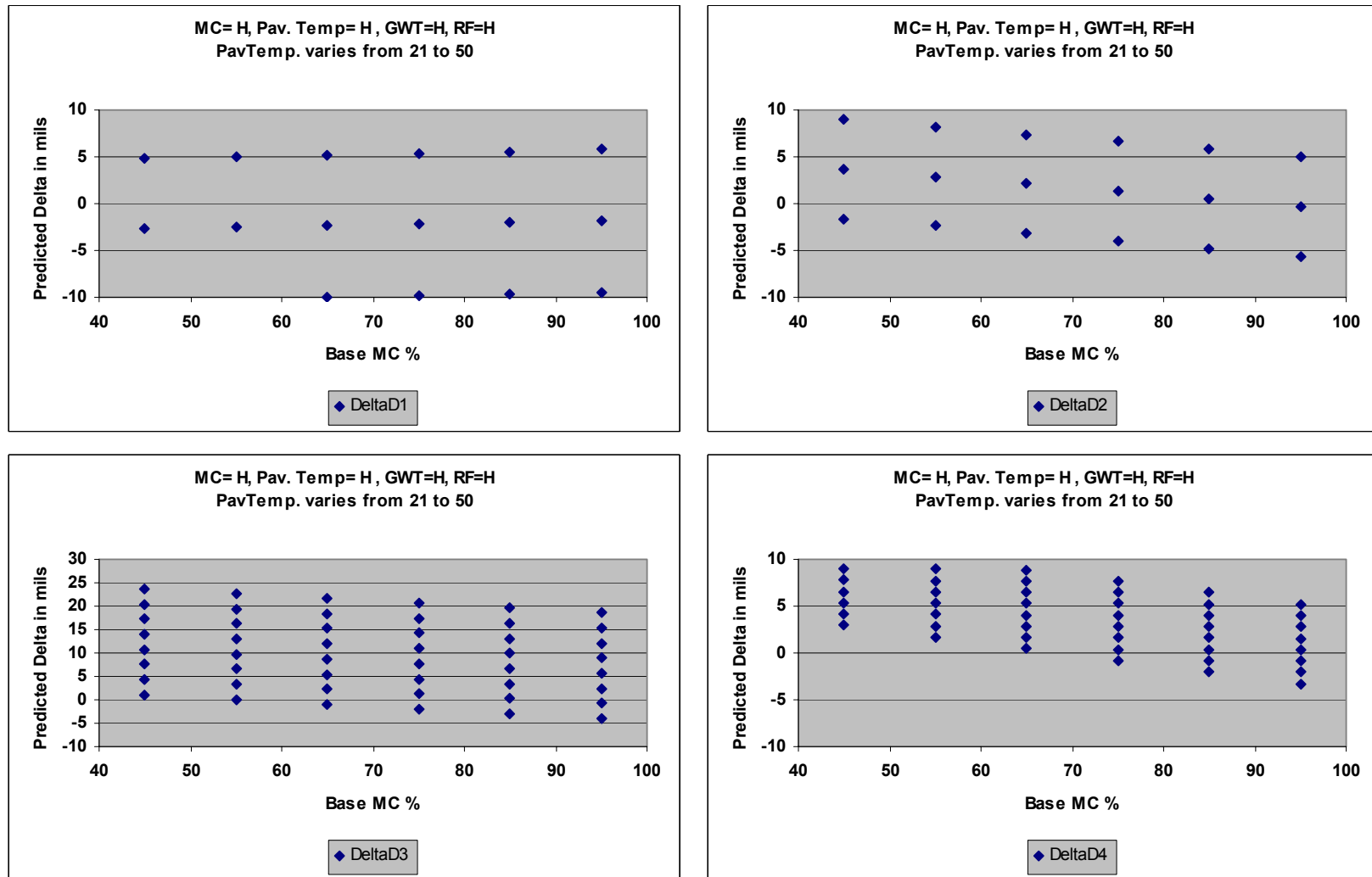


Figure B.24: Variation of Delta Deflection with MC and Pavement Temperature
MC=H, PavTemp=H, GWT= H, RF=H

MATERIAL CHARACTERIZATION AND SEASONAL VARIATION IN MATERIAL PROPERTIES

Appendix B: Results of Sensitivity Analysis for Regression Models

July 22, 2005

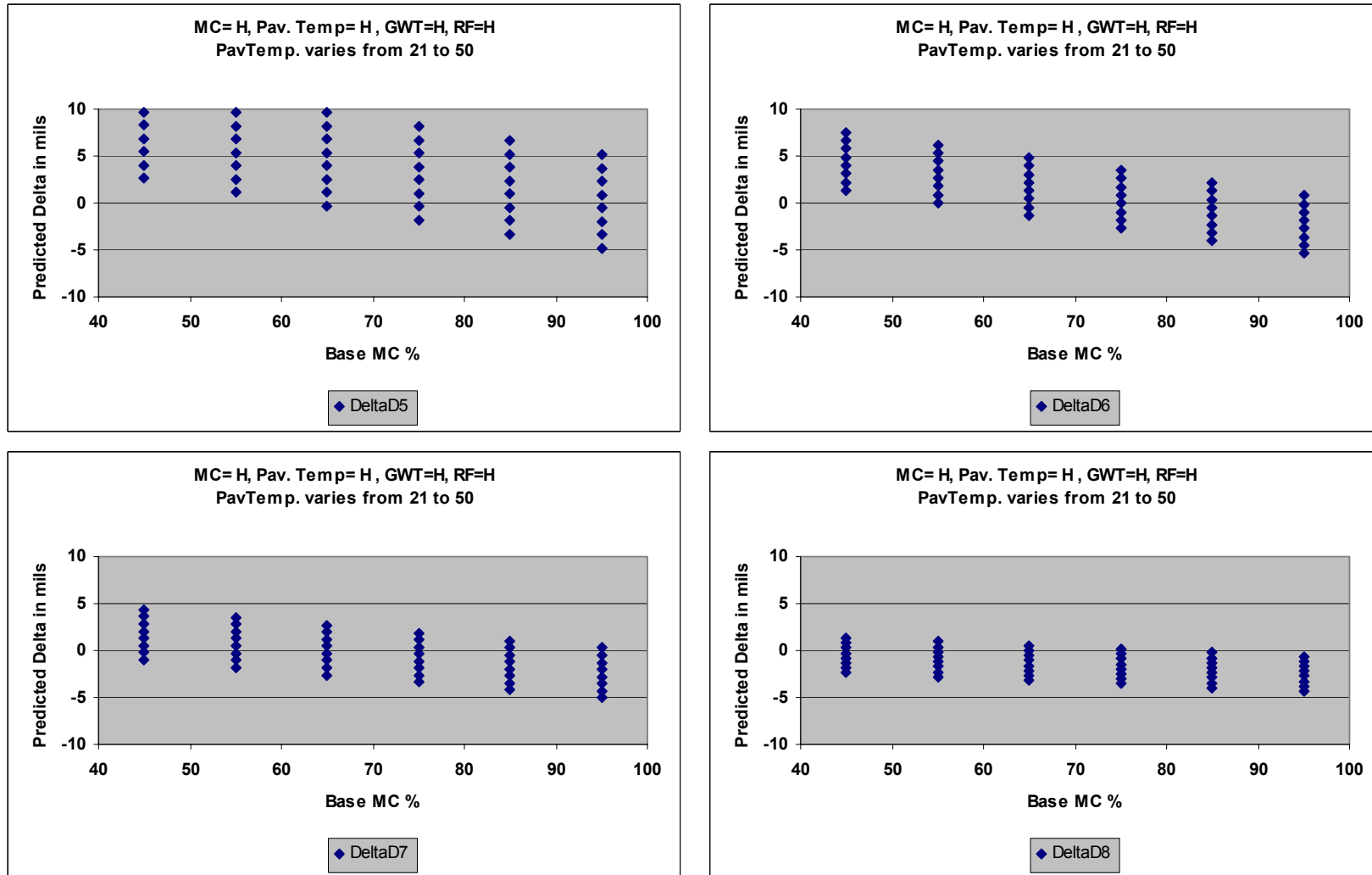


Figure B.25: Variation of Delta Deflection with MC and Pavement Temperature
MC=H, PavTemp=H, GWT= H, RF=H